



**PHOTOCATALYTIC C-H BONDS FUNCTIONALIZATION OF
CARBOXYLIC ACIDS AND ALKYLARENES**

Thesis submitted in accordance with the requirements of the University of
Liverpool for the degree of Doctor in Philosophy

by

Renpeng Guan

August 2023

Acknowledgements

First of all, I am very grateful to my supervisor Professor Jianliang Xiao. Thank you for the great opportunity of conducting my PhD study with you. Thank you for your continuous guidance and support over the whole PhD period. Thank you for your contagious passion on research. It encourages me to continue my experiment exploration when I face difficulty.

I want to thank Chinese Scholarship Council and University of Liverpool for funding me for PhD. I also want to thank Dr. Xiaofeng Wu. Not only for his valuable discussions and suggestions for my projects, but also for his concern to help me overcome the tough period like the Covid-19 Pandemic.

Thank you to my colleague Professor Zhiliang Huang. Your patience and guidance really help me to be familiar with the lab work and start my PhD study successfully. You have offered me valuable suggestions and help for both my projects and my papers. I also appreciate you for caring me in daily life.

Thanks to the whole family for your endless support. Honestly, finishing my PhD as well as living an unfamiliar country are challenging for me. Your encouragement and concern really support me to finish my PhD study. When I feel frustrated, your concern is my motional spirit. It helps me to overcome the dilemma I faced. I also think you for your open attitude. Thank you for supporting me when I want to chase my dream.

A big thanks goes to Guanhong. Thanks for your help since we flying from Hangzhou to UK. You help me to be familiar with Liverpool and the daily life when I first come here. It is a good time living with you as the roommate. I also appreciate your help in the lab, especially in the assistance of HPLC detection.

Thanks to all past and current members of the Xiao group. I will never forget our together working time. To Elliot for his help in photo reactors and his advice in my projects. To Tianlin for his assistance in my projects. Thanks to Zhenyu, Leiming, Sydney, Ilkan, Prashant and Ramachandran.

Finally, I want to appreciate our university. It is really a meaningful experience and important memory for me. I will remember alma mater forever.

Abstract

C-H functionalization is a meaningful but challenge issue. The construction of C-C bond or C-X bonds can afford different feedstocks for organic synthesis. Therefore, developing new methods for such reactions is an important task in organic chemistry. Chapter 1 presents a general introduction to C-C and C-X bond forming reactions, focusing on C-H functionalization of carboxylic acids and arenes.

Chapter 2 describes the decarboxylative oxygenation of carboxylic acids to aldehydes and ketones. A new protocol using a novel and efficient Mn catalyst and O₂ as oxidant for this transformation is developed. A series of different carboxylic acids, including benzylic acids, amino acids, fatty acids and drug molecules, can be successfully transformed to the corresponding valuable aldehydes and ketones.

Chapter 3 describes the selective transformation of carboxylic acids to a variety of products, including peroxides, carbonyls and alcohols. Cheap and commercial-available Ce(III) catalysts are employed for this selective transformation of carboxylic acids using air as oxidants. The selectivity of products can be tuned to favour peroxides, carbonyls or alcohols with excellent selectivity and high yields by the selection of bases.

Chapter 4 describes a Ce-catalysed Ritter type C-H amidation of alkylarenes with nitriles. A wide range of benzylic amides can be afforded in good yields and high selectivity, as well as expanding scope of nitriles seen in previous reports. Mechanistic studies indicate that a bromide intermediate is formed in the reactions, which is transformed to corresponding amides.

Chapter 5 presents the exploration of oxidative C-H functionalization of cyclododecane for the construction of C-O bonds. Three different products, cyclododecanone, cyclododecanol and hydroperoxycyclododecane, can be afforded with high selectivity in different photocatalytic or thermal catalytic systems.

Publications

- **Chemoselective Decarboxylative Oxygenation of Carboxylic Acids to Access Ketones, Aldehydes, and Peroxides**
Guan, R.; Chen, G.; Bennett, E.L.; Xiao, J. *Org. Lett.* **2023**, *25*, 2482–2486.
- **Non-Heme Manganese(II) Complex-Catalysed Oxidative Cleavage of 1,2-Diols via Alcohol-Assisted O₂ Activation**
Huang, Z.; Guan, R.; Bennett, E.L.; Xiao, J. *Green Chem.* **2022**, *24*, 3814-3823.
- **Chemical Recycling of Polystyrene to Valuable Chemicals via Selective Acid-Catalyzed Aerobic Oxidation under Visible Light**
Huang, Z.; Shanmugam, M.; Liu, Z.; Brookfield, A.; Bennett, E.L.; Guan, R.; Vega Herrera, D.E.; Lopez-Sanchez, J.A.; Slater, A.G.; McInnes, E.J; and Qi, X.; Xiao, J. *J. Am. Chem. Soc.* **2022**, *144*, 6532-6542.
- **Decarboxylative Oxygenation of Carboxylic Acids with O₂ via a Non-Heme Manganese Catalyst**
Guan, R.; Bennett, E.L.; Huang, Z.; and Xiao, J. *Green Chem.* **2022**, *24*, 2946-2952.
- **Oxidative Cleavage of Alkenes by O₂ with a Non-Heme Manganese Catalyst**
Huang, Z.; Guan, R.; Shanmugam, M.; Bennett, E.L.; Robertson, C.M.; Brookfield, A.; McInnes, E.J.; Xiao, J. *J. Am. Chem. Soc.* **2021**, *143*, 10005-10013.

Definitions and Abbreviations

ns	Nanosecond
ms	Microsecond
nm	Nanometer
vs	Versus
SCE	Saturated calomel electrode
v	Volt
<i>t</i> BuCN	<i>Tert</i> -butyl isocyanide
Me	Methyl
OMe	Methoxy
<i>t</i> Bu	<i>Tert</i> -butyl
EtCN	Propionitrile
NaBH ₄	Sodium borohydride
Mn(OTf) ₂	Manganese bis(trifluoromethanesulfonate)
dtbpy	4,4'-Di- <i>tert</i> -butyl-2,2'-dipyridyl
SHE	Standard Hydrogen Electrode
o	Ortho
p	Para
m	Meta
Fe(OTf) ₂	Iron(II) trifluoromethanesulfonate
Cu(OTf) ₂	Copper(II) trifluoromethanesulfonate
CoCl ₂	Cobalt(II) chloride
MnCl ₂	Manganese(II) chloride
DCE	1,2-Dichloroethane
EtOH	Ethanol
THF	Tetrahydrofuran
MeOH	Methanol
TFE	2,2,2-Trifluoroethanol
NaOAc	Sodium acetate
¹ O ₂	Singlet oxygen
Ru(bpy) ₃	Tris(bipyridine)ruthenium(II) chloride

Ir(dFppy) ₃	Tris[3,5-difluoro-2-(2-pyridinyl)phenyl]- Iridium
DPA	9,10-Diphenylanthracene
KIE	Kinetic isotope effect
NaIO ₄	Sodium periodate
<i>n</i> -Bu ₄ NIO ₄	Tetrabutylammonium (meta)periodate
HgF ₂	Mercury(II) fluoride
Pb(OAc) ₄	Lead(IV) acetate
PhI(OAc) ₂	(Diacetoxiodo)benzene
K ₂ S ₂ O ₈	Potassium persulfate
Mes-AcrClO ₄	9-Mesityl-10-methylacridinium perchlorate
CeCl ₃	Cerium(III) chloride
CeBr	Cerium(III) bromide
[Ir(dF(Me)ppy) ₂ (dtbbpy)]PF ₆	Iridium(III) bis[2-(2,4-difluorophenyl)-5- methylpyridine-N,C ₂₀]-4,40-di- <i>tert</i> -butyl- 2,20-bipyridine hexafluorophosphate
Ce(<i>Ot</i> Bu) ₄	(<i>tert</i> -butoxo)Cerium(IV)
NaBH ₄	Sodium borohydride
KOAc	Potassium acetate
LiOAc	Lithium acetate
CsOAc	Caesium acetate
Na ₂ CO ₃	Sodium carbonate
NaOH	Sodium hydroxide
Et ₃ N	Triethylamine
DBU	1,8-Diazabicyclo(5.4.0)undec-7-ene
Ce ₂ (C ₂ O ₄) ₃	Cerium Oxalate Hydrate
NH ₄ Ce(NO ₃) ₆	Ceric ammonium nitrate
Ce(OAc) ₃	Cerium (III) acetate
CeF ₃	Cerium(III) fluoride
CeF ₄	Cerium(IV) fluoride
HIO ₃	Iodic acid
DDQ	2,3-Dichloro-5,6-dicyano-1,4-benzoquinone

$\text{Na}_2\text{S}_2\text{O}_8$	Sodium persulfate
TAC	Trisaminocyclopropenium
H_2SO_4	Sulfuric acid
$\text{Sc}(\text{OTf})_3$	Scandium(III) triflate
$\text{Yt}(\text{OTf})_3$	Ytterbium(III) trifluoromethanesulfonate
$\text{La}(\text{OTf})_3$	Lanthanum(III) trifluoromethanesulfonate
CBr_3COOH	Tribromoacetic acid
CCl_3COOH	Trichloroacetic acid
CCl_2COOH	Dichloroacetic acid
CF_3COOH	Trifluoroacetic acid
$\text{Fe}(\text{ClO}_4)_2$	Iron(II) perchlorate
CuCr_2O_4	Copper chromite

Contents

Acknowledgements	I
Abstract	III
Publications	V
Definitions and Abbreviations	VI
Chapter 1: Introduction	1
1.1 Catalytic C-H bonds functionalization	1
- 1.1.1 Photocatalytic C-H bonds functionalization	1
- 1.1.2 Transition-metal-catalysed C-H bonds functionalization	7
- 1.1.3 Electrocatalytic C-H bonds functionalization	12
1.2 Functionalization of carboxylic acids	16
1.3 Ritter and Ritter-type reaction	21
- 1.3.1 Ritter reaction	21
- 1.3.2 Ritter-type reaction	23
1.4 Molecular oxygen in oxidation reactions	25
1.5 Aims of this thesis	29
1.6 References	30
Chapter 2: Decarboxylative Oxygenation of Carboxylic Acids to Aldehydes and Ketones via a Non-Heme Manganese Catalyst	38
2.1 Introduction	38
2.2 Results and discussion	40
- 2.2.1 Optimization experiments	40

- 2.2.2 Substrate scope	43
- 2.2.3 Exploration of possible mechanism	46
2.3 Conclusions	52
2.4 Experimental details	53
- 2.4.1 Details of photoreactors	53
- 2.4.2 Preparation of substrates	54
- 2.4.3 Optimization of experimental conditions	64
- 2.4.4 Mechanistic studies	65
2.5 Analytical data of products	71
2.6 References	83
Chapter 3: Chemoselective Decarboxylative Oxygenation of Carboxylic	
Acids to Access Ketones, Aldehydes, Alcohols and Peroxides	92
3.1 Introduction	92
3.2 Results and discussion	95
- 3.2.1 Optimization experiments	95
- 3.2.2 Substrate scope	97
- 3.2.3 Exploration of possible mechanism	105
3.3 Conclusions	115
3.4 Experimental details	115
- 3.4.1 Details of photoreactors	115
- 3.4.2 Preparation of substrates	115
- 3.4.3 Mechanistic studies	121
3.5 Analytical data of products	129
- 3.5.1 Hydroperoxide products	129

- 3.5.2 Aldehyde and ketone products	136
- 3.5.3 Alcohol products	142
3.6 References	148
Chapter 4: Photocatalytic Ritter-type Benzylic C-H	
Amidation of Alkylarenes	156
4.1 Introduction	156
4.2 Results and discussion	159
- 4.2.1 Optimization experiments	159
- 4.2.2 Substrate scope	161
- 4.2.3 Exploration of possible mechanism	164
4.3 Conclusions	173
4.4 Experimental details	174
- 4.4.1 Details of photoreactors	174
- 4.4.2 Preparation of substrates	174
- 4.4.3 Details of solvents	178
- 4.4.4 Mechanistic studies	179
4.5 Analytical data of products	184
4.6 References	198
Chapter 5: Exploration of Photocatalytic Oxidation of Cycloalkanes	203
5.1 Introduction	203
5.2 Exploration of oxygenation of cyclododecane	205
5.3 Conclusions and future work	212
5.4 Experimental details	213

- 5.4.1 Details of photoreactors	213
- 5.4.2 Synthesis of catalysts	213
- 5.4.3 General procedure for selective oxidation of cyclododecane	214
5.5 Analytical data of products	215
5.6 References	219
Chapter 6: Conclusions and Perspectives	223

Chapter 1

Introduction

1.1 Catalytic C-H bonds functionalization

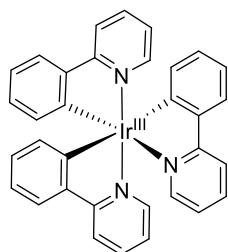
C-H bonds have become the focus of intense work since the start of chemical research because of their ubiquitous presence in organic chemistry.¹⁻² The direct installation of new C-C/C-X bonds from readily available C-H bonds without pre-activation of the substrates makes C-H bonds functionalization atom- and step-economic.³ Although great progress has been achieved over the past two decades, selective and efficient activation and transformation of strong C-H bonds still remains a challenging issue.⁴ To deal with this challenge, different catalytic strategies have been investigated, many of which have been proved to be good solutions. Over the past two decades, a series of good processes have been achieved in the field of catalytic C-H functionalization, including exploration of scope of transformations and types of catalytic manifolds which enable C-H functionalization.⁵ Among the current catalytic strategies used in organic chemistry, photocatalysis, transition-metal-catalysis and electrocatalysis all have been utilized for the selective functionalization of C-H bonds.⁶⁻⁸ These strategies have been widely employed in selective functionalization of natural products,⁹⁻¹⁰ petroleum feedstocks,⁵ pharmaceutical derivatives¹¹ and polymers are selected examples presented below.^{7, 12}

1.1.1 Photocatalytic C-H bonds functionalization

Photocatalytic C-H bonds functionalization normally employs inorganic/organometallic or organic photoredox catalysts.¹³ For inorganic/organometallic catalysts, their advantages include high molar absorptivity, long triplet lifetime (~100 ns to 1 ms) and efficient intersystem crossing.¹⁴⁻¹⁵ Common photocatalysts employed in current research are Ir(III) or Ru(II) complexes and their derivatives, which can change their excited state properties and absorption

ability by altering their ligands set. The absorption windows of Ir(III) and Ru(II) photocatalysts are between 390-480 nm. Some selected common Ir(III) and Ru(II) photocatalysts are shown in Scheme 1.1.

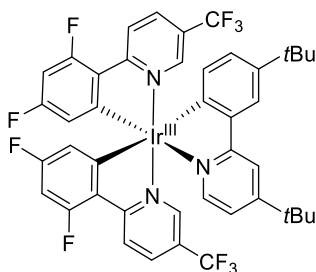
a) Common Ir photocatalysts



Ir(ppy)₃

$$E_{1/2} (M^+/M^*) = -1.73$$

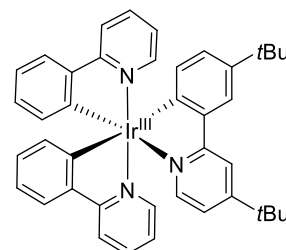
$$E_{1/2} (M^*/M^-) = +0.31$$



Ir(dF(CF₃)ppy)₃(dtbbpy)

$$E_{1/2} (M^+/M^*) = -0.89$$

$$E_{1/2} (M^*/M^-) = +1.21$$

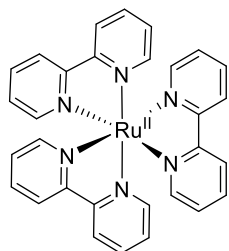


Ir(ppy)₂(dtbbpy)

$$E_{1/2} (M^+/M^*) = -0.96$$

$$E_{1/2} (M^*/M^-) = +0.66$$

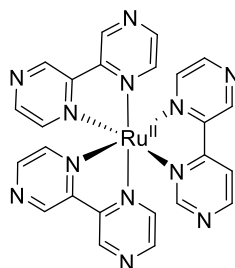
b) Common Ru photocatalysts



Ru(bpy)₃

$$E_{1/2} (M^+/M^*) = -0.81$$

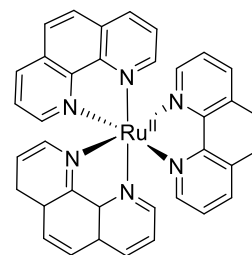
$$E_{1/2} (M^*/M^-) = +0.77$$



Ru(bpz)₃

$$E_{1/2} (M^+/M^*) = -0.26$$

$$E_{1/2} (M^*/M^-) = +1.45$$



Ru(phen)₃

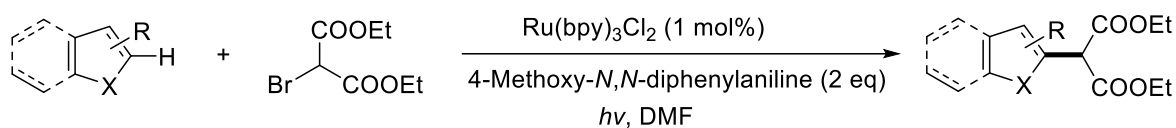
$$E_{1/2} (M^+/M^*) = -0.87$$

$$E_{1/2} (M^*/M^-) = +0.82$$

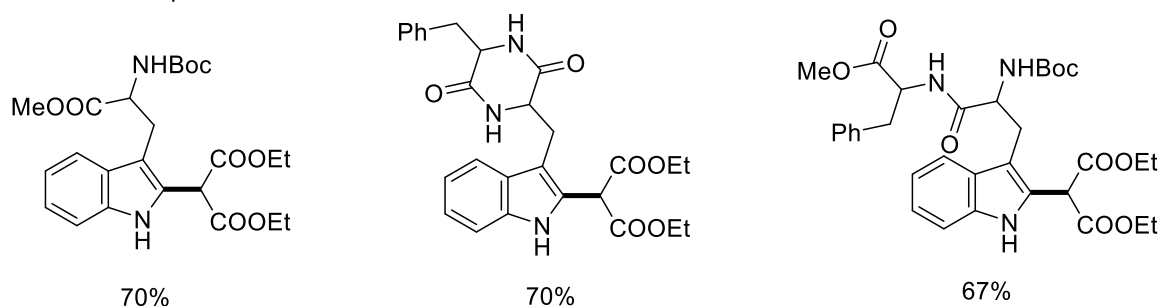
Scheme 1.1 Abbreviations and excited-state redox values (vs SCE) of common Ir and Ru photocatalysts.¹⁴

Both Ir^{III} and Ru^{II} photocatalysts have successfully catalysed aromatic and aliphatic C-H functionalization. For example, Stephenson and co-workers have reported the intermolecular heteroaryl C-H alkylation.¹⁶ In their work, Ru(bpy)₃Cl₂ was employed as the catalyst and the construction of C-C bond was realized by intermolecular coupling of heteroaromatics with bromomalonate (Scheme 1.2). This coupling reaction relies on the added reductant, 4-methoxy-*N,N*-diphenylaniline, which can help to prevent the undesired formation of possible alkylated enamine side products from a reductive hydrogen atom transfer of trialkylamines. A series of

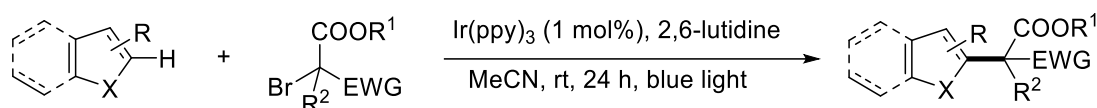
heteroaromatic compounds, including indoles, azaindoles, pyrroles, and furans underwent C2 functionalization successfully, affording corresponding products in moderate to good yields.



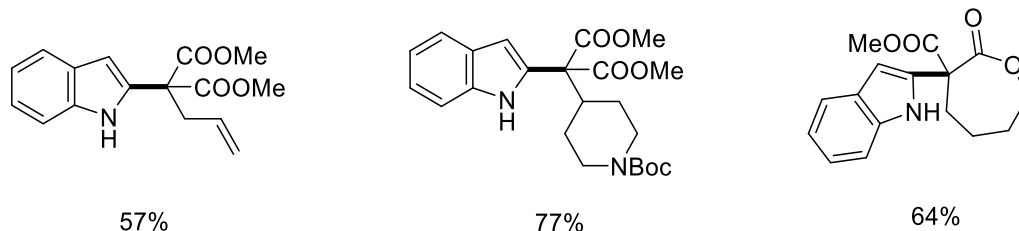
Selected examples



Scheme 1.2 C2 functionalization of heteroarene by intermolecular heteroaryl C-H alkylation.



Selected examples

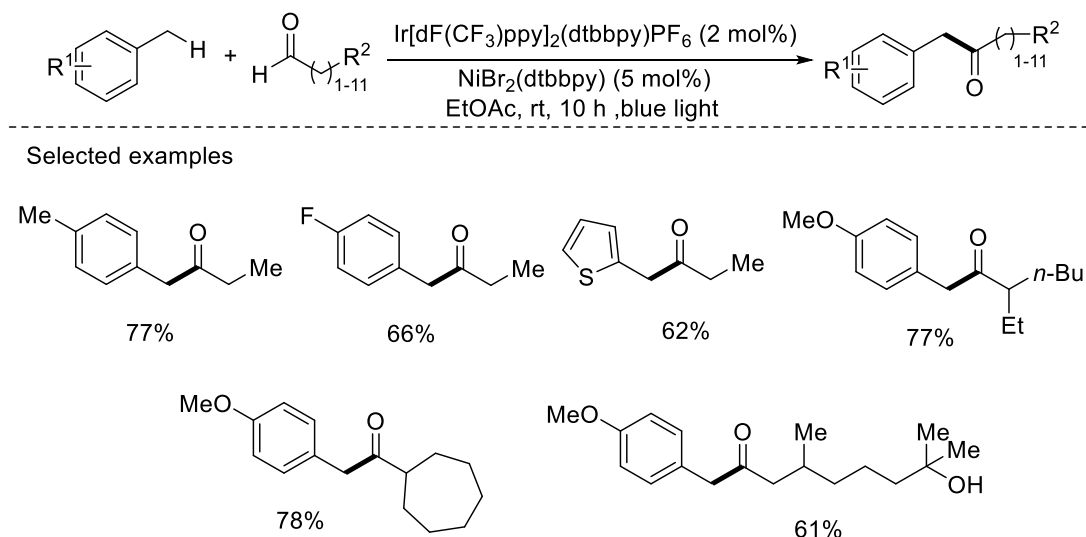


Scheme 1.3 Exploration of different bromides for an intermolecular heteroaryl C-H alkylation.

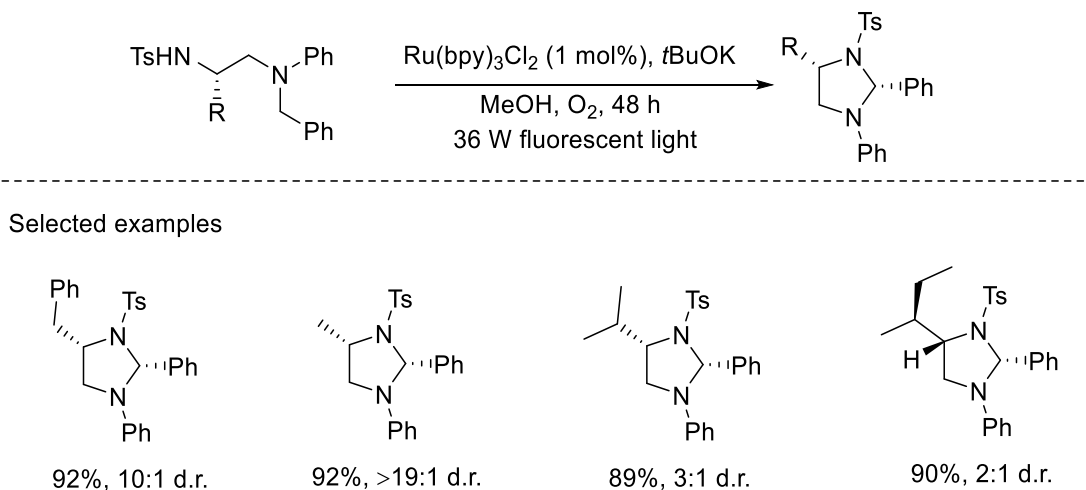
In their following work, Stephenson and co-workers explored the scope of the bromoacetate partner by employing Ir(ppy)_3 as the photocatalyst (Scheme 1.3).¹⁷ The requirement of an extra reductant can be eliminated in this work because Ir(ppy)_3 allows direct reduction of the tertiary bromide from the excited state ($E^*_{\text{ox}} = -1.73$ V vs SCE). A wide range of tertiary bromoacetates containing an electron-deficient group with different functional groups, such as primary or secondary allyl, alkyl, or benzyl substitution, were all tolerated in this work.

The C-H functionalization of alkylbenzenes for new C-C bonds have been reported by Murakami and co-workers (Scheme 1.4).¹⁸ A dehydrogenative C-H/C-H cross-coupling

reaction of alkylbenzenes with aldehydes to form α -aryl ketones was performed under blue light irradiation, which employed an iridium and nickel dual catalytic system. A series of aromatic and aliphatic aldehydes can undergo the dehydrogenative cross-coupling reaction successfully. Electron-donating groups, such as Me, OMe, *t*Bu et al., and halide groups, including F, Cl and Br, all are eligible substituents on the benzene ring.



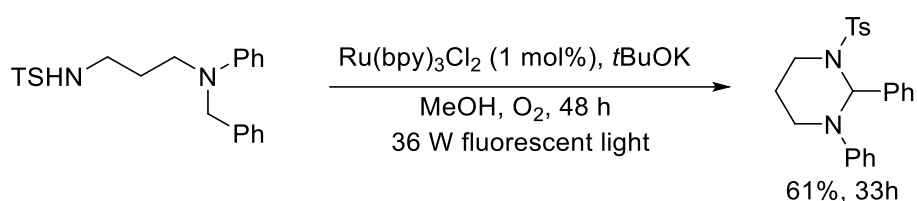
Scheme 1.4 Dehydrogenative coupling of benzylic and aldehydic C-H bonds.



Scheme 1.5 Visible light induced the asymmetric synthesis of tetrahydroimidazole derivatives.

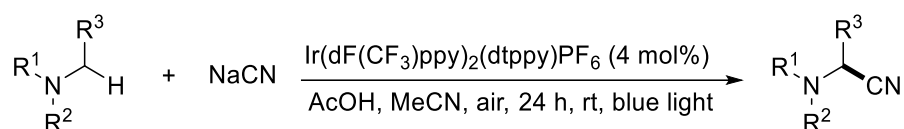
On the other hand, aliphatic C-H functionalization can be realized with Ru and Ir photocatalysts. W. J. Xiao and co-workers employed $\text{Ru}(\text{bpy})_3\text{Cl}_2$ in the formation of tetrahydroimidazoles via addition of an intramolecular sulfonamide to iminiums.¹⁹ As shown in Scheme 1.5, their strategy exhibited high diastereoselectivity, and the desired tetrahydroimidazoles were afforded in good yields. It is significant that this method can be

applied in the synthesis of biologically important tetrahydropyrimidine derivatives (Scheme 1.6).

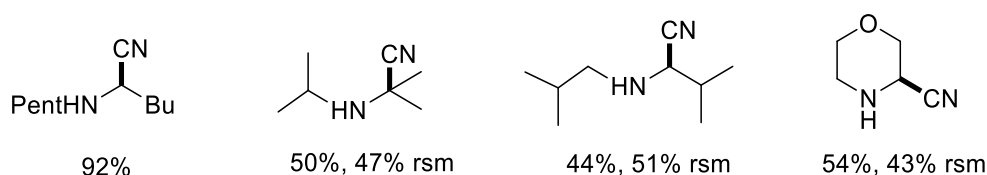


Scheme 1.6 Synthesis of biologically important tetrahydropyrimidine derivatives.

$\text{Ir(dF(CF}_3\text{)ppy)}_2\text{(dtpy)PF}_6$ has been successfully applied in C-H cyanation reaction (Scheme 1.7).²⁰ In this work, inexpensive NaCN is employed as the cyanide source and air is the external oxidant, leading to highly functional group tolerance in mild conditions. Secondary and tertiary aliphatic amines, and biologically active compounds (drugs) proceeded successfully, affording corresponding nitriles in up to 99% yields.



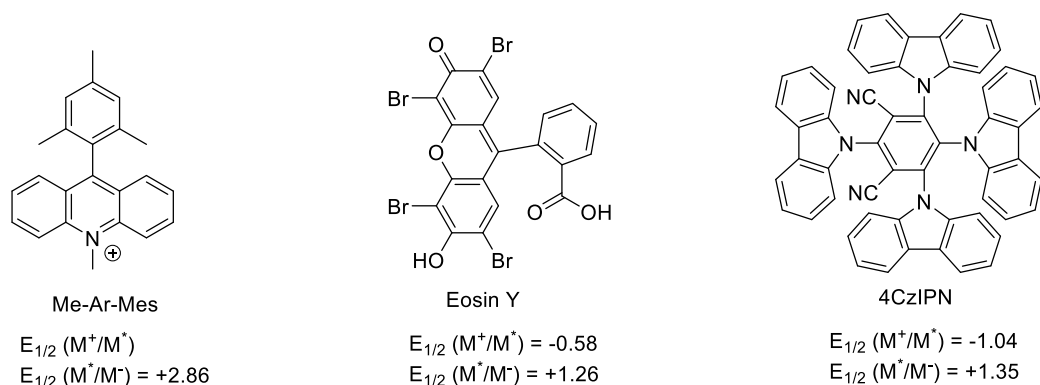
Selected examples



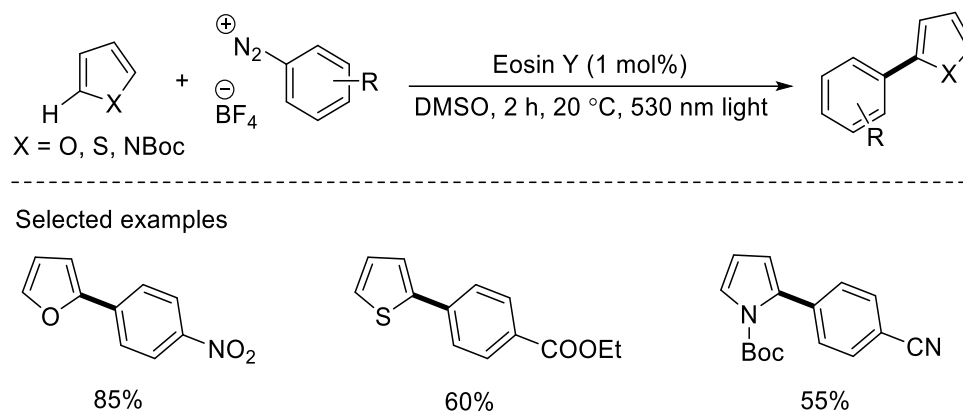
Scheme 1.7 C-H cyanation of tertiary aliphatic amine derived iminium ions.

Apart from the above inorganic photocatalysts, a series of organic catalysts have also been successfully employed in photocatalytic C-H functionalization (Scheme 1.8). In comparison with inorganic/organometallic catalysts, excited-state organic photoredox catalysts have a larger redox window.²¹ It may be the key to realize some specific transformations or access particular substrates, which are inaccessible by metal-based photocatalytic systems. Although the absorption profile of organic catalysts is similar to that of inorganic/organometallic-based systems, organic catalysts have lower extinction coefficients. Normally, they operate via S1

states rather than T1 states, leading to a larger redox window at the expense of shorter lifetimes overall (10-50 ns).⁵



Scheme 1.8 Abbreviations and excited-state redox values (vs SCE) of common organic photocatalysts.

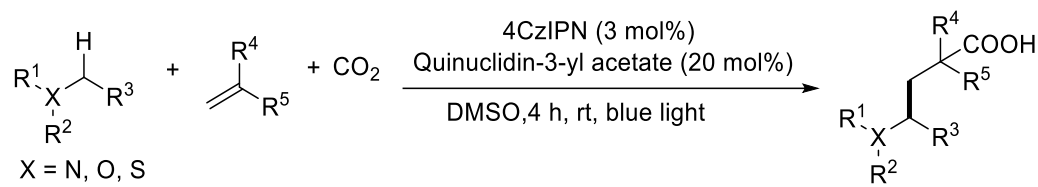


Scheme 1.9 C-H heteroarylation via Eosin Y.

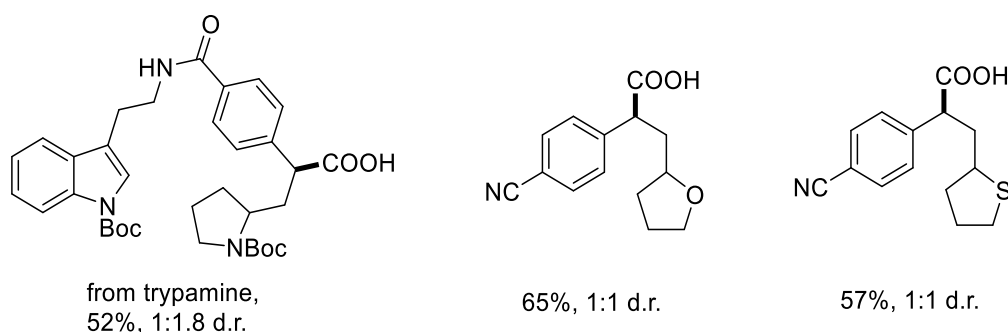
(Hetero)aryl C-H functionalization can be realized by using organic photocatalysts. For example, König and co-authors reported a metal-free arylation of heteroarenes employing Eosin Y as catalyst (Scheme 1.9).²² In this work, an aryl radical was formed via single electron reduction with photoexcited Eosin Y, which underwent the addition to a heteroarene in a Minisci-type fashion. The oxidation and deprotonation of resulting cyclohexadienyl radical intermediate afforded the final products. Generally, furan, thiophene, and pyrrole derivatives with a broad scope of diazonium salts were transformed to arylation products in moderate to good yields.

Meanwhile, aliphatic C-H functionalization by organic photocatalysts also has been demonstrated in previous work. Wu and co-authors employed 4CzIPN in carbocarboxylation of alkenes with CO₂ (Scheme 1.10).²³ In this report, the added quinuclidine catalysed the

hydrogen atom transfer, leading to the formation of α -heteroatom radicals. These radicals were trapped with alkenes in the presence of CO_2 , affording the carbocarboxylated products. A wide substrate scope can be observed because a series of different substrates, including amides, ethers, and thioethers, can be coupled with electron-deficient alkenes.



Selected examples



Scheme 1.10 Carbocarboxylation of alkenes via 4CzIPN.

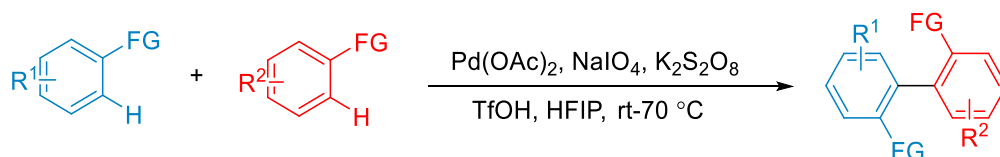
1.1.2 Transition-metal-catalysed C-H bonds functionalization

Transition-metal-catalysed C-H functionalization is an important synthetic strategy in terms of high step- and atom-economy.²⁴⁻²⁵ In C-H functionalization of aromatic heterocycles, these heterocycles normally guide the regioselectivity of C-H functionalisation reactions because of their influence on the electron density of different C-H positions.²⁶⁻²⁷ However, in C-H functionalisation of arenes or aliphatic compounds, the differences in intrinsic reactivity are less noticeable and selective cleavage of a specific C-H bond is more difficult.²⁸⁻²⁹ To overcome this problem, directing groups, consisting of a coordinating moiety, are employed to direct a metal catalyst into the proximity of a certain C-H bond in the molecule, contributing to its selective cleavage and following functionalisation.³⁰ After a few decades research, a variety of C-H functionalization reactions assisted by different directing groups, including

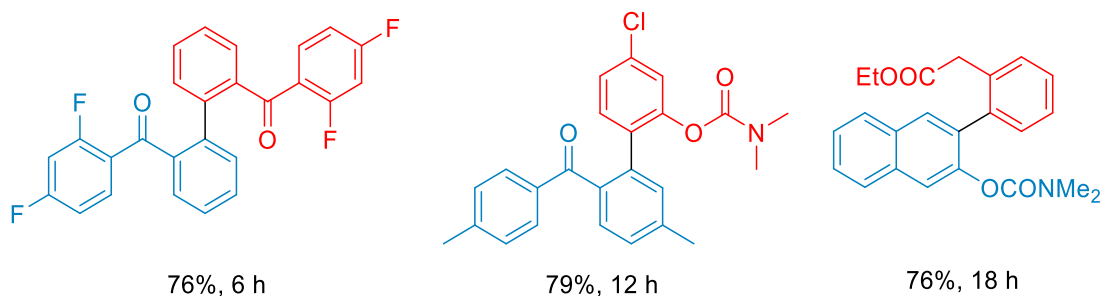
ketones, aldehydes, carboxylic acids, esters, monodentate amides, et al., have been reported.²⁴

Generally, Pd, Ru, Rh, Ir and Co complexes have been utilized as catalysts.

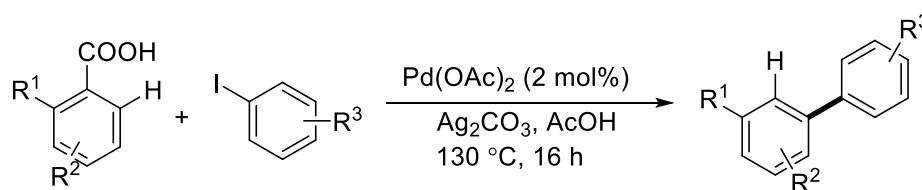
For example, Rao and Zhang have reported the Pd-catalysed arylation (Scheme 1.11).³¹ This work is a dimerization of aromatic ketones, affording 2,2'-dicarbonylated biaryls. Ketones, esters and carbamates have been utilized as directing groups in this work. Substituted benzophenone derivatives and alkyl-aryl ketones proceeded well, affording the homodimers in good yields. More importantly, hetero-coupling products (61-82%) can be produced by two different ketone substrates.



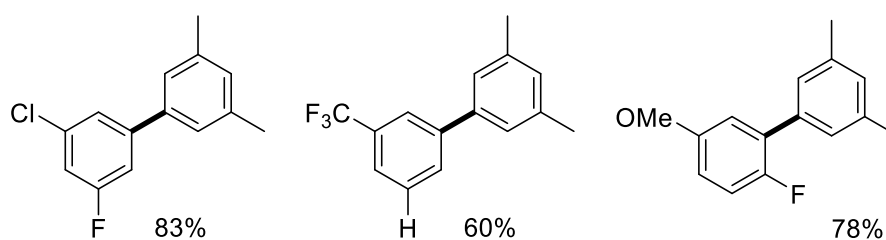
Selected examples



Scheme 1.11 Pd-catalysed dimerization of aromatic ketones.



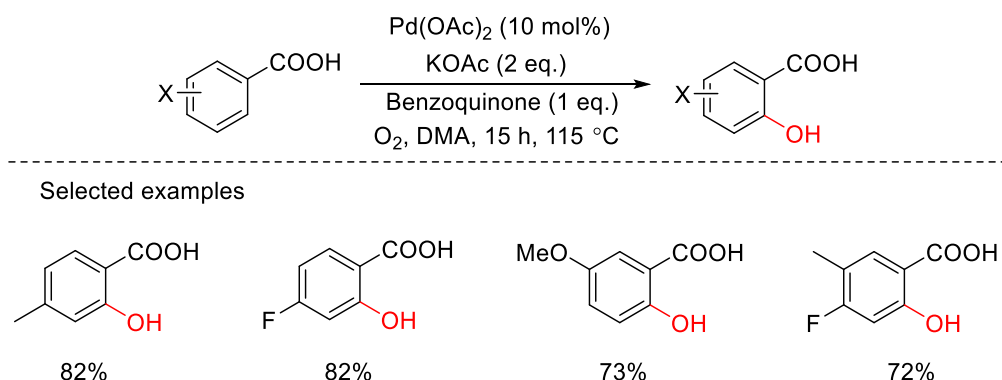
Selected examples



Scheme 1.12 Pd-catalysed *meta*-arylation of 2-substituted benzoic acids.

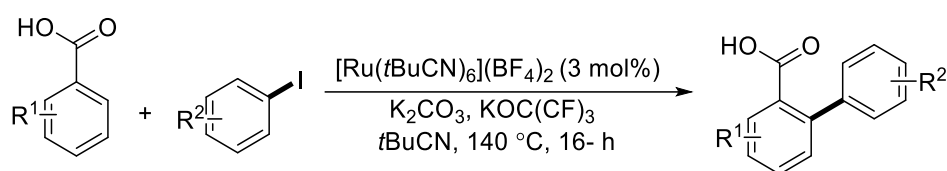
A Pd-catalysed *meta*-C-H functionalisation using carboxylic acids as directing groups was reported by Larrosa and co-workers (Scheme 1.12).³² Their strategy employed *ortho*-substituted benzoic acids and substituted iodoarenes as coupling partners. A wide range of *meta*-substituents on iodoarenes were tolerated in this process, affording various *meta*-substituted biaryl compounds in one step. Protodecarboxylation of benzoic acids and the direct decarboxylative *ipso*-arylation before the desired arylation were successfully prevented.

Yu and Co-workers have developed a Pd(II)-catalysed protocol for *ortho*-C-H hydroxylation of aromatic carboxylic acids with 1 atm of O₂ or air under nonacidic conditions (Scheme 1.13).³³ Arenes bearing electron-donating and electron-withdrawing groups all were tolerated. It is worth noticing that the well-known directing group acetamide did not scramble the regioselectivity. It has been proved that this reaction goes through a direct oxygenation of the aryl-palladium intermediates.

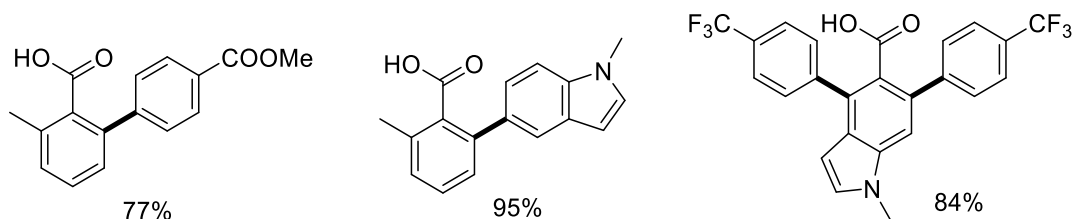


Scheme 1.13 Pd-catalysed *ortho*-hydroxylation of aromatic carboxylic acids.

On the other hand, Ru-catalysed approaches have also been explored. Larrosa and co-workers have reported a Ru-catalysed arylation using carboxylic acid as a directing group (Scheme 1.14).³⁴ A variety of aryl iodides and different substituted acids were tolerated in the reaction, affording the di-arylated products in good yields. As well, this protocol is applicable to indole carboxylic acids in various positions and even in certain cases without any protection of the indole nitrogen.

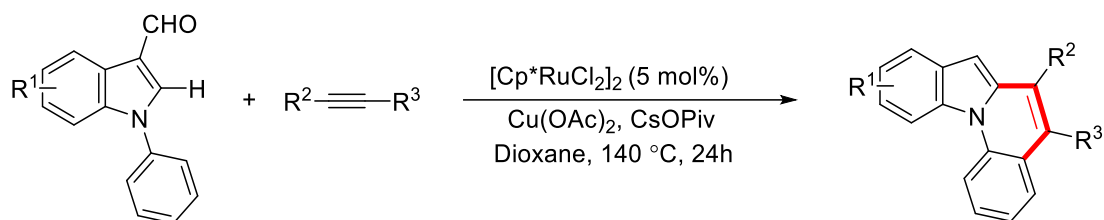


Selected examples

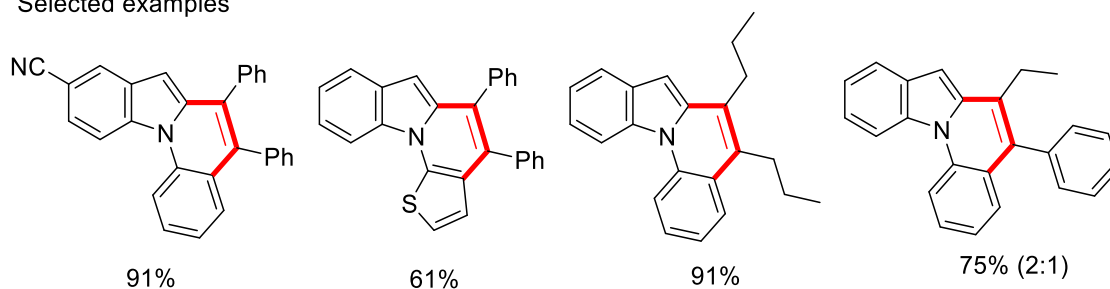


Scheme 1.14 Ru-catalysed arylation of carboxylic acids.

You and co-workers have employed Rh-catalyst for C-H activation/cyclization via aldehyde as a traceless directing group (Scheme 1.15).³⁵ In their work, 2-aryl-3-formylindoles were used as starting materials. Aldehydes may direct an alkenylation at C2-position of the indole core. A Rh-catalysed decarbonylation process and further activation of a C-H bond of the N-aryl group afforded a variety of appealing indolo[1,2-*a*]quinolones in high yields.



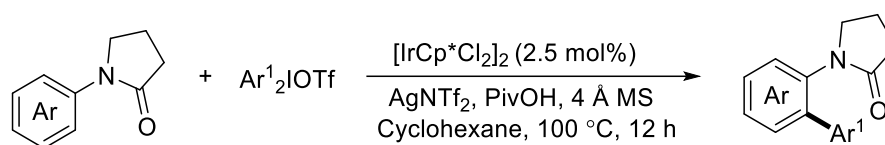
Selected examples



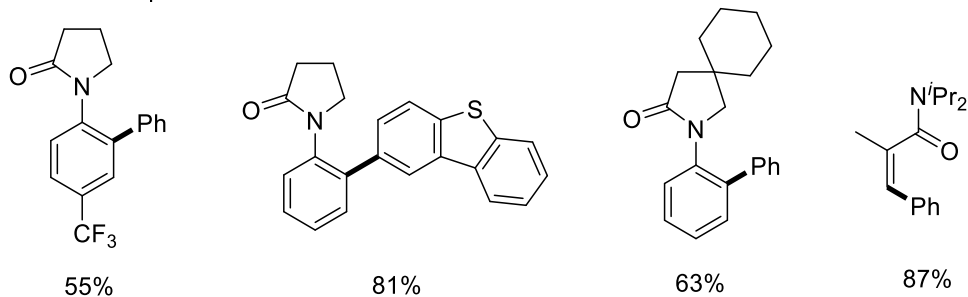
Scheme 1.15 Ru-catalysed selective (hetero)aromatic C-H activation/cyclization.

As well, the investigation of Ir and Co catalysts in C-H functionalization has been reported. Shi and Yuan have reported the Ir-catalysed arylation with diaryliodonium salts (Scheme 1.16).³⁶ A previously reported protocol for *o*-arylation of *O*-methyl ketoximes³⁷ was applied to *N*-aryl-2-pyrrolidinone. This protocol shows good functional group tolerance, though the

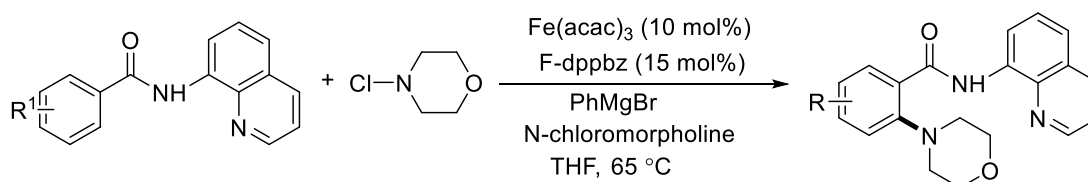
yields of products may be affected by electronic effects. Those products with electron-donating groups were afforded in higher yields than those with electron-withdrawing groups.



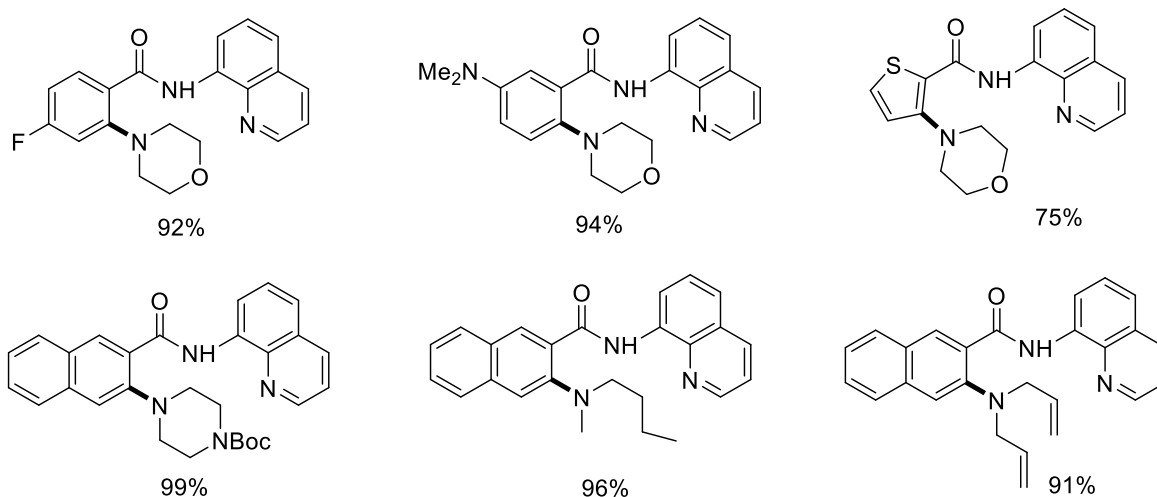
Selected examples



Scheme 1.16 Ir-catalysed arylation with diaryliodonium salts.



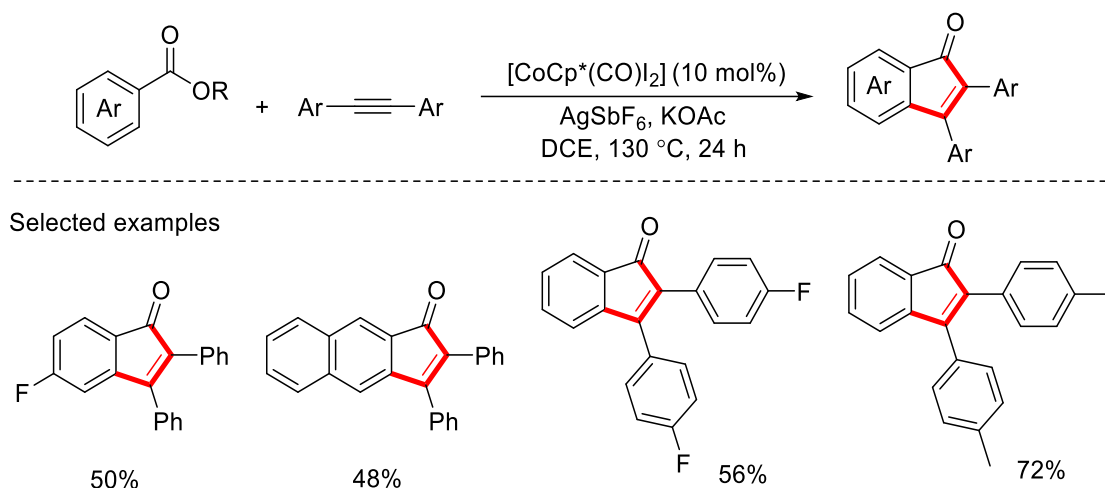
Selected examples



Scheme 1.17 Iron-catalysed *ortho*-amination of aromatic carboxamides with *N*-chloroamines.

Meanwhile, Nakamura and co-workers have reported an Fe-catalysed *ortho*-amination of aromatic carboxamides with *N*-chloroamines (Scheme 1.17).³⁸ Their work employed arenes possessing an 8-quinolinylamide group as a directing group, which are *ortho*-aminated with *N*-chloroamines and *N*-benzoyloxyamines in the presence of an Fe/diphosphine catalyst and an

organometallic base. The target anthranilic acid derivatives can be afforded in high yields. The whole reaction includes a Fe-catalysed C-H activation step and following reaction of the resulting Fe intermediate with *N*-chloroamine. The structure of the directing group and the control of the electronic properties of the diphosphine ligand allowed selective formation of the aminated product.



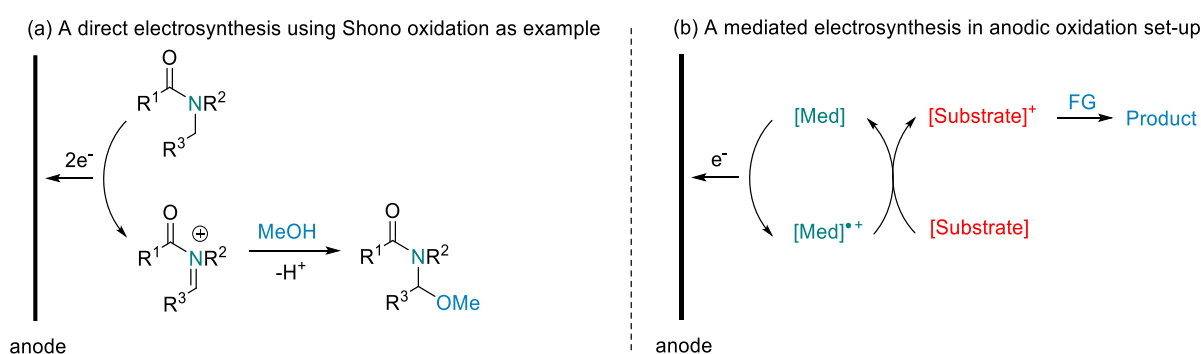
Scheme 1.18 Co-catalysed annulation of esters and alkynes.

Zhang and co-workers have reported the Co-catalysed alkenylation reactions with consecutive annulation to access indenones (Scheme 1.18).³⁹ A variety of esters with different functional groups and symmetrical aryl alkynes were tolerated in their protocol, affording corresponding indenones in moderate to good yields, though their strategy is slightly sensitive to electronic effects. In comparison with substrates with electron-donating groups, those substrates with electron-withdrawing groups showed slightly lower yields.

1.1.3 Electrocatalytic C-H bonds functionalization

Organic electrochemistry is recognized as an environmentally-friendly strategy, employing ‘electrons’ as the traceless redox reagent in synthetic organic transformations, which can replace toxic and dangerous redox reagents.⁴⁰⁻⁴¹ Generally, electrosynthesis for desirable compounds involves the electron transfer between an electrode and a molecule (substrate or mediator) and the following chemical reaction.⁴² The reaction can be realized by direct or mediated electrolysis. For direct electrolysis, a heterogeneous electron-transfer

between an electrode and a substrate leads to the generation of a reactive intermediate. Then, the following chemical reaction of the reactive intermediate and another molecule or functional group affords desired products.⁴³ As shown in Scheme 1.19(a), a Shono oxidation of amines via direct electrolysis is presented as an example.⁴⁴⁻⁴⁵ The iminium intermediate formed by the oxidation of an amine (or amide) substrate can undergo nucleophilic addition with nucleophiles to afford the functionalized product.

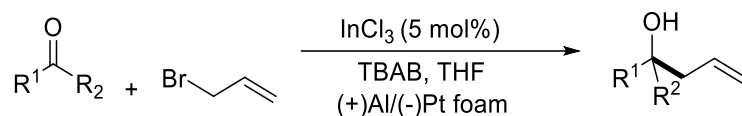


Scheme 1.19 Direct (a) and indirect (b) electrosynthesis in the context of anodic oxidation reactions.

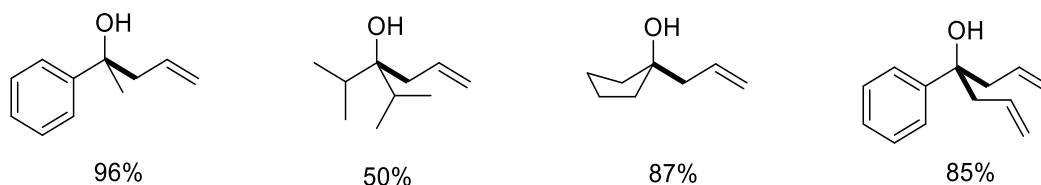
On the other hand, in mediated electrosynthesis, a redox mediator which has a lower redox potential than the substrates undergoes electron-transfer at the electrode, affording an electrochemically generated reagent for the following reaction (Scheme 1.19(b)).⁴⁶ During the last two decades, the use of different molecular metal electrocatalysts, such as In, Co, Ni, Pd, and other transition metals, as the mediator have been developed.⁴⁷⁻⁴⁸ Molecular electrocatalysis involves a metal-mediated electron transfer to a substrate. In most cases, the molecular metal catalyst plays an important role in the bond-breaking and bond-forming steps for the desired product.

The addition of organohalides to carbonyls is considered a powerful reaction to construct new carbon-carbon bonds with the concomitant formation of alcohols. Hilt and Smolko have developed an In-electrocatalysed allylation of aldehydes and ketones with allyl bromides to obtain alcohols (Scheme 1.20).⁴⁹ It was proposed that electrochemical reduction of In(III) to In(I) may happen in the reaction, which was followed by activation of allyl bromide. The catalytic allylations was facilitated by In(I) species on a preparative scale with aldehydes,

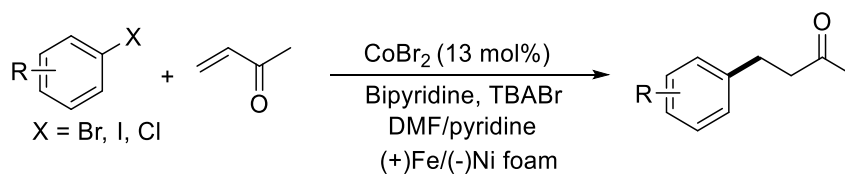
ketones, and even carboxylic esters as carbonyl components. A sacrificial anode such as aluminum was found to be critical for the reaction.



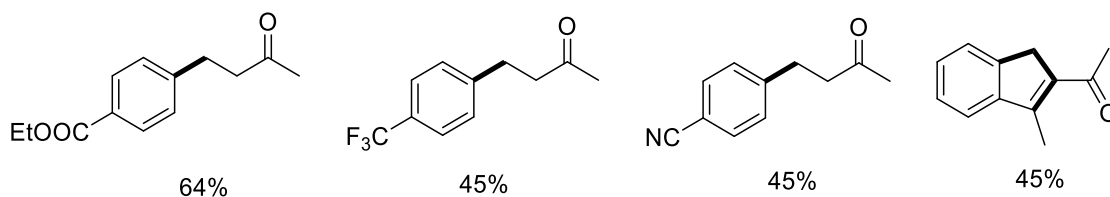
Selected examples



Scheme 1.20 In-electrocatalysed allylation of aldehydes and ketones with allyl bromides.



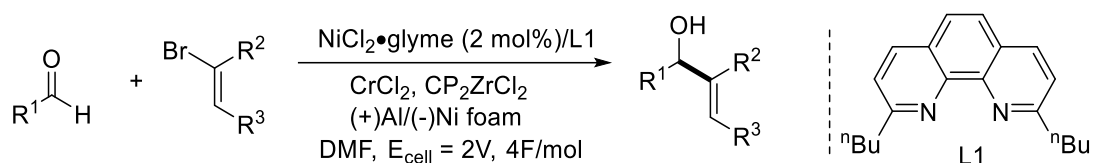
Selected examples



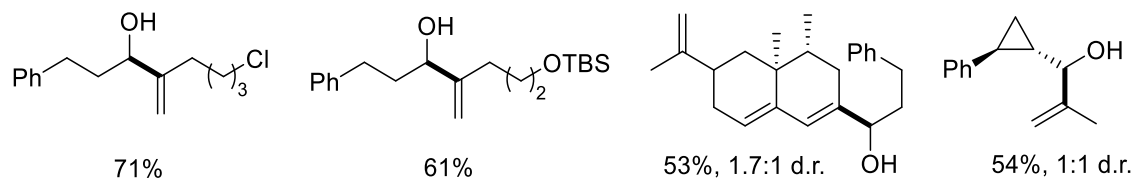
Scheme 1.21 Co-mediated electrocatalytic addition of aryl halides to activated olefins.

Gosmini and co-workers have reported the electrochemical addition of aryl halides onto activated olefins via using iron as a sacrificial anode (Scheme 1.21).⁵⁰ In their work, CoBr₂ and bipyridine were used to realize this conjugate addition reaction. The reaction conditions were compatible with a variety of substitutes in aryl group, though the yields of addition products were moderate (22-70%).

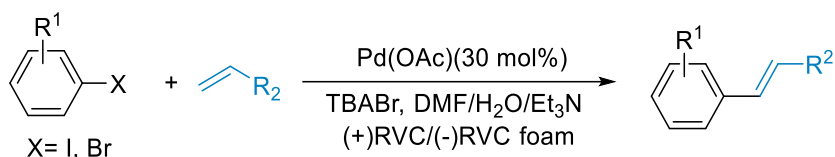
The Baran, Blackmond, and Reisman groups have reported a highly general and practical electrocatalytic Nozaki-Hiyama-Kishi coupling using a Ni catalyst (Scheme 1.22).⁵¹ Their strategy successfully avoids the use of superstoichiometric metallic reducing agents, and it showed wide substrate scope. Kishi's asymmetric variant, multiple realistic substrate classes and noncanonical substrate classes all were tolerated in their strategy.



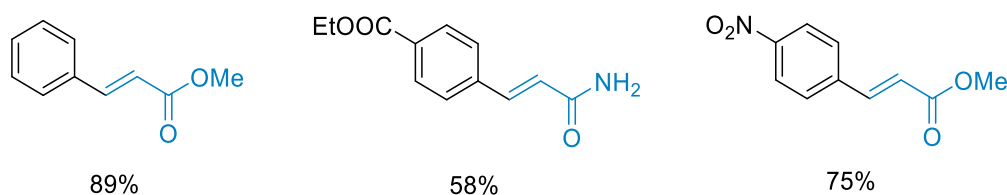
Selected examples



Scheme 1.22 Electrocatalytic Nozaki-Hiyama-Kishi coupling.



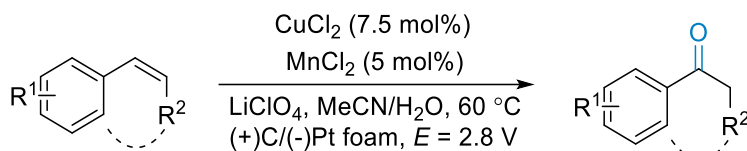
Selected examples



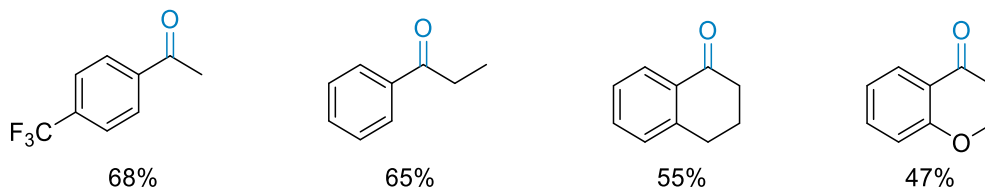
Scheme 1.23 Pd-catalysed electrochemical Heck coupling reaction.

Moeller and co-workers have developed the Pd-catalysed electrochemical Heck coupling reactions (Scheme 1.23).⁵² Impressively, their developed methodology allows the occurrence of Heck reactions at room temperatures and without the use of ligands. A variety of aryl iodides were coupled with a range of activated terminal olefins to afford substituted styrenes in good yields. Their work also inspires the following work about selective Pd-catalysed reactions, such as Suzuki and allylation reactions.⁵³⁻⁵⁴

On the other hand, transition metals, including Fe, Cu and Mn, also have been utilized in the electrocatalytic C-H bonds functionalization. A good example can be found in a Cu/Mn-catalyzed Wacker oxidation of alkenes by Pericàs and co-workers (Scheme 1.24).⁵⁵ In their protocol, a wide range of styrene derivatives undergo Wacker-Tsuji type oxidation to afford acetophenone derivatives in good yields. Both endocyclic and acyclic alkenes performed well in the reactions.



Selected examples



Scheme 1.24 Cu/Mn-Wacker-Tsuji type oxidation of styrene derivatives.

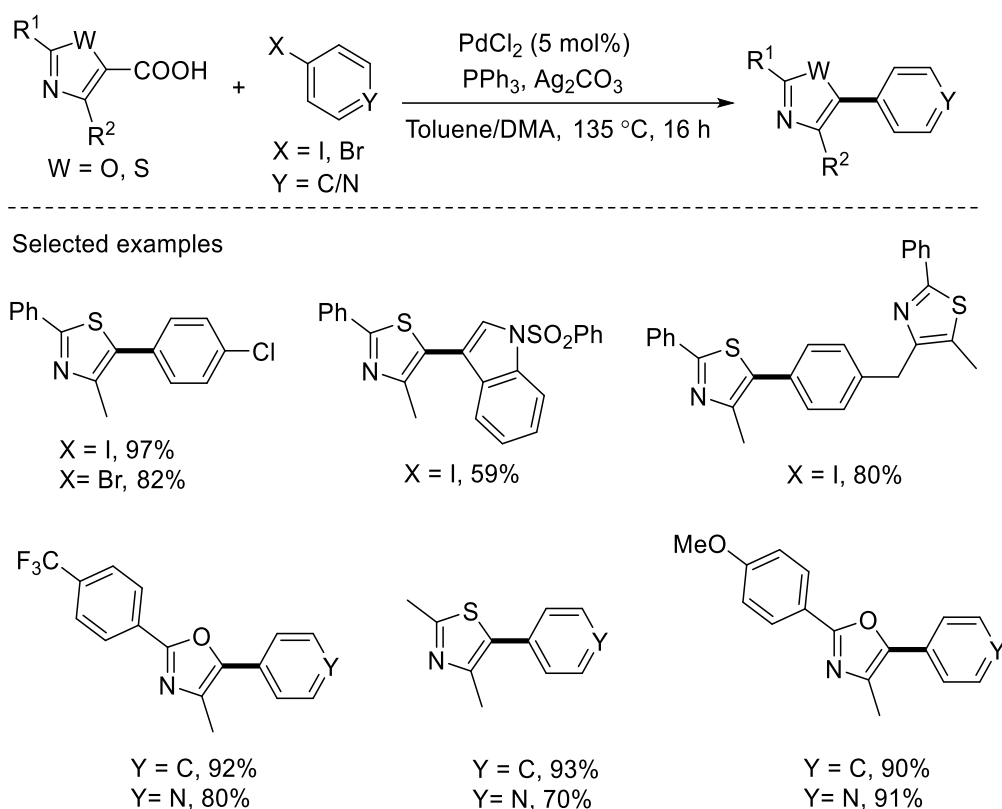
1.2 Functionalization of carboxylic acids

C-H functionalization concerns the transformation of a C-H bond to a C-C or C-heteroatom (C-X) bond.⁵⁶⁻⁵⁷ By employing various efficient directing groups, replacing specific C-H bonds with C-C, C-O, C-N, or other C-heteroatom bonds can create a wide variety of organic scaffolds. Highly effective catalytic systems enable the selective introduction of new functional groups at the ortho, meta, or para positions of aromatic compounds.⁵⁸⁻⁵⁹ One of the drawbacks of this directing group-based C-H functionalization is the requirement of two additional steps, including introducing and later removing complex moieties. Therefore, the ideal directing groups for C-H functionalization are those that are small, ubiquitously available, and can be easily removed or transformed.⁶⁰

It is interesting to find that the carboxylate group is qualified for those prerequisites. Carboxylate groups are abundant in organic molecules. It is possible to remove the carboxylate without leaving any trace by catalytic extrusion of volatile CO₂ for further conversion to a wealth of other moieties in interest. The use of carboxylates as tracelessly cleavable directing group has been studied since 19th century.^{59, 61-63}

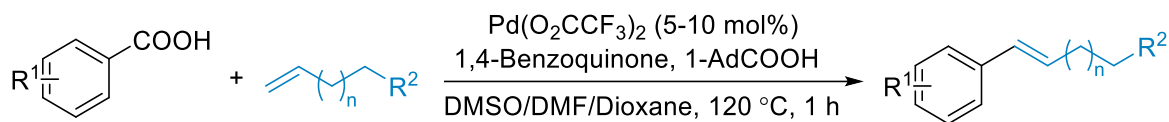
Carboxylate groups can also serve as leaving groups in a wealth of decarboxylative couplings with formation of C-C or C-X bonds.⁶⁴ After the continuous study in the last few decades, the decarboxylative cross-coupling reaction using carboxylates as leaving groups

have been well established.⁶⁴ A series of metal catalysts, such as chosen based on Pd, Ru, Rh, Cu, Ag et al., have been employed in the decarboxylative cross-coupling reactions. The decarboxylative metallation of a carboxylic acid substrate affords an intermediate containing a C-metal bond. In the next step, the organometallic intermediate participates in the cross-coupling reaction with specific partners, leading to the formation of a new C-C bond or C-X bonds.⁶⁵



Scheme 1.25 Decarboxylative cross-coupling of azoyl carboxylic acids with aryl halides.

The decarboxylative cross-coupling of carboxylic acids with aryl halides can forge the formation of C-C bonds. Greaney and Zhang have reported the decarboxylative cross-coupling of azoyl carboxylic acids with aryl halides (Scheme 1.25).⁶⁶ In their strategy, a bimetallic system of Pd and Ag was employed, where a variety of bromide and iodide coupling partners were tolerated. A variety of 5-arylated oxazoles and thiazoles were afforded in good yields. Meanwhile, a double coupling reaction using *o*-bromomethyl iodobenzene was proceeded successfully, affording the novel sp² and sp³ coupled product in 80% yield.



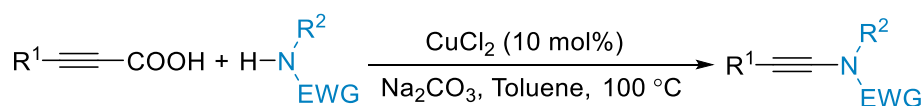
$n = 1$, $R^2 = \text{CO}_2\text{Et}$, regioselectivity = 13:1-63:1, E:Z > 16:1;

$n = 0$, $R^2 = \text{Ph}$ or CO_2^iBu , 48-99%;

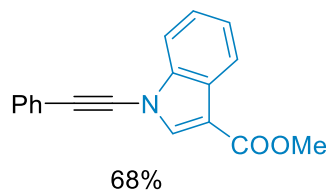
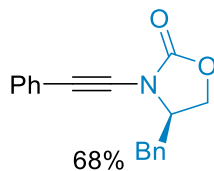
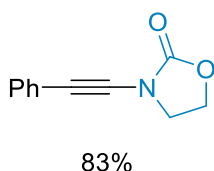
$n = 0$, $R^2 = \text{OAc}$, regioselectivity = 8:1-29:1, E:Z > 16:1.

Scheme 1.26 Decarboxylative cross-coupling of aryl carboxylic acids with aryl halides.

Another good example for the formation C-C bonds is the decarboxylative Heck reaction. As reported by Su and co-workers (Scheme 1.26),⁶⁷ a $\text{Pd}(\text{O}_2\text{CCF}_3)_2$ /benzoquinone catalytic system was designed for decarboxylative olefination of arenecarboxylic acids. The key to this efficient catalyst system is the use of 1-adamantanecarboxylic acid as additive. The decarboxylative Heck reaction of arenecarboxylic acids tolerated a series of olefins, including unactivated alkyl-substituted olefins, electron-deficient olefin, and styrene.

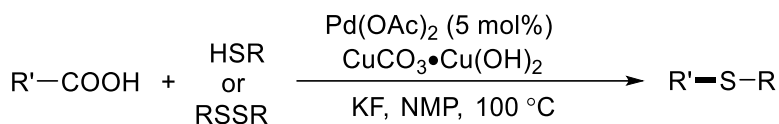


Selected examples

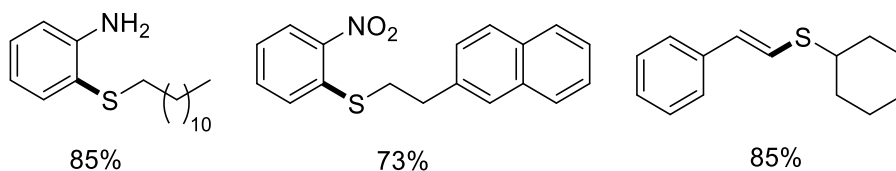


Scheme 1.27 Cu-catalysed aerobic oxidative amidation of propiolic acids via decarboxylative coupling.

On the other hand, decarboxylative C-heteroatom cross-coupling also has been studied. The Cu-catalysed decarboxylative C-N cross-coupling of alkynyl carboxylic acids with amides and N-heterocycles has been reported by Jiao and Jia (Scheme 1.27).⁶⁸ It is worth noting that air was compatible in their strategy, and it was employed as the oxidant in their work. Their strategy realized the first sp-carbon-heteroatom bond formation via decarboxylation.

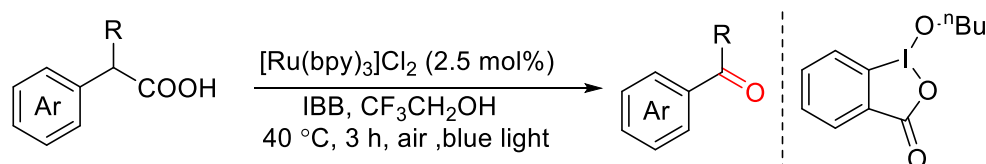


Selected examples

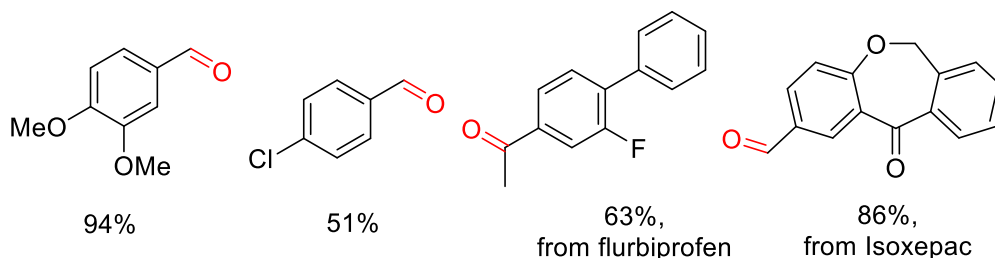


Scheme 1.28 Synthesis of aryl sulfides by decarboxylative C-S cross-couplings.

Liu and Co-workers have reported the decarboxylative C-S cross-coupling reaction (Scheme 1.28).⁶⁹ A Pd/Cu bimetallic catalyst system was employed in this work. Electron-deficient aromatic acids and heteroaromatic acids underwent the decarboxylative C-S cross-coupling to afford alkyl aryl thioethers or diaryl thioethers as final products in good yields.



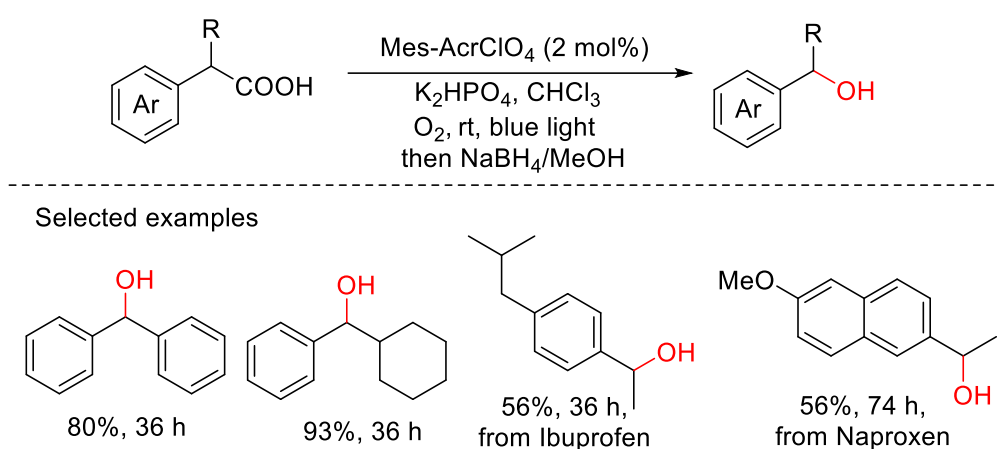
Selected examples



Scheme 1.29 Ru-catalyzed decarboxylative oxidation of arylacetic acids.

Apart from the use of carboxylic acids as direct groups in decarboxylative cross-coupling reactions, functionalization of carboxylic acids via oxidative decarboxylative reactions has also attracted wide attention in recent years.⁷⁰⁻⁷¹ Decarboxylative oxidation of carboxylic acids is a direct and promising method for the construction of C-O bond. It involves decarboxylation and the following oxidation steps, affording valuable carbonyls or alcohols as the final products. In the last few decades, decarboxylative oxidation of benzylic carboxylic acids has been well studied, affording corresponding aldehydes and ketones in good yields and high selectivity.

A good example found in the literature was reported by Itami and co-workers.⁷² They employed Ru as catalyst and hypervalent iodine 1-butoxy 1- λ^3 -benzo[*d*][1,2]iodaoxol-3(1*H*)-one (IBB) as additive (Schem 1.29). It is worth noting that air was used as the oxidant in this decarboxylative oxidation. A variety of arylacetic acids as well as drug molecules can be converted to corresponding aldehydes and ketones in good to excellent yields. Strategies about the transformation of carboxylic acids to other oxidation products, such as alcohols and peroxides, have been rarely reported however.

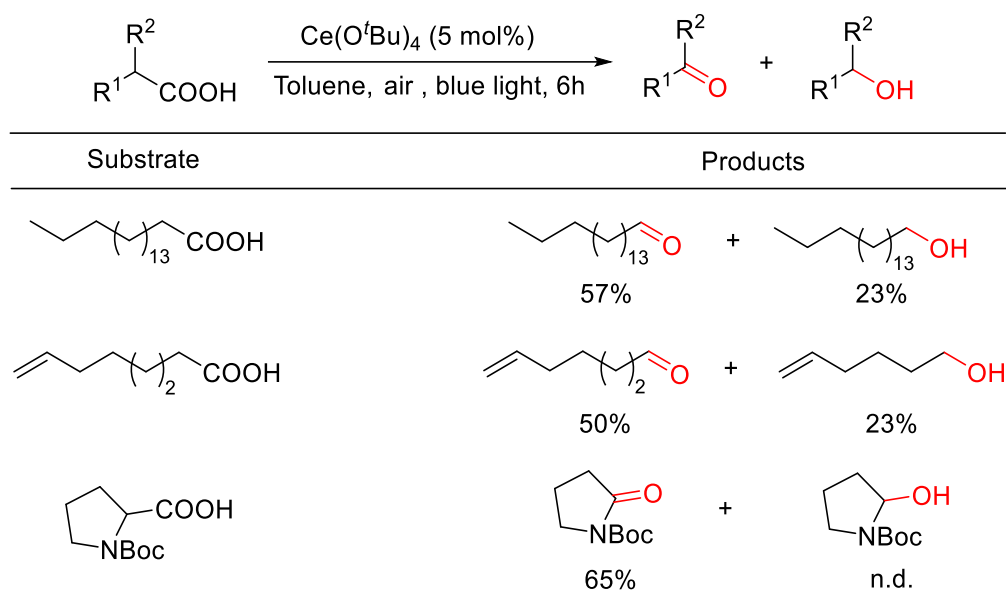


Scheme 1.30 Photocatalytic decarboxylative hydroxylation of arylacetic acids.

Decarboxylative hydroxylation can realize the transformation of carboxylic acids to alcohols via decarboxylative oxidation and the following reduction. Lu and co-workers have reported a photocatalytic decarboxylative hydroxylation of arylacetic acids using an organic catalyst Mes-AcrClO₄ (Scheme 1.30).⁷³ Their strategy includes the decarboxylative oxidation of carboxylic acids to corresponding aldehydes and ketones, which were then reduced by NaBH₄ to target alcohols. It is worth noticing that aliphatic acids, including cyclohexanecarboxylic acid and adamantane-1-carboxylic acid, proceeded successfully, though the yields of corresponding alcohols are moderate.

Decarboxylative oxidation or hydroxylation of aliphatic acids is still a challenging issue. A good forward step has been achieved by Mashima and co-workers (Scheme 1.31).⁷⁰ A direct decarboxylative oxygenation of aliphatic acids has been realized with Ce(O^{*t*}Bu)₄ as catalyst and air as oxidant. Long-chain fatty acids and amino acids all can be converted to

corresponding aldehydes or ketones and alcohols. Although impressive results have been achieved in their work, the drawbacks in their strategy include the low selectivity of products and low yields of target alcohol products. Therefore, the decarboxylative C-H functionalization of carboxylic acids still requires further investigation.

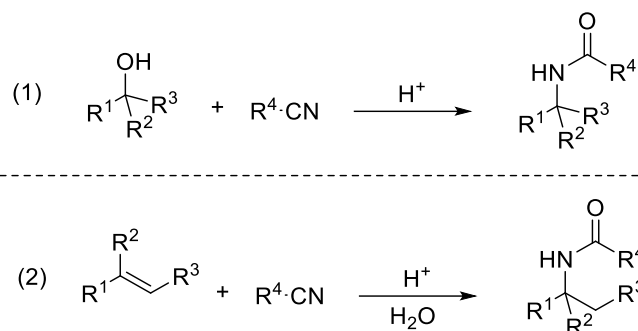


Scheme 1.31 Photocatalytic decarboxylative hydroxylation of arylacetic acids.

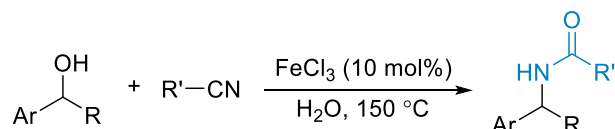
1.3 Ritter and Ritter-type reaction

1.3.1 Ritter reaction

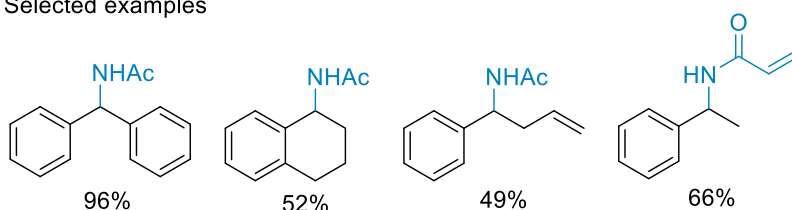
The Ritter reaction has attracted wide attention since it was reported by Ritter in 1948.⁷⁴⁻⁷⁵ It allows the formation of amides, which are ubiquitous motifs in both natural products and various synthetic materials.⁷⁶ It provides a rapid approach for the preparation of biologically active molecules, such as antibiotic,⁷⁷ anti-influenza⁷⁸ and antimicrobial drugs.⁷⁹ Generally, alcohols and olefins are applied as the precursors of carbocations in traditional Ritter reaction (Scheme 1.32). A carbocation generated in-situ from an alcohol, an alcohol derivative or an olefin, is trapped by a nitrile to generate a nitrilium species, which is transformed to an amide after hydrolysis. The addition of water is required when olefins are employed as substrates. In the case of alcohols, the alcohol itself can generate a hydroxide ion and the process becomes atom-economical.



Scheme 1.32 Classic examples of Ritter reaction.

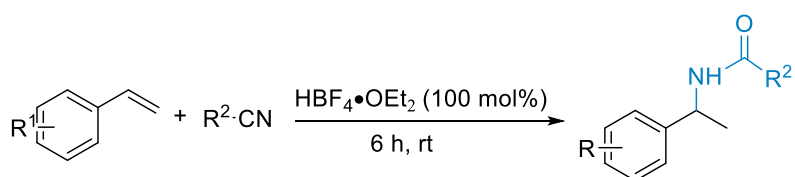


Selected examples

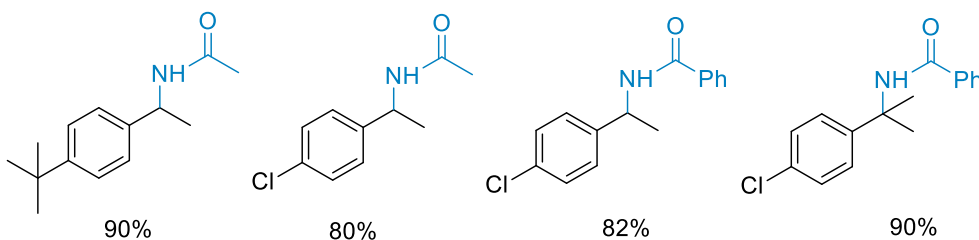


Scheme 1.33 FeCl₃-catalyzed Ritter reactions between benzylic alcohols and nitriles.

In the following investigation, many efforts have been made in catalytic Ritter reactions, where good results have been achieved via different catalysts. For example, Cossy and co-workers reported a FeCl₃-catalyzed Ritter reaction between benzylic alcohols and nitriles (Scheme 1.33).⁸⁰ Various benzylic amides can be obtained from the reaction of the different benzylic alcohols or benzhydrol derivatives with a variety of different nitriles in moderate to good yields. Water was added for fast conversions of the alcohols.



Selected examples



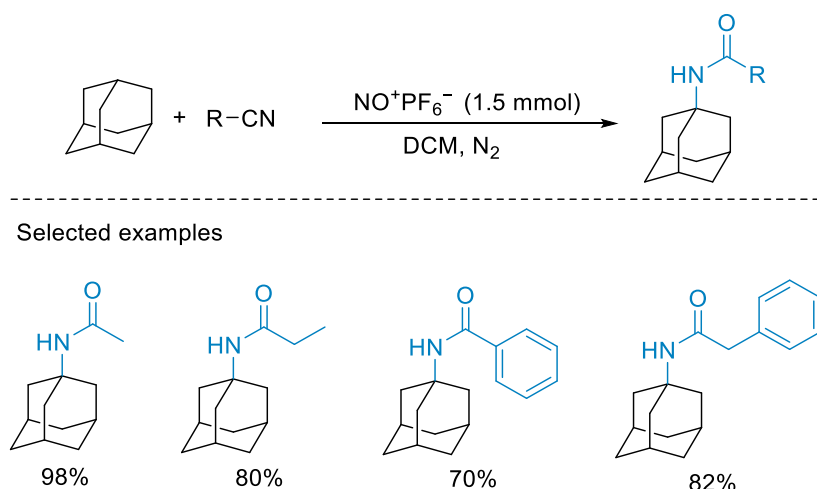
Scheme 1.34 Ritter reactions between olefins and nitriles using HBF₄•OEt₂.

Reddy and co-workers explored the Ritter reaction of alkenes with nitriles for the synthesis of secondary amides, in which tetrafluoroboric acid etherate ($\text{HBF}_4 \cdot \text{OEt}_2$) was employed as the catalyst (Scheme 1.34).⁸¹ A variety of vinyl arenes reacted with nitriles successfully, affording corresponding secondary amides in good yields. As well, sterically hindered 2-vinyl dihydronaphthalene, indene, naphthalene, and cycloalkanes were tolerated.

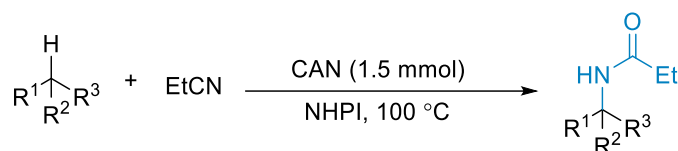
1.3.2 Ritter-type reaction

In addition to the use of alcohols and alkenes as reaction partners, other substrates such as alkanes, alkylarenes, carboxylic acids and aldehydes, have been employed as alternatives to form carbonium intermediates.⁸² Olah and co-workers reported a Ritter-type reaction of adamantane using NO^+PF_6^- as the oxidant (Scheme 1.35).⁸³ A variety of *N*-(1-adamantyl)amides were produced in good yields by the reactions between adamantane and different nitriles.

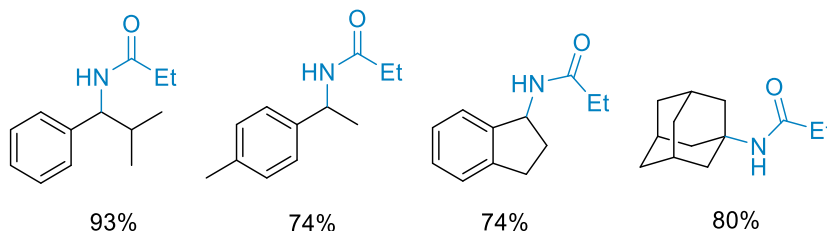
In the following investigation, Ishii and co-workers investigated the Ritter-type amidation of alkylbenzenes by using *N*-hydroxyphthalimide (NHPI) and ammonium hexanitratocerate(IV) (CAN) as catalysts (Scheme 1.36).⁸⁴ Different alkylbenzene or adamantane derivatives can be transformed to corresponding amides with good selectivity in this NHPI-CAN catalytic system using EtCN as the nitrile source.



Scheme 1.35 Ritter-type reaction of adamantane with nitriles.

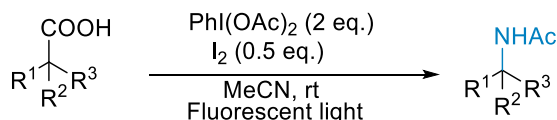


Selected examples

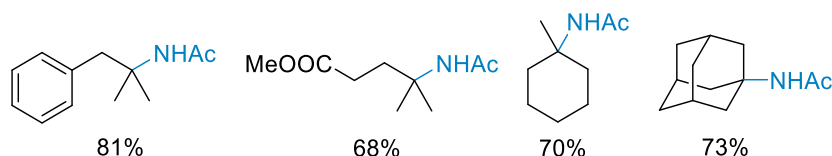


Scheme 1.36 Ritter-type reaction of alkanes and aryl alkanes.

Kiyokawa and Minakata explored the decarboxylative Ritter-type reaction of carboxylic acids with acetonitrile for the synthesis of α -tertiary amine derivatives (Scheme 1.37).⁸⁵ In their strategy, a combination of I_2 and $\text{PhI}(\text{OAc})_2$ was employed. A wide range of carboxylic acids bearing an α -quaternary carbon center proceeded successfully, affording corresponding amides in good yields. In addition, oxalic acid monoalkyl esters prepared from alcohols were also tolerated in this strategy.

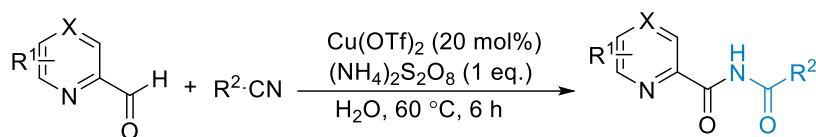


Selected examples

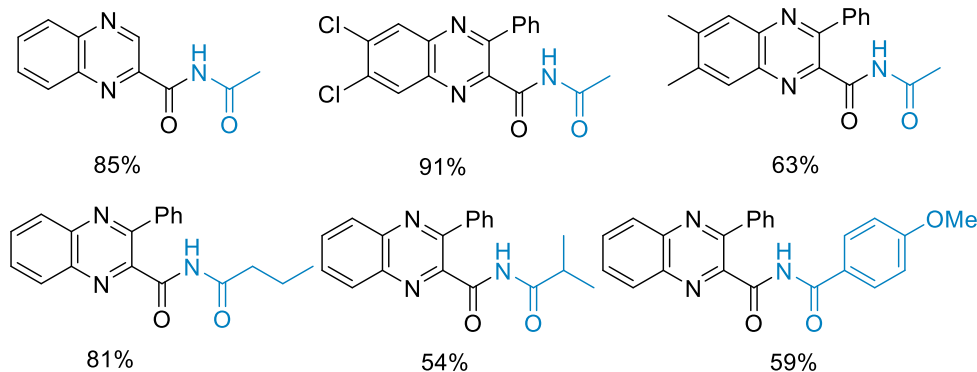


Scheme 1.37 Hypervalent iodine (III)-mediated Ritter-type reaction of carboxylic acids with acetonitrile.

On the other hand, Jin and Liu reported a Cu-catalysed Ritter-type reaction of *N*-heteroaryl aldehydes with nitriles, in which $(\text{NH}_4)_2\text{S}_2\text{O}_8$ was used as the oxidant (Scheme 1.38).⁸⁶ This protocol featured wide substrate scope of *N*-heteroaryl aldehydes and atom economy. The mechanistic studies indicated that a radical triggered Ritter-type reaction may happen, and the C–O bond was formed by using water as the oxygen source.



Selected examples



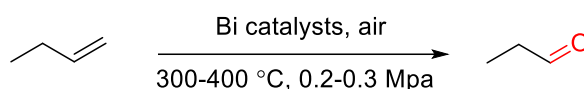
Scheme 1.38 Cu-catalyzed Ritter-type reaction of *N*-heteroaryl aldehydes with nitriles.

Although the Ritter-type C-H amidation is a promising issue, relevant reports are limited. One of the challenging issues of this reaction probably is the relatively low reactivity and poor selectivity of the C(sp³)–H bonds. Therefore, developing new catalytic systems to address this problem and obtain amides in good selectivity and yields still requires more efforts and attention.

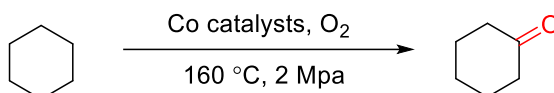
1.4 Molecular oxygen in oxidation reactions

Oxidation reaction plays an important role in chemical industry. Over 90% of the feedstocks in oxidation reaction are derived from hydrocarbons, which are the most reduced organic chemicals on our planet.⁸⁷ To date, oxidation is the second largest process after polymerization, and it contributes around 30% of total production in the chemical industry.⁸⁸ The oxidation of different hydrocarbon compounds affords a variety of valuable chemicals and intermediates, including aldehydes, ketones, epoxides, alcohols, and organic acids.⁸⁹ Among current oxidation reactions in chemical industry, some reactions, such as oxidation of propene to acrolein, oxidation of cyclohexane to cyclohexanone and oxidation of ethylene to ethylene oxide, are well-known and have been well established (Scheme 1.39).⁹⁰

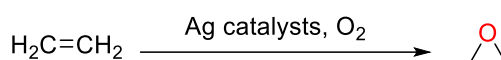
a) Oxidation of propene to acrolein



b) Oxidation of cyclohexane to cyclohexanone

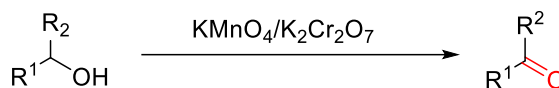


c) Oxidation of ethylene to ethylene oxide

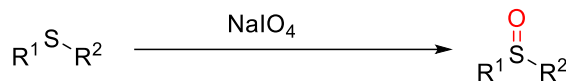


Scheme 1.39 Examples of oxidation reactions in chemical industries.

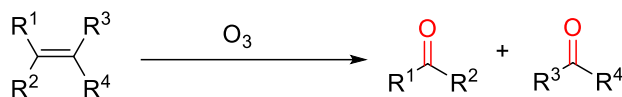
a) Oxidation of alcohols to aldehydes and ketones



b) Oxidation of sulfides to sulfoxides



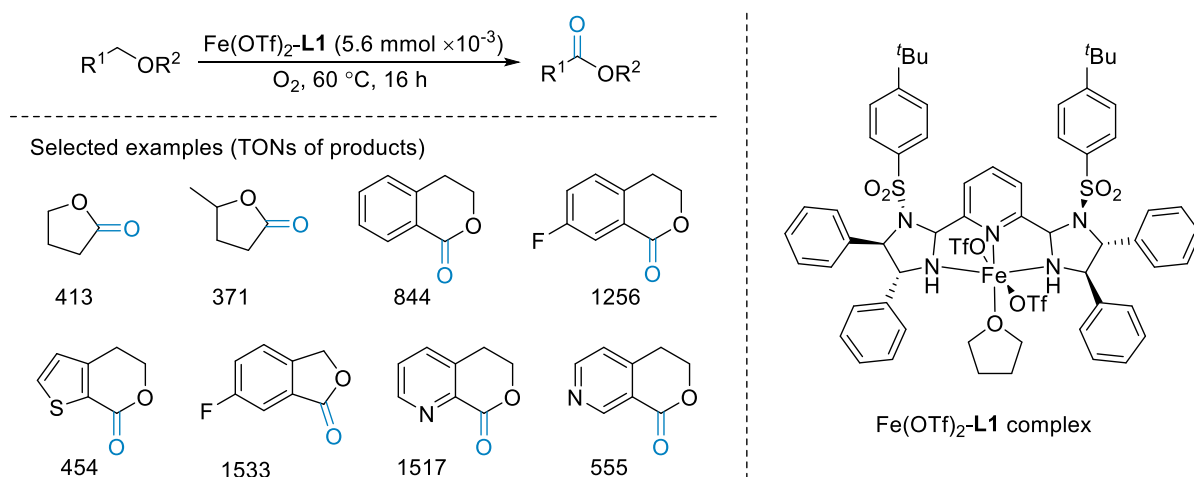
c) Oxidation of olefins to carbonyl compounds



Scheme 1.40 Examples of oxidation reactions employing toxic oxidants.

The wide use of oxidation reactions has prompted us to search more sustainable and green oxidation processes due to some notable drawbacks in common oxidation procedures, such as formation of non-selective byproducts, limited applicability, and use of toxic oxidants.⁹¹ Further optimization of the current oxidation strategies, including oxidants, catalysts, reaction temperature and pressure, etc remains necessary. Furthermore, there is a strong incentive to develop both new and green oxidation strategies according to the Principle of Green Chemistry.⁹²⁻⁹³ Particularly, it is highly desirable to replace the environmentally unfriendly or energetically inefficient reactions.

A representative example is the oxidation of alcohols to aldehydes or ketones, which has been widely recognised as one of the most fundamental reactions.⁸⁸ The usually employed oxidation reagents, such as stoichiometric amount of permanganate and dichromate, lead to the production of a large amount of heavy-metal wastes (Scheme 1.40a). Meanwhile, the permanganate and dichromate are toxic and expensive. In the other important reactions, such as oxidation of sulfides to sulfoxides and oxidative cleavage of alkenes, toxic periodates and hazardous O₃, are used (Scheme 1.40b, c). Therefore, the exploration of green and cheap oxidants, such as O₂ and H₂O₂, in both foundational and new chemical reactions is urgent. Among these oxidants, obviously, the employment of O₂ as oxidant is more attractive because O₂ is the cheapest, most abundant and easily-available oxidising agent in nature. As well, the employment of O₂ normally leads to the formation of H₂O as the by-product.

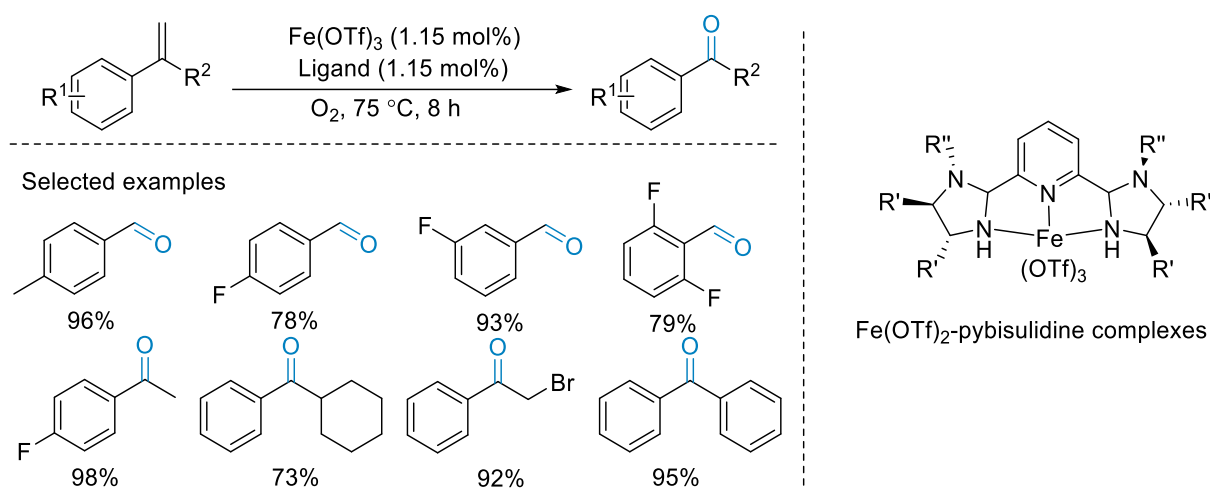


Scheme 1.41 Fe-catalysed aerobic oxidation of ethers.

Our group reported a series of strategies for the oxidation of ethers, olefins and diols using O₂ as oxidant. In 2014, our group reported a Fe-catalysed aerobic oxidation of ethers (Scheme 1.41).⁹⁴ A novel Fe(OTf)₂-pybisulidone complex was synthesized for selective oxidation of tetrahydrofuran substrates, isochromans and phthalans, affording corresponding products in high TONs. Mechanistic studies indicated that a two-step reaction pathway was involved. A peroxobisether intermediate may be formed by dehydrogenative incorporation of O₂ into the

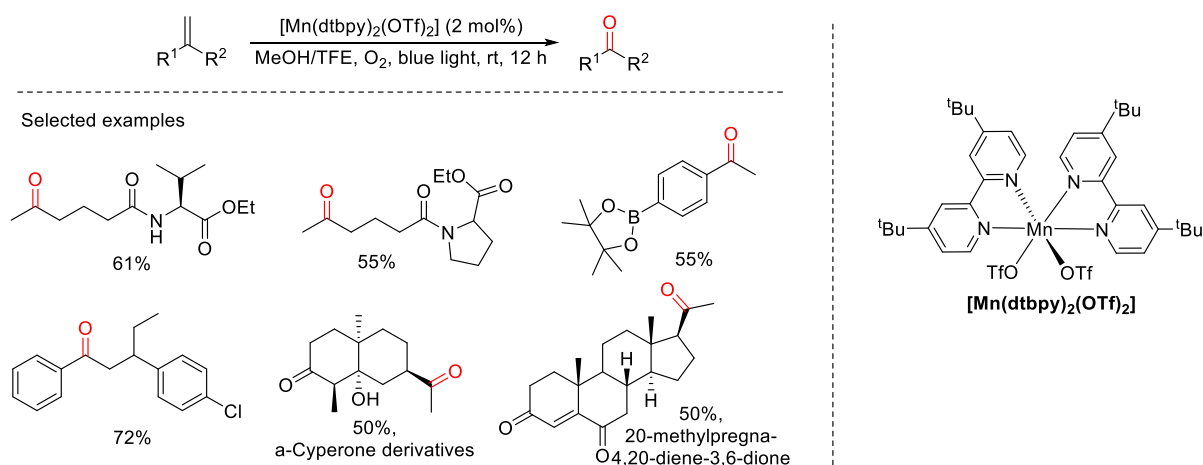
ether, which then underwent the cleavage of the peroxy bond to afford two ester molecules.

Stoichiometric H₂ was released in each step.



Scheme 1.42 Fe-catalysed oxidation of α - and β -substituted styrenes.

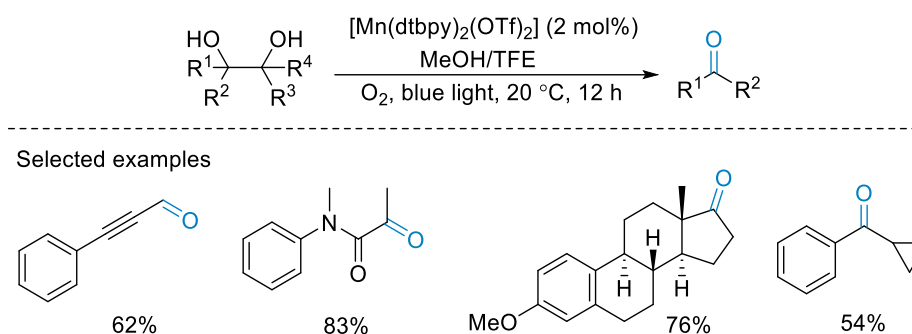
In the following investigation, our group employed a Fe(OTf)₃-pybisulidine complex in the oxidation of olefins (Scheme 1.42).⁹⁵ A wide range of α - and β -substituted styrenes with different functional groups were oxidized to corresponding aldehydes and ketones in good yields with high chemo-selectivity.



Scheme 1.43 Mn-catalysed oxidation of activated and non-activated alkenes.

In 2021, a new Mn-catalysis strategy for oxidative cleavage of alkenes was reported by our group (Scheme 1.43).⁹⁶ A non-heme Mn catalyst [Mn(dtbp)₂(OTf)₂] was synthesized to catalysed, under blue light irradiation, oxidative cleavage of both activated and non-activated alkenes under mild conditions, affording corresponding aldehydes and ketones in good yields. Mechanistic studies indicated that a Mn-oxo species was formed by reaction of the Mn

precatalyst, MeOH and O₂, which may generate active Mn(IV)=O species for the oxidation of alkenes.



Scheme 1.44 Mn-catalysed oxidation of diols.

In the following study of our group, the [Mn(dtbp)₂(OTf)₂] complex was employed in oxidative cleavage of 1,2-diols under blue light irradiation (Scheme 1.44).⁹⁷ A wide range of valuable carbonyl products and five-membered heterocycles with different functional groups were afforded in good yields.

1.5 Aims of this thesis

This introduction has highlighted by examples about C-X (X = C, N, O) bond forming reactions involving C-H functionalization. In particular, it focuses on the C-H functionalization of carboxylic acids and arenes. To date, the aerobic C-H functionalization of carboxylic acids and arenes is still a challenging issue. O₂ is a green, clean and abundant oxidant, and the use of O₂ fulfils the requirement of green chemistry. Therefore, developing new strategies for O₂ activation and subsequent oxidative C-H functionalization is important and meaningful.

We hope it can be seen that this thesis has gone some way to achieving this goal. Chapter 2 presents a cheap and novel Mn-catalyst for photocatalytic decarboxylative oxygenation of carboxylic acids. The construction of C-O bonds has been realized with this Mn-catalytic system, where a variety of carboxylic acids are transformed to aldehydes and ketones in good yields.

In Chapter 3, we have developed a new Ce catalytic system to realize the selective transformation of carboxylic acids. Transformation of C-H bonds to different C-O bonds has

been realized, in which carboxylic acids have been selectively transformed to peroxides, aldehydes, ketones and alcohols. Its selectivity can be simply changed by using different bases.

In Chapter 4, we focus on the Ritter-type C-H amidation of alkylarenes. We have developed a new Ce-catalytic system for the amidation of a wide range of alkyl arenes with nitriles. In particular, a variety of different nitriles are tolerated in our strategy, affording corresponding amides in good yields.

In Chapter 5, we have explored more challenging oxidation of aliphatic cyclic alkanes. Three different catalytic systems have been studied for selective oxidation of cyclic alkanes to the corresponding ketones, alcohols and peroxides using air or H₂O₂ as oxidant. The good selectivity and yield of these products obtained thus far indicate the high potential of our method in future work.

1.6 References

1. Davies, H. M.; Du Bois, J.; Yu, J. Q., C-H Functionalization in Organic Synthesis. *Chem. Soc. Rev.* **2011**, *40*, 1855-1856.
2. Bruckl, T.; Baxter, R. D.; Ishihara, Y.; Baran, P. S., Innate and Guided C-H Functionalization Logic. *Acc. Chem. Res.* **2012**, *45*, 826-839.
3. Murakami, K.; Yamada, S.; Kaneda, T.; Itami, K., C-H Functionalization of Azines. *Chem. Rev.* **2017**, *117*, 9302-9332.
4. Qin, Y.; Zhu, L.; Luo, S., Organocatalysis in Inert C–H Bond Functionalization. *Chem. Rev.* **2017**, *117*, 9433-9520.
5. Holmberg-Douglas, N.; Nicewicz, D. A., Photoredox-Catalyzed C-H Functionalization Reactions. *Chem. Rev.* **2022**, *122*, 1925-2016.
6. Arndtsen, B. A.; Bergman, R. G.; Mobley, T. A.; Peterson, T. H., Selective Intermolecular Carbon-Hydrogen Bond Activation by Synthetic Metal Complexes in Homogeneous Solution. *Acc. Chem. Res.* **2002**, *28*, 154-162.
7. Williamson, J. B.; Lewis, S. E.; Johnson, R. R., 3rd; Manning, I. M.; Leibfarth, F. A., C-H Functionalization of Commodity Polymers. *Angew. Chem. Int. Ed.* **2019**, *58*, 8654-8668.
8. Davies, H. M.; Manning, J. R., Catalytic C-H Functionalization by Metal Carbenoid and Nitrenoid Insertion. *Nature* **2008**, *451*, 417-424.

9. Gutekunst, W. R.; Baran, P. S., C-H Functionalization Logic in Total Synthesis. *Chem. Soc. Rev.* **2011**, *40*, 1976-1991.
10. Abrams, D. J.; Provencher, P. A.; Sorensen, E. J., Recent Applications of C-H Functionalization in Complex Natural Product Synthesis. *Chem. Soc. Rev.* **2018**, *47*, 8925-8967.
11. Cernak, T.; Dykstra, K. D.; Tyagarajan, S.; Vachal, P.; Krska, S. W., The Medicinal Chemist's Toolbox for Late Stage Functionalization of Drug-Like Molecules. *Chem. Soc. Rev.* **2016**, *45*, 546-576.
12. Yang, Y.; Nishiura, M.; Wang, H.; Hou, Z., Metal-Catalyzed C-H Activation for Polymer Synthesis and Functionalization. *Coord. Chem. Rev.* **2018**, *376*, 506-532.
13. Bellotti, P.; Huang, H. M.; Faber, T.; Glorius, F., Photocatalytic Late-Stage C-H Functionalization. *Chem. Rev.* **2023**, *123*, 4237-4352.
14. Prier, C. K.; Rankic, D. A.; MacMillan, D. W., Visible Light Photoredox Catalysis with Transition Metal Complexes: Applications in Organic Synthesis. *Chem. Rev.* **2013**, *113*, 5322-5363.
15. Arias-Rotondo, D. M.; McCusker, J. K., The Photophysics of Photoredox Catalysis: A Roadmap for Catalyst Design. *Chem. Soc. Rev.* **2016**, *45*, 5803-5820.
16. Narayanam, J. M.; Stephenson, C. R., Visible Light Photoredox Catalysis: Applications in Organic Synthesis. *Chem. Soc. Rev.* **2011**, *40*, 102-113.
17. Stephenson, C.; Swift, E.; Williams, T., Intermolecular Photocatalytic C-H Functionalization of Electron-Rich Heterocycles with Tertiary Alkyl Halides. *Synlett* **2016**, *27*, 754-758.
18. Zhang, Y.; Zhang, T.; Das, S., Selective Functionalization of Benzylic Csp³-H bonds to Synthesize Complex Molecules. *Chem* **2022**, DOI: 10.1016/j.chempr.2022.10.005
19. Xuan, J.; Cheng, Y.; An, J.; Lu, L. Q.; Zhang, X. X.; Xiao, W. J., Visible Light-Induced Intramolecular Cyclization Reactions of Diamines: A New Strategy to Construct Tetrahydroimidazoles. *Chem. Commun.* **2011**, *47*, 8337-8339.
20. Yilmaz, O.; Oderinde, M. S.; Emmert, M. H., Photoredox-Catalyzed C_α-H Cyanation of Unactivated Secondary and Tertiary Aliphatic Amines: Late-Stage Functionalization and Mechanistic Studies. *J. Org. Chem.* **2018**, *83*, 11089-11100.
21. Romero, N. A.; Nicewicz, D. A., Organic Photoredox Catalysis. *Chem. Rev.* **2016**, *116*, 10075-10166.

22. Hari, D. P.; Schroll, P.; Konig, B., Metal-Free, Visible-Light-Mediated Direct C-H Arylation of Heteroarenes with Aryl Diazonium Salts. *J. Am. Chem. Soc.* **2012**, *134*, 2958-2961.
23. Hou, J.; Ee, A.; Cao, H.; Ong, H. W.; Xu, J. H.; Wu, J., Visible-Light-Mediated Metal-Free Difunctionalization of Alkenes with CO₂ and Silanes or C(sp³)-H Alkanes. *Angew. Chem. Int. Ed.* **2018**, *57*, 17220-17224.
24. Sambigioglio, C.; Schonbauer, D.; Blicke, R.; Dao-Huy, T.; Pototschnig, G.; Schaaf, P.; Wiesinger, T.; Zia, M. F.; Wencel-Delord, J.; Besset, T.; Maes, B. U. W.; Schnurch, M., A Comprehensive Overview of Directing Groups Applied in Metal-Catalysed C-H Functionalisation Chemistry. *Chem. Soc. Rev.* **2018**, *47*, 6603-6743.
25. Wu, Y.; Pi, C.; Wu, Y.; Cui, X., Directing Group Migration Strategy in Transition-Metal-Catalysed Direct C-H Functionalization. *Chem. Soc. Rev.* **2021**, *50*, 3677-3689.
26. Lewis, J. C.; Bergman, R. G.; Ellman, J. A., Direct Functionalization of Nitrogen Heterocycles via Rh-Catalyzed C-H Bond Activation. *Acc. Chem. Res.* **2008**, *41*, 1013-1025.
27. Campos, K. R., Direct sp³ C-H Bond Activation Adjacent to Nitrogen in Heterocycles. *Chem. Soc. Rev.* **2007**, *36*, 1069-1084.
28. Ye, J.; Lautens, M., Palladium-Catalysed Norbornene-Mediated C-H Functionalization of Arenes. *Nat. Chem.* **2015**, *7*, 863-870.
29. White, M. C.; Zhao, J., Aliphatic C-H Oxidations for Late-Stage Functionalization. *J. Am. Chem. Soc.* **2018**, *140*, 13988-14009.
30. Ros, A.; Fernandez, R.; Lassaletta, J. M., Functional Group Directed C-H Borylation. *Chem. Soc. Rev.* **2014**, *43*, 3229-3243.
31. Zhang, C.; Rao, Y., Weak Coordination Promoted Regioselective Oxidative Coupling Reaction for 2,2'-Difunctional Biaryl Synthesis in Hexafluoro-2-Propanol. *Org. Lett.* **2015**, *17*, 4456-4459.
32. Cornella, J.; Righi, M.; Larrosa, I., Carboxylic Acids as Traceless Directing Groups for Formal *meta*-Selective Direct Arylation. *Angew. Chem. Int. Ed.* **2011**, *50*, 9429-9432.
33. Zhang, Y. H.; Yu, J. Q., Pd(II)-Catalyzed Hydroxylation of Arenes with 1 atm of O₂ or air. *J. Am. Chem. Soc.* **2009**, *131*, 14654-14655.
34. Simonetti, M.; Cannas, D. M.; Panigrahi, A.; Kujawa, S.; Kryjewski, M.; Xie, P.; Larrosa, I., Ruthenium-Catalyzed C-H Arylation of Benzoic Acids and Indole Carboxylic Acids with Aryl Halides. *Chemistry* **2017**, *23*, 549-553.

35. Liu, X.; Li, X.; Liu, H.; Guo, Q.; Lan, J.; Wang, R.; You, J., Aldehyde as a Traceless Directing Group for Rh(III)-Catalyzed C-H Activation: A Facile Access to Diverse Indolo[1,2-*a*]quinolines. *Org. Lett.* **2015**, *17*, 2936-2939.
36. Gao, P.; Liu, L.; Shi, Z.; Yuan, Y., Iridium(III)-Catalyzed Regioselective Direct Arylation of sp² C-H Bonds with Diaryliodonium Salts. *Org. Biomol. Chem.* **2016**, *14*, 7109-7113.
37. Gao, P.; Guo, W.; Xue, J.; Zhao, Y.; Yuan, Y.; Xia, Y.; Shi, Z., Iridium(III)-Catalyzed Direct Arylation of C-H Bonds with Diaryliodonium Salts. *J. Am. Chem. Soc.* **2015**, *137*, 12231-12240.
38. Matsubara, T.; Asako, S.; Ilies, L.; Nakamura, E., Synthesis of Anthranilic Acid Derivatives through Iron-Catalyzed Ortho Amination of Aromatic Carboxamides with *N*-Chloroamines. *J. Am. Chem. Soc.* **2014**, *136*, 646-649.
39. Yu, W.; Zhang, W.; Liu, Z.; Zhang, Y., Cobalt(III)-Catalyzed Annulation of Esters and Alkynes: A Facile Route to Indenones. *Chem. Commun.* **2016**, *52*, 6837-6840.
40. Liang, S.; Xu, K.; Zeng, C. C.; Tian, H. Y.; Sun, B. G., Recent Advances in the Electrochemical α -C-H Bond Functionalization of Carbonyl Compounds. *Adv. Syn. Catal.* **2018**, *360*, 4266-4292.
41. Chakraborty, P.; Mandal, R.; Garg, N.; Sundararaju, B., Recent Advances in Transition Metal-Catalyzed Asymmetric Electrocatalysis. *Coord. Chem. Rev.* **2021**, *444*, 214065.
42. Karkas, M. D., Electrochemical Strategies for C-H Functionalization and C-N Bond Formation. *Chem. Soc. Rev.* **2018**, *47*, 5786-5865.
43. Malapit, C. A.; Prater, M. B.; Cabrera-Pardo, J. R.; Li, M.; Pham, T. D.; McFadden, T. P.; Blank, S.; Minter, S. D., Advances on the Merger of Electrochemistry and Transition Metal Catalysis for Organic Synthesis. *Chem. Rev.* **2022**, *122*, 3180-3218.
44. Shono, T.; Hamaguchi, H.; Matsumura, Y., Electroorganic chemistry. XX. Anodic Oxidation of Carbamates. *J. Am. Chem. Soc.* **2002**, *97*, 4264-4268.
45. Shono, T., Electroorganic Chemistry in Organic Synthesis. *Tetrahedron* **1984**, *40*, 811-850.
46. Francke, R.; Little, R. D., Redox Catalysis in Organic Electrosynthesis: Basic Principles and Recent Developments. *Chem. Soc. Rev.* **2014**, *43*, 2492-2521.
47. Cheung, K.; Wong, W.; Ma, D.; Lai, T.; Wong, K., Transition Metal Complexes as Electrocatalysts-Development and Applications in Electro-Oxidation Reactions. *Coord. Chem. Rev.* **2007**, *251*, 2367-2385.
48. Ma, C.; Fang, P.; Liu, Z. R.; Xu, S. S.; Xu, K.; Cheng, X.; Lei, A.; Xu, H. C.; Zeng, C.; Mei, T. S., Recent Advances in Organic Electrosynthesis Employing Transition Metal Complexes as Electrocatalysts. *Sci. Bull.* **2021**, *66*, 2412-2429.

49. Hilt, G.; Smolko, K. I., Electrochemical Regeneration of Low-Valent Indium(I) Species as Catalysts for C-C Bond Formations. *Angew. Chem. Int. Ed.* **2001**, *40*, 3399-3402.
50. Gomes, P.; Gosmini, C.; Nédélec, J. Y.; Périchon, J., Cobalt Bromide as Catalyst in Electrochemical Addition of Aryl Halides onto Activated Olefins. *Tetrahedron Lett.* **2000**, *41*, 3385-3388.
51. Gao, Y.; Hill, D. E.; Hao, W.; McNicholas, B. J.; Vantourout, J. C.; Hadt, R. G.; Reisman, S. E.; Blackmond, D. G.; Baran, P. S., Electrochemical Nozaki-Hiyama-Kishi Coupling: Scope, Applications, and Mechanism. *J. Am. Chem. Soc.* **2021**, *143*, 9478-9488.
52. Tian, J.; Moeller, K. D., Electrochemically Assisted Heck Reactions. *Org. Lett.* **2005**, *7*, 5381-5383.
53. Hu, L.; Stuart, M.; Tian, J.; Maurer, K.; Moeller, K. D., Building Addressable Libraries: Site-Selective Use of Pd(0) Catalysts on Microelectrode Arrays. *J. Am. Chem. Soc.* **2010**, *132*, 16610-16616.
54. Yeh, N. H.; Zhu, Y.; Moeller, K. D., Electroorganic Synthesis and the Construction of Addressable Molecular Surfaces. *ChemElectroChem* **2019**, *6*, 4134-4143.
55. Lai, J.; Pericas, M. A., Manganese/Copper Co-catalyzed Electrochemical Wacker-Tsuji-Type Oxidation of Aryl-Substituted Alkenes. *Org. Lett.* **2020**, *22*, 7338-7342.
56. Lu, H.; Zhang, X. P., Catalytic C-H Functionalization by Metalloporphyrins: Recent Developments and Future Directions. *Chem. Soc. Rev.* **2011**, *40*, 1899-1909.
57. Doyle, M. P.; Goldberg, K. I., C-H functionalization. *Acc. Chem. Res.* **2012**, *45*, 777.
58. Labinger, J. A., Platinum-Catalyzed C-H Functionalization. *Chem. Rev.* **2017**, *117*, 8483-8496.
59. Wei, Y.; Hu, P.; Zhang, M.; Su, W., Metal-Catalyzed Decarboxylative C-H Functionalization. *Chem. Rev.* **2017**, *117*, 8864-8907.
60. Pichette Drapeau, M.; Goossen, L. J., Carboxylic Acids as Directing Groups for C-H Bond Functionalization. *Chemistry* **2016**, *22*, 18654-18677.
61. Shi, G.; Zhang, Y., Carboxylate-Directed C-H Functionalization. *Adv. Syn. Catal.* **2014**, *356*, 1419-1442.
62. Davies, D. L.; Macgregor, S. A.; McMullin, C. L., Computational Studies of Carboxylate-Assisted C-H Activation and Functionalization at Group 8-10 Transition Metal Centers. *Chem. Rev.* **2017**, *117*, 8649-8709.
63. Lai, X. L.; Shu, X. M.; Song, J.; Xu, H. C., Electrophotocatalytic Decarboxylative C-H Functionalization of Heteroarenes. *Angew. Chem. Int. Ed.* **2020**, *59*, 10626-10632.

64. Rodriguez, N.; Goossen, L. J., Decarboxylative Coupling Reactions: A Modern Strategy for C-C Bond Formation. *Chem. Soc. Rev.* **2011**, *40*, 5030-5048.
65. Shang, R.; Liu, L., Transition Metal-Catalyzed Decarboxylative Cross-Coupling Reactions. *Sci. China Chem.* **2011**, *54*, 1670-1687.
66. Zhang, F.; Greaney, M. F., Decarboxylative Cross-Coupling of Azoyl Carboxylic Acids with Aryl Halides. *Org. Lett.* **2010**, *12*, 4745-4747.
67. Hu, P.; Kan, J.; Su, W.; Hong, M., Pd(O₂CCF₃)₂/Benzoquinone: A Versatile Catalyst System for the Decarboxylative Olefination of Arene Carboxylic Acids. *Org. Lett.* **2009**, *11*, 2341-2344.
68. Jia, W.; Jiao, N., Cu-Catalyzed Oxidative Amidation of Propiolic Acids under Air via Decarboxylative Coupling. *Org. Lett.* **2010**, *12*, 2000-2003.
69. Duan, Z.; Ranjit, S.; Zhang, P.; Liu, X., Synthesis of Aryl Sulfides by Decarboxylative C-S Cross-Couplings. *Chemistry* **2009**, *15*, 3666-3669.
70. Shirase, S.; Tamaki, S.; Shinohara, K.; Hirosawa, K.; Tsurugi, H.; Satoh, T.; Mashima, K., Cerium(IV) Carboxylate Photocatalyst for Catalytic Radical Formation from Carboxylic Acids: Decarboxylative Oxygenation of Aliphatic Carboxylic Acids and Lactonization of Aromatic Carboxylic Acids. *J. Am. Chem. Soc.* **2020**, *142*, 5668-5675.
71. Guan, R.; Bennett, E. L.; Huang, Z.; Xiao, J., Decarboxylative Oxygenation of Carboxylic Acids with O₂ via a Non-Heme Manganese Catalyst. *Green Chem.* **2022**, *24*, 2946-2952.
72. Sakakibara, Y.; Cooper, P.; Murakami, K.; Itami, K., Photoredox-Catalyzed Decarboxylative Oxidation of Arylacetic Acids. *Chem. Asian J.* **2018**, *13*, 2410-2413.
73. Song, H. T.; Ding, W.; Zhou, Q. Q.; Liu, J.; Lu, L. Q.; Xiao, W. J., Photocatalytic Decarboxylative Hydroxylation of Carboxylic Acids Driven by Visible Light and Using Molecular Oxygen. *J. Org. Chem.* **2016**, *81*, 7250-7255.
74. Ritter, J. J.; Minieri, P. P., A New Reaction of Nitriles; Amides from Alkenes and Mononitriles. *J. Am. Chem. Soc.* **1948**, *70*, 4045-4048.
75. Ritter, J. J.; Kalish, J., A New Reaction of Nitriles; Synthesis of *t*-Carbinamines. *J. Am. Chem. Soc.* **1948**, *70*, 4048-4050.
76. Guérinot, A.; Reymond, S.; Cossy, J., Ritter Reaction: Recent Catalytic Developments. *Eur. J. Org. Chem.* **2011**, *2012*, 19-28.
77. Nair, V.; Rajan, R.; Rath, N. P., A CAN-Induced Cyclodimerization-Ritter Trapping Strategy for the One-Pot Synthesis of 1-Amino-4-Aryltetralins from Styrenes. *Org. Lett.* **2002**, *4*, 1575-1577.

78. Leiva, R.; Gazzarrini, S.; Esplugas, R.; Moroni, A.; Naesens, L.; Sureda, F. X.; Vazquez, S., Ritter Reaction-Mediated Syntheses of 2-Oxaadamantan-5-amine, A Novel Amantadine Analog. *Tetrahedron Lett.* **2015**, *56*, 1272-1275.
79. Stepanovs, D.; Posevins, D.; Turks, M., Crystal Structures of Two (+/-)-Exo-*N*-Isobornyl-Acetamides. *Acta. Crystallogr. E. Crystallogr. Commun.* **2015**, *71*, 1117-1120.
80. Anxionnat, B.; Guérinot, A.; Reymond, S.; Cossy, J., FeCl₃-Catalyzed Ritter Reaction. Synthesis of Amides. *Tetrahedron Lett.* **2009**, *50*, 3470-3473.
81. Subba Reddy, B. V.; Sivasankar Reddy, N.; Madan, C.; Yadav, J. S., HBF₄·OEt₂ as a Mild and Versatile Reagent for the Ritter Amidation of Olefins: A Facile Synthesis of Secondary Amides. *Tetrahedron Lett.* **2010**, *51*, 4827-4829.
82. Chen, M. E.; Chen, X. W.; Hu, Y. H.; Ye, R.; Lv, J. W.; Li, B.; Zhang, F. M., Recent Advances of Ritter Reaction and its Synthetic Applications. *Org. Chem. Front.* **2021**, *8*, 4623-4664.
83. Olah, G. A.; Balaram Gupta, B. G., Synthetic Methods and Reactions. 86. Novel Synthesis of *N*-(1-Adamantyl)amides from Adamantane. *J. Org. Chem.* **2002**, *45*, 3532-3533.
84. Sakaguchi, S.; Hirabayashi, T.; Ishii, Y., First Ritter-Type Reaction of Alkylbenzenes Using *N*-Hydroxyphthalimide as a Key Catalyst. *Chem. Commun.* **2002**, *5*, 516-517.
85. Kiyokawa, K.; Watanabe, T.; Fra, L.; Kojima, T.; Minakata, S., Hypervalent Iodine(III)-Mediated Decarboxylative Ritter-Type Amination Leading to the Production of α -Tertiary Amine Derivatives. *J. Org. Chem.* **2017**, *82*, 11711-11720.
86. Bao, H.; Zhou, B.; Jin, H.; Liu, Y., Copper-Catalyzed Three-Component Reaction of *N*-Heteroaryl Aldehydes, Nitriles, and Water. *Org. Biomol. Chem.* **2019**, *17*, 5021-5028.
87. Stahl, S. S.; Alsters, P. L., *Liquid Phase Aerobic Oxidation Catalysis: Industrial Applications and Academic Perspectives*. John Wiley & Sons: **2016**.
88. Guo, Z.; Liu, B.; Zhang, Q.; Deng, W.; Wang, Y.; Yang, Y., Recent Advances in Heterogeneous Selective Oxidation Catalysis for Sustainable Chemistry. *Chem. Soc. Rev.* **2014**, *43*, 3480-3524.
89. Smith, M., *Organic Synthesis*. Academic Press: **2016**.
90. Caron, S.; Dugger, R. W.; Ruggeri, S. G.; Ragan, J. A.; Ripin, D. H., Large-Scale Oxidations in the Pharmaceutical Industry. *Chem. Rev.* **2006**, *106*, 2943-2989.
91. Sheldon, R. A.; Arends, I.; Hanefeld, U., *Green Chemistry and Catalysis*. John Wiley & Sons: **2007**.
92. Anastas, P.; Warner, J., *Green Chemistry: Theory and Practice*, Oxford University Press: **1998**.

93. Anastas, P. T.; Kirchhoff, M. M., Origins, Current Status, and Future Challenges of Green Chemistry. *Acc. Chem. Res.* **2002**, *35*, 686-694.
94. Gonzalez-de-Castro, A.; Robertson, C. M.; Xiao, J., Dehydrogenative α -Oxygenation of Ethers with an Iron Catalyst. *J. Am. Chem. Soc.* **2014**, *136*, 8350-8360.
95. Gonzalez-de-Castro, A.; Xiao, J., Green and Efficient: Iron-Catalyzed Selective Oxidation of Olefins to Carbonyls with O₂. *J. Am. Chem. Soc.* **2015**, *137*, 8206-8218.
96. Huang, Z.; Guan, R.; Shanmugam, M.; Bennett, E. L.; Robertson, C. M.; Brookfield, A.; McInnes, E. J. L.; Xiao, J., Oxidative Cleavage of Alkenes by O₂ with a Non-Heme Manganese Catalyst. *J. Am. Chem. Soc.* **2021**, *143*, 10005-10013.
97. Huang, Z.; Guan, R.; Bennett, E. L.; Xiao, J., Non-Heme Manganese(II) Complex-Catalysed Oxidative Cleavage of 1,2-Diols via Alcohol-Assisted O₂ Activation. *Green Chem.* **2022**, *24*, 3814-3823.

Chapter 2

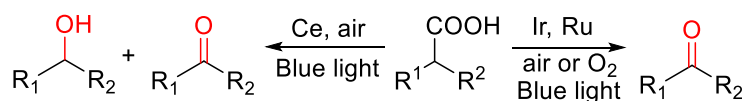
Decarboxylative Oxygenation of Carboxylic Acids to Aldehydes and Ketones via a Non-Heme Manganese Catalyst

2.1 Introduction

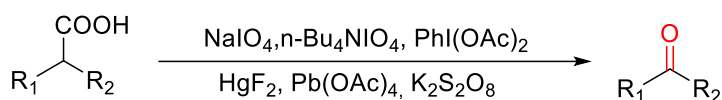
Carboxylic acids are cheap, non-toxic and stable substrates, and they are abundant, easily-available in nature and industry. Carboxylic acids have wide applications in organic chemistry. They often play an important role as feedstocks in organic, material and polymer synthesis.¹⁻² Therefore, a great number of carboxylic acid transformations have been reported in the last few decades. Particularly, the construction of C-C and C-X bonds using carboxylic acids as starting materials via decarboxylation has attracted wide attention.³⁻¹⁷ However, the research value of decarboxylative oxygenation of carboxylic acids to valuable carbonyl products including aldehydes and ketones has been underestimated, and research about this direct transformation with wide substrate scope, good yields and high efficiency remains limited. Carbonyl products are important building blocks of organic chemistry.¹⁸⁻²³ In industrial production, the synthesis of aldehydes and ketones can be realized by a series of strategies, such as carbonylation of alkenes and oxidation of hydrocarbons.²⁴⁻²⁵ However, harsh conditions such as high pressure, high temperature, and toxic reagents are often required for these synthesis processes. For instance, whilst hydroformylation is a dominant technology to prepare aldehydes, over 100 °C and 200 atm syngas with cobalt catalysts are required. Although much milder conditions are employed for Rh-based catalysts, Rh catalysts are toxic and expensive.²⁶ Therefore, exploring rapid and efficient synthesis of aldehydes and ketones under mild conditions with cheap catalysts and substrates is a worthy endeavor. Considering the easy availability of various carboxylic acids, they are suitable substrates for this endeavor.

Decarboxylative oxygenation of carboxylic acids is a challenging issue. The catalyst for this transformation requires the ability of promoting both decarboxylation and oxidation. So far, only three reports have demonstrated decarboxylative oxygenation of carboxylic acids via photoredoxcatalysis using O₂ under mild conditions. Two of these require precious Ir or Ru photocatalysts,²⁷⁻²⁸ while the third produces a mixture of aldehydes/ketones and alcohols as the products (Scheme 2.1a).²⁹ Other strategies have been reported; however, stoichiometric strong oxidants were employed in these strategies, e.g. NaIO₄,³⁰ *n*-Bu₄NIO₄,³¹ PhI(OAc)₂,³² HgF₂,³³ Pb(OAc)₄³⁴ and K₂S₂O₈³⁵ (Scheme 2.1b), or a high reaction temperature was required (Scheme 2.1c). In this chapter, a highly selective decarboxylative oxygenation of carboxylic acids to aldehydes or ketones by O₂ (1 atm) is reported. This reaction is promoted by a non-heme Mn(II) catalyst and visible light under mild conditions (Scheme 2.1d).

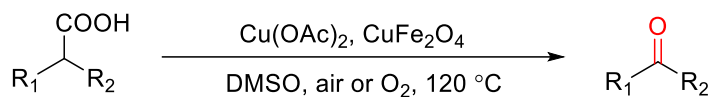
a) Photocatalytic systems



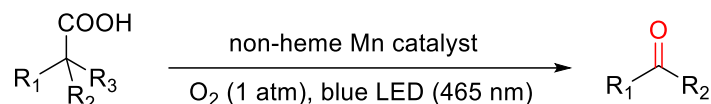
b) Chemical methods using oxidants



c) High temperature methods



d) This work



Scheme 2.1 Decarboxylative oxygenation of carboxylic acids.

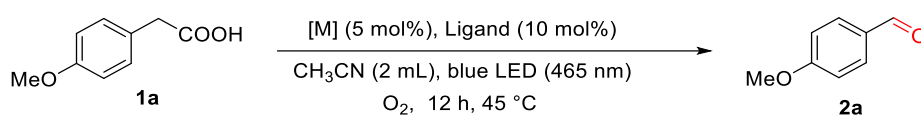
The use of inexpensive and benign O₂ for selective oxidation with first-row, biologically relevant metal complexes as catalysts is a challenging issue for the synthetic chemist.³⁶⁻³⁸ Some

biomimetic Mn and Fe complexes bearing heme and non-heme polydentate ligands have been developed. They were successfully employed to catalyse a series of oxidation reactions with O₂, including the oxidation of carboxylic acids, hydrocarbons and alcohols.^{30, 36, 39-43} However, significant drawbacks remain in most cases, e.g. unsatisfactory selectivity due to poorly controlled radical-type pathways and the requirement for stoichiometric co-reductants. To date, only a limited number of biomimetic metal complexes are able to catalyse the aerobic oxidation in a controlled manner without the assistance of a co-reductant.⁴⁴⁻⁴⁹ Following on from our group's previous study of aerobic cleavage of alkenes with a non-heme Mn(II) complex,⁵⁰ the decarboxylative oxygenation of carboxylic acids to aldehydes/ketones by O₂ with this and related complexes has been developed in this thesis.

2.2 Results and Discussion

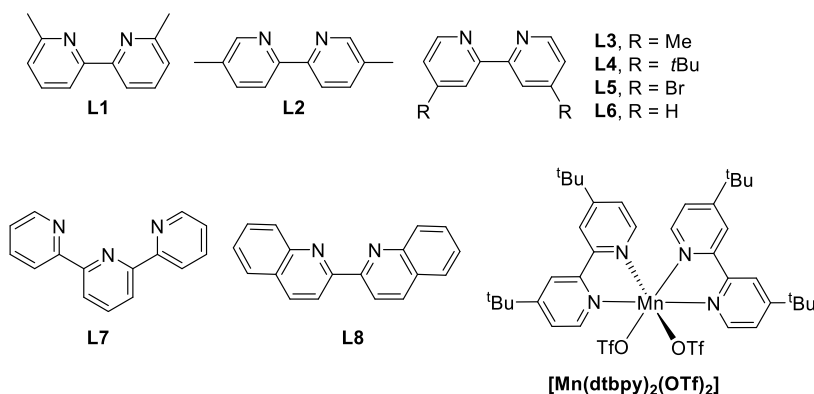
2.2.1 Optimization experiments

This study started from the examination of the decarboxylative oxygenation of 4-methoxybenzeneacetic acid (**1a**) with O₂ (1 atm) (Table 2.1). Our previous work showed that the photocatalytic system comprised of Mn(OTf)₂ and **L4** was effective for O₂ activation in the presence of blue light.⁵⁰ Therefore, the photocatalytic system was initially tested. To our delight, the desired oxygenation product **2a** could be obtained in 90% yield (Table 2.1, entry 6). [Mn(dtbpy)₂(OTf)₂] formed in situ is likely to be the catalytic species, as the isolated [Mn(dtbpy)₂(OTf)₂] complex displayed a similar activity (Table 2.1, entry 1). It is unsurprising that the ligand-free Mn(OTf)₂ showed no catalytic activity for the target reaction (Table 2.1, entry 2), as it is less likely to produce activated oxygen species from O₂ ($E^0_{\text{Mn(III)/Mn(II)}} = 1.56$ V/SHE, $E^0_{\text{O}_2/\text{H}_2\text{O}} = 0.82$ V/SHE, neutral conditions). A range of substituted bipyridines (**L1-L8**) were further tested to explore the effect of ligand, revealing **L4** to give the best yield of **2a** (Table 2.1, entries 3-10).

Table 2.1 Optimization of reaction conditions^{a, b}

Entry	[M]	Ligand	Yield (%)
1	[Mn(dt bpy) ₂ (OTf) ₂]	/	87
2	Mn(OTf) ₂	/	0
3	Mn(OTf) ₂	L1	33
4	Mn(OTf) ₂	L2	46
5	Mn(OTf) ₂	L3	61
6	Mn(OTf) ₂	L4	90
7	Mn(OTf) ₂	L5	41
8	Mn(OTf) ₂	L6	64
9	Mn(OTf) ₂	L7	14
10	Mn(OTf) ₂	L8	41
11	Fe(OTf) ₂	L4	16
12	Cu(OTf) ₂	L4	4
13	CoCl ₂	L4	42
14	MnCl ₂	L4	53
15 ^c	[Mn(dt bpy) ₂ (OTf) ₂]	/	0
16 ^d	Mn(OTf) ₂	L4	62

^aReaction conditions: **1a** (0.5 mmol), [M] (5 mol%), ligand (10 mol%), CH₃CN (2 mL), blue light (465 nm), 45 °C, O₂ (1 atm), 12 h. ^bNMR yields, determined using mesitylene (20 μL) as internal standard. ^cN₂ (1 atm). ^dAir instead of O₂.



The combinations of **L4** with other metal salts, such as Fe(OTf)₂, Cu(OTf)₂ and CoCl₂, were ineffective, affording much lower yields of **2a** (Table 2.1, entries 11-13). Meanwhile, MnCl₂ is less effective than Mn(OTf)₂, as can be seen in Table 2.1, entry 14. As is clear, both

O₂ and blue light are essential for this transformation; in their absence, no target product was observed (Table 2.1, entry 15, and Figure 2.1). In addition, the aerobic oxygenation reaction presented the highest reactivity in acetonitrile after evaluation of the solvents (Table 2.2). A series of different solvents, including DCE, EtOH, THF, MeOH, acetone, ethyl acetate, hexane and TFE, were screened. However, only low to moderate yields of **2a** were obtained. The screening established the following optimized conditions: Mn(OTf)₂ (5 mol%), **L4** (10 mol%) as ligand, O₂ as oxidant in CH₃CN at 45 °C with blue light irradiation.

Table 2.2 Oxidative decarboxylation/oxidation of acid **1a** in different solvents^{a, b}

Reaction scheme: 4-methoxybenzoic acid (**1a**) reacts with [Mn(dtbpv)₂(OTf)₂] (5 mol%), solvent (2 mL) under Blue LED (465 nm), O₂, 12 h, 45 °C to yield 4-methoxybenzaldehyde (**2a**).

Entry	Catalyst	Solvent	Time (h)	Yield (%)
1	[Mn(dtbpv) ₂ (OTf) ₂]	DCE	12	59
2	[Mn(dtbpv) ₂ (OTf) ₂]	EtOH	12	28
3	[Mn(dtbpv) ₂ (OTf) ₂]	THF	12	14
4	[Mn(dtbpv) ₂ (OTf) ₂]	MeOH	12	29
5	[Mn(dtbpv) ₂ (OTf) ₂]	Acetone	12	41
6	[Mn(dtbpv) ₂ (OTf) ₂]	Ethyl acetate	12	37
7	[Mn(dtbpv) ₂ (OTf) ₂]	Hexane	12	35
8	[Mn(dtbpv) ₂ (OTf) ₂]	TFE	12	50
9 ^c	[Mn(dtbpv) ₂ (OTf) ₂]	Acetonitrile	12	72
10	[Mn(dtbpv) ₂ (OTf) ₂]	Acetonitrile	6	67
11	[Mn(dtbpv) ₂ (OTf) ₂]	Acetonitrile	9	79

^aReaction conditions: **1a** (0.5 mmol), [Mn(dtbpv)₂(OTf)₂] (5 mol%), solvent (2 mL), under blue LED light (465 nm, 9 W) at 45 °C under O₂ atmosphere (1 atm) for 12 h. ^bNMR yields are given. ^c20 °C.

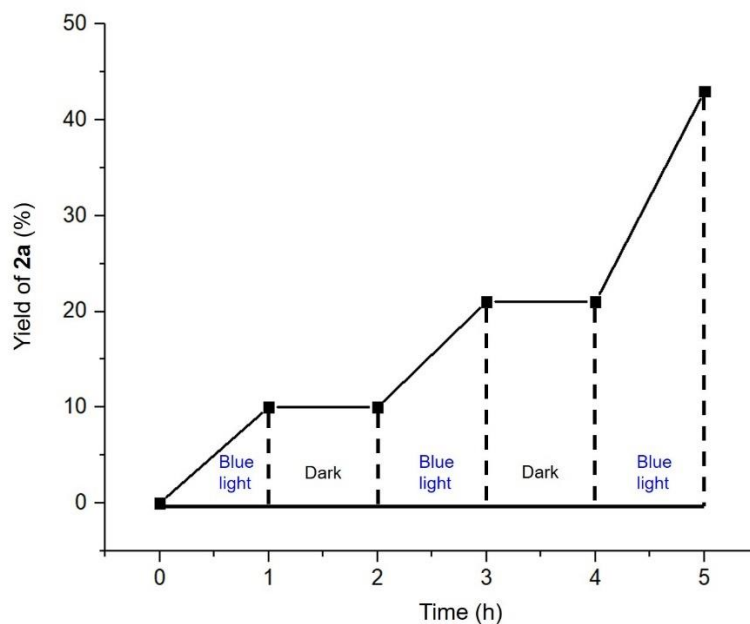
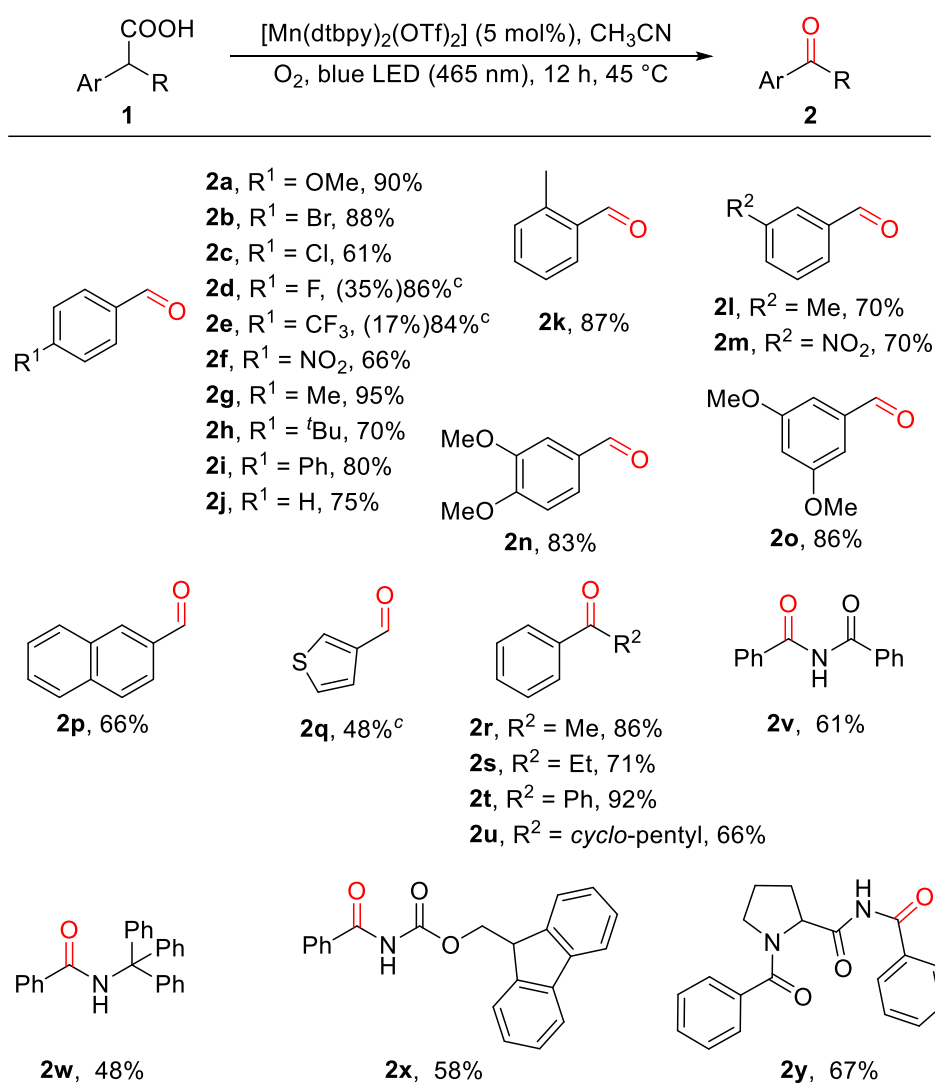


Figure 2.1 Decarboxylative oxidation of **1a** under light on/off conditions. Reaction conditions: **1a** (0.5 mmol), [Mn(dtbpv)₂(OTf)₂] (5 mol%), CH₃CN (2 mL), 1,3,5-tribromobenzene (62.4 mg) as internal standard, blue LED light (465 nm, 9 W), 45 °C, O₂ atmosphere.

2.2.2 Substrate scope

A series of benzylic carboxylic acids were first examined to test the generality of this decarboxylative oxygenation protocol. As shown in Scheme 2.2, a variety of phenyl acetic acids bearing electron-donating or electron-withdrawing groups on the phenyl ring reacted well (**2a-2o**), affording the desirable aldehyde products in good to excellent yields. In terms of phenyl acetic acids bearing electronic-withdraw groups, they were usually less reactive. For example, *para*-F-substituted acid (**1d**) and *para*-CF₃-substituted acid (**1e**) showed low reactivity for the oxidation under the standard conditions, giving the corresponding aldehydes in 35% and 17% yields, respectively. However, we found that the oxidation efficiency was improved by introducing a catalytic amount of NaOAc as an additive (Table 2.3). With the addition of NaOAc, the yields of **2d** and **2e** were improved to 86% and 84%, respectively. Meanwhile, 2-naphthyl acetic acid and a *S*-heterocycle were tolerated, affording corresponding **2p** and **2q** in moderate yields, respectively. Notably, a range of amino acids including a

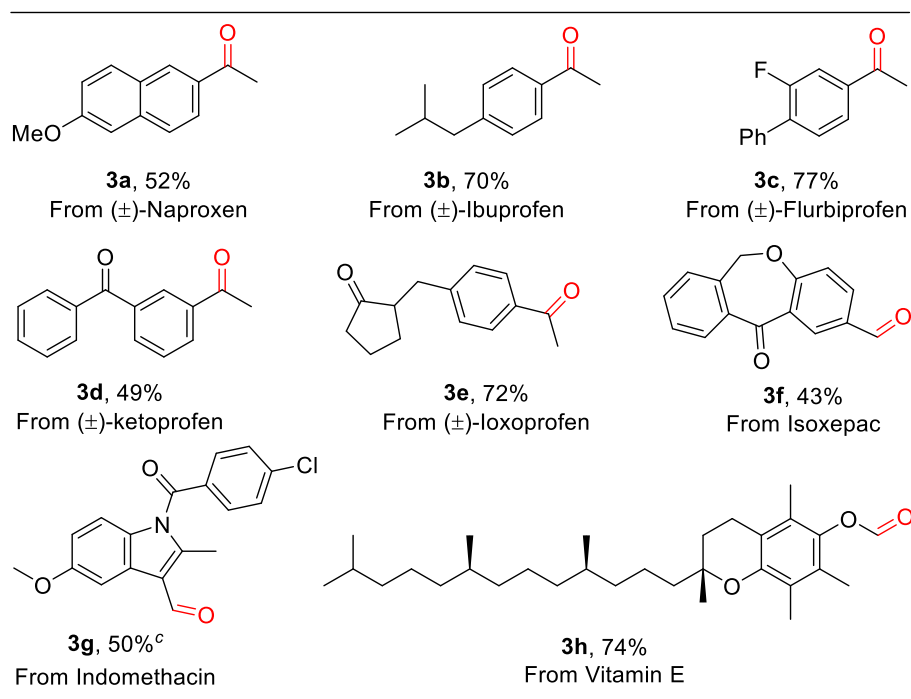
dipeptide were oxidized to the corresponding amide products in a highly selective manner (**2v-2y**), showing potential applications in bio-conjugate chemistry.



Scheme 2.2 Oxidation of mono- and di-substituted benzylic carboxylic acids.^{a, b} Reaction conditions: **1** (0.5 mmol), $[\text{Mn}(\text{dtbpy})_2(\text{OTf})_2]$ (5 mol%) (in situ prepared), CH_3CN (2 mL), blue light (465 nm), 45 °C, O_2 (1 atm), 12 h. ^bIsolated yields are given. ^c CH_3COONa (30 mol%) was added.

It is worth noting that a variety of drug molecules with functionalized aryl acetic acid scaffolds were also selectively oxidized by O_2 under the optimum conditions. As shown in Scheme 2.3, naproxen, ibuprofen, flubiprofen, ketoprofen, ioxoprofen, isoxepac and indomethacin all proceeded successfully, and the corresponding aldehydes or ketones were afforded in good yields (**3a-3g**). Moreover, the ability of this photo-Mn protocol in late-stage decarboxylative oxygenation was tested by using vitamin E as substrate. Notably, the aldehyde

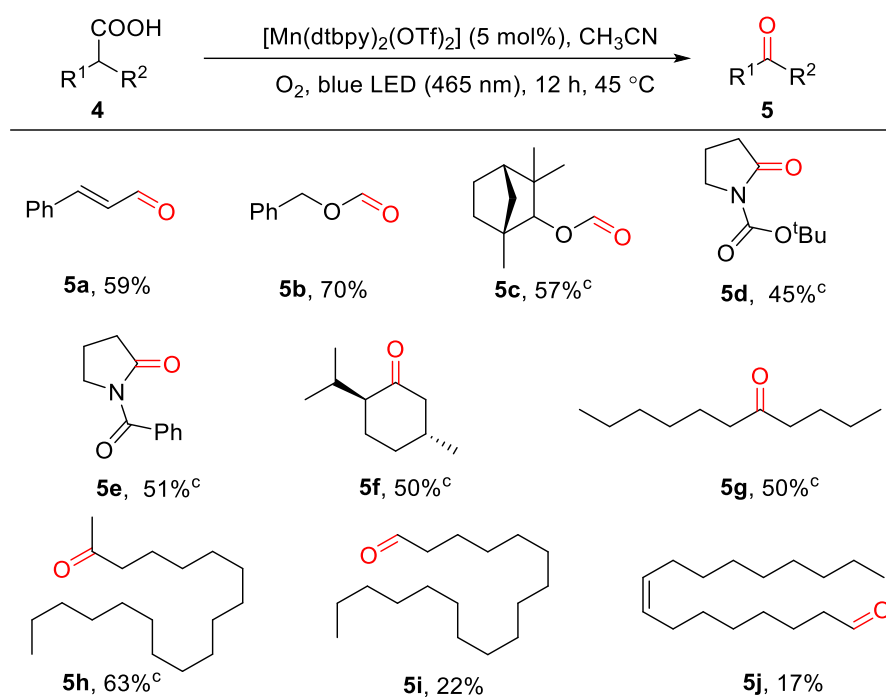
product **3h** was afforded in 74% yield. The relatively active benzylic C-H bonds, tertiary C-H bonds, and indole ring remained intact in the reaction, showing the high chemoselectivity of this oxidation protocol.



Scheme 2.3 Oxidation of pharmaceutical molecules.^{a, b} ^aReaction conditions: carboxylic acids (0.5 mmol), [Mn(dtbpv)₂(OTf)₂] (5 mol%), CH₃CN (2 mL), blue light (465 nm), 45 °C, O₂ (1 atm), 12 h. ^bIsolated yields are given. ^cCH₃COONa (30 mol%) was added.

Moreover, we tested the oxidation of more challenging enoic acids and aliphatic carboxylic acids.⁵¹⁻⁵² As can be seen in Scheme 2.4, the C=C double bonds in enoic acids, usually sensitive to oxidation conditions, remained intact during the oxidation (**5a**). Meanwhile, it is noting that aliphatic acids bearing different functionalities, including ether, carbamate, and amide reacted smoothly to afford the corresponding carbonyl products with blue or UV light irradiation (**5b-5e**). These good results highlight the high chemoselectivity and hence great application potential of this method. Secondary cyclic or long-chain aliphatic acids were also oxidatively decarboxylated to furnish the target carbonyls in good yields (**5f-5h**, 50-63%) under the irradiation of UV-light. The primary stearic acid and oleic acid also were tolerated; however, their yields were low (**5i** and **5j**). Generally, our protocol shows a wider substrate scope when compared with MacMillan's work in 2019.²⁷ Not only can the cyclic aliphatic acids be oxidized

selectively, but also saturated or unsaturated long-chain fatty acids could be oxidized, which are usually challenging substrates.⁵³



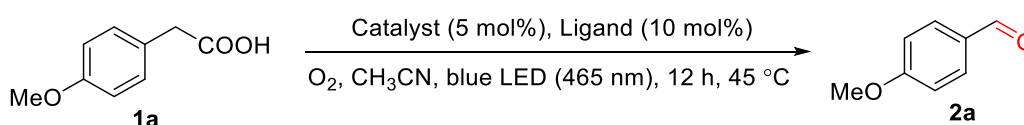
Scheme 2.4 Oxidation of aliphatic acids.^{a, b} ^aReaction conditions: **4** (0.5 mmol), [Mn(dtbp)₂(OTf)₂] (5 mol%), CH₃CN (2 mL), blue LED light (465 nm), 45 °C, O₂ atmosphere (1 atm), 12 h. ^bIsolated yields are given. ^cDCE/CH₃CN (1:1, 2 mL), ultraviolet light (365 nm).

2.2.3 Exploration of possible mechanism

A series of experiments were performed to shed light on possible reaction pathways in the decarboxylative oxygenation of carboxylic acids. As reported by Boger's group, ¹O₂ is generated in the presence of rose bengal under light irradiation and it can efficiently transfer pyrrole-2-carboxylic acids to the corresponding ketones.⁵⁴ Therefore, it is important to determine whether ¹O₂ is the oxidative species in our photo-Mn enabled oxidative decarboxylation. As shown in Table 2.4, a range of well-known photosensitizers including Eosin Y disodium salt, Ru(bpy)₃, Ir(dFppy)₃ and rose bengal (Table 2.4, entries 1-4), which can generate ¹O₂ under blue light, were used individually as replacement catalysts for the decarboxylative oxygenation of **1a** under the standard reaction conditions. However, these photosensitizers showed significantly lower catalytic performance. No reaction was observed when Ir(dFppy)₃ was employed as the catalyst, which worked well in MacMillan's work

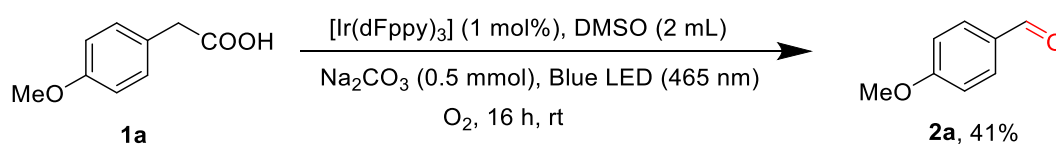
(Scheme 2.5).²⁷ Meanwhile, a well-known $^1\text{O}_2$ trap, 9,10-diphenylanthracene (DPA) which can react rapidly with $^1\text{O}_2$ to give an endoperoxide product ($k \approx 1.3 \times 10^6 \text{ M}^{-1} \text{ s}^{-1}$), was used to detect the formation of $^1\text{O}_2$ in decarboxylative oxygenation.⁵⁵ When DPA was added to the oxidative decarboxylation of **1a** under the standard conditions (Table 2.4, entry 5), **2a** was obtained in 70% yield, and no endoperoxide was detected. These observations appear to rule out the involvement of $^1\text{O}_2$ in the reaction pathway.

Table 2.4 Decarboxylative oxidation of **1a** in the presence of well-known photosensitizers or singlet oxygen trap^{a, b}

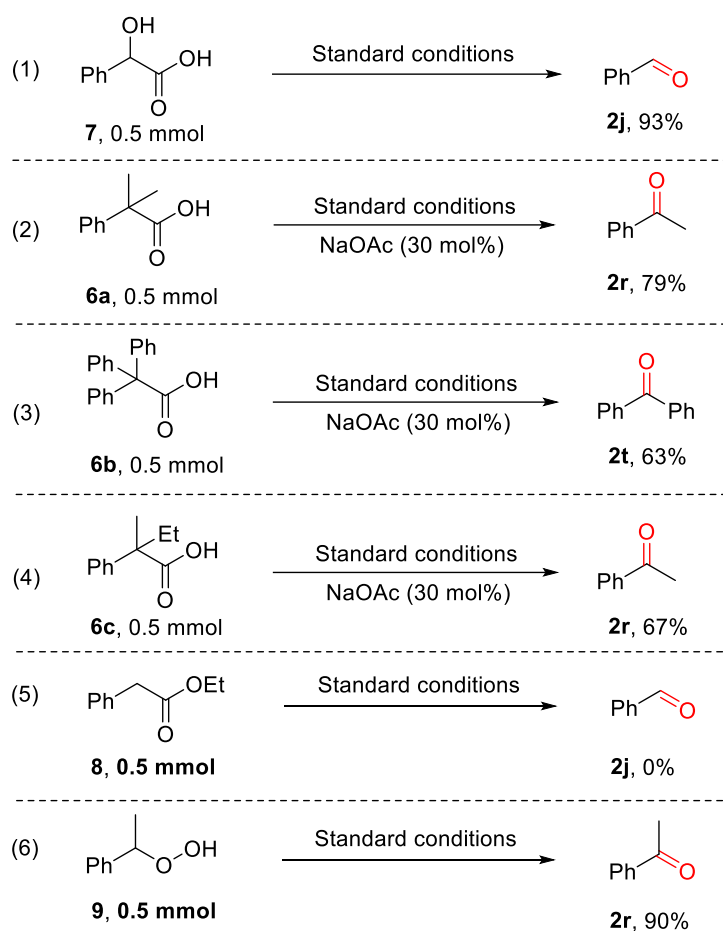


Entry	Catalyst	Yield (%)
1	Eosin Y disodium salt	37
2	[Ru(bpy) ₃ •6H ₂ O]	49
3	[Ir(dFppy) ₃]	0 ^c
4	Rose bengal	4
5	[Mn(dt bpy) ₂ (OTf) ₂]	70

^aReaction conditions: acid (0.5 mmol), catalyst (5 mol%), CH₃CN (2 mL), blue light (465 nm), 45 °C, O₂ (1 atm), 12 h. ^bNMR yields, determined using mesitylene as internal standard. ^cConversion was observed under the conditions reported by MacMillan's group.²⁷ (see Scheme 2.5) ^dDPA (0.1 mmol) was added.



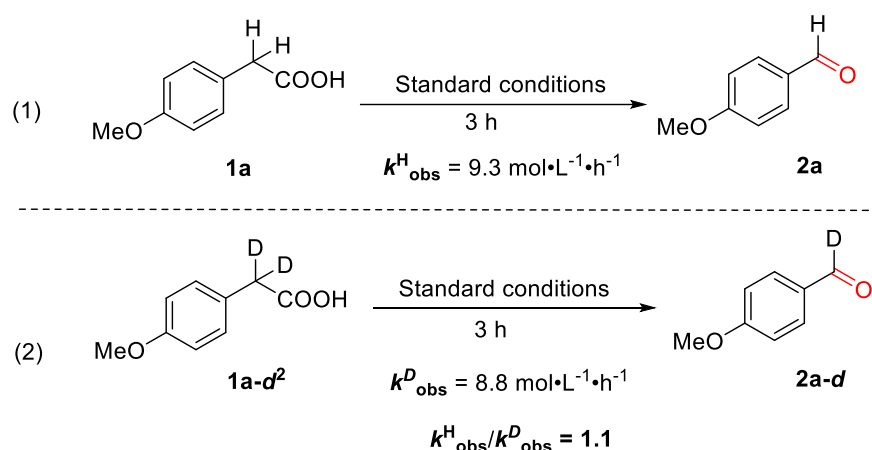
Scheme 2.5 Decomposition of **1a** by [Ir(dFppy)₃] under MacMillan's conditions.²⁷



Scheme 2.6 Control experiments to shed light on the mechanism^{a, b} ^aConditions: substrate (0.5 mmol), [Mn(dtbpv)₂(OTf)₂] (5 mol%), CH₃CN (2 mL), blue light (465 nm), 45 °C, O₂ (1 atm), 12 h, CH₃COONa (30 mol%) where applicable; ^bNMR yields, determined using mesitylene as internal standard.

Previous studies on decarboxylative oxygenation of phenylacetic acids by Mn-based enzymes indicate that the hydroxylation of C-H bond in the benzylic position is the initiation step of this oxidation reaction. For instance, phenylacetic acid was converted to 2-hydroxy-2-phenylacetic acid, which was the key intermediate for the further oxidative decarboxylation process.⁵⁶⁻⁵⁸ Because of this possibility, several control experiments were performed to determine whether a similar hydroxylation process occurs as the key step in our strategy. Firstly, the potential intermediate 2-hydroxy-2-phenylacetic acid (**7**) was subjected to the standard reaction conditions, affording **2j** in 93% yield (Scheme 2.6, eq. 1). This result indicates that **7** could be involved in the oxidative decarboxylation reaction under the current conditions. However, the desired decarboxylative oxygenation proceeded successfully as well

when phenylacetic acids bearing two alkyl or phenyl groups on benzylic position (Scheme 2.6, eqs. 2-4). Apparently, the ketone products were obtained via a C-C bond cleavage process due to the formation of the strong C=O bond. This indicates the involvement of a radical fragmentation pathway in decarboxylative oxygenation. In addition, ethyl 2-phenylacetate (**8**) showed no reactivity under standard conditions (Scheme 2.6, eq. 5). Meanwhile, when (1-hydroperoxyethyl)benzene (**9**) was employed (Scheme 2.6, eq. 6), **2r** was afforded in an excellent yield. These observations may indicate the involvement of the acid moiety and the formation of peroxide intermediates in the decarboxylative oxygenation reaction.



Scheme 2.7 Kinetic isotope effect studied under the optimized conditions.

Further insight was obtained by following the kinetic isotope effect (KIE) (Scheme 2.7). Parallel reactions using acids **1a** and **1a-d²** were conducted, affording the rate constants based on the initial rates $k^{\text{H}}_{\text{obs}} = 9.3$ and $k^{\text{D}}_{\text{obs}} = 8.8$, respectively. Considering the KIE values of *ca* 1.1, the cleavage of the C-H bond on the benzylic position is less likely to be involved in the turnover limiting step. This result further supports the notion that the oxidative decarboxylation is not initiated by the benzylic C-H bond hydroxylation.

Subsequently, UV-Vis experiments were conducted to investigate the reaction of carboxylic acids with the $[\text{Mn}(\text{dtbpy})_2(\text{OTf})_2]$ complex. As shown in Figure 2.2, an obvious decrease of the absorbance of **1a** at 230 nm was observed when 1 equivalent of $[\text{Mn}(\text{dtbpy})_2(\text{OTf})_2]$ was added. Meanwhile, compared with that of $[\text{Mn}(\text{dtbpy})_2(\text{OTf})_2]$, a

significant absorption decrease of the spectrum of the mixture of $[\text{Mn}(\text{dtbpy})_2(\text{OTf})_2]$ and **1a** was shown at around 295 nm and 306 nm. These observations indicate that $[\text{Mn}(\text{dtbpy})_2(\text{OTf})_2]$ reacts with **1a** to form a new Mn(II) species. Further structural information of the new Mn(II) species was obtained by HRMS. As shown in Figure 2.3, the experimental and calculated mass spectra of the molecular ion suggests that the carboxylate-coordinated $[\text{Mn}(\text{dtbpy})_2(\mathbf{1a-H})(\text{OTf})]$ is likely to be formed by losing a HOTf from the parent complex.

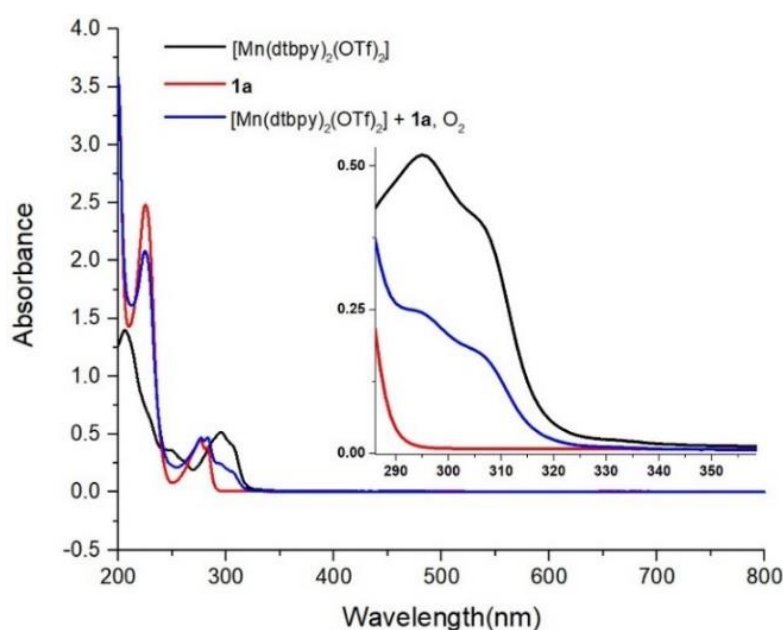


Figure 2.2 UV-Vis spectra of $[\text{Mn}(\text{dtbpy})_2(\text{OTf})_2]$, **1a** and the mixture of $[\text{Mn}(\text{dtbpy})_2(\text{OTf})_2]$ and **1a** without blue light irradiation (Concentration of $[\text{Mn}(\text{dtbpy})_2(\text{OTf})_2]$ and **1a**: 25 μM in CH_3CN).

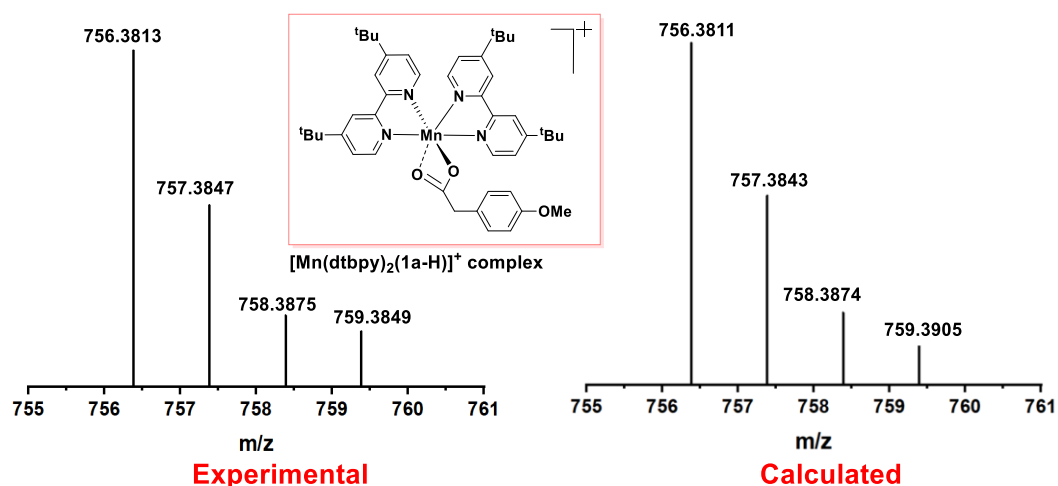


Figure 2.3 HRMS spectrum of $[\text{Mn}(\text{dtbpy})_2(\mathbf{1a-H})(\text{OTf})]^+$ formed in the in-situ reaction of $[\text{Mn}(\text{dtbpy})_2(\text{OTf})_2]$ with **1a**.

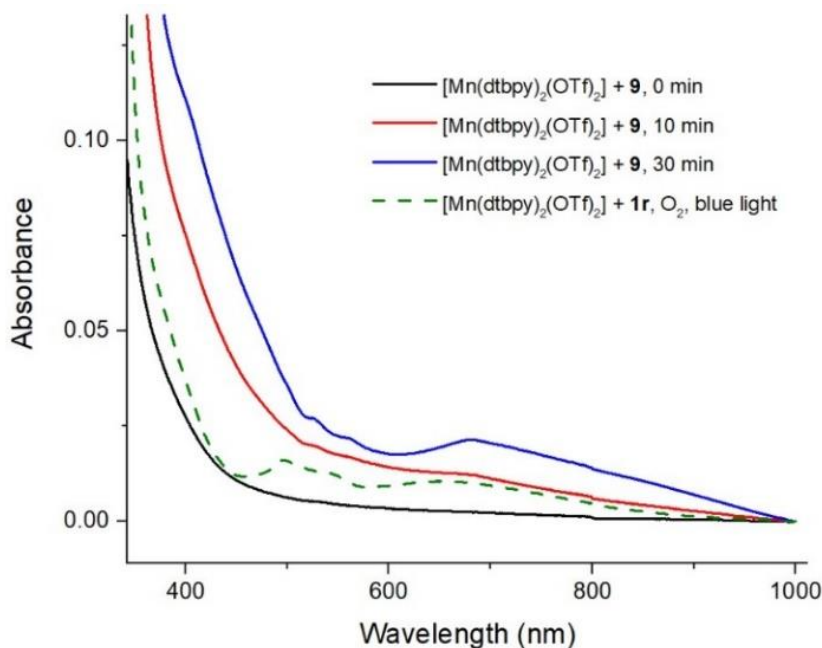
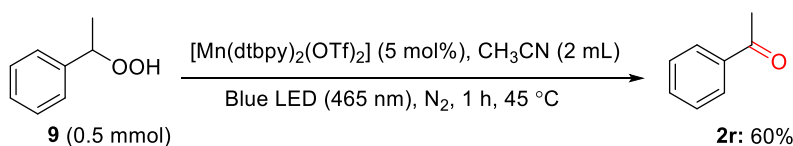
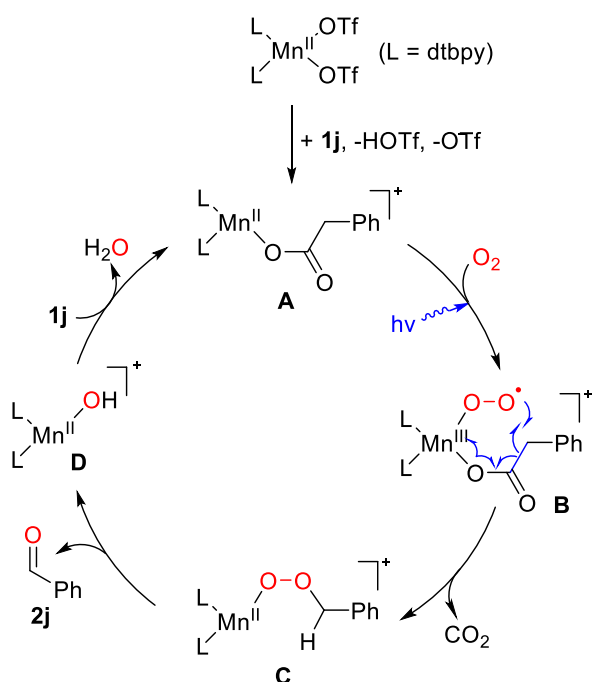


Figure 2.4 In-situ UV-Vis monitoring of the mixture of $[\text{Mn}(\text{dtbpv})_2(\text{OTf})_2]$ and **9** and the UV-vis spectra of the mixture of $[\text{Mn}(\text{dtbpv})_2(\text{OTf})_2]$ and **1r** with blue light irradiation for 2 h (Concentration of each compound: 25 μM in CH_3CN).



Scheme 2.8 Transformation of **9** under standard conditions with N_2 for 1 h.

We envisioned that the reaction of $[\text{Mn}(\text{dtbpv})_2(\mathbf{1a-H})(\text{OTf})]$ with O_2 may produce a Mn-peroxide intermediate in the decarboxylative oxidation under blue light.^{28, 58} To explore this possibility, UV-Vis experiment of a mixture of $[\text{Mn}(\text{dtbpv})_2(\text{OTf})_2]$ and **1r**, which was expected to afford $[\text{Mn}(\text{dtbpv})_2(\mathbf{1r-H})(\text{OTf})]$, was performed. When the mixture was irradiated by blue light under O_2 (Fig. 2.4, green dash line), an obvious absorption at *ca* 685 nm was observed. In particular, a similar absorption band was also found in the spectrum of the mixture of $[\text{Mn}(\text{dtbpv})_2(\text{OTf})_2]$ and **9** without blue light irradiation under N_2 . This absorption band increased over time and then reached saturation before beginning to decrease (Figure 2.4). Finally, the product **2r** was formed in 60% yield after 60 mins (Scheme 2.8). Based on these observations, a peroxide intermediate may be involved and complexed with the Mn catalyst in the process of decarboxylative oxidation. Comparing with the previous literature, the absorption at 685 nm is likely to arise from a Mn-peroxide species.⁵⁹⁻⁶¹



Scheme 2.9 A plausible mechanism of decarboxylative oxygenation of carboxylic acids (possible coordination of solvent or other molecules is omitted).

Based on the observations above and previous literature,^{18, 29} a plausible mechanism is proposed by taking the oxidation of phenylacetic acid (**1j**) as an example. As shown in Scheme 2.9, the intermediate **A**, formed by the reaction of **1j** with the Mn(II) precatalyst, is oxidized by O₂ to afford the key species **B** under blue light irradiation.^{36, 62-64} Then, the benzylic carbon of the coordinated acid was attacked by this unstable superoxide radical driven by the release of CO₂, affording the Mn(II)-peroxide **C**. Further decomposition of the unstable species **C** produces the carbonyl product and a Mn(II)-OH species **D**, which reacts with phenylacetic acid, regenerating **A**.

2.3 Conclusions

In conclusion, we have developed a selective, practical decarboxylative oxygenation protocol, which uses a non-heme Mn(II) complex as the catalyst and molecular oxygen as the oxidant under blue light irradiation. With this protocol, readily available carboxylic acids, including benzylic acids, amino acids, aliphatic acids, long-chain fatty acids and pharmaceutical molecules, can be easily converted to a wide range of valuable aldehydes, ketones, and amides in good yields under mild conditions. Mechanistic studies indicated that

peroxide intermediates may be involved in the reactions, which can be further transformed to final carbonyl products.

2.4 Experimental details

2.4.1 Details of photoreactors

Information for the blue LEDs: 2.95 V blue LED SMD, Lumileds LUXEON Rebel LXML-PB01-0040; dominant wavelength or Peak Wavelength (minimum: 460 nm, typical: 465 nm, maximum: 485 nm); typical spectral half-width (20 nm); typical temperature coefficient of dominant or Peak Wavelength (0.05 nm/°C); typical total included angle (160°); typical view angle (125°). Each hole on the photoreactor is fitted with three LEDs, giving a total power for each reaction tube as 9 W. Reactor temperature after 12 h irradiation is 45 °C.

Information for LEDs with various wavelengths:

UV LEDs (365 nm): 3.0 V UV LED SMD, LUMINUS SST-10-UV-E365-00; dominant wavelength or peak wavelength (minimum: 365 nm, typical: 365 nm, maximum: 370 nm); typical spectral half-width (10 nm); typical total included angle (160°); typical view angle (130°). Each hole on the photoreactor is fitted with three LEDs, giving a total power for each reaction tube as 9 W. Reactor temperature after 12 h irradiation is around 20 °C.

UV LEDs (405 nm): 3.0 V UV LED SMD, LUMINUS SST-10-UV-F405-00; dominant wavelength or peak wavelength (minimum: 405 nm, typical: 405 nm, maximum: 410 nm); typical spectral half-width (10 nm); typical total included angle (160°); typical view angle (130°). Each hole on the photoreactor is fitted with three LEDs, giving a total power for each reaction tube as 9 W.

Cyan LEDs (505 nm): 2.90 V cyan LED SMD, Lumileds LUXEON Rebel LXML-PE01-0080; dominant wavelength or peak wavelength (minimum: 495 nm, typical: 505 nm, maximum: 515 nm); typical spectral half-width (30 nm); typical temperature coefficient of dominant or Peak Wavelength (0.04 nm/°C); typical total included angle (160°); typical view

angle (125°). Each hole on the photoreactor is fitted with three LEDs, giving a total power for each reaction tube as 9 W.



Figure 2.5 Blue light photoreactor.

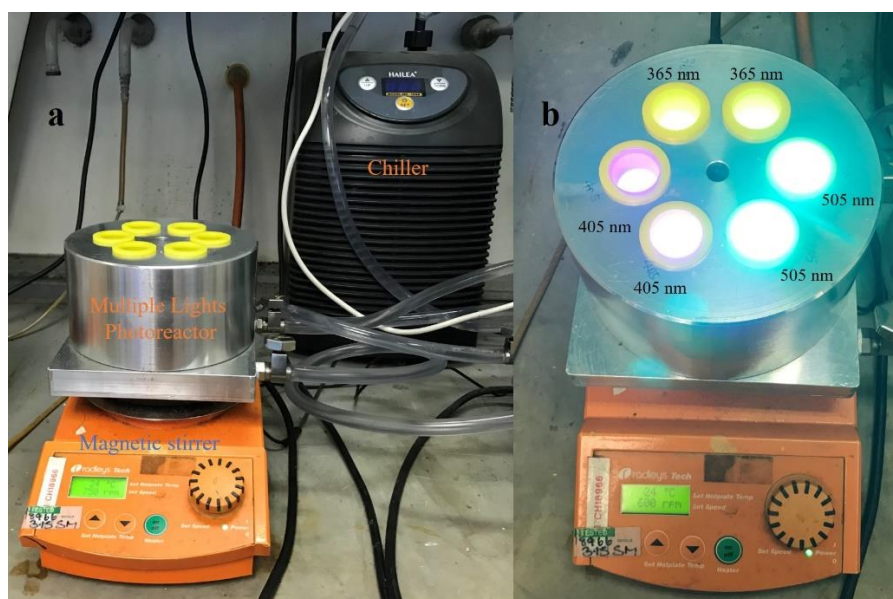
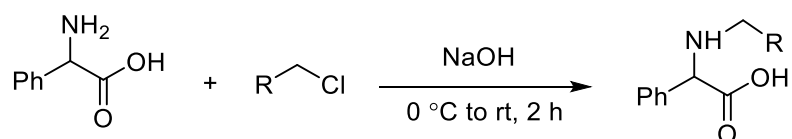


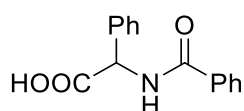
Figure 2.6 Multi-wavelength photoreactor.

2.4.2 Preparation of substrates

Synthesis of 2-(Benzylamino)-2-phenylacetic acid and 2-(((9H-Fluoren-9-yl)methoxy)carbonyl)amino)-2-phenylacetic acid



2-(Benzylamino)-2-phenylacetic acid (**1v**) and 2-([(9*H*-Fluoren-9-yl)methoxy]carbonyl]amino)-2-phenylacetic acid (**1x**) were synthesized according to the literature.⁶⁵ A mixture of 2.0 M NaOH (50 mL) and phenyl glycine (3.0 g, 19.85 mmol) were added to a 250 mL round-bottom flask equipped with a magnetic stirrer. Then, the solution was cooled to 0 °C in an ice bath. After that, benzoyl chloride or 9-fluorenylmethoxycarbonyl chloride (1.1 equiv., 21.83 mmol) was added to the mixture over the course of 20 mins. In the next step, the reaction was warmed to room temperature and stirred for 2 h. After completion of the reaction, 2.0 M HCl was added dropwise to make the solution slightly acidic (pH 5-6), and the mixture was extracted with ethyl acetate (75 mL × 5). The combined organic phase was dried over magnesium sulfate and concentrated to obtain **1v** or **1x**.



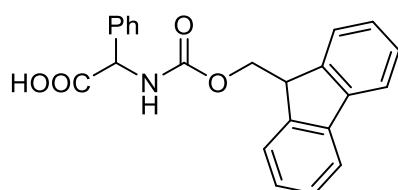
2-(Benzylamino)-2-phenylacetic acid (1v)⁶⁵

¹H NMR (400 MHz, DMSO-*d*₆) δ 12.94 (s, 1H), 9.05 (d, *J* = 7.5 Hz, 1H), 7.94 (dd, *J* = 7.2, 1.8 Hz, 2H), 7.56 – 7.32 (m, 8H), 5.64 (d, *J* = 7.5 Hz, 1H).

¹³C NMR (101 MHz, DMSO-*d*₆) δ 171.98, 166.37, 137.16, 131.51, 128.44, 128.23, 128.20, 127.94, 127.75, 56.88.

HRMS (ESI) calcd for C₁₅H₁₃NO₃ [M+Na]⁺: 278.0788; found: 278.0787.

Melting point: 170-172 °C.



2-([(9*H*-Fluoren-9-yl)methoxy]carbonyl]amino)-2-phenylacetic acid (1x)⁶⁶

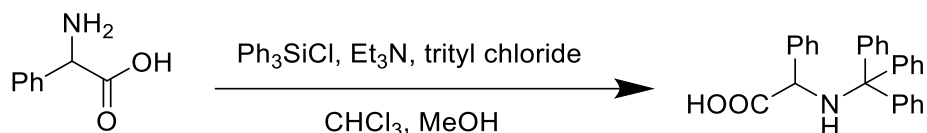
¹H NMR (400 MHz, DMSO-*d*₆) δ 12.89 (s, 1H), 8.23 (d, *J* = 8.1 Hz, 1H), 7.89 (d, *J* = 7.6 Hz, 2H), 7.76 (d, *J* = 7.6 Hz, 2H), 7.48 – 7.21 (m, 9H), 5.18 (d, *J* = 8.1 Hz, 1H), 4.31 – 4.17 (m, 3H).

^{13}C NMR (101 MHz, $\text{DMSO-}d_6$) δ 172.14, 155.88, 143.89, 143.79, 140.75, 137.39, 128.45, 127.90, 127.81, 127.69, 127.12, 127.10, 125.46, 125.42, 120.12, 65.99, 58.20, 46.65.

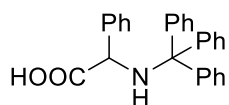
HRMS (ESI) calcd for $\text{C}_{23}\text{H}_{19}\text{NO}_4$ $[\text{M}+\text{Na}]^+$: 396.1207; found: 396.1198.

Melting point: 187-189 °C.

Synthesis of 2-(Triphenylmethylthio)acetic acid



2-(Triphenylmethylthio)acetic acid (**1w**) was synthesized according to the literature.⁶⁷ A mixture of 2-phenylglycine (1.81 g, 12 mmol) and triphenylsilyl chloride (Ph_3SiCl , 2.17g, 20 mmol) in 25 mL of CHCl_3 was heated under reflux for 2 h. After cooling to room temperature, triethylamine (Et_3N , 3.34 g, 33 mmol) and trityl chloride (2.79 g, 10 mmol) were added, and the mixture was stirred at room temperature for 20 h. Then, MeOH (1.60g, 50 mmol) was added and stirred for 0.5 h. The reaction mixture was concentrated under reduced pressure and the residue was dissolved in ethyl acetate (50 mL). The organic layer was washed with 10% aqueous citric acid (50 mL \times 3), and brine (50 mL) and dried over MgSO_4 . The solvent was evaporated, and the oily crude product was recrystallized from CHCl_3 /hexane to give **1w** as a colourless solid.



2-(Triphenylmethylthio)acetic acid (**1w**)

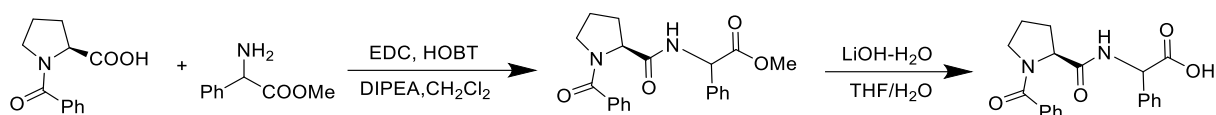
^1H NMR (400 MHz, Chloroform-*d*) δ 7.47 (d, $J = 7.1$ Hz, 2H), 7.44 – 7.37 (m, 8H), 7.36 – 7.28 (m, 2H), 7.17 (t, $J = 7.6$ Hz, 6H), 7.06 (t, $J = 7.3$ Hz, 3H), 4.36 (s, 1H).

^{13}C NMR (101 MHz, Chloroform-*d*) δ 177.26, 145.34, 139.26, 129.67, 128.86, 128.71, 127.91, 127.13, 126.74, 72.09, 60.22.

HRMS (ESI) calcd for $\text{C}_{27}\text{H}_{23}\text{NO}_2$ $[\text{M}+\text{Na}]^+$: 416.1621; found: 416.1623.

Melting point: 195-197 °C.

Synthesis of 2-(Triphenylmethylthio)acetic acid

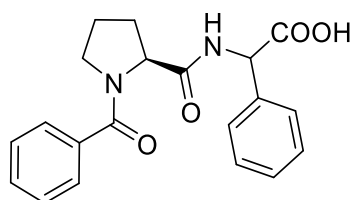


2-((S)-1-Benzoylpyrrolidine-2-carboxamido)-2-phenylacetic acid (**1y**) was synthesized according to the literature.⁶⁸ Methyl 2-amino-2-phenylacetate hydrochloride (2.01 g, 1.0 equiv., 10 mmol) was weighed into a round-bottom flask with a stirrer bar, diluted with CH₂Cl₂ (108 mL), and cooled to 0 °C in an ice bath. To this solution, diisopropyl ethylamine (1.74 mL, 1.0 equiv., 10 mmol) was added dropwise. Next, reagents were added in the following order: 1) *N*-benzoyl-*L*-proline (**4e**) (2.19 g, 1.0 equiv., 10 mmol), 2) hydroxybenzotriazole (HOBt, 20% by weight H₂O, 1.49 g, 1.1 equiv.), and 3) 1-ethyl-3-(3-dimethylaminopropyl)carbodiimide hydrochloride (EDC, 1.92 g, 1.0 equiv., 10 mmol), and the reaction was warmed to room temperature. The reaction was then stirred overnight or until complete consumption of the carboxylic acid coupling partner was observed by TLC (typically: 1% acetic acid in ethyl acetate eluent).

The reaction contents were added to an appropriately sized separatory funnel and washed with a 1:1 volume each of saturated NaHCO₃ solution, 10 wt% aqueous citric acid, and brine. Following each of the first two washes, the aqueous layer was extracted with CH₂Cl₂ (× 2), and the combined organic layers were combined for the next wash. The combined organic layers were then dried over Na₂SO₄, filtered, and concentrated *in vacuo* to provide crude ester product (assumed quantitative yield) which was taken on without further purification to the next step. (Note 1: in order to achieve a dry solid after purification, it may be necessary to dry the pure oil *in vacuo* from hexane several times to completely remove residual CH₂Cl₂, followed by placement on a high vacuum line for 24 h. Note 2: in the case of using a free amine methyl ester in place of a hydrochloride salt, DIPEA (0.1 equiv.) was used).

Then the ester product underwent hydrolysis to afford the final acid product (**1y**). To a glass round-bottom flask with Teflon stir bar was added crude ester product in 3:1 of THF:H₂O (30 mL, 0.5 M). The solution was cooled to 0 °C in an ice bath, and LiOH (2.1 g, 5.0 equiv., 50 mmol) was added in 1 portion. The reaction was held at 0 °C for 10 mins, and then warmed to room temperature and stirred for 24 h, or until complete conversion of the ester was observed by TLC.

Upon complete conversion, the reaction was cooled back down to 0 °C, and acidified to a pH of < 2 via dropwise addition of 10 wt% aqueous KHSO₄. The solution was then diluted with ethyl acetate (~1:1 v/v) and the two layers were separated via a separatory funnel. The pH of the aqueous layer was then taken. If it was found to be > 4/5, the aqueous layer was re-acidified with 10 wt% aqueous KHSO₄ to pH < 2. It was then extracted with ethyl acetate (× 2), making sure to retain an acidic pH before each extraction. The organic layers were combined and washed with water (× 1) and brine (× 1), dried over MgSO₄, filtered, and concentrated *in vacuo* to afford the crude acid product (**1y**), which was purified via flash chromatography on silica gel.



2-((S)-1-Benzoylpyrrolidine-2-carboxamido)-2-phenylacetic acid (1y**)**

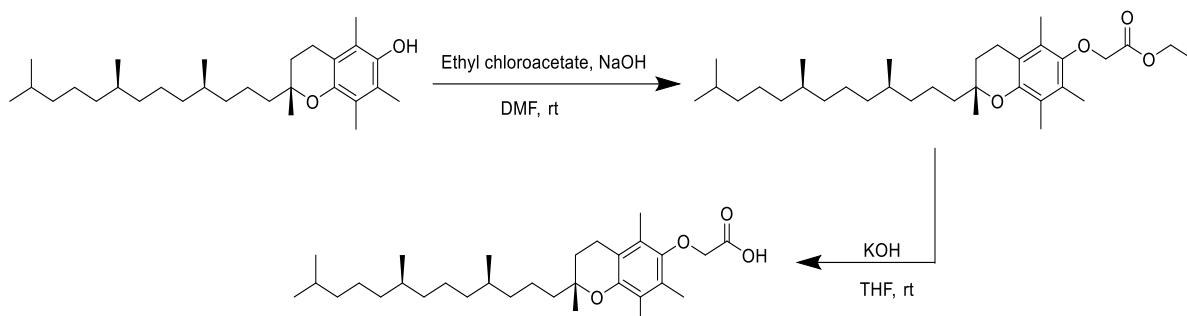
¹H NMR (400 MHz, Chloroform-*d*) δ 9.05 (s, 1H), 8.13 (dd, *J* = 45.1, 6.8 Hz, 1H), 7.56-7.28 (m, 10H), 5.61 (dd, *J* = 15.4, 6.8 Hz, 1H), 4.92 (dt, *J* = 45.3, 6.8 Hz, 1H), 3.59-3.4 (m, 2H), 2.23-1.68 (m, 4H).

¹³C NMR (101 MHz, Chloroform-*d*) δ 172.52, 172.26, 170.97, 136.40, 135.36, 130.34, 128.65, 128.60, 128.23, 127.05, 127.01, 59.94, 56.60, 50.47, 28.51, 25.01.

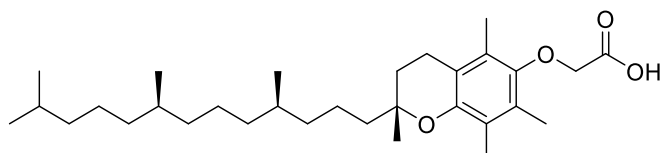
HRMS (ESI) calcd for C₂₀H₂₀N₂O₄ [M+Na]⁺: 375.1315; found: 375.1311.

Melting point: 157-158 °C.

Synthesis of 2-((*R*)-2,5,7,8-tetramethyl-2-((*4R,8R*)-4,8,12-trimethyltridecyl)chroman-6-yloxy)acetic acid



2-((*R*)-2,5,7,8-Tetramethyl-2-((*4R,8R*)-4,8,12-trimethyltridecyl)chroman-6-yloxy)acetic acid was synthesized according to the literature.⁶⁹ To a mixture of (*2R*)-2,5,7,8-tetramethyl-2-[(*4R,8R*)-(4,8,12-trimethyltridecyl)]-6-chroman-ol (1.7 g, 4.25 mmol) in DMF (50 mL), ethyl chloroacetate (0.6 g, 4.85 mmol) and powdered NaOH (240 mg, 6 mmol) were added, and the mixture was stirred at room temperature and monitored by TLC until there was no starting material remaining. Then, the aqueous was extracted with ethyl acetate (75 mL × 2), and the combined ethyl acetate fractions were washed with brine (100 mL × 2) and water (100 mL × 1), and dried over MgSO₄. After removal of the solvent, the ester product was obtained as a colourless oil compound, and it was used in the next step without purification. A mixture of ester compound (1 g, 1.92 mmol) in THF (10 mL) and 10% KOH (30 mL) was stirred at room temperature for 5 h, and then the THF was evaporated, and the residue was neutralized with HCl and extracted with CH₂Cl₂. Afterwards, it was washed with water, and dried over MgSO₄. The solvent was evaporated to give the acid product as pale yellow oil without purification.



2-((*R*)-2,5,7,8-tetramethyl-2-((*4R,8R*)-4,8,12-trimethyltridecyl)chroman-6-yloxy)acetic acid

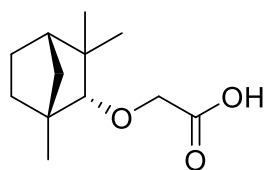
^1H NMR (400 MHz, Chloroform-*d*) δ 4.32 (m, $J = 25.6$ Hz, 2H), 2.57 (q, $J = 5.8, 4.9$ Hz, 2H), 2.17 (s, 3H), 2.13 (s, 3H), 2.09 (s, 3H), 1.79 (qt, $J = 13.3, 6.8$ Hz, 2H), 1.61 – 1.48 (m, 3H), 1.42 – 1.20 (m, 15H), 1.16 – 1.02 (m, 6H), 0.86 (m, 12H).

^{13}C NMR (101 MHz, Chloroform-*d*) δ 172.41, 148.59, 146.80, 127.28, 125.41, 123.31, 117.83, 75.03, 69.12, 39.99, 39.36, 37.44, 37.39, 37.37, 37.27, 32.78, 32.68, 31.14, 27.96, 24.79, 24.42, 23.83, 22.71, 22.61, 21.01, 20.60, 19.73, 19.67, 12.72, 11.86, 11.77.

HRMS (CI) calcd for $\text{C}_{31}\text{H}_{52}\text{O}_4$ $[\text{M}+\text{H}]^+$: 489.3938; found: 489.3941.

Synthesis of (*1R-endo*)-[(1,3,3-Trimethylbicyclo[2.2.1]hept-2-yl)oxy]-acetic acid

(*1R-endo*)-[(1,3,3-Trimethylbicyclo[2.2.1]hept-2-yl)oxy]-acetic acid (**4c**) was synthesized according to the literature.⁷⁰ To a suspension of NaH (1 g, 60% dispersion in mineral oil, 25.0 mmol) in dry THF (35 mL) under Ar at 0 °C, was added a solution of (*1R,2R,4S*)-1,3,3-trimethylbicyclo[2.2.1]heptan-2-ol (11.3 mmol) in THF (5 mL). After the mixture was stirred for 1 h, a solution of 2-bromo-acetic acid (0.99 g, 7.1 mmol) in THF (20 mL) was added and the mixture was heated to reflux overnight. The mixture was then quenched with methanol (20 mL), diluted with water, and washed with ether. The aqueous layer was then acidified with concentrated HCl to pH 4, and extracted with ethyl acetate. The combined ethyl acetate extracts were dried (Na_2SO_4) and filtered, and the solvent was evaporated to give **4c**.



(*1R-endo*)-[(1,3,3-Trimethylbicyclo[2.2.1]hept-2-yl)oxy]-acetic acid (**4c**)

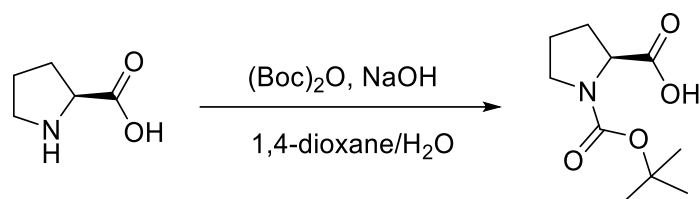
^1H NMR (400 MHz, Chloroform-*d*) δ 4.22 – 4.00 (m, 2H), 3.04 (s, 1H), 1.74 – 1.66 (m, 3H), 1.49 – 1.40 (m, 2H), 1.14 – 1.01 (m, 8H), 0.94 (s, 3H).

^{13}C NMR (101 MHz, Chloroform-*d*) δ 172.48, 95.08, 68.75, 49.22, 48.47, 41.35, 39.60, 31.42, 25.96, 25.85, 20.57, 20.00.

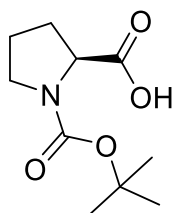
HRMS (CI) calcd for $\text{C}_{12}\text{H}_{20}\text{O}_3$ $[\text{M}+\text{H}]^+$: 213.1486; found: 213.1495.

Melting point: 89-90 °C.

Synthesis of (*tert*-Butoxycarbonyl)proline



(*tert*-Butoxycarbonyl)proline (**4d**) was synthesized according to the literature.⁷¹ To a solution of *L*-proline (1.15 g, 10 mmol) in 1,4-dioxane (15 mL) was added NaOH (0.48 g, 12 mmol), H₂O (10 mL) at 0 °C. After stirring for 20 mins, di-*tert*-butyl dicarbonate (Boc₂O, 2.76 mL, 12 mmol) was added. Then, the reaction was stirred at room temperature and detected by TLC until the reaction was finished. The mixture was diluted with H₂O and washed with Et₂O (× 1). The aqueous layer was acidified with 10% HCl to pH 1 and extracted with ethyl acetate. The organic layer was dried over MgSO₄ and evaporated, affording **4e** as colourless crystals.



(*tert*-Butoxycarbonyl)proline (**4d**)

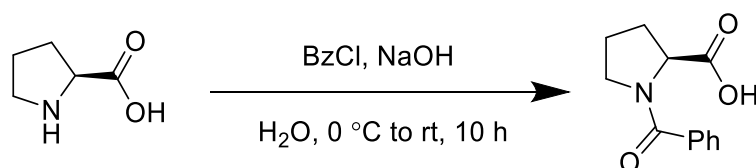
¹H NMR (400 MHz, Chloroform-*d*) δ 11.40 (s, 1H), 4.37 – 4.11 (m, 1H), 3.54 – 3.25 (m, 2H), 2.27 – 1.72 (m, 4H), 1.38 (m, 9H).

¹³C NMR (101 MHz, Chloroform-*d*) δ 178.14, 176.44, 155.34, 153.91, 80.56, 80.25, 58.82, 58.72, 46.63, 46.19, 30.65, 29.16, 28.23, 28.09, 24.11, 23.48.

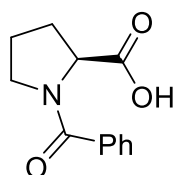
HRMS (ESI) calcd for C₁₀H₁₇NO₄ [M+Na]⁺: 238.1050; found: 238.1053.

Melting point: 130-132 °C.

Synthesis of *N*-Benzoyl-*L*-proline



N-Benzoyl-*L*-proline (**4e**) was synthesized according to the literature.⁷² To a solution of *L*-proline (4.00 g, 34.7 mmol) and NaOH (2.78 g, 69.5 mmol) in H₂O (64 mL) was added benzoyl chloride (BzCl, 4.0 mL, 34.7 mmol) dropwise at 0 °C. The mixture was stirred for 10 h at room temperature. The mixture was diluted with H₂O and washed with Et₂O (× 1). The aqueous layer was acidified with 10% HCl to pH = 1 and extracted with ethyl acetate. The organic layer was dried over MgSO₄ and evaporated to afford **4e** as colourless crystals.



***N*-Benzoyl-*L*-proline (**4e**)**

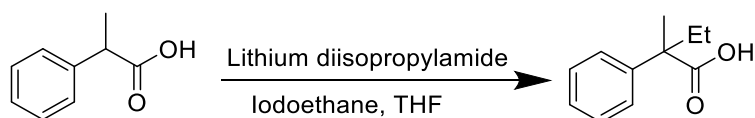
¹H NMR (400 MHz, Chloroform-*d*) δ 10.09 (s, 1H), 7.59 – 7.53 (m, 2H), 7.48 – 7.38 (m, 3H), 4.74 (t, *J* = 6.0 Hz, 1H), 3.62-3.52 (m, 2H), 2.34 – 2.22 (m, 2H), 2.06-1.98 (m, 1H), 1.94-1.84 (m, 1H).

¹³C NMR (101 MHz, Chloroform-*d*) δ 174.35, 171.20, 135.30, 130.56, 128.36, 127.22, 59.75, 50.37, 28.55, 25.16.

HRMS (ESI) calcd for C₁₂H₁₃NO₃ [M+Na]⁺: 242.0788; found: 242.0784.

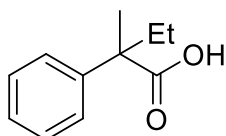
Melting point: 150-152 °C.

Synthesis of 2-methyl-2-phenylbutanoic acid



Acid **6c** was synthesized according to the literature.⁷³ A solution containing 2-phenylpropanoic acid (10.0 mmol) in dry tetrahydrofuran (5 mL) was added to lithium diisopropylamide (25.0 mmol) in dry tetrahydrofuran (20 mL) at 0 °C. The suspension was stirred for 1 hour at 25 °C and then for 30 minutes at 60 °C. The mixture was then cooled to 0 °C and iodoethane (25.0 mmol) was added dropwise and the reaction stirred at 25 °C for 21 hours. The mixture was quenched with saturated ammonium chloride (aq), acidified with

concentrated sulfuric acid and the layers separated. The aqueous layer was then extracted with diethyl ether (50 mL \times 2). The ether layers were combined and washed with 20% K_2CO_3 (50 mL), dried over magnesium sulfate, filtered and concentrated in *vacuo*. The acid **6c** was then used without further purification.



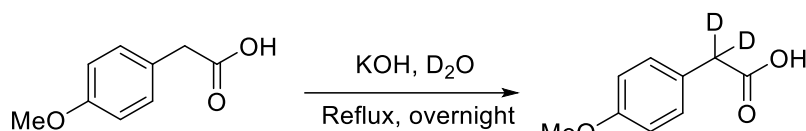
2-Methyl-2-phenylbutanoic acid (**6c**)⁷⁴

1H NMR (400 MHz, Chloroform-*d*) δ 7.43 – 7.20 (m, 5H), 2.05 (m, 2H), 1.57 (s, 3H), 0.86 (t, J = 6.6 Hz, 3H).

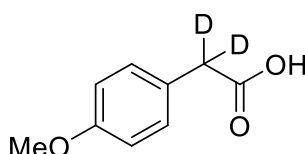
^{13}C NMR (101 MHz, Chloroform-*d*) δ 182.68, 142.80, 128.37, 126.86, 126.25, 50.35, 31.59, 21.67, 9.02.

Melting point: 135-136 °C.

Synthesis of 2-(4-Methoxyphenyl)acetic-2,2- d^2 acid



Acid **1a- d^2** was synthesized according to the literature.⁷⁵ A mixture of 2-(4-methoxyphenyl)acetic acid (1.83 g), anhydrous potassium hydroxide (2.24 g, 40.0 mmol) and deuterium oxide (7.5 mL) was heated to reflux overnight. After the reaction, the mixture was cooled to room temperature. The reaction mixture was acidified to pH = 2 with 6 N HCl. The solution was then extracted with diethyl ether (50 mL \times 3). The combined organic layers were washed with brine, and dried over Na_2SO_4 . After evaporating the combined organic layers *in vacuo*, **1h- d^2** was afforded as a colourless powder.



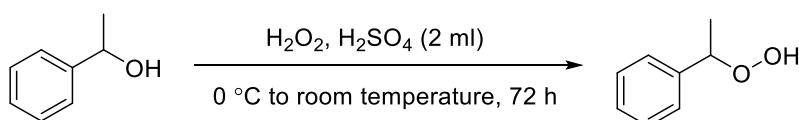
2-(4-Methoxyphenyl)acetic-2,2- d^2 acid (**1h- d^2**)⁷⁶

^1H NMR (400 MHz, Chloroform-*d*) δ 7.21 (d, J = 8.6 Hz, 2H), 6.88 (d, J = 8.6 Hz, 2H), 3.80 (s, 3H).

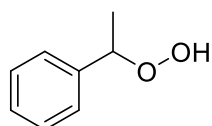
^{13}C NMR (101 MHz, Chloroform-*d*) δ 178.23, 158.83, 130.34, 125.21, 114.05, 55.22, 39.81 (m).

Melting point: 78-80 °C.

Synthesis of 1-phenylethyl hydroperoxide (**9**)



1-Phenylethyl hydroperoxide (**9**) was *in situ* synthesized according to the literature.⁷⁷ To a cooled (0 °C) solution of H_2O_2 (25.05 ml, 0.25 mol, 30 wt% in H_2O) and H_2SO_4 (0.25 mL, 4.5 mmol) was added 1-phenylethanol (1.15 g, 9 mmol). The reaction mixture was stirred vigorously for 72 h at ambient temperature and partitioned between Et_2O (20 mL) and water (30 mL). The aqueous layer was extracted with Et_2O (2×20 mL). The combined fractions were dried over MgSO_4 , concentrated *in vacuo* and purified by flash chromatography (hexane/ethyl acetate 9:1) to yield the hydroperoxide.



1-Phenylethyl hydroperoxide (**9**)

^1H NMR (400 MHz, Chloroform-*d*) δ 7.74 (b, 1H), 7.43 – 7.30 (m, 5H), 5.09 (q, J = 6.6 Hz, 1H), 1.48 (d, J = 6.6 Hz, 3H).

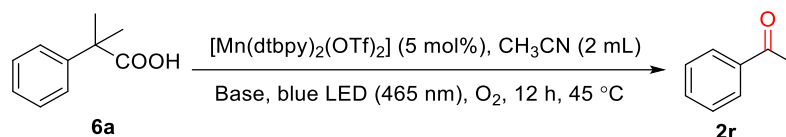
^{13}C NMR (101 MHz, Chloroform-*d*) δ 141.37, 128.68, 128.28, 126.51, 83.79, 20.08.

2.4.3 Optimization of experimental conditions

To an oven dried Schlenk tube, $[\text{Mn}(\text{dtbpy})_2(\text{OTf})_2]$ (5 mol%) was *in situ* synthesized. Then, acid (0.5 mmol), base and CH_3CN (1 mL) were added under N_2 . The reaction tube was then fitted with an oxygen balloon, and was allowed to stir at room temperature under blue light for 12 h. After the reaction, mesitylene (17.3 mg) as internal standard, water (2 mL) and

CDCl₃ (2 mL) were added. Finally, the product yield of **2r** was obtained by ¹H NMR analysis of the organic layer.

Table 2.3 Effect of bases on oxidative decarboxylation/oxidation of acid **6a**^{a, b}



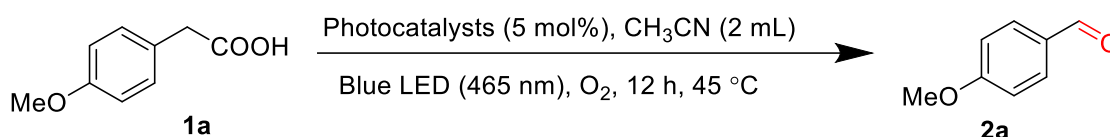
Entry	Base	Content	Yield (%)
1	KOH	10 mol%	48
2	NaOH	10 mol%	49
3	LiOH	10 mol%	50
4	K ₂ CO ₃	10 mol%	44
5	Na ₂ CO ₃	10 mol%	39
6	NaOAc	10 mol%	53
7	NaOAc	30 mol%	79
8	NaOAc	90 mol%	79
9	KOAc	30 mol%	46
10	LiOAc	30 mol%	73

^aReaction conditions: **6a** (0.5 mmol), [Mn(dtbpy)₂(OTf)₂] (5 mol%), base, solvent (2 mL), under blue LED light (465 nm, 9 W) at 45 °C under O₂ atmosphere (1 atm) for 12 h. ^bNMR yields are given.

2.4.4 Mechanistic studies

Control experiments

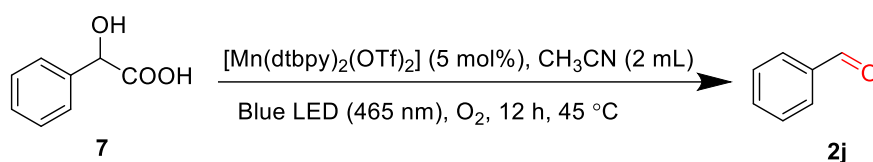
Decarboxylative oxygenation of 2-(4-methoxyphenyl)acetic acid (**1a**) with well-known photosensitizers capable of producing singlet oxygen



To an oven dried Schlenk tube, a photocatalyst (5 mol%) and **1a** (0.5 mmol) were added. Then the reaction tube was placed under vacuum and purged with nitrogen at least three times. The reaction tube was fitted with an oxygen balloon, and CH₃CN (2 mL) was added under

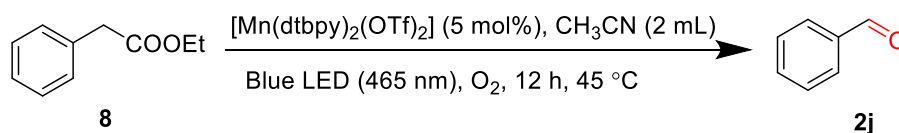
N₂. The reaction tube was allowed to stir at room temperature under blue light (465 nm) for 12 h. After the reaction, mesitylene (17.3 mg) as internal standard, water (2 mL) and CDCl₃ (2 mL) were added. Finally, the product yield of **2a** was obtained by ¹H NMR analysis of the organic layer. The photocatalysts tested were Eosin Y disodium salt, [Ru(bpy)₃•6H₂O], [Ir(dFppy)₃] and rose Bengal.

Decarboxylative oxygenation of 2-hydroxy-2-phenylacetic acid (**7**)



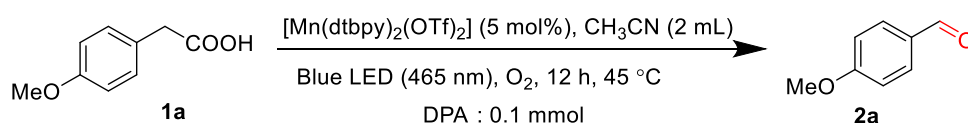
To an oven dried Schlenk tube, [Mn(dtbp)₂(OTf)₂] (5 mol%) was *in situ* synthesized. Then, 2-hydroxy-2-phenylacetic acid (**7**, 0.5 mmol) and CH₃CN (1 mL) were added under N₂. The reaction tube was then fitted with an oxygen balloon, and was allowed to stir at room temperature under blue light (465 nm) for 12 h. After the reaction, mesitylene (17.3 mg) as internal standard, water (2 mL) and CDCl₃ (2 mL) were added. Finally, the product yield of **2j** was obtained by ¹H NMR analysis of the organic layer.

Decarboxylative oxygenation of ethyl 2-phenylacetate (**8**)



To an oven dried Schlenk tube, [Mn(dtbp)₂(OTf)₂] (5 mol%) was *in situ* synthesized. Then, ethyl 2-phenylacetate (**8**, 0.5 mmol) and CH₃CN (1 mL) were added under N₂. The reaction tube was then fitted with an oxygen balloon, and was allowed to stir at room temperature under blue light (465 nm) for 12 h. After reaction, mesitylene (17.3 mg) as internal standard, water (2 mL) and CDCl₃ (2 mL) were added. Finally, the product yield of **2j** was obtained by ¹H NMR analysis of the organic layer.

Singlet oxygen trap experiment



To an oven dried Schlenk tube, $[\text{Mn}(\text{dtbpy})_2(\text{OTf})_2]$ (5 mol%) was *in situ* synthesized. Then, **1a** (0.5 mmol), 9,10-diphenylanthracene (33 mg, 0.1 mmol, singlet oxygen trap) and CH_3CN (2 ml) were added under N_2 . The reaction tube was then fitted with an oxygen balloon, and was allowed to stir at room temperature under blue light (465 nm) for 12 h. The product yield of **2a** (70%) was obtained by ^1H NMR analysis with mesitylene (17.3 mg) as internal standard. In the meantime, no 9,10-diphenyl-4a,9,9a,10-tetrahydro-9,10-epidioxyanthracene was observed by ^1H NMR analysis. These results indicated that singlet oxygen was not involved as the key intermediate during the decarboxylative oxygenation.

Light on/off experiments

To an oven dried Schlenk tube, $[\text{Mn}(\text{dtbpy})_2(\text{OTf})_2]$ (5 mol%) was *in situ* synthesized and 1,3,5-tribromobenzene (62.4 mg) as internal standard were added. CH_3CN (2 mL) was injected through a syringe, and **1a** (0.5 mmol) was added under N_2 . The reaction tube was then fitted with an oxygen balloon, and was allowed to stir at room temperature under blue light. After 1 h, 0.1 mL of the reaction mixture was taken out for ^1H NMR analysis; in the meantime, the reaction tube was further stirred in the dark. After 1 h, 0.1 mL of the reaction mixture was taken out for ^1H NMR analysis, and the reaction tube was exposed to blue light again for another 1 h, followed by ^1H NMR analysis. This on/off process was further repeated.

UV-Vis experiment

$[\text{Mn}(\text{dtbpy})_2(\text{OTf})_2]$: To an oven dried Schlenk tube, $[\text{Mn}(\text{dtbpy})_2(\text{OTf})_2]$ (5 mol%, 0.5 mmol) was *in situ* synthesized, and then CH_3CN (1 mL) was added under N_2 . 0.1 mL of the solution was then taken out and diluted to 10 mL for UV-Vis analysis.

1a: **1a** (0.5 mmol) was dissolved in CH_3CN (2 mL). 0.1 mL of the solution was then taken out and diluted to 10 mL for UV-Vis analysis.

The mixture of $[\text{Mn}(\text{dtbpy})_2(\text{OTf})_2]$ and **1a** in the absence of blue light: To an oven dried Schlenk tube, $[\text{Mn}(\text{dtbpy})_2(\text{OTf})_2]$ (5 mol%) was *in situ* synthesized. Then **1a** (0.5 mmol) and

CH₃CN (1 mL) was added under N₂. The reaction tube was then fitted with an oxygen balloon, and was allowed to stir at room temperature in dark for 1 h. Then, 0.1 mL of the solution was taken out and diluted to 10 mL for UV-Vis analysis.

The mixture of [Mn(dtbpy)₂(OTf)₂] and **1a** in the presence of blue light: To an oven dried Schlenk tube, [Mn(dtbpy)₂(OTf)₂] (5 mol%) was *in situ* synthesized. Then **1a** (0.5 mmol) and CH₃CN (1 mL) were added under N₂. The reaction tube was then fitted with an oxygen balloon, and was allowed to stir at room temperature under blue light (465 nm) for 1 h. 0.1 mL of the solution was then taken out and diluted to 10 mL for UV-Vis analysis.

In situ UV-Vis monitoring of the mixture of [Mn(dtbpy)₂(OTf)₂] and **9**: To an oven dried Schlenk tube, [Mn(dtbpy)₂(OTf)₂] (5 mol%) was *in situ* synthesized, and then CH₃CN (1 mL) was added under N₂. 0.1 mL of the solution was then taken out and diluted to 10 mL. After the addition of 2 mL of the solution to a cuvette, **9** (50 25 μmol) was added to the cuvette and UV-Vis monitoring was started immediately. The mixture was monitored by UV-Vis again at 10 mins and 30 mins.

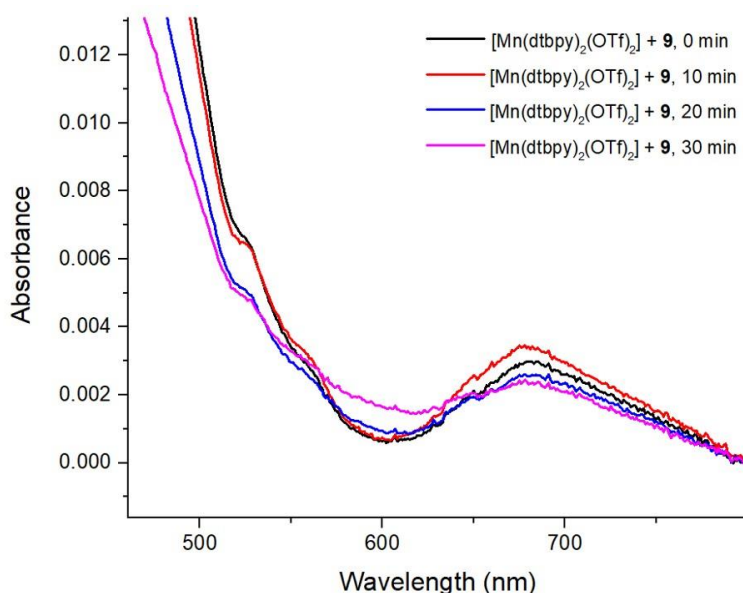


Figure 2.7 UV-Vis analysis of the mixture of [Mn(dtbpy)₂(OTf)₂] and **9**.

The mixture of [Mn(dtbpy)₂(OTf)₂] and **9**: To an oven dried Schlenk tube, [Mn(dtbpy)₂(OTf)₂] (5 mol%) was *in situ* synthesized, and then **9** (0.5 mmol) and CH₃CN (1

mL) were added under N₂. It was then allowed to stir at room temperature in the dark. 0.1 mL of the solution was taken out every 10 mins, and it was diluted to 10 mL for UV-Vis analysis.

Kinetic behaviours of decarboxylative oxygenation of acid **1r and 1-phenylethyl hydroperoxide (**9**)**

Decarboxylative oxygenation of **1r**: To an oven dried Schlenk tube, [Mn(dtbpy)₂(OTf)₂] (5 mol%) was *in situ* synthesized and 1,3,5-tribromobenzene (62.4 mg) as internal standard was added. CH₃CN (1 mL) was injected through a syringe, and acid **1r** (0.5 mmol) was added under N₂. The reaction tube was then allowed to stir under blue light. Every 20 min, 0.1 mL of the reaction mixture was taken out for ¹H NMR analysis.

Decarboxylative oxygenation of **9**: To an oven dried Schlenk tube, [Mn(dtbpy)₂(OTf)₂] (5 mol%) was *in situ* synthesized and 1,3,5-tribromobenzene (62.4 mg) as internal standard was added. CH₃CN (1 mL) was injected through a syringe, and 1-phenylethyl hydroperoxide (**9**) (0.5 mmol) was added under N₂. The reaction tube was then allowed to stir under blue light. Every 20 min, 0.1 mL of the reaction mixture was taken out for ¹H NMR analysis.

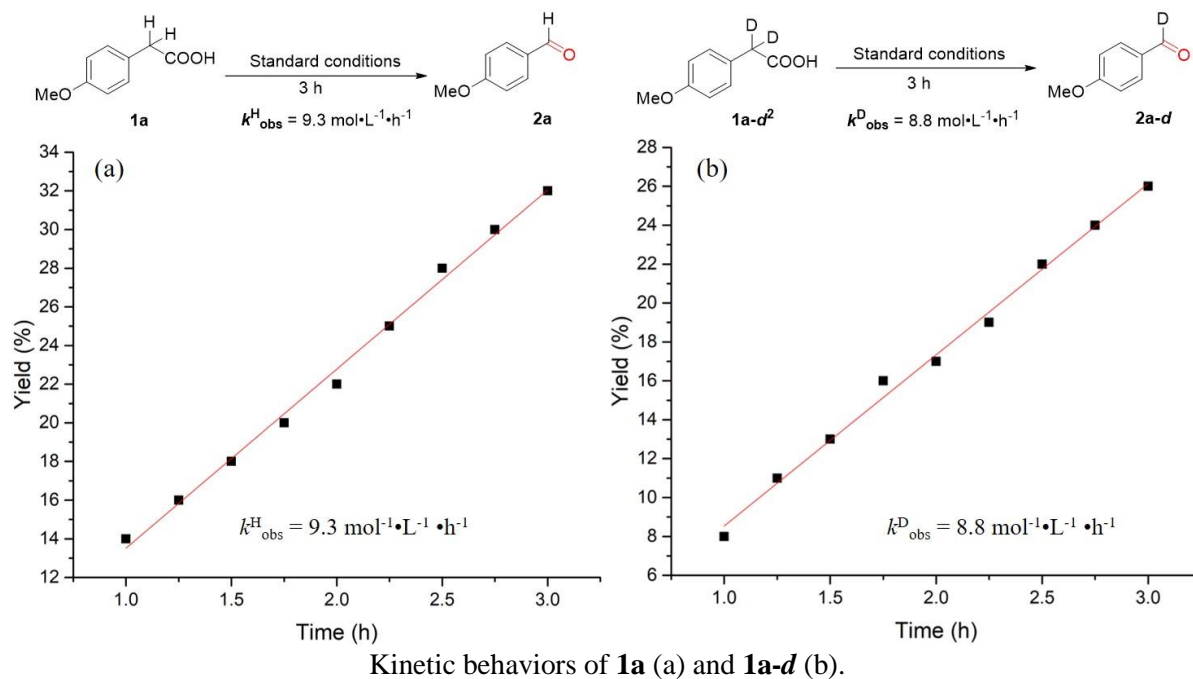
Reaction of 1-phenylethyl hydroperoxide (9**) without blue light irradiation under N₂.**

To an oven dried Schlenk tube, [Mn(dtbpy)₂(OTf)₂] (5 mol%) was *in situ* synthesized. CH₃CN (1 mL) was injected through a syringe, and **9** (0.5 mmol) was added under N₂. The reaction tube was allowed to stir at room temperature for 1 h. After the reaction, mesitylene (17.3 mg) as internal standard, water (2 mL) and CDCl₃ (2 mL) were added. Finally, the product yield of **2r** was obtained by ¹H NMR analysis of the organic layer.

Kinetic isotope effect (KIE) experiment

To an oven dried Schlenk tube, [Mn(dtbpy)₂(OTf)₂] (5 mol%) was *in situ* synthesized and 1,3,5-tribromobenzene (62.4 mg) as internal standard was added. CH₃CN (1 mL) was injected through a syringe, and **1a** (0.5 mmol) was added under N₂. The reaction tube was then fitted with an oxygen balloon, and was allowed to stir at room temperature under blue light. Every

15 mins, 0.1 mL of the reaction mixture was taken out for ^1H NMR analysis. Meanwhile, the deuterated acid **1a-d²** was tested in the experiment using the same procedures. The yields of **2a** and **2a-d** between 1 h and 3 h were collected and analysed by Origin 2016 to get corresponding $k_{\text{obs}}^{\text{H}}$ and $k_{\text{obs}}^{\text{D}}$ values.



Kinetic behaviors of **1a** (a) and **1a-d** (b).

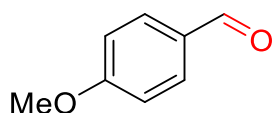
HRMS analysis of $[\text{Mn}(\text{dtbpy})_2(\mathbf{1a-H})(\text{OTf})_2]$ complex

To an oven dried Schlenk tube, $[\text{Mn}(\text{dtbpy})_2(\text{OTf})_2]$ (5 mol%) was *in situ* synthesized. CH_3CN (1 mL) was injected through a syringe, and **1a** (0.5 mmol) was added under N_2 . The reaction tube was then fitted with an oxygen balloon, and was allowed to stir in the dark for 2 h. Then, the solution was analysed by HRMS.

$[\text{Ir}(\text{dFppy})_3]$ -catalysed decarboxylative oxygenation of **1a**

The dose of $[\text{Ir}(\text{dFppy})_3]$, solvent and base was chosen according to MacMillan's work.¹⁵ To an oven dried Schlenk tube, $[\text{Ir}(\text{dFppy})_3]$ (1 mol%), **1a** (0.5 mmol), Na_2CO_3 (0.5 mmol) and DMSO (2 mL) were added under N_2 . The reaction tube was then fitted with an oxygen balloon, and was allowed to stir at room temperature under blue light for 16 h. After the reaction, mesitylene (17.3 mg) as internal standard, water (2 mL) and CDCl_3 (2 mL) were added. Finally, the product yield of **2a** was obtained by ^1H NMR analysis of the organic layer.

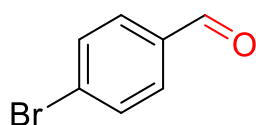
2.5 Analytical data of products



4-Methoxybenzaldehyde (2a)⁷⁸

¹H NMR (400 MHz, Chloroform-*d*) δ 9.87 (s, 1H), 7.82 (d, $J = 8.8$ Hz, 2H), 6.99 (d, $J = 8.8$ Hz, 2H), 3.87 (s, 3H).

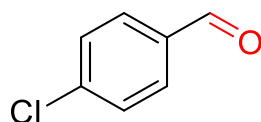
¹³C NMR (101 MHz, Chloroform-*d*) δ 190.72, 164.54, 131.91, 129.90, 114.25, 55.52.



4-Bromobenzaldehyde (2b)⁷⁹

¹H NMR (400 MHz, Chloroform-*d*) δ 9.97 (s, 1H), 7.74 (d, $J = 8.5$ Hz, 2H), 7.68 (d, $J = 8.5$ Hz, 2H).

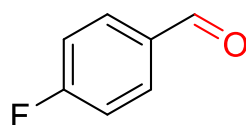
¹³C NMR (101 MHz, Chloroform-*d*) δ 191.00, 135.04, 132.41, 130.93, 129.74.



4-Chlorobenzaldehyde (2c)⁷⁹

¹H NMR (400 MHz, Chloroform-*d*) δ 9.99 (s, 1H), 7.83 (d, $J = 8.5$ Hz, 2H), 7.52 (d, $J = 8.5$ Hz, 2H).

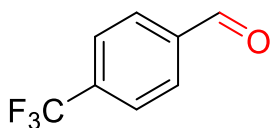
¹³C NMR (101 MHz, Chloroform-*d*) δ 190.83, 140.95, 134.70, 130.89, 129.45.



4-Fluorobenzaldehyde (2d)⁸⁰

¹H NMR (400 MHz, Chloroform-*d*) δ 9.94 (s, 1H), 7.90 – 7.86 (m, 2H), 7.20 – 7.16 (m, 2H).

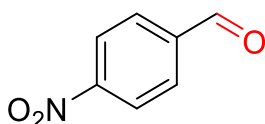
¹³C NMR (101 MHz, Chloroform-*d*) δ 190.42, 166.43 (d, $J_{C-F} = 256.7$ Hz), 132.90 (d, $J_{C-F} = 2.7$ Hz), 132.14 (d, $J_{C-F} = 9.7$ Hz), 116.25 (d, $J_{C-F} = 22.3$ Hz).



4-(Trifluoromethyl)benzaldehyde (2e)⁸¹

¹H NMR (400 MHz, Chloroform-*d*) δ 9.94 (s, 1H), 7.93 – 7.83 (m, 2H), 7.21-7.15 (m, 2H).

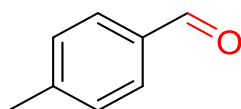
¹³C NMR (101 MHz, Chloroform-*d*) δ 191.08, 138.65, 135.62 (q, J_{C-F} = 32.7 Hz), 129.91, 126.11 (q, J_{C-F} = 3.7 Hz), 123.42 (d, J_{C-F} = 272.8 Hz).



4-Nitrobenzaldehyde (2f)⁷⁹

¹H NMR (400 MHz, Chloroform-*d*) δ 10.16 (s, 1H), 8.39 (d, J = 8.7 Hz, 2H), 8.07 (d, J = 8.7 Hz, 2H).

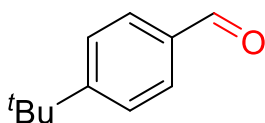
¹³C NMR (101 MHz, Chloroform-*d*) δ 190.25, 151.08, 140.01, 130.44, 124.26.



4-Methylbenzaldehyde (2g)⁷⁹

¹H NMR (400 MHz, Chloroform-*d*) δ 9.96 (s, 1H), 7.77 (d, J = 8.1 Hz, 2H), 7.33 (d, J = 8.1 Hz, 2H), 2.43 (s, 3H).

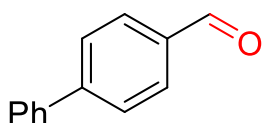
¹³C NMR (101 MHz, Chloroform-*d*) δ 191.91, 145.48, 134.16, 129.78, 129.65, 21.82.



4-(Tert-butyl)benzaldehyde (2h)⁷⁹

¹H NMR (400 MHz, Chloroform-*d*) δ 9.98 (s, 1H), 7.82 (d, J = 8.4 Hz, 2H), 7.55 (d, J = 8.4 Hz, 2H), 1.35 (s, 9H).

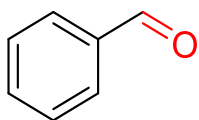
¹³C NMR (101 MHz, Chloroform-*d*) δ 191.96, 158.38, 134.04, 129.64, 125.94, 35.30, 31.03.



4-Phenylbenzaldehyde (2i)⁸¹

^1H NMR (400 MHz, Chloroform-*d*) δ 10.06 (s, 1H), 7.96 (d, $J = 8.4$ Hz, 2H), 7.76 (d, $J = 8.4$ Hz, 2H), 7.71 – 7.58 (m, 2H), 7.51-7.40 (m, 3H).

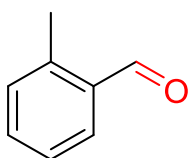
^{13}C NMR (101 MHz, Chloroform-*d*) δ 191.88, 147.15, 139.67, 135.16, 130.23, 128.98, 128.43, 127.64, 127.32.



Benzaldehyde (2j)⁷⁸

^1H NMR (400 MHz, Chloroform-*d*) δ 10.02 (s, 1H), 7.91 – 7.85 (m, 2H), 7.66 – 7.60 (m, 1H), 7.53 (t, $J = 7.5$ Hz, 2H).

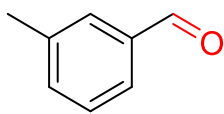
^{13}C NMR (101 MHz, Chloroform-*d*) δ 192.40, 136.37, 134.44, 129.72, 128.97.



2-Methylbenzaldehyde (2k)⁸²

^1H NMR (400 MHz, Chloroform-*d*) δ 10.27 (s, 1H), 7.80 (dd, $J = 7.6, 1.5$ Hz, 1H), 7.48 (td, $J = 7.5, 1.6$ Hz, 1H), 7.36 (t, $J = 7.5$ Hz, 1H), 7.26 (d, $J = 8.0$ Hz, 1H), 2.68 (s, 3H).

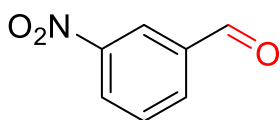
^{13}C NMR (101 MHz, Chloroform-*d*) δ 192.77, 140.59, 134.14, 133.61, 132.02, 131.74, 126.30, 19.56.



3-Methylbenzaldehyde (2l)⁸³

^1H NMR (400 MHz, Chloroform-*d*) δ 9.99 (s, 1H), 7.68 (m, 2H), 7.43 (m, 2H), 2.44 (s, 3H).

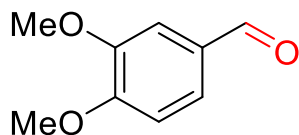
^{13}C NMR (101 MHz, Chloroform-*d*) δ 192.59, 138.90, 136.47, 135.27, 130.00, 128.86, 127.21, 21.17.



3-Nitrobenzaldehyde (2m)⁸⁴

^1H NMR (400 MHz, Chloroform-*d*) δ 10.13 (s, 1H), 8.72 (s, 1H), 8.50 (dd, $J = 8.2, 1.2$ Hz, 1H), 8.24 (d, $J = 7.6$ Hz, 1H), 7.77 (t, $J = 7.9$ Hz, 1H).

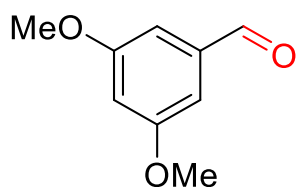
^{13}C NMR (101 MHz, Chloroform-*d*) δ 189.73, 148.76, 137.36, 134.63, 130.36, 128.55, 124.42.



3,4-Dimethoxybenzaldehyde (2n)⁸⁵

^1H NMR (400 MHz, Chloroform-*d*) δ 9.82 (s, 1H), 7.43 (dd, $J = 8.1, 1.9$ Hz, 1H), 7.38 (d, $J = 1.9$ Hz, 1H), 6.95 (d, $J = 8.1$ Hz, 1H), 3.92 (d, $J = 10.2$ Hz, 6H).

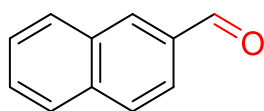
^{13}C NMR (101 MHz, Chloroform-*d*) δ 190.77, 154.37, 149.51, 130.03, 126.75, 110.29, 108.84, 56.07, 55.89.



3,5-Dimethoxybenzaldehyde (2o)⁸⁶

^1H NMR (400 MHz, Chloroform-*d*) δ 9.91 (s, 1H), 7.02 (d, $J = 2.4$ Hz, 2H), 6.71 (t, $J = 2.3$ Hz, 1H), 3.85 (s, 6H).

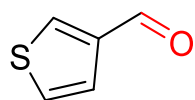
^{13}C NMR (101 MHz, Chloroform-*d*) δ 191.90, 161.23, 138.38, 107.10, 55.62.



2-Naphthaldehyde (2p)⁸⁷

^1H NMR (400 MHz, Chloroform-*d*) δ 10.16 (s, 1H), 8.33 (s, 1H), 8.02 – 7.89 (m, 4H), 7.66 – 7.57 (m, 2H).

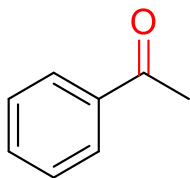
^{13}C NMR (101 MHz, Chloroform-*d*) δ 192.20, 136.41, 134.50, 134.08, 132.60, 129.49, 129.07, 129.06, 128.04, 127.05, 122.73.



Thiophene-3-carbaldehyde (2q)⁸⁸

^1H NMR (400 MHz, Chloroform-*d*) δ 9.94 (s, 1H), 8.13 (dd, $J = 2.9, 1.2$ Hz, 1H), 7.56 (dd, $J = 5.1, 1.2$ Hz, 1H), 7.38 (m, 1H).

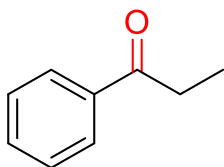
^{13}C NMR (101 MHz, Chloroform-*d*) δ 184.95, 143.03, 136.68, 127.38, 125.37.



Acetophenone (2r)⁷⁹

^1H NMR (400 MHz, Chloroform-*d*) δ 7.96 (d, $J = 7.0$ Hz, 2H), 7.57 (t, $J = 7.4$ Hz, 1H), 7.47 (t, $J = 7.5$ Hz, 2H), 2.61 (s, 3H).

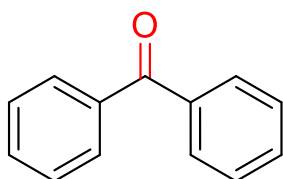
^{13}C NMR (101 MHz, Chloroform-*d*) δ 198.12, 137.10, 133.07, 128.54, 128.27, 26.59.



Propiophenone (2s)⁸³

^1H NMR (400 MHz, Chloroform-*d*) δ 7.97 (d, $J = 7.0$ Hz, 2H), 7.55 (t, $J = 7.4$ Hz, 1H), 7.46 (t, $J = 7.5$ Hz, 2H), 3.01 (q, $J = 7.3$ Hz, 2H), 1.23 (t, $J = 7.2$ Hz, 3H).

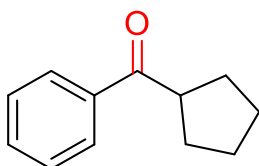
^{13}C NMR (101 MHz, Chloroform-*d*) δ 200.78, 136.90, 132.83, 128.51, 127.93, 31.75, 8.21.



Benzophenone (2t)⁸²

^1H NMR (400 MHz, Chloroform-*d*) δ 7.81 (d, $J = 6.9$ Hz, 4H), 7.59 (t, $J = 7.4$ Hz, 2H), 7.48 (t, $J = 7.6$ Hz, 4H).

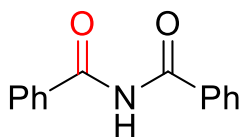
^{13}C NMR (101 MHz, Chloroform-*d*) δ 196.64, 137.52, 132.34, 129.97, 128.20.



Cyclopentyl(phenyl)methanone (2u)⁸⁹

¹H NMR (400 MHz, Chloroform-*d*) δ 7.98 (d, $J = 7.0$ Hz, 2H), 7.54 (t, $J = 7.3$ Hz, 1H), 7.46 (t, $J = 7.5$ Hz, 2H), 3.72 (p, $J = 7.9$ Hz, 1H), 1.92 (q, $J = 6.2, 5.5$ Hz, 4H), 1.77 – 1.62 (m, 4H).

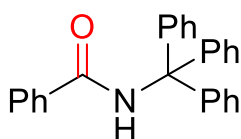
¹³C NMR (101 MHz, Chloroform-*d*) δ 202.76, 136.92, 132.65, 128.46, 128.42, 46.34, 29.96, 26.29.



N-benzoylbenzamide (2v)⁹⁰

¹H NMR (400 MHz, Chloroform-*d*) δ 9.09 (s, 1H), 7.86 (dd, $J = 8.3, 1.3$ Hz, 4H), 7.68 – 7.55 (m, 2H), 7.49 (t, $J = 7.7$ Hz, 4H).

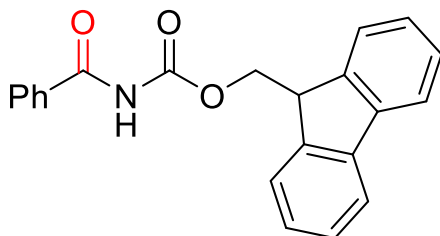
¹³C NMR (101 MHz, Chloroform-*d*) δ 166.46, 133.31, 133.03, 128.80, 127.93.



N-tritylbenzamide (2w)⁹¹

¹H NMR (400 MHz, Chloroform-*d*) δ 7.85 – 7.82 (m, 3H), 7.41 – 7.40 (m, 3H), 7.29-7.23 (m, 15H).

¹³C NMR (101 MHz, Chloroform-*d*) δ 159.60, 145.79, 136.71, 130.71, 129.78, 128.58, 128.53, 127.73, 126.75, 78.26.

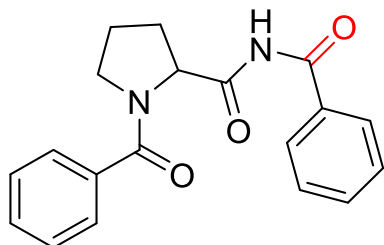


(9H-fluoren-9-yl)methyl benzoylcarbamate (2x)

¹H NMR (400 MHz, Chloroform-*d*) δ 8.26 (s, 1H), 7.83 (d, $J = 7.2$ Hz, 2H), 7.78 (d, $J = 7.5$ Hz, 2H), 7.67 (d, $J = 7.5$ Hz, 2H), 7.58 (t, $J = 7.4$ Hz, 1H), 7.48 (t, $J = 7.6$ Hz, 2H), 7.42 (t, $J = 7.5$ Hz, 2H), 7.33 (t, $J = 7.4$ Hz, 2H), 4.58 (d, $J = 6.8$ Hz, 2H), 4.31 (t, $J = 6.8$ Hz, 1H).

^{13}C NMR (101 MHz, Chloroform-*d*) δ 164.84, 151.31, 143.28, 141.29, 133.03, 132.90, 128.83, 127.89, 127.68, 127.21, 125.04, 120.04, 67.97, 46.68.

HRMS (ESI) calcd for $\text{C}_{22}\text{H}_{17}\text{NO}_3$ $[\text{M}+\text{Na}]^+$: 366.1101; found: 366.1097.

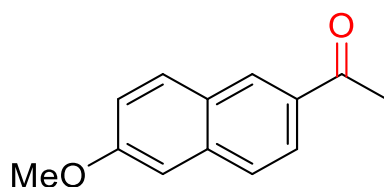


***N*,1-Dibenzoylpyrrolidine-2-carboxamide (2y)**

^1H NMR (400 MHz, Chloroform-*d*) δ 10.57 (s, 1H), 7.97 (d, $J = 7.7$ Hz, 2H), 7.53 (m, 3H), 7.48 – 7.38 (m, 5H), 5.21 (dd, $J = 8.1, 4.3$ Hz, 1H), 3.61 – 3.50 (m, 2H), 2.54-2.48 (m, 1H), 2.22-2.17 (m, 1H), 2.11-2.04 (m, 1H), 1.94-1.86 (m, 1H).

^{13}C NMR (101 MHz, Chloroform-*d*) δ 171.34, 170.79, 165.42, 135.64, 132.97, 132.65, 130.36, 128.80, 128.40, 127.89, 126.94, 61.02, 50.51, 26.75, 25.07.

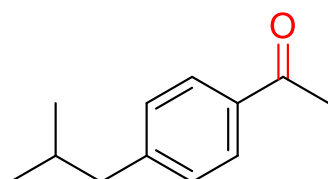
HRMS (ESI) calcd for $\text{C}_{19}\text{H}_{18}\text{N}_2\text{O}_3$ $[\text{M}+\text{Na}]^+$: 345.1210; found: 345.1214.



1-(6-Methoxynaphthalen-2-yl)ethan-1-one (3a)⁹²

^1H NMR (400 MHz, Chloroform-*d*) δ 8.38 (s, 1H), 8.00 (dd, $J = 8.6, 1.8$ Hz, 1H), 7.84 (d, $J = 9.0$ Hz, 1H), 7.76 (d, $J = 8.6$ Hz, 1H), 7.23 – 7.12 (m, 2H), 3.94 (s, 3H), 2.69 (s, 3H).

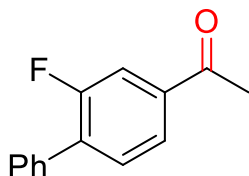
^{13}C NMR (101 MHz, Chloroform-*d*) δ 197.80, 159.71, 137.23, 132.58, 131.06, 130.00, 127.77, 127.04, 124.61, 119.67, 105.71, 55.37, 26.51.



1-(4-Isobutylphenyl)ethan-1-one (3b)⁹²

^1H NMR (400 MHz, Chloroform-*d*) δ 7.88 (d, $J = 8.2$ Hz, 2H), 7.23 (d, $J = 8.2$ Hz, 2H), 2.58 – 2.52 (m, 5H), 1.93-1.87 (m, 1H), 0.91 (d, $J = 6.6$ Hz, 6H).

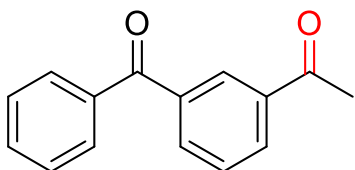
^{13}C NMR (101 MHz, Chloroform-*d*) δ 197.84, 147.53, 134.92, 129.23, 128.26, 45.33, 30.07, 26.49, 22.28.



1-(2-Fluoro-[1,1'-biphenyl]-4-yl)ethan-1-one (3c)²⁸

^1H NMR (400 MHz, Chloroform-*d*) δ 7.80 (dd, $J = 8.0, 1.7$ Hz, 1H), 7.74 (dd, $J = 11.2, 1.7$ Hz, 1H), 7.61 – 7.51 (m, 3H), 7.48 (t, $J = 7.3$ Hz, 2H), 7.42 (t, $J = 7.3$ Hz, 1H), 2.63 (s, 3H).

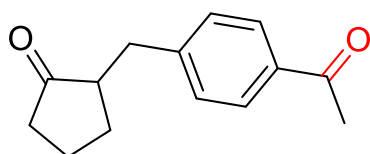
^{13}C NMR (101 MHz, Chloroform-*d*) δ 196.43, 159.63 (d, $J_{\text{C-F}} = 249.8$ Hz), 137.77 (d, $J_{\text{C-F}} = 6.3$ Hz), 134.63, 133.75 (d, $J_{\text{C-F}} = 13.7$ Hz), 130.89 (d, $J_{\text{C-F}} = 3.4$ Hz), 128.96 (d, $J_{\text{C-F}} = 3.1$ Hz), 128.47, 124.30 (d, $J_{\text{C-F}} = 3.4$ Hz), 115.86 (d, $J_{\text{C-F}} = 24.0$ Hz), 26.61.



1-(3-Benzoylphenyl)ethan-1-one (3d)⁹²

^1H NMR (400 MHz, Chloroform-*d*) δ 8.36 (s, 1H), 8.18 (d, $J = 7.8$ Hz, 1H), 7.98 (d, $J = 7.6$ Hz, 1H), 7.79 (d, $J = 8.8$ Hz, 2H), 7.60 (q, $J = 7.9$ Hz, 2H), 7.50 (t, $J = 7.6$ Hz, 2H), 2.64 (s, 3H).

^{13}C NMR (101 MHz, Chloroform-*d*) δ 197.23, 195.79, 138.02, 137.13, 136.95, 134.19, 132.83, 131.71, 129.98, 129.64, 128.69, 128.46, 26.70.

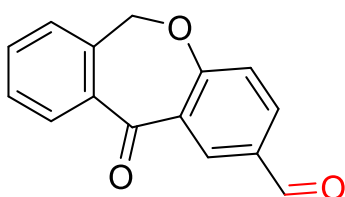


2-(4-Acetylbenzyl)cyclopentan-1-one (3e)

^1H NMR (400 MHz, Chloroform-*d*) δ 7.81 (d, $J = 8.1$ Hz, 2H), 7.19 (d, $J = 8.1$ Hz, 2H), 3.12 (dd, $J = 13.9, 4.3$ Hz, 1H), 2.61 – 2.53 (m, 1H), 2.51 (s, 3H), 2.34 – 2.25 (m, 2H), 2.08 – 1.94 (m, 2H), 1.92 – 1.87 (m, 1H), 1.71 – 1.62 (m, 1H), 1.52–1.41 (m, 1H).

^{13}C NMR (101 MHz, Chloroform-*d*) δ 219.45, 197.67, 145.76, 135.30, 129.05, 128.51, 50.58, 37.97, 35.48, 29.05, 26.49, 20.45.

HRMS (ESI) calcd for $\text{C}_{14}\text{H}_{16}\text{O}_2$ $[\text{M}+\text{Na}]^+$: 239.1043; found: 239.1046.

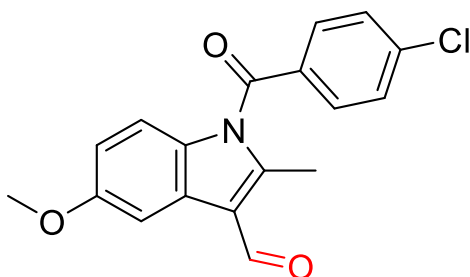


11-Oxo-6,11-dihydrodibenzo[*b,e*]oxepine-2-carbaldehyde (3f)⁹³

^1H NMR (400 MHz, Chloroform-*d*) δ 9.99 (s, 1H), 8.73 (d, $J = 2.2$ Hz, 1H), 8.02 (dd, $J = 8.6, 2.2$ Hz, 1H), 7.88 (d, $J = 7.6$ Hz, 1H), 7.60 (t, $J = 7.5$ Hz, 1H), 7.51 (t, $J = 7.6$ Hz, 1H), 7.41 (d, $J = 7.4$ Hz, 1H), 7.16 (d, $J = 8.5$ Hz, 1H), 5.28 (s, 2H).

^{13}C NMR (101 MHz, Chloroform-*d*) δ 190.34, 190.13, 165.51, 140.28, 137.41, 134.49, 133.39, 133.18, 130.90, 129.70, 129.37, 128.12, 124.98, 122.13, 73.59.

HRMS (CI) calcd for $\text{C}_{15}\text{H}_{10}\text{O}_3$ $[\text{M}+\text{H}]^+$: 239.0703; found: 239.0692.

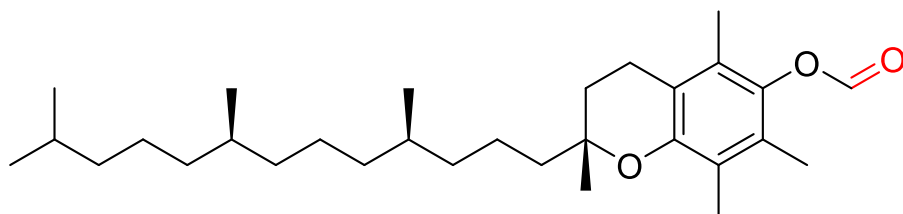


1-(4-Chlorobenzoyl)-5-methoxy-2-methyl-1H-indole-3-carbaldehyde (3g)⁹²

^1H NMR (400 MHz, Chloroform-*d*) δ 10.32 (s, 1H), 7.80 (s, 1H), 7.70 (d, $J = 8.3$ Hz, 2H), 7.50 (d, $J = 8.4$ Hz, 2H), 6.73 (s, 2H), 3.87 (s, 3H), 2.76 (s, 3H).

^{13}C NMR (101 MHz, Chloroform-*d*) δ 185.71, 168.20, 157.16, 148.46, 140.88, 132.04, 131.65, 130.59, 129.46, 126.93, 118.34, 114.25, 113.84, 103.27, 55.72, 12.62.

HRMS (CI) calcd for $\text{C}_{18}\text{H}_{14}\text{ClNO}_3$ $[\text{M}+\text{H}]^+$: 328.0735; found: 328.0734.

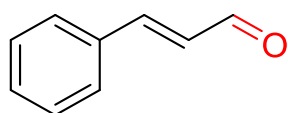


(R)-2,5,7,8-Tetramethyl-2-((4R,8R)-4,8,12-trimethyltridecyl)chroman-6-yl formate (3h)

^1H NMR (400 MHz, Chloroform-*d*) δ 8.31 (s, 1H), 2.60 (t, $J = 6.8$ Hz, 2H), 2.10 (s, 3H), 2.06 (s, 3H), 2.02 (s, 3H), 1.86-1.72 (m, 2H), 1.54 – 1.51 (m, 2H), 1.43-1.35 (m, 4H), 1.28 – 1.24 (m, 11H), 1.16 – 1.03 (m, 7H), 0.88 – 0.84 (m, 12H).

^{13}C NMR (101 MHz, Chloroform-*d*) δ 160.02, 149.77, 139.73, 126.56, 124.85, 123.32, 117.61, 75.20, 40.02, 39.37, 37.45, 37.40, 37.38, 37.28, 32.77, 32.69, 31.03, 27.97, 24.80, 24.43, 23.90, 22.71, 22.62, 21.02, 20.62, 19.74, 19.68, 13.09, 12.24, 11.84.

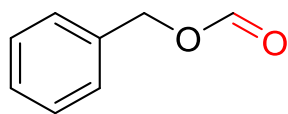
HRMS (ESI) calcd for $\text{C}_{30}\text{H}_{50}\text{O}_3$ $[\text{M}+\text{Na}]^+$: 481.3653; found: 481.3649



Cinnamaldehyde (5a)⁷⁹

^1H NMR (400 MHz, Chloroform-*d*) δ 9.71 (d, $J = 7.7$ Hz, 1H), 7.60 – 7.53 (m, 2H), 7.51 – 7.39 (m, 4H), 6.72 (dd, $J = 16.0, 7.7$ Hz, 1H).

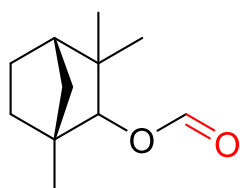
^{13}C NMR (101 MHz, Chloroform-*d*) δ 193.68, 152.76, 133.97, 131.24, 129.07, 128.56, 128.46.



Benzyl formate (5b)⁹⁴

^1H NMR (400 MHz, Chloroform-*d*) δ 8.15 (s, 1H), 7.39 – 7.33 (m, 5H), 5.21 (s, 2H).

^{13}C NMR (101 MHz, Chloroform-*d*) δ 160.76, 135.17, 128.64, 128.49, 128.35, 65.68.

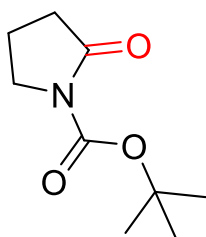


(1R,4S)-1,3,3-trimethylbicyclo[2.2.1]heptan-2-yl formate (5c)

^1H NMR (400 MHz, Chloroform-*d*) δ 8.17 (s, 1H), 4.47 (s, 1H), 1.71 (dd, $J = 20.4, 9.0$ Hz, 3H), 1.60 (d, $J = 10.5$ Hz, 1H), 1.51 – 1.40 (m, 1H), 1.21 (d, $J = 8.9$ Hz, 1H), 1.11-1.04 (m, 7H), 0.80 (s, 3H).

^{13}C NMR (101 MHz, Chloroform-*d*) δ 161.53, 86.37, 48.26, 48.23, 41.36, 39.20, 29.68, 26.52, 25.77, 20.31, 19.24.

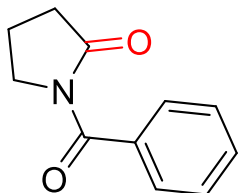
HRMS (CI) calcd for $\text{C}_{11}\text{H}_{18}\text{O}_2$ $[\text{M}+\text{H}]^+$: 183.1380; found: 183.1381.



tert-butyl 2-oxopyrrolidine-1-carboxylate (5d)⁹⁵

^1H NMR (400 MHz, Chloroform-*d*) δ 3.74 (t, $J = 7.2$ Hz, 2H), 2.50 (t, $J = 8.1$ Hz, 2H), 2.00 (q, $J = 9.2, 7.7$ Hz, 2H), 1.52 (s, 9H).

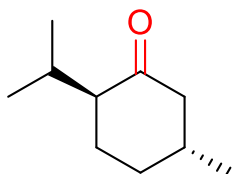
^{13}C NMR (101 MHz, Chloroform-*d*) δ 174.27, 150.24, 82.75, 46.45, 32.95, 28.01, 17.38.



1-Benzoylpyrrolidin-2-one (5e)⁹⁶

^1H NMR (400 MHz, Chloroform-*d*) δ 7.60 (d, $J = 8.4$ Hz, 2H), 7.51 (t, $J = 7.4$ Hz, 1H), 7.40 (t, $J = 7.7$ Hz, 2H), 3.95 (t, $J = 7.1$ Hz, 2H), 2.59 (t, $J = 8.0$ Hz, 2H), 2.17-2.09 (m, 2H).

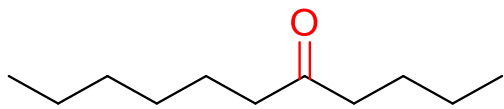
^{13}C NMR (101 MHz, Chloroform-*d*) δ 174.45, 170.61, 134.28, 131.82, 128.83, 127.70, 46.46, 33.23, 17.59.



(2*S*,5*R*)-2-Isopropyl-5-methylcyclohexan-1-one (5f)⁹⁷

^1H NMR (400 MHz, Chloroform-*d*) δ 2.37 – 2.29 (m, 1H), 2.16 – 1.81 (m, 6H), 1.43-1.31 (m, 2H), 1.00 (d, $J = 6.3$ Hz, 3H), 0.91 (d, $J = 6.8$ Hz, 3H), 0.85 (d, $J = 6.8$ Hz, 3H).

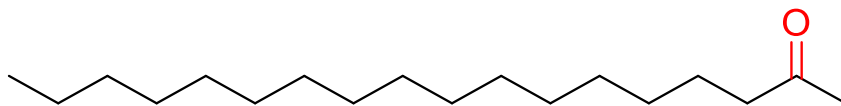
^{13}C NMR (101 MHz, Chloroform-*d*) δ 212.42, 55.89, 50.86, 35.46, 33.92, 27.86, 25.89, 22.27, 21.20, 18.69.



Undecan-5-one (5g)⁹⁸

^1H NMR (400 MHz, Chloroform-*d*) δ 2.39 (t, $J = 7.5$ Hz, 4H), 1.57-1.51 (m, 4H), 1.35 – 1.26 (m, 8H), 0.92 – 0.86 (m, 6H).

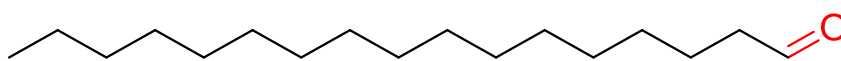
^{13}C NMR (101 MHz, Chloroform-*d*) δ 211.73, 42.83, 42.52, 31.61, 28.94, 25.99, 23.86, 22.49, 22.38, 14.02, 13.86.



Octadecan-2-one (5h)⁹⁹

^1H NMR (400 MHz, Chloroform-*d*) δ 2.40 (t, $J = 7.5$ Hz, 2H), 2.12 (s, 3H), 1.61 – 1.50 (m, 2H), 1.30-1.24 (m, 26H), 0.87 (t, $J = 6.6$ Hz, 3H).

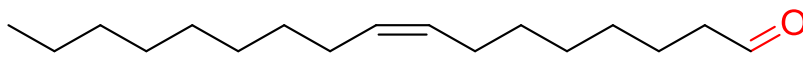
^{13}C NMR (101 MHz, Chloroform-*d*) δ 209.32, 43.81, 31.91, 29.81, 29.67, 29.65, 29.64, 29.59, 29.46, 29.39, 29.34, 29.17, 23.86, 22.67, 14.09.



Heptadecanal (5i)¹⁰⁰

^1H NMR (400 MHz, Chloroform-*d*) δ 9.76 (s, 1H), 2.42 (t, $J = 7.4, 1.9$ Hz, 2H), 1.63 (t, $J = 7.1$ Hz, 2H), 1.30-1.26 (m, 26H), 0.88 (t, $J = 6.7$ Hz, 3H).

^{13}C NMR (101 MHz, Chloroform-*d*) δ 202.98, 43.92, 31.92, 29.69, 29.65, 29.63, 29.57, 29.42, 29.35, 29.16, 22.68, 22.09, 14.11.



(Z)-heptadec-8-enal (5j)¹⁰¹

¹H NMR (400 MHz, Chloroform-*d*) δ 9.76 (s, 1H), 5.39-5.30 (m, 2H), 2.42 (td, *J* = 7.4, 1.9 Hz, 2H), 2.03-2.00 (m, 4H), 1.65-1.61 (m, 2H), 1.36 – 1.25 (m, 18H), 0.88 (t, *J* = 6.7 Hz, 3H).

¹³C NMR (101 MHz, Chloroform-*d*) δ 202.87, 130.31, 130.14, 129.55, 129.33, 43.88, 31.89, 29.75, 29.50, 29.31, 29.05, 28.97, 27.21, 27.08, 22.67, 22.05, 14.10.

2.6 References

1. Simonetta, M.; Carra, S.; Ebersson, L.; Koskikallio, J.; Sneed, R.; Kucherov, V.; Yanovskaya, L.; Bergelson, L.; Shemyakin, M.; Kwart, H., *Carboxylic Acids and Esters*, Wiley: **1969**.
2. Večeřa, M.; Gasparič, J., *Carboxylic Acids and Their Derivatives*. In *Detection and Identification of Organic Compounds*, Springer: **1971**.
3. Yoon, T. P.; Ischay, M. A.; Du, J., Visible Light Photocatalysis as a Greener Approach to Photochemical Synthesis. *Nat. Chem.* **2010**, *2*, 527-532.
4. Kautzky, J. A.; Wang, T.; Evans, R. W.; MacMillan, D. W. C., Decarboxylative Trifluoromethylation of Aliphatic Carboxylic Acids. *J. Am. Chem. Soc.* **2018**, *140*, 6522-6526.
5. Rodriguez, N.; Goossen, L. J., Decarboxylative Coupling Reactions: A Modern Strategy for C-C Bond Formation. *Chem. Soc. Rev.* **2011**, *40*, 5030-5048.
6. Pichette Drapeau, M.; Goossen, L. J., Carboxylic Acids as Directing Groups for C-H Bond Functionalization. *Chemistry* **2016**, *22*, 18654-18677.
7. Bhadra, S.; Dzik, W. I.; Goossen, L. J., Decarboxylative Etherification of Aromatic Carboxylic Acids. *J. Am. Chem. Soc.* **2012**, *134*, 9938-9941.
8. Johnston, C. P.; Smith, R. T.; Allmendinger, S.; MacMillan, D. W., Metallaphotoredox-Catalysed sp³-sp³ Cross-Coupling of Carboxylic Acids with Alkyl Halides. *Nature* **2016**, *536*, 322-325.
9. Ventre, S.; Petronijevic, F. R.; MacMillan, D. W., Decarboxylative Fluorination of Aliphatic Carboxylic Acids via Photoredox Catalysis. *J. Am. Chem. Soc.* **2015**, *137*, 5654-5657.
10. Chu, L.; Lipshultz, J. M.; MacMillan, D. W., Merging Photoredox and Nickel Catalysis: The Direct Synthesis of Ketones by the Decarboxylative Arylation of α-Oxo Acids. *Angew. Chem. Int. Ed.* **2015**, *54*, 7929-7933.
11. Chu, L.; Ohta, C.; Zuo, Z.; MacMillan, D. W., Carboxylic Acids as a Traceless Activation Group for Conjugate Additions: A Three-Step Synthesis of (+/-)-Pregabalin. *J. Am. Chem. Soc.* **2014**, *136*, 10886-10889.

12. Zuo, Z.; MacMillan, D. W., Decarboxylative Arylation of α -Amino Acids via Photoredox Catalysis: A One-Step Conversion of Biomass to Drug Pharmacophore. *J. Am. Chem. Soc.* **2014**, *136*, 5257-5260.
13. Bu, F.; Lu, L.; Hu, X.; Wang, S.; Zhang, H.; Lei, A., Electrochemical Oxidative Decarboxylation and 1,2-Aryl Migration towards the Synthesis of 1,2-Diaryl Ethers. *Chem. Sci.* **2020**, *11*, 10000-10004.
14. Yuan, Y.; Zhou, Z.; Zhang, L.; Li, L. S.; Lei, A., Electrochemical Oxidative C3 Acyloxylation of Imidazo[1,2-*a*]pyridines with Hydrogen Evolution. *Org. Lett.* **2021**, *23*, 5932-5936.
15. Liang, Y.; Strieth-Kalthoff, F.; Bellotti, P.; Glorius, F., Catalytic One-Carbon Homologation of α -Amino Acids to β -Amino Aldehydes. *Chem. Catal.* **2021**, *1*, 1427-1436.
16. Zheng, C.; Wang, Y.; Xu, Y.; Chen, Z.; Chen, G.; Liang, S. H., Ru-Photoredox-Catalyzed Decarboxylative Oxygenation of Aliphatic Carboxylic Acids through *N*-(acyloxy)phthalimide. *Org. Lett.* **2018**, *20*, 4824-4827.
17. Wang, L.; Wang, T.; Cheng, G. J.; Li, X.; Wei, J. J.; Guo, B.; Zheng, C.; Chen, G.; Ran, C.; Zheng, C., Direct C–H Arylation of Aldehydes by Merging Photocatalyzed Hydrogen Atom Transfer with Palladium Catalysis. *ACS Catal.* **2020**, *10*, 7543-7551.
18. Feng, Q.; Song, Q., Aldehydes and Ketones Formation: Copper-Catalyzed Aerobic Oxidative Decarboxylation of Phenylacetic Acids and α -Hydroxyphenylacetic Acids. *J. Org. Chem.* **2014**, *79*, 1867-1871.
19. Liu, M.; Wang, H.; Zeng, H.; Li, C. J., Silver(I) as a Widely Applicable, Homogeneous Catalyst for Aerobic Oxidation of Aldehydes toward Carboxylic Acids in Water-"Silver Mirror": From Stoichiometric to Catalytic. *Sci. Adv.* **2015**, *1*, e1500020.
20. Li, J.; Wang, H.; Qiu, Z.; Huang, C. Y.; Li, C. J., Metal-Free Direct Deoxygenative Borylation of Aldehydes and Ketones. *J. Am. Chem. Soc.* **2020**, *142*, 13011-13020.
21. Lv, L.; Zhu, D.; Li, C. J., Direct Dehydrogenative Alkyl Heck-Couplings of Vinylarenes with Umpolung Aldehydes Catalyzed by Nickel. *Nat. Commun.* **2019**, *10*, 715.
22. Lv, L.; Zhu, D.; Tang, J.; Qiu, Z.; Li, C. C.; Gao, J.; Li, C. J., Cross-Coupling of Phenol Derivatives with Umpolung Aldehydes Catalyzed by Nickel. *ACS Catal.* **2018**, *8*, 4622-4627.
23. Wang, H.; Dai, X. J.; Li, C. J., Aldehydes as Alkyl Carbanion Equivalents for Additions to Carbonyl Compounds. *Nat. Chem.* **2017**, *9*, 374-378.
24. Cornils, B.; Herrmann, W. A.; Rasch, M., Otto Roelen, Pioneer in Industrial Homogeneous Catalysis. *Angew. Chem. Int. Ed.* **1994**, *33*, 2144-2163.
25. Bruckner, R., *Advanced Organic Chemistry: Reaction Mechanisms*. Elsevier: **2001**.

26. Weissermel, K.; Arpe, H. J., *Industrial Organic Chemistry*. John Wiley & Sons: **2008**.
27. Faraggi, T. M.; Li, W.; MacMillan, D. W. C., Decarboxylative Oxygenation via Photoredox Catalysis. *Israel J. Chem.* **2019**, *60*, 410-415.
28. Sakakibara, Y.; Cooper, P.; Murakami, K.; Itami, K., Photoredox-Catalyzed Decarboxylative Oxidation of Arylacetic Acids. *Chem. Asian J.* **2018**, *13*, 2410-2413.
29. Shirase, S.; Tamaki, S.; Shinohara, K.; Hirosawa, K.; Tsurugi, H.; Satoh, T.; Mashima, K., Cerium(IV) Carboxylate Photocatalyst for Catalytic Radical Formation from Carboxylic Acids: Decarboxylative Oxygenation of Aliphatic Carboxylic Acids and Lactonization of Aromatic Carboxylic Acids. *J. Am. Chem. Soc.* **2020**, *142*, 5668-5675.
30. Araghi, M.; Bokaei, F., Manganese(III) Porphyrin Supported on Multi-Wall Carbon Nanotubes: A Highly Efficient and Reusable Biomimetic Catalyst for Oxidative Decarboxylation of α -Arylcarboxylic Acids and Oxidation of Alkanes with Sodium Periodate. *Polyhedron* **2013**, *53*, 15-19.
31. Tangestaninejad, S.; Mirkhani, V., Efficient and Mild Oxidative Decarboxylation of Aryl-substituted Carboxylic Acids by Iron and Manganese Porphyrin Periodate Systems. *J. Chem. Res.* **1998**, *12*, 820-821.
32. Gholamreza, K.; Roxana, A., Biomimetic Decarboxylation of Carboxylic Acids with $\text{PhI}(\text{OAc})_2$ Catalyzed by Manganese Porphyrin $[\text{Mn}(\text{TPP})\text{OAc}]$. *Chem. Res. Chin. Uni.* **2008**, *24*, 464-468.
33. Farhadi, S.; Zaringhadam, P.; Sahamieh, R. Z., Photolytic Decarboxylation of α -Arylcarboxylic Acids Mediated by HgF_2 under a Dioxygen Atmosphere. *Tetrahedron Lett.* **2006**, *47*, 1965-1968.
34. Pocker, Y.; Davis, B. C., Oxidative Cleavage by Lead(IV). I. The Mechanism of Decarboxylation of 2-Hydroxycarboxylic Acids. *J. Am. Chem. Soc.* **1973**, *95*, 6216-6223.
35. Mete, T. B.; Khopade, T. M.; Bhat, R. G., Oxidative Decarboxylation of Arylacetic Acids in Water: One-Pot Transition-Metal-Free Synthesis of Aldehydes and Ketones. *Tetrahedron Lett.* **2017**, *58*, 2822-2825.
36. Sahu, S.; Goldberg, D. P., Activation of Dioxygen by Iron and Manganese Complexes: A Heme and Nonheme Perspective. *J. Am. Chem. Soc.* **2016**, *138*, 11410-11428.
37. Zhu, B.; Shen, T.; Huang, X.; Zhu, Y.; Song, S.; Jiao, N., Selective Aerobic Oxygenation of Tertiary Allylic Alcohols with Molecular Oxygen. *Angew. Chem. Int. Ed.* **2019**, *58*, 11028-11032.
38. Liang, Y. F.; Jiao, N., Oxygenation via C-H/C-C Bond Activation with Molecular Oxygen. *Acc. Chem. Res.* **2017**, *50*, 1640-1653.

39. Paria, S.; Que, L., Jr.; Paine, T. K., Oxidative Decarboxylation of Benzilic Acid by a Biomimetic Iron(II) Complex: Evidence for an Iron(IV)-Oxo-Hydroxo Oxidant from O₂. *Angew. Chem. Int. Ed.* **2011**, *50*, 11129-11132.
40. Baglia, R. A.; Zaragoza, J. P. T.; Goldberg, D. P., Biomimetic Reactivity of Oxygen-Derived Manganese and Iron Porphyrinoid Complexes. *Chem. Rev.* **2017**, *117*, 13320-13352.
41. Prokop, K. A.; Goldberg, D. P., Generation of an Isolable, Monomeric Manganese(V)-Oxo Complex from O₂ and Visible Light. *J. Am. Chem. Soc.* **2012**, *134*, 8014-8017.
42. Prokop, K. A.; Neu, H. M.; de Visser, S. P.; Goldberg, D. P., A manganese(V)-Oxo π -Cation Radical Complex: Influence of One-Electron Oxidation on Oxygen-Atom Transfer. *J. Am. Chem. Soc.* **2011**, *133*, 15874-15877.
43. Fukuzumi, S.; Kotani, H.; Prokop, K. A.; Goldberg, D. P., Electron- and Hydride-Transfer Reactivity of an Isolable Manganese(V)-Oxo Complex. *J. Am. Chem. Soc.* **2011**, *133*, 1859-1869.
44. Riaño, S.; Fernández, D.; Fadini, L., Oxidative Cleavage of *vic*-Diols Catalyzed by Manganese (III) Complexes in Ionic Liquids. *Catal. Commun.* **2008**, *9*, 1282-1285.
45. Barroso, S.; Blay, G.; Fernández, I.; Pedro, J. R.; Ruiz-García, R.; Pardo, E.; Lloret, F.; Muñoz, M. C., Chemistry and Reactivity of Mononuclear Manganese Oxamate Complexes: Oxidative Carbon–Carbon Bond Cleavage of *vic*-Diols by Dioxygen and Aldehydes Catalyzed by a *trans*-Dipyridine Manganese(III) Complex with a Tetradentate *o*-Phenylenedioxamate Ligand. *J. Mol. Catal. A.* **2006**, *243*, 214-220.
46. Guo, M.; Zhang, J.; Zhang, L.; Lee, Y. M.; Fukuzumi, S.; Nam, W., Enthalpy-Entropy Compensation Effect in Oxidation Reactions by Manganese(IV)-Oxo Porphyrins and Nonheme Iron(IV)-Oxo Models. *J. Am. Chem. Soc.* **2021**, *44*, 18559-18570.
47. Guo, M.; Lee, Y. M.; Fukuzumi, S.; Nam, W., Biomimetic Metal-Oxidant Adducts as Active Oxidants in Oxidation Reactions. *Coord. Chem. Rev.* **2021**, *435*, 213807.
48. Li, G.; Kates, P. A.; Dilger, A. K.; Cheng, P. T.; Ewing, W. R.; Groves, J. T., Manganese-Catalyzed Desaturation of N-Acyl Amines and Ethers. *ACS Catal.* **2019**, *9*, 9513-9517.
49. Liu, W.; Huang, X.; Cheng, M. J.; Nielsen, R. J.; Goddard, W. A., 3rd; Groves, J. T., Oxidative Aliphatic C-H Fluorination with Fluoride Ion Catalyzed by a Manganese Porphyrin. *Science* **2012**, *337*, 1322-1325.
50. Huang, Z.; Guan, R.; Shanmugam, M.; Bennett, E. L.; Robertson, C. M.; Brookfield, A.; McInnes, E. J. L.; Xiao, J., Oxidative Cleavage of Alkenes by O₂ with a Non-Heme Manganese Catalyst. *J. Am. Chem. Soc.* **2021**, *143*, 10005-10013.

51. Uttry, A.; van Gemmeren, M., Direct C(sp³)-H Activation of Carboxylic Acids. *Synthesis* **2019**, *52*, 479-488.
52. Kiyokawa, K.; Yahata, S.; Kojima, T.; Minakata, S., Hypervalent Iodine(III)-Mediated Oxidative Decarboxylation of β,λ -Unsaturated Carboxylic Acids. *Org. Lett.* **2014**, *16*, 4646-4649.
53. Herman, N. A.; Zhang, W., Enzymes for Fatty Acid-Based Hydrocarbon Biosynthesis. *Curr. Opin. Chem. Biol.* **2016**, *35*, 22-28.
54. Boger, D. L.; Baldino, C. M., Singlet Oxygen Mediated Oxidative Decarboxylation of Pyrrole-2-carboxylic Acids. *J. Org. Chem.* **2002**, *56*, 6942-6944.
55. You, Y., Chemical Tools for the Generation and Detection of Singlet Oxygen. *Org. Biomol. Chem.* **2018**, *16*, 4044-4060.
56. Sheet, D.; Paine, T. K., Aerobic Alcohol Oxidation and Oxygen Atom Transfer Reactions Catalyzed by a Nonheme Iron(II)- α -Keto Acid Complex. *Chem. Sci.* **2016**, *7*, 5322-5331.
57. Neidig, M. L.; Decker, A.; Choroba, O. W.; Huang, F.; Kavana, M.; Moran, G. R.; Spencer, J. B.; Solomon, E. I., Spectroscopic and Electronic Structure Studies of Aromatic Electrophilic Attack and Hydrogen-Atom Abstraction by Non-Heme Iron Enzymes. *Proc. Natl. Acad. Sci. USA.* **2006**, *103*, 12966-12973.
58. Choroba, O. W.; Williams, D. H.; Spencer, J. B., Biosynthesis of the Vancomycin Group of Antibiotics: Involvement of an Unusual Dioxygenase in the Pathway to (S)-4-Hydroxyphenylglycine. *J. Am. Chem. Soc.* **2000**, *122*, 5389-5390.
59. Kitajima, N.; Komatsuzaki, H.; Hikichi, S.; Osawa, M.; Moro-oka, Y., A Monomeric Side-On Peroxo Manganese(III) Complex: Mn(O₂)(3,5-iPr₂pzH)(HB(3,5-iPr₂pz)₃). *J. Am. Chem. Soc.* **2002**, *116*, 11596-11597.
60. Jackson, T. A.; Karapetian, A.; Miller, A. F.; Brunold, T. C., Probing the Geometric and Electronic Structures of the Low-Temperature Azide Adduct and the Product-Inhibited Form of Oxidized Manganese Superoxide Dismutase. *Biochemistry* **2005**, *44*, 1504-1520.
61. Groni, S.; Blain, G.; Guillot, R.; Policar, C.; Anxolabehere-Mallart, E., Reactivity of Mn^{II} with Superoxide. Evidence for a [Mn^{III}OO]⁺ Unit by Low-Temperature Spectroscopies. *Inorg. Chem.* **2007**, *46*, 1951-1953.
62. Kovacs, J. A., Tuning the Relative Stability and Reactivity of Manganese Dioxygen and Peroxo Intermediates via Systematic Ligand Modification. *Acc. Chem. Res.* **2015**, *48*, 2744-2753.
63. Coggins, M. K.; Sun, X.; Kwak, Y.; Solomon, E. I.; Rybak-Akimova, E.; Kovacs, J. A., Characterization of Metastable Intermediates Formed in the Reaction Between a Mn(II)

Complex and Dioxygen, Including a Crystallographic Structure of a Binuclear Mn(III)-Peroxo Species. *J. Am. Chem. Soc.* **2013**, *135*, 5631-5640.

64. Sankaralingam, M.; Lee, Y. M.; Jeon, S. H.; Seo, M. S.; Cho, K. B.; Nam, W., A Mononuclear Manganese(III)-Hydroperoxo Complex: Synthesis by Activating Dioxygen and Reactivity in Electrophilic and Nucleophilic Reactions. *Chem. Commun.* **2018**, *54*, 1209-1212.

65. Dietrich, J.; Gokhale, V.; Wang, X.; Hurley, L. H.; Flynn, G. A., Application of a Novel [3+2] Cycloaddition Reaction to Prepare Substituted Imidazoles and Their Use in the Design of Potent DFG-Out Allosteric B-Raf Inhibitors. *Bioorg. Med. Chem.* **2010**, *18*, 292-304.

66. Bain, J. D.; Wacker, D. A.; Kuo, E. E.; Chamberlin, A. R., Site-Specific Incorporation of Non-Natural Residues into Peptides: Effect of Residue Structure on Suppression and Translation Efficiencies. *Tetrahedron* **1991**, *47*, 2389-2400.

67. Megumi, K.; Arif, F, N, B, M.; Matsumoto, S.; Akazome, M., Design and Evaluation of Salts between *N*-Trityl Amino Acid and *tert*-Butylamine as Inclusion Crystals of Alcohols. *Cryst. Growth Des.* **2012**, *12*, 5680-5685.

68. Osberger, T. J.; Rogness, D. C.; Kohrt, J. T.; Stepan, A. F.; White, M. C., Oxidative Diversification of Amino Acids and Peptides by Small-Molecule Iron Catalysis. *Nature* **2016**, *537*, 214-219.

69. Abdel-Hafez, S. H.; Abdelwahab, A. B.; Kirsch, G., Design, Synthesis and Cytotoxic Activity of Vitamin E Bearing Selenium Compounds Against Human Breast Cancer Cell Line (MCF-7). *Phosphorus. Sulfur.* **2017**, *192*, 1114-1118.

70. Seizert, C. A.; Ferreira, E. M., An Examination of the Scope and Stereochemistry of the Ireland-Claisen Rearrangement of Boron Ketene Acetals. *Chemistry* **2014**, *20*, 4460-4468.

71. Yang, J.; Ke, C.; Zhang, D.; Liu, X.; Feng, X., Enantioselective Synthesis of 2,2,3-Trisubstituted Indolines via Bimetallic Relay Catalysis of α -Diazoketones with Enones. *Org. Lett.* **2018**, *20*, 4536-4539.

72. Sasano, Y.; Nagasawa, S.; Yamazaki, M.; Shibuya, M.; Park, J.; Iwabuchi, Y., Highly Chemoselective Aerobic Oxidation of Amino Alcohols into Amino Carbonyl Compounds. *Angew. Chem. Int. Ed.* **2014**, *53*, 3236-3240.

73. Cottrell, I. F.; Cowley, A. R.; Croft, L. J.; Hymns, L.; Moloney, M. G.; Nettleton, E. J.; Kirsty Smithies, H.; Thompson, A. L., Acyloxylactonisations Mediated by Lead Tetracarboxylates. *Tetrahedron* **2009**, *65*, 2537-2550.

74. Cheng, X. F.; Li, Y.; Su, Y. M.; Yin, F.; Wang, J. Y.; Sheng, J.; Vora, H. U.; Wang, X. S.; Yu, J. Q., Pd(II)-Catalyzed Enantioselective C-H Activation/C-O Bond Formation: Synthesis of Chiral Benzofuranones. *J. Am. Chem. Soc.* **2013**, *135*, 1236-1239.
75. Liang, H.; Xu, G. Q.; Feng, Z. T.; Wang, Z. Y.; Xu, P. F., Dual Catalytic Switchable Divergent Synthesis: An Asymmetric Visible-Light Photocatalytic Approach to Fluorine-Containing gamma-Keto Acid Frameworks. *J. Org. Chem.* **2019**, *84*, 60-72.
76. Chronakis, N.; Orfanopoulos, M., Ene Reaction of Arylallyl Alkenes with C60. A Mechanistic Approach. *Org. Lett.* **1999**, *1*, 1909-1912.
77. Driver, T. G.; Harris, J. R.; Woerpel, K. A., Kinetic Resolution of Hydroperoxides with Enantiopure Phosphines: Preparation of Enantioenriched Tertiary Hydroperoxides. *J. Am. Chem. Soc.* **2007**, *129*, 3836-3837.
78. Cui, T.; Ma, L.; Wang, S.; Ye, C.; Liang, X.; Zhang, Z.; Meng, G.; Zheng, L.; Hu, H. S.; Zhang, J.; Duan, H.; Wang, D.; Li, Y., Atomically Dispersed Pt-N₃C₁ Sites Enabling Efficient and Selective Electrocatalytic C-C Bond Cleavage in Lignin Models under Ambient Conditions. *J. Am. Chem. Soc.* **2021**, *143*, 9429-9439.
79. Wang, Y.; Li, P.; Wang, J.; Liu, Z.; Wang, Y.; Lu, Y.; Liu, Y.; Duan, L.; Li, W.; Sarina, S.; Zhu, H.; Liu, J., Visible-Light Photocatalytic Selective Oxidation of C(sp³)-H Bonds by Anion-Cation Dual-Metal-Site Nanoscale Localized Carbon Nitride. *Catal. Sci. Technol.* **2021**, *11*, 4429-4438.
80. Uyanik, M.; Fukatsu, R.; Ishihara, K., Bromine-Catalyzed Aerobic Oxidation of Alcohols. *Chem. Asian J.* **2010**, *5*, 456-460.
81. Meng, S. S.; Lin, L. R.; Luo, X.; Lv, H. J.; Zhao, J. L.; Chan, A. S. C., Aerobic Oxidation of Alcohols with Air Catalyzed by Decacarbonyldimanganese. *Green Chem.* **2019**, *21*, 6187-6193.
82. Behera, P. K.; Choudhury, P.; Sahu, S. K.; Sahu, R. R.; Harvat, A. N.; McNulty, C.; Stitgen, A.; Scanlon, J.; Kar, M.; Rout, L., Oxygen Bridged Bimetallic CuMoO₄ Nanocatalyst for Benzylic Alcohol Oxidation; Mechanism and DFT Study. *Asian J. Org. Chem.* **2021**, *10*, 1117-1122.
83. Uygur, M.; Kuhlmann, J. H.; Pérez-Aguilar, M. C.; Piekarski, D. G.; García Mancheño, O., Metal- and Additive-Free C-H Oxygenation of Alkylarenes by Visible-Light Photoredox Catalysis. *Green Chem.* **2021**, *23*, 3392-3399.
84. Ma, R.; Xiao, Z.; Zhong, W.; Lu, C.; Shen, Z.; Zhao, D.; Liu, X., The Superiority of Cuprous Chloride to Iodide in the Selective Aerobic Oxidation of Benzylic Alcohols at Ambient Temperature. *Appl. Organomet. Chem.* **2021**, *35*, e6245.

85. Ma, L.; Zhou, H.; Kong, X.; Li, Z.; Duan, H., An Electrocatalytic Strategy for C–C Bond Cleavage in Lignin Model Compounds and Lignin under Ambient Conditions. *ACS Sustain. Chem. Eng.* **2021**, *9*, 1932-1940.
86. Dogga, B.; Kumar, C. S. A.; Joseph, J. T., Palladium-Catalyzed Reductive Carbonylation of (Hetero) Aryl Halides and Triflates Using Cobalt Carbonyl as CO Source. *Eur. J. Org. Chem.* **2020**, *2021*, 309-313.
87. Tian, Y.; Guo, X.; Li, M.; Li, C.; Hu, X.; Jin, L.; Sun, N.; Hu, B.; Shen, Z., SBA-15 Supported 1-Methyl-2-azaadamantane N-Oxyl (1-Me-AZADO) as Recyclable Catalyst for Oxidation of Alcohol. *Org. Lett.* **2021**, *23*, 3928-3932.
88. Dharpure, P. D.; Bhowmick, A.; Warghude, P. K.; Bhat, R. G., Visible-Light Mediated Facile Dithiane Deprotection under Metal Free Conditions. *Tetrahedron Lett.* **2020**, *61*, 151407.
89. Lee, G. S.; Won, J.; Choi, S.; Baik, M. H.; Hong, S. H., Synergistic Activation of Amides and Hydrocarbons for Direct C(sp³)-H Acylation Enabled by Metallaphotoredox Catalysis. *Angew. Chem. Int. Ed.* **2020**, *59*, 16933-16942.
90. Liou, Y. C.; Su, Y. H.; Ku, K. C.; Edukondalu, A.; Lin, C. K.; Ke, Y. S.; Karanam, P.; Lee, C. J.; Lin, W., Organophosphane-Promoted Synthesis of Functionalized α,β -Unsaturated Alkenes and Furanones via Direct β -Acylation. *Org. Lett.* **2019**, *21*, 8339-8343.
91. Indalkar, K. S.; Khatri, C. K.; Chaturbhuj, G. U., Sulfated polyborate: A Mild, Efficient Catalyst for Synthesis of *N*-*tert*-butyl/*N*-trityl Protected Amides via Ritter Reaction. *J. Chem. Sci.* **2017**, *129*, 415-420.
92. Gangadurai, C.; Illa, G. T.; Reddy, D. S., FeCl₃-Catalyzed Oxidative Decarboxylation of Aryl/Heteroaryl Acetic Acids: Preparation of Selected API Impurities. *Org. Biomol. Chem.* **2020**, *18*, 8459-8466.
93. Ge, L.; Wang, D. X.; Xing, R.; Ma, D.; Walsh, P. J.; Feng, C., Photoredox-Catalyzed Oxo-Amination of Aryl Cyclopropanes. *Nat. Commun.* **2019**, *10*, 4367.
94. Li, Z.; Chu, J.; Meng, D.; Wen, Y.; Xing, X.; Miao, H.; Hu, M.; Yu, C.; Wei, Z.; Yang, Y.; Li, Y., Photocatalytic Chemical CO₂ Fixation by Cu-BDC Nanosheet@Macroporous–Mesoporous-TiO₂ under Mild Conditions. *ACS Catal.* **2019**, *9*, 8659-8668.
95. Tayama, E.; Ishikawa, Y., Bronsted Acid-Catalyzed Aza-Ferrier Reaction of N,O-Allenyl Acetals: Synthesis of β -Amino- α -methylene Aldehydes. *J. Org. Chem.* **2020**, *85*, 9405-9414.
96. Humphries, P. S.; Bersot, R.; Kincaid, J.; Mabery, E.; McCluskie, K.; Park, T.; Renner, T.; Riegler, E.; Steinfeld, T.; Turtle, E. D.; Wei, Z. L.; Willis, E., Carbazole-Containing Amides

and Ureas: Discovery of Cryptochrome Modulators as Antihyperglycemic Agents. *Bioorg. Med. Chem. Lett.* **2018**, *28*, 293-297.

97. Palav, A.; Misal, B.; Ganwir, P.; Badani, P.; Chaturbhuj, G., Rapid, Chemoselective and Mild Oxidation Protocol for Alcohols and Ethers with Recyclable *N*-Chloro-*N*-(phenylsulfonyl)benzenesulfonamide. *Tetrahedron Lett.* **2021**, *73*, 153094.

98. Mori, N.; Togo, H., Facile Oxidative Conversion of Alcohols to Esters using Molecular Iodine. *Tetrahedron* **2005**, *61*, 5915-5925.

99. Puls, F.; Linke, P.; Kataeva, O.; Knolker, H. J., Iron-Catalyzed Wacker-type Oxidation of Olefins at Room Temperature with 1,3-Diketones or Neocuproine as Ligands*. *Angew. Chem. Int. Ed.* **2021**, *60*, 14083-14090.

100. Hu, C.; Li, G.; Mu, Y.; Wu, W.; Cao, B.; Wang, Z.; Yu, H.; Guan, P.; Han, L.; Li, L.; Huang, X., Discovery of Anti-TNBC Agents Targeting PTP1B: Total Synthesis, Structure-Activity Relationship, *In Vitro* and *In Vivo* Investigations of Jamunones. *J. Med. Chem.* **2021**, *64*, 6008-6020.

101. Subba Reddy, B. V.; Anusha, B.; Subba Reddy, U. V.; Yadav, J. S.; Suresh Reddy, C., A Concise and Convergent Total Synthesis of Two Novel Cytotoxic Hydroquinones, Lanneaquinol and (*R*)-2'-Hydroxylanneaquinol. *Helv. Chim. Acta* **2013**, *96*, 1983-1990.

Chapter 3

Chemoselective Decarboxylative Oxygenation of Carboxylic Acids to Access Ketones, Aldehydes, Alcohols and Peroxides

3.1 Introduction

Control of chemoselectivity is one of the most enduring and important topics in organic synthesis.¹ Decarboxylative oxygenation of carboxylic acids is a good example, which could afford three different products, a peroxide, a carbonyl or an alcohol, in a de-homologation manner (Scheme 3.1a). This is potentially a tremendously interesting and meaningful reaction, because of the abundance and easy availability of the substrate and the huge importance of each product. Carboxylic acids are probably the most easily accessible functionality in biological and chemical synthesis.² Most of carboxylic acids are widespread in nature, e.g. keto-acids, fatty acids and amino acids, or are produced at large industrial scale, e.g. benzoic acid, formic acid, acetic acid and acrylic acid, and they are simple to handle and easy to store.³⁻

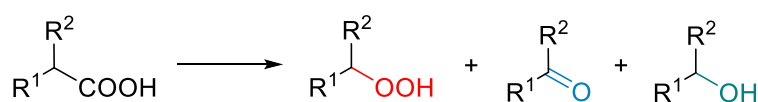
6

Carbonyl compounds, e.g. aldehydes and ketones, are widely used as starting materials and precursors in the organic synthesis of a wide range of chemicals including drugs, vitamins and fragrances.⁷ The importance of them can hardly be overstated. Meanwhile, alcohols, especially aliphatic alcohols, are important feedstocks for the large-scale synthesis of detergents, plasticizers and surfactants.⁸ In comparison, the role of organic peroxides in organic synthesis has been less important. However, their importance in many biological processes, e.g. biodegradation, aging and drug development, is obvious. In addition, they are widely employed in oxidation reactions as oxidants and in polymerization processes as initiators.⁹⁻¹⁰

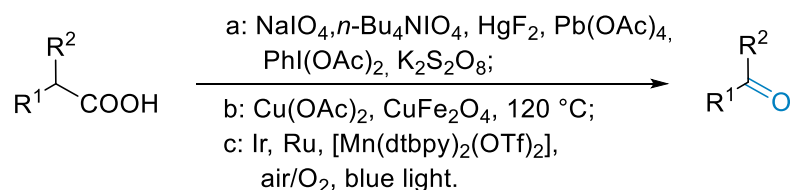
Thus, it is a valuable and meaningful endeavor to develop a method for selective decarboxylative oxygenation of carboxylic acids to peroxides, carbonyls and alcohols. This is

particularly so with the latter two classes of compounds. Whilst the synthesis of aldehydes and ketones via decarboxylation of carboxylic acids (*vide infra*) has been investigated by various methods including that described in Chapter 2, methods to access organic peroxides have been limited. And those reported methods usually rely on harsh conditions and/or suffer from a limited substrate scope.¹¹ For instance, only a few methods are feasible for the formation of both benzylic and aliphatic peroxides using benign, green and economic oxidants, i.e. O₂¹² or H₂O₂.¹³

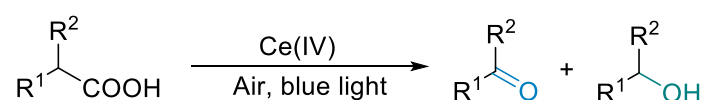
(a) Possible products from decarboxylative oxygenation of carboxylic acids



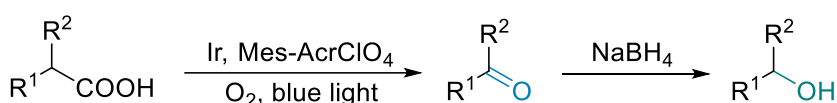
(b) Decarboxylative oxygenation of carboxylic acids to aldehydes or ketones



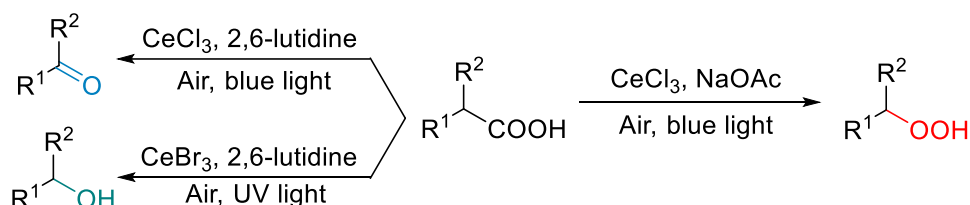
(c) Decarboxylative oxygenation of carboxylic acids to carbonyls + alcohols



(d) Decarboxylative oxygenation of carboxylic acids to alcohols



(e) Our work: Selective decarboxylative oxygenation of carboxylic acids



Scheme 3.1 Decarboxylative oxygenation of carboxylic acids to form various products.

Alcohols are often prepared via hydrogenation of carboxylic acids, which usually rely on harsh conditions, i.e. high pressure and temperature. For instance, fatty alcohols are produced

as detergents at large industrial scale from hydrogenation of fatty acids at 200-300 bar and 250-350 °C.¹⁴⁻¹⁵ In comparison, oxidative decarboxylation of fatty acids could offer an alternative, much milder route to access fatty alcohols that are odd numbered via de-homologation. However, it is challenging to control the chemoselectivity of the decarboxylative oxygenation, because peroxides and alcohols are easy to be further oxidized to the more stable carbonyl compounds. Indeed, although peroxides are generally believed to be a key intermediate in the decarboxylative oxygenation reaction in previous reports,¹⁶⁻¹⁸ only one example has shown the possibility of synthesis of peroxides from decarboxylation and their use in intramolecular cyclization.¹⁸ In addition, chemoselective synthesis of alcohols from the decarboxylation without resorting to a strong reductant has not been reported yet.

The decarboxylative oxygenation of carboxylic acids to aldehydes or ketones has been well documented (Scheme 3.1b). However, stoichiometric amounts of oxidants, such as NaIO₄,¹⁹ *n*-Bu₄NIO₄,²⁰ HgF₂,²¹ Pb(OAc)₄,²² PhI(OAc)₂,²³ and K₂S₂O₈,²⁴ or high temperature are required for most earlier methods. Recently, photocatalytic oxidative decarboxylation of carboxylic acids with O₂ has been developed, and a range of catalysts such as [Ir(dF(Me)ppy)₂(bpy)]PF₆, [Ru(bpy)₃]Cl₂, [Mn(dtbp)₂(OTf)₂] or acridiniums have been employed under blue or visible light irradiation.^{16, 25-26} In addition to the noble metal catalysts, the earth-abundant cerium has been found to be efficient catalyst for decarboxylation of carboxylic acids.²⁷⁻³⁰ Particularly, a Ce(IV) carboxylate cluster, generated from Ce(O*t*Bu)₄, catalyses efficient aerobic decarboxylative oxygenation of carboxylic acids to afford carbonyl compounds together with a small amount (*ca* 20%) of alcohols by-products under blue light (Scheme 3.1c).¹⁸ These reactions most likely proceed via the intermediary of peroxides, formed upon the interception of decarboxylation-generated carbon radical by O₂.¹⁶⁻¹⁷ It has been shown that the peroxides can be reduced to alcohols with NaBH₄ in situ under the oxidation conditions

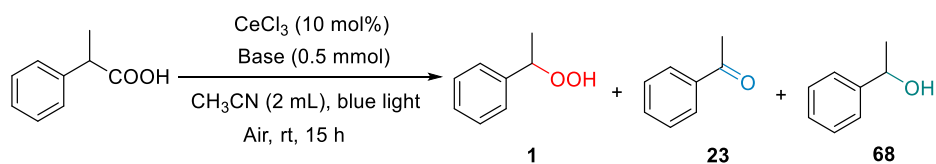
or post oxidative decarboxylation (Scheme 3.1d).³¹⁻³² However, it is desirable to develop a safer route to alcohols that avoids simultaneous use of an oxidant and a strong reductant.

In Chapter 2, our Mn-catalysis system realized the transformation of carboxylic acids to carbonyls. However, controlling the selectivity of decarboxylative oxygenation to afford other products, such as alcohols and peroxides, remains challenging. In this chapter, we report a photocatalytic method that enables, for the first time, selective formation of aldehydes/ketones, peroxides and alcohols via aerobic decarboxylative oxygenation of carboxylic acids with simple, cheap cerium halides as catalyst (Scheme 3.1e).

3.2 Results and discussion

3.2.1 Optimization experiments

Table 3.1 Optimization of selective transformation of carboxylic acids^{a,b}



Entry	Catalyst	Base	Yield (%)		
			1	23	68
1	CeCl ₃	NaOAc	94	2	0
2	CeCl ₃	/	49	22	0
3	CeCl ₃	2,6-lutidine	0	74	22
4	CeCl ₃	KOAc	37	8	0
5	CeCl ₃	LiOAc	38	42	0
6	CeCl ₃	CsOAc	33	9	0
7	CeCl ₃	Na ₂ CO ₃	37	2	0
8	CeCl ₃	NaOH	9	1	0
9	CeCl ₃	Pyridine	0	51	10
10	CeCl ₃	Et ₃ N	0	37	0
11	CeCl ₃	DBU	0	10	0
12 ^c	CeCl ₃	NaOAc	0	0	0
13	/	NaOAc	0	0	0
14 ^d	CeCl ₃	NaOAc	0	0	0

^aReaction conditions: α -methylphenylacetic acid (0.5 mmol), CeCl₃ (10 mol%), base (0.5 mmol), CH₃CN (2 mL), air, blue light (465 nm, 9 W), room temperature, 15 h. ^bNMR yields are given, determined using mesitylene (20 μ L) as internal standard. ^cReaction in dark. ^dN₂ instead of air.

We started from searching optimum conditions for selective decarboxylative oxygenation of carboxylic acids. We examined CeCl_3 as a potential catalyst for the model reaction of α -methylphenylacetic acid with 1 bar of air under the irradiation of blue light (465 nm, 9 W), which was inspired by the remarkable ability of Ce(III/IV) in engaging photoredox reactions.³³⁻³⁶ In comparison with $\text{Ce}(\text{O}t\text{Bu})_4$,¹⁸ CeCl_3 is much cheaper and more easily available. The results are shown in Table 3.1. As can be seen, much to our surprise, the hydroperoxide **1** was obtained in an excellent yield of 94% when 1 equivalent of NaOAc was employed as base. The formation of hydroperoxides has been observed before, but in a significantly lower yield.¹⁸ Without the addition of the base, it is interesting that α -methylphenylacetic acid was transformed to a mixture of **1** and 1-phenylethanone (**23**) in 49% and 22% yield, respectively (Table 3.1, entry 2).

Aiming to alter the reaction selectivity, a range of bases in the reaction were screened. Obviously, the base plays a decisive role in affecting the selectivity of products (Table 3.1, entries 1, 3-11). Whilst the addition of NaOAc led to almost exclusive formation of the peroxide **1**, the addition of 2,6-lutidine as base afforded the ketone **23** and alcohol **68** in yields similar to those obtained with $\text{Ce}(\text{O}t\text{Bu})_4$.¹⁸ Lower yields were afforded with other bases including KOAc, LiOAc, CsOAc, Na_2CO_3 , NaOH, pyridine, Et_3N and DBU (Table 3.1, entries 4-11). It is interesting to find that the formation of the peroxide is strongly promoted by NaOAc and to a less degree by Na_2CO_3 but suppressed by amine bases. The difference in yield observed with the different acetate bases (Table 3.1, entries 1 and 4-6) may be at least partly due to their varying solubilities in the solvent used (Table 3.2). This dramatic effect of bases on the chemoselectivity of decarboxylative oxygenation has not been noted in previous studies. Taking NaOAc and 2,6-lutidine as the optimum base for the formation of **1** and **23**, respectively, the effect of other cerium compounds as possible catalysts was examined (Table 3.3); but none was better than CeCl_3 in forming **1** or **23**. Selective formation of alcohols was

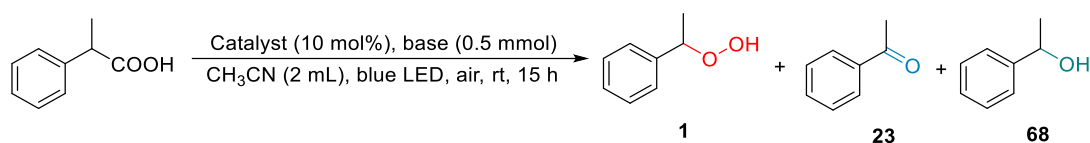
achieved upon further studies (*vide infra*). As may be expected, blue light, CeCl₃, and air are all essential components for the decarboxylative oxygenation to occur (Table 3.1, entries 12-14).

Table 3.2 Estimated solubility of bases in CH₃CN^a

Base	NaOAc	KOAc	LiOAc	CsOAc
Solubility ^b	7.3%	5.1%	0.8%	0.4%

^aMeasured at ambient temperature (Details can be seen in Section 3.3.3); ^bSolubility (wt. %).

Table 3.3 Screening of Ce catalysts for selective decarboxylative oxygenation of α -methylphenylacetic acid^{a,b}



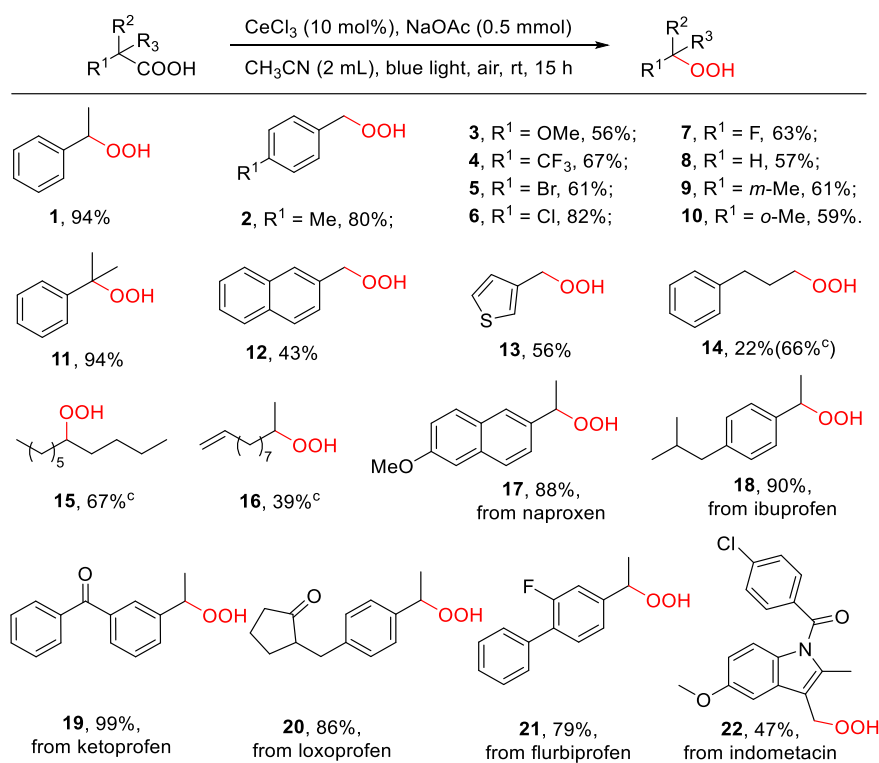
Entry	Catalyst	Base	Yield (%)		
			1	23	68
1	Ce(OAc) ₃	NaOAc	88	2	0
2	CeBr ₃	NaOAc	89	4	0
3	Ce ₂ (C ₂ O ₄) ₃	NaOAc	90	1	0
4	CeF ₃	NaOAc	11	0	0
5	CeF ₄	NaOAc	50	1	0
6	NH ₄ Ce(NO ₃) ₆	NaOAc	84	1	0
7	Ce(OAc) ₃	2,6-lutidine	0	51	28
8	CeBr ₃	2,6-lutidine	0	36	17
9	Ce ₂ (C ₂ O ₄) ₃	2,6-lutidine	0	2	0
10	CeF ₃	2,6-lutidine	0	6	0
11	CeF ₄	2,6-lutidine	0	0	3
12	NH ₄ Ce(NO ₃) ₆	2,6-lutidine	0	0	5

^aReaction conditions: α -methylphenylacetic acid (0.5 mmol), catalyst (10 mol%), base (0.5 mmol), CH₃CN (2 mL), under air, blue LED (465 nm, 9W), room temperature, overnight. ^bNMR yields are given.

3.2.2 Substrate scope

The decarboxylative oxygenation of a variety of carboxylic acids was investigated to demonstrate the generality of our protocol. Firstly, we examined the scope for the formation of hydroperoxides. As shown in Scheme 3.2, selective decarboxylative oxygenation of a variety of phenylacetic acids proceeded well and the corresponding hydroperoxide products were

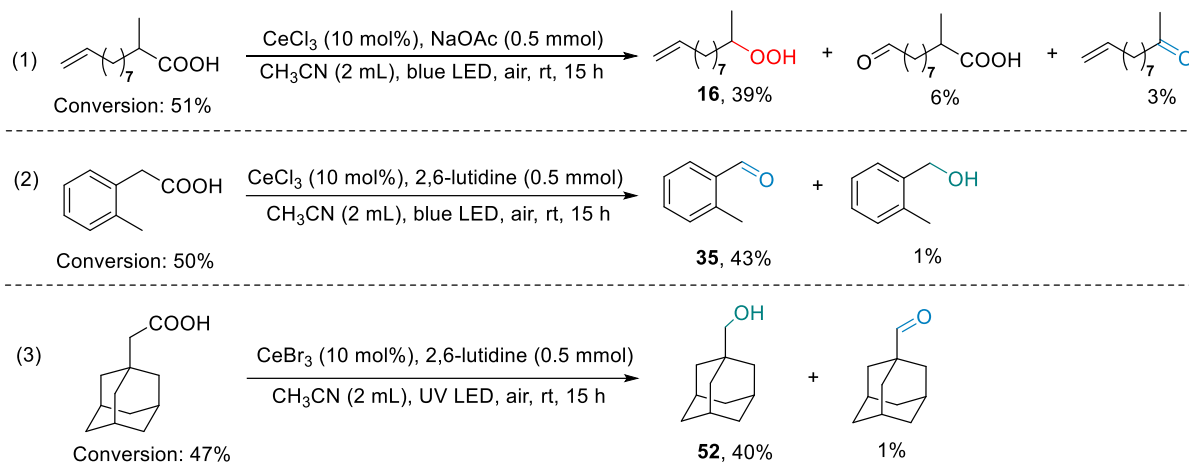
afforded in good yields (46-94%). All the halogen-substituted (*p*-CF₃-, *p*-Br-, *p*-Cl-, and *p*-F-) phenylacetic acids underwent decarboxylative oxygenation successfully, affording the corresponding hydroperoxide products (**4-7**) in good yields. Meanwhile, a thiopheneacetic acid worked, without poisoning the catalyst, so did 2-naphthylacetic acid, albeit in moderate yields. In comparison with *p*-substituted hydroperoxide (**2**), *m*-substituted (**9**) and *o*-substituted (**10**) hydroperoxide products showed lower yields (61% and 59%). These results may indicate that the position of substitutes affects the yields. This might result from some steric hindrance.³⁷ Notably, the secondary (**1**) and tertiary peroxides (**11**) were obtained in significantly higher yields (94%) than the primary analogue (**2**), indicating the involvement of benzylic radical in the formation of the peroxide products.



Scheme 3.2 Decarboxylative oxygenation of carboxylic acids to hydroperoxides.^{a,b} ^aReaction conditions: acid (0.5 mmol), CeCl₃ (10 mol%), NaOAc (0.5 mmol), CH₃CN (2 mL), blue light (465 nm, 9 W), air, room temperature, 15 h. ^bIsolated yields are given. ^cNa₂CO₃ (0.5 mmol) instead of NaOAc, and N₂/O₂ (1:2) mixture instead of air.

Transformation of more challenging aliphatic acids to corresponding peroxides (**14-16**) is also feasible, though a higher O₂ concentration (N₂/O₂ volume: 1:2; 1 bar) and Na₂CO₃ as the

base were required. As shown in Scheme 3.2, a lower yield of **14** was obtained under the condition of using air and NaOAc. Worth noting is that the oxidation-prone C=C bond remained intact in **16**, and byproducts were formed in very low yields (Scheme 3.3, eq. 1). Meanwhile, no benzylic oxidation was observed in the formation of **14**.



Scheme 3.3 Selective decarboxylative oxygenation of different acids.

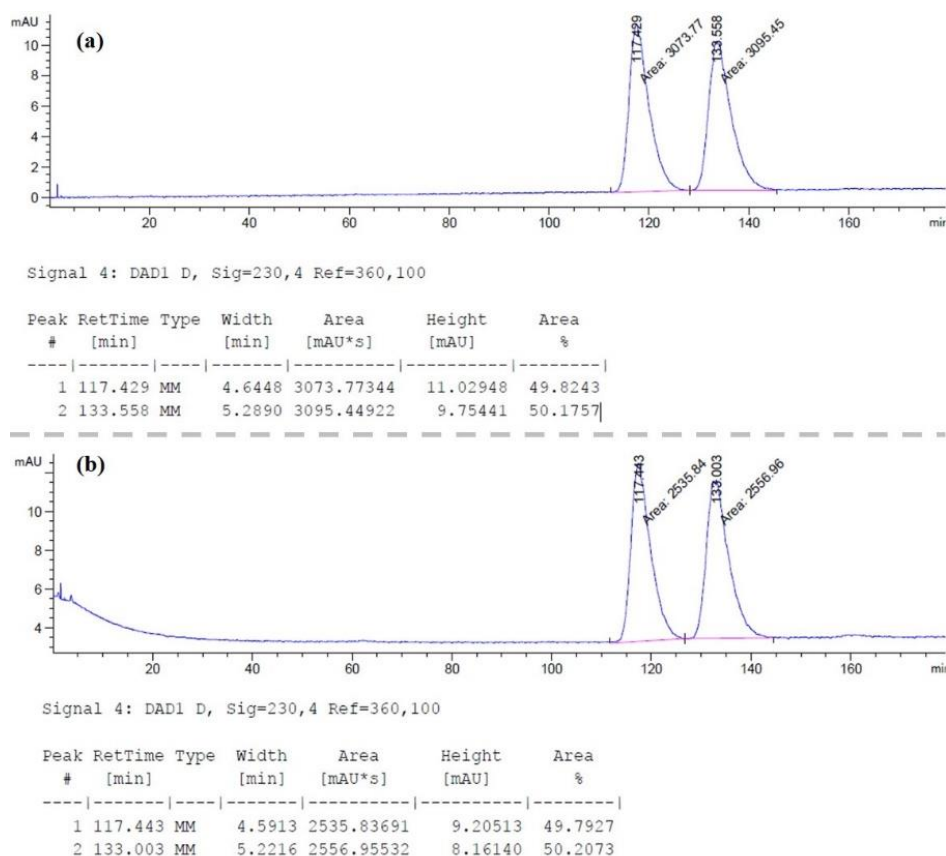
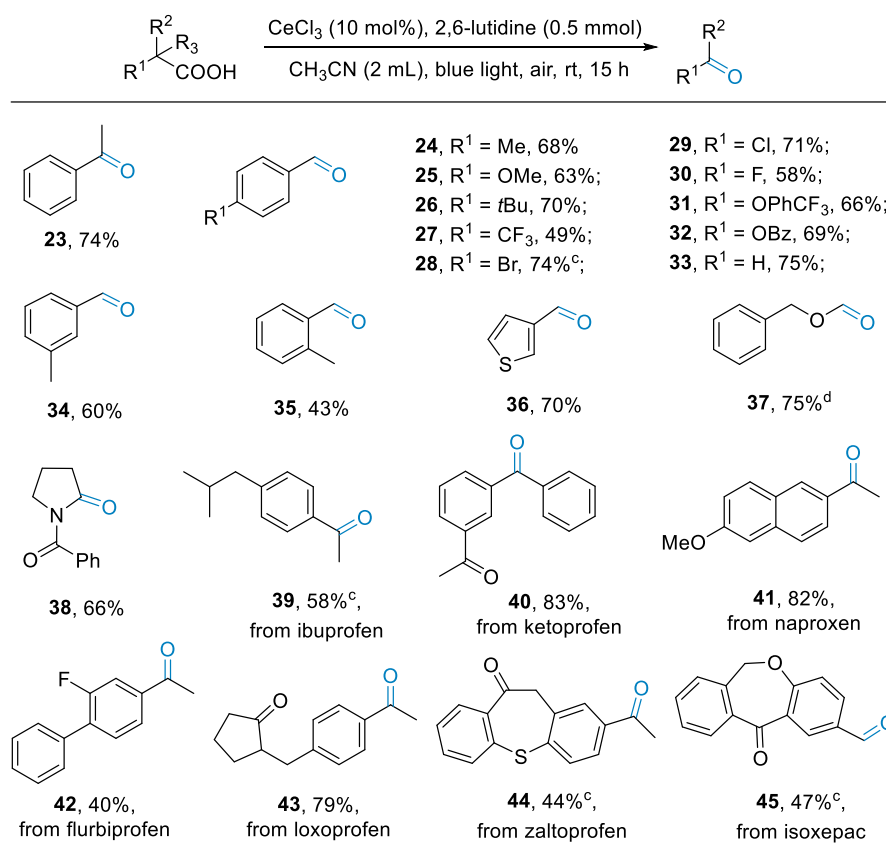


Figure 3.1 HPLC traces of hydroperoxides from (*S*)-naproxen (a) and racemic naproxen. (b) The results show the oxidation reaction to be non-enantioselective.

Furthermore, a series of anti-inflammatory drugs, such as naproxen, ibuprofen, ketoprofen, loxoprofen, flurbiprofen and indomethacin proceeded well in the reaction, affording the corresponding hydroperoxide products (**17-22**) in moderate to high yields (47-99%). Such peroxides could provide metabolites for drug study, as they may form under enzymatic oxidation.³⁸

The decarboxylative oxygenation of (*S*)-naproxen was examined under the same conditions as for racemic naproxen (**17**). As shown in Figure 3.1, the resulting peroxide was racemic. The result indicates again that a benzylic radical intermediate is likely to be involved in the decarboxylative oxygenation. Although it is generally assumed that peroxy species are formed from the reaction of triplet O₂ with the carbon radical,^{16-18, 39} the isolation of a range of peroxides as potentially useful products in oxidative decarboxylation is firstly reported here.

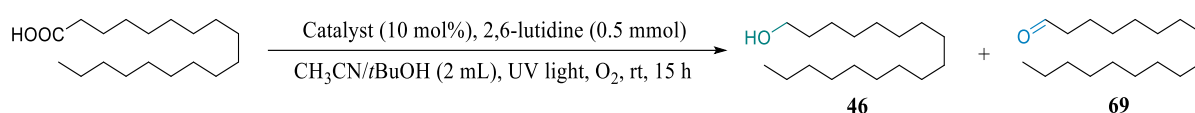


Scheme 3.4 Decarboxylative oxygenation of carboxylic acids to aldehydes and ketones.^{a,b} ^aReaction conditions: acid (0.5 mmol), CeCl₃ (10 mol%), 2,6-lutidine (0.5 mmol), CH₃CN (2 mL), blue light (465 nm, 9 W), air, room temperature, 15 h. ^bIsolated yields are given. ^cPyridine (0.5 mmol) instead of 2,6-lutidine. ^dUV (365 nm, 9 W) instead of blue light.

The selectivity of the oxidative decarboxylation can be channelled to carbonyl products by simply changing the base from NaOAc to 2,6-lutidine. As shown in Scheme 3.4, a wide range of aldehydes and ketones were obtained from the selective decarboxylative oxygenation of acids, demonstrating the high adaptability and practicability of our strategy. Firstly, a variety of phenylacetic acids bearing different functional groups underwent decarboxylative oxygenation successfully, affording the corresponding aldehyde and ketone products (**23-35**) in moderate to good yields (43-75%). To showcase the chemoselectivity of this transformation, *o*-tolylacetic acid was selected as an example substrate. As shown in Scheme 3.3 (eq. 2), only a trace of the alcohol byproduct was detected. Phenylacetic acids bearing both electron-withdrawing halide substituents, including -CF₃, -Br, -Cl, and -F, and electron-donating substituents, e.g. *m*-Me and *o*-Me, were tolerated in the decarboxylative oxygenation.

Moreover, an acid bearing a heteroatom ring, i.e. thiophene, processed well, affording **36** in a good yield (70%). Notably, 2-(phenylmethoxy)acetic acid with an oxygen atom in the carbon chain was also tolerated, without the weak benzylic C-H bond being compromised (**37**). An amino acid derivative reacted smoothly, affording the corresponding amide product **38** in a good yield (66%).

As with the reaction leading to peroxides, a series of drug molecules, including ibuprofen, ketoprofen, naproxen, flurbiprofen, loxoprofen, zaltoprofen and isoxepac, were shown to work well. As seen in Scheme 3.4, the corresponding aldehyde or ketone products (**39-45**) were formed in moderate to excellent yields (40-83%). These derivatives not only are useful in the study of drug metabolism, but also may serve as substrates for further reactions or as useful scaffolds to build new bioactive molecules.⁴⁰⁻⁴¹

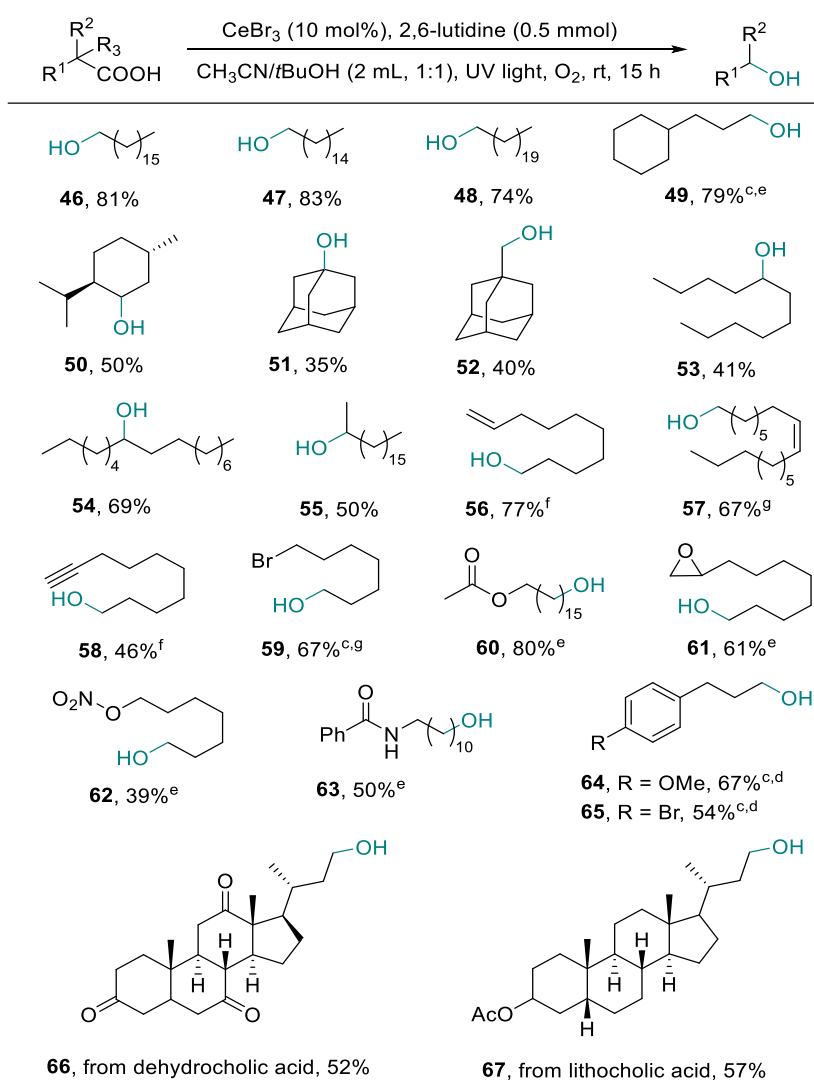
Table 3.4 Screening experimental conditions for selective decarboxylative oxygenation of stearic acid^{a,b}

Entry	Catalyst	Solvent	Base	Yield (%)	
				46	69
1	CeBr ₃	CH ₃ CN/ <i>t</i> BuOH	/	52	13
2	CeBr ₃	CH ₃ CN/ <i>t</i> BuOH	2,6-lutidine	81	16
3	/	CH ₃ CN/ <i>t</i> BuOH	2,6-lutidine	4	0
4	CeBr ₃	CH ₃ CN	2,6-lutidine	55	16
5	CeBr ₃	<i>t</i> BuOH	2,6-lutidine	12	5
6	CeBr ₃	CH ₃ CN/ <i>t</i> BuOH	Pyridine	51	7
7	CeBr ₃	CH ₃ CN/toluene	2,6-lutidine	39	6
8	CeBr ₃	CH ₃ CN/chloroform	2,6-lutidine	10	0
9	CeBr ₃	CH ₃ CN/acetone	2,6-lutidine	38	4
10	CeBr ₃	CH ₃ CN/ethyl acetate	2,6-lutidine	19	4
11	CeBr ₃	<i>t</i> BuOH/toluene	2,6-lutidine	5	0
12	CeBr ₃	<i>t</i> BuOH/chloroform	2,6-lutidine	25	3
13	CeBr ₃	<i>t</i> BuOH/acetone	2,6-lutidine	37	5
14	CeBr ₃	<i>t</i> BuOH/ethyl acetate	2,6-lutidine	34	4
15	CeCl ₃	CH ₃ CN/ <i>t</i> BuOH	2,6-lutidine	61	9
16 ^c	CeBr ₃	CH ₃ CN/ <i>t</i> BuOH	2,6-lutidine	0	0
17 ^d	CeBr ₃	CH ₃ CN/ <i>t</i> BuOH	2,6-lutidine	0	0
18 ^e	CeBr ₃	CH ₃ CN/ <i>t</i> BuOH	2,6-lutidine	36	0
19 ^f	CeBr ₃	CH ₃ CN/ <i>t</i> BuOH	2,6-lutidine	12	0
20	Ce(OAc) ₃	CH ₃ CN/ <i>t</i> BuOH	2,6-lutidine	4	0
21	Ce ₂ (C ₂ O ₄) ₃	CH ₃ CN/ <i>t</i> BuOH	2,6-lutidine	0	8
22	CeF ₃	CH ₃ CN/ <i>t</i> BuOH	2,6-lutidine	25	1
23	CeF ₄	CH ₃ CN/ <i>t</i> BuOH	2,6-lutidine	9	4
24	NH ₄ Ce(NO ₃) ₆	CH ₃ CN/ <i>t</i> BuOH	2,6-lutidine	40	8
25	/	CH ₃ CN/ <i>t</i> BuOH	/	0	0
26 ^g	CeCl ₃	CH ₃ CN	2,6-lutidine	6	2

^aReaction conditions: stearic acid (0.5 mmol), catalyst (10 mol%), base (0.5 mmol), CH₃CN/*t*BuOH (2 mL), O₂ (1 atm), UV LED (365 nm, 9W), room temperature, 15 h. ^bNMR yields are given. ^cReaction in dark. ^dN₂ instead of O₂. ^eAir instead of O₂. ^fBlue LED (465 nm) instead of UV LED. ^gBlue LED (465 nm) instead of UV LED, air instead of O₂.

Most notably, the chemoselectivity of the oxidative decarboxylation could be turned to alcohols. Considering the potential of the method in supplementing hydroformylation of α -

olefins followed by hydrogenation for fatty alcohols or hydrogenation of carboxylic acids for the same,¹¹ we first explored this alternative route for the synthesis of aliphatic alcohols from aliphatic carboxylic acids. In comparison with the stable benzylic carbons, these substrates are more challenging to undergo decarboxylation because of their less stability. Indeed, the decarboxylative oxygenation of stearic acid under the established conditions only afforded the expected 1-heptadecanol (**46**) in an unsatisfactory yield (Table 3.4, entry 26).

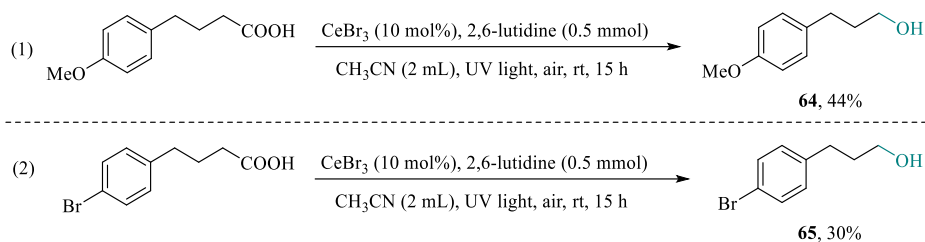


Scheme 3.5 Decarboxylative oxygenation of carboxylic acids to alcohols^{a,b} ^aReaction conditions: acid (0.5 mmol), CeBr₃ (10 mol%), 2,6-lutidine (0.5 mmol), CH₃CN/*t*BuOH (1:1, 2 mL), UV light (365 nm, 9 W), O₂, room temperature, 15 h. ^bIsolated yields are given. ^cNMR yields are given (Inaccurate isolated yields because of low boiling points of products), determined using mesitylene (20 μL) as internal standard. ^dBlue light (465 nm, 9 W) instead of UV light. ^e22 h. ^fNo addition of 2,6-lutidine. ^gNo addition of 2,6-lutidine, 22 h.

Further optimization helped to improve the transformation of stearic acid to 1-heptadecanol. After a series of optimization experiments, a more effective catalytic system using CeBr₃ with 2,6-lutidine under the irradiation of 365 nm light in CH₃CN/tBuOH and 1 bar of O₂ was identified under such conditions, and 1-heptadecanol was isolated in a high yield of 81% (Table 3.4, entry 2). The decarboxylative oxygenation of a variety of acid substrates were subsequently carried out and the results are shown in Scheme 3.5. Heptadecanoic acid and docosanoic acid were converted to the one-carbon-shorter fatty alcohols with good yields (**47** and **48**) as well as the cyclohexyl-terminated butanoic acid (**49** and **50**). Meanwhile, sterically bulky secondary and tertiary acids (**51-55**) were tolerated, although their corresponding products were afforded in lower yields. The high chemoselectivity of this transformation can be seen in the reaction of 2-(adamantan-1-yl)acetic acid. As shown in Scheme 3.3, only 1% of adamantane-1-carbaldehyde was formed as byproduct.

Notably, a series of fatty acids with a range of diverse functional groups, including alkene, alkyne, halogen, ester, heterocycle, nitrooxy and amide, were successfully oxidatively decarboxylated to alcohols (**56-63**). Note that for the fatty acids with C=C double and C≡C triple bonds, lower yields of alcohol products were afforded by the addition of 2,6-lutidine. For the aryl-terminated butanoic acids, blue instead of UV light was applied; the latter led to lower yields (Scheme 3.6). Moreover, drug molecules with complicated structures, such as the bile acids dehydrocholic acid and lithocholic acid (**66** and **67**), proceeded well. It is remarkable that the oxidation-sensitive alkene, alkyne and epoxy units survived in the reaction as well as secondary and tertiary C-H bonds. These results highlight the high selectivity of the protocol and its practical potential for late-stage decarboxylative oxygenation of bioactive molecules and drugs. It is difficult to access such functionalized alcohols (**56-63**, **66-67**) via common hydrogenation reactions. To the best of our knowledge, this is the first time that aliphatic acids,

including fatty acids, have been selectively transformed to alcohols in a de-homologation manner under mild conditions with high selectivity and good yields.



Scheme 3.6 Decarboxylative oxygenation of phenylbutanoic acids to alcohols under UV light.

3.2.3 Exploration of possible mechanism

Whilst the mechanism of decarboxylative oxygenation of carboxylic acids to carbonyl products has been widely studied,^{18, 25-26} the chemoselective formation of isolable peroxides and alcohols prompted us to look into the mechanism concerning particularly what controls the selectivity of the reaction. Firstly, HRMS measurement of a mixture of CeCl_3 with phenylacetic acid was conducted. As shown in Figure 3.2, a cerium species $[\text{Ce}(\text{PA-H})_2]^+$ appeared to be formed in the reaction, which could result from the coordination of two PA molecules with a Ce(III) centre.⁴²⁻⁴³ The coordination of carboxylates to Ce(IV) oxo species was also reported.¹⁸ Thus, it is likely that the selective decarboxylative oxygenation starts from the coordination of carboxylic acids to CeX_3 . Indeed, esters do not engage in the reaction (Scheme 3.7).

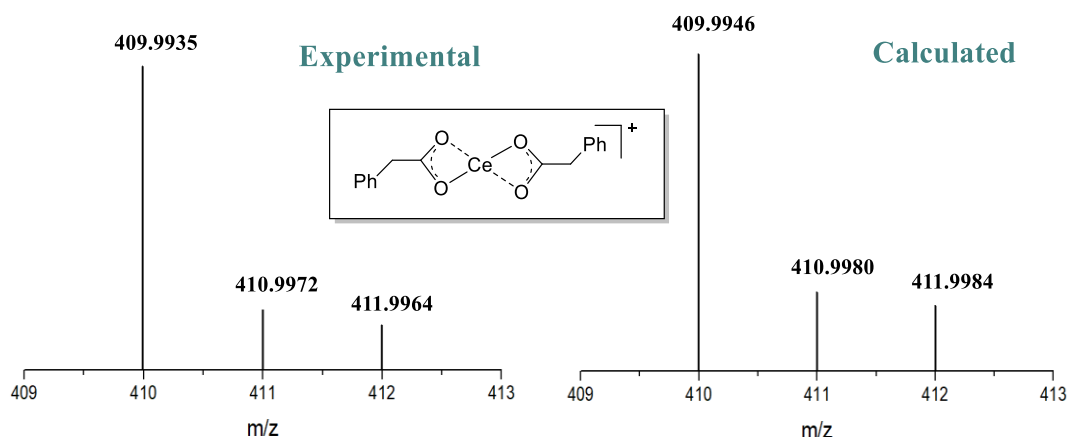
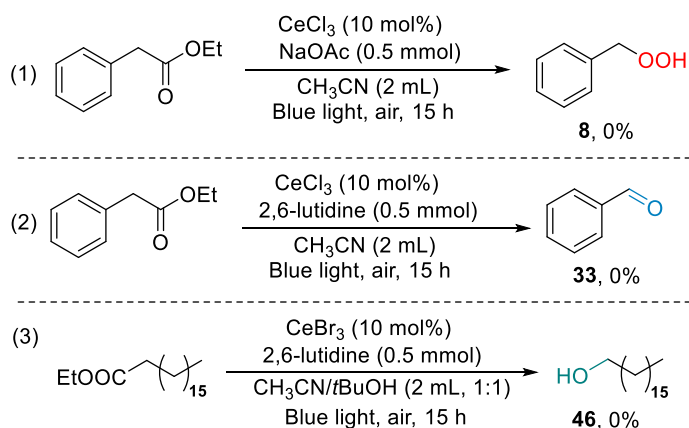


Figure 3.2 (a) HRMS spectra of Ce(III) complex formed in the in situ reaction of CeCl_3 with phenylacetic acid. Conditions: CeCl_3 (0.05 mmol), CH_3CN (2 mL), NaOAc or 2,6-lutidine (0.5 mmol), blue light, air, 465 nm.



Scheme 3.7 Decarboxylative oxygenation of phenylbutanoic acids to alcohols under UV light.

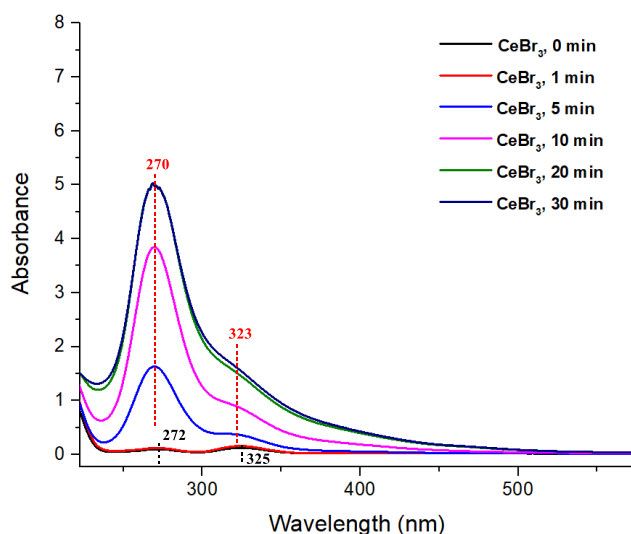


Figure 3.3 UV-Vis spectra of CeBr_3 under blue light irradiation. Conditions: CeBr_3 (0.05 mmol), $\text{CH}_3\text{CN}/t\text{BuOH}$ (2 mL, 1:1), air, 465 nm. Details can be seen in Section 3.3.3.

Next, we conducted experiments to identify possible active Ce species involved in the decarboxylative oxygenation process. The experimental conditions were altered because of low solubility of CeCl_3 in CH_3CN . CeBr_3 was selected as the catalyst because of its greater solubility in $\text{CH}_3\text{CN}/t\text{BuOH}$. The UV-Vis spectra of CeBr_3 recorded under air are shown in Figure 3.3. Two weak absorption bands at around 272 and 325 nm were observed without blue light irradiation.⁴⁴ After irradiation, a new absorption band and a shoulder at around 270 and 323 nm appeared, respectively, which overlapped with the previous absorption bands. These new bands increased quickly in intensity with irradiation time, indicating the easy transformation of Ce(III) to Ce(IV) species.^{34, 45} Same experiments were performed either

under N₂ atmosphere or in the dark; no change of the absorption bands of CeBr₃ was observed (Figure 3.4).

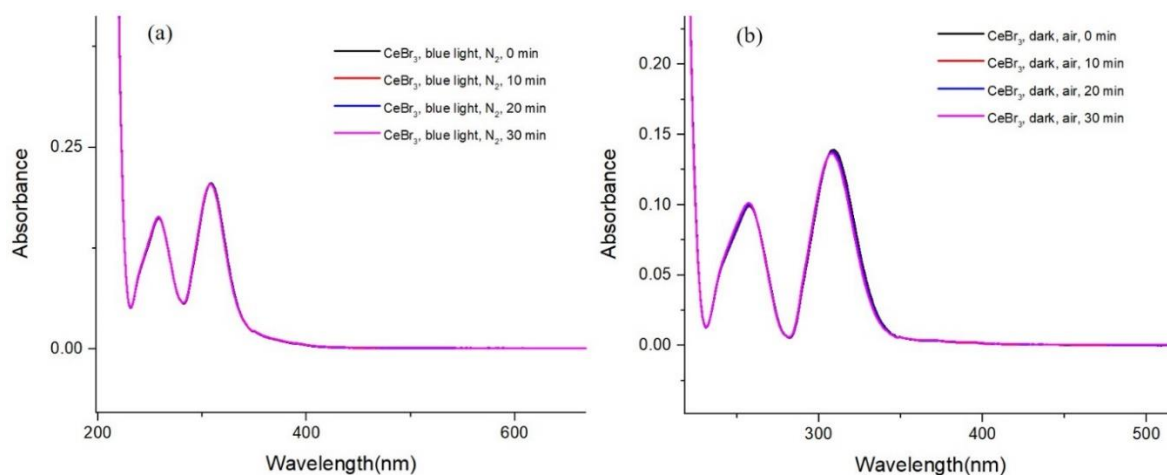


Figure 3.4 (a) UV-Vis spectra of CeBr₃ with N₂ under blue light irradiation. Conditions: CeBr₃ (0.05 mmol), CH₃CN/*t*BuOH (2 mL, 1:1), N₂, 465 nm. (b) UV-Vis spectra of CeBr₃ with air under dark. Conditions: CeBr₃ (0.05 mmol), CH₃CN/*t*BuOH (2 mL, 1:1), air, dark. Details can be seen in Section 3.3.3.

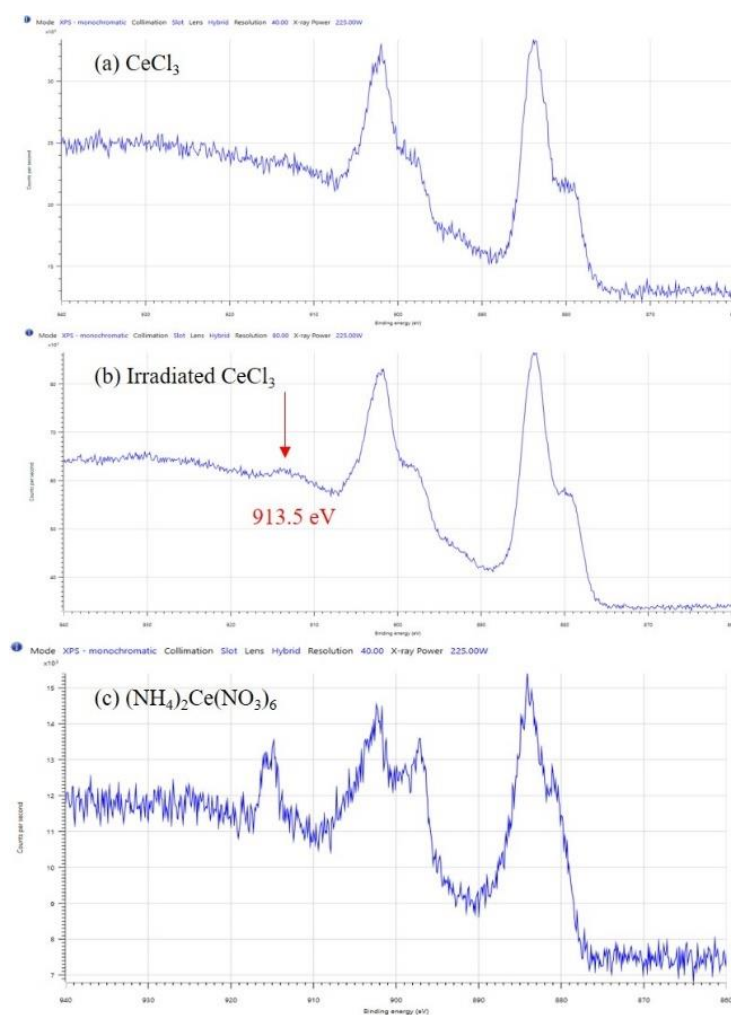


Figure 3.5 XPS spectra of CeCl₃, irradiated CeCl₃ and (NH₄)₂Ce(NO₃)₆.

Furthermore, XPS studies were conducted to find support for the formation of Ce(IV) species. As shown in Figure 3.5, a peak at 913.5 eV was observed, indicating the formation of Ce(IV) upon blue light irradiation of CeCl₃ in air. Mashima, Tsurugi and co-workers have shown that Ce(III) compounds can be oxidized to complex oxo-bridged Ce(IV) species under thermal heating conditions.^{33, 46}

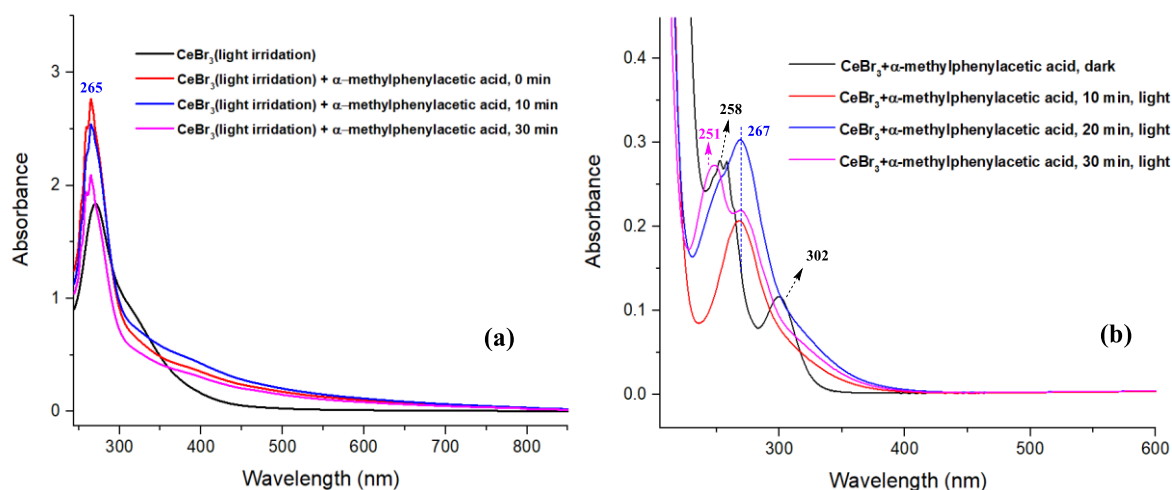


Figure 3.6 (a) UV-Vis spectra of the mixture of α -methylphenylacetic acid and CeBr₃ (photo/O₂-oxidized) (0.5 mmol of α -methylphenylacetic acid was added after the irradiation in **Figure 3.3**). (b) UV-Vis of the mixture of CeBr₃ and α -methylphenylacetic acid with or without light. Conditions: CeBr₃ (0.05 mmol), α -methylphenylacetic acid (0.05 mmol), CH₃CN/*t*BuOH (2 mL, 1:1), air, dark to blue light. Details can be seen in Section 3.3.3.

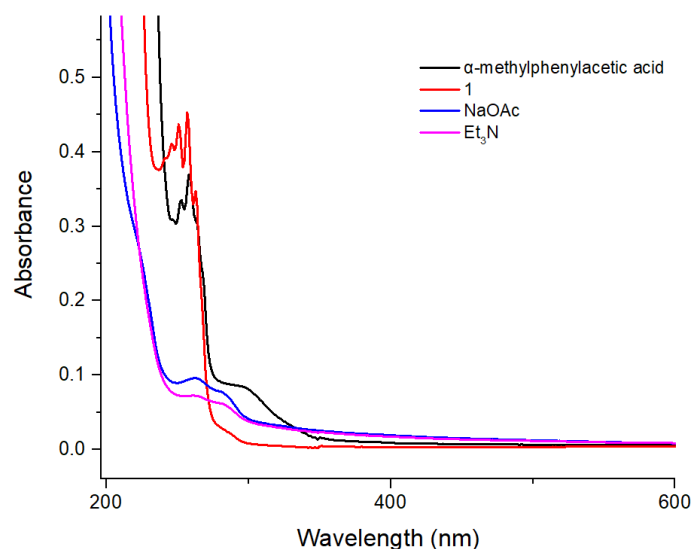


Figure 3.7 UV-Vis spectra of α -methylphenylacetic acid, **1**, NaOAc and Et₃N. Conditions: α -methylphenylacetic acid (0.1 mmol), **1** (0.1 mmol), NaOAc(0.1 mmol), Et₃N (0.1 mmol), CH₃CN/*t*BuOH (2 mL, 1:1), air, dark to blue light. Details can be seen in Section 3.3.3.

The resulting Ce(IV) species reacts with acid substrates. Thus, as shown in Figure 3.6(a), a new absorption band at around 265 nm due to the acid was observed when the CeBr₃ catalyst, initially irradiated at 465 nm for 30 min, reacted with α -methylphenylacetic acid (10 eq.) in the dark. This new absorption band decreased with time due to the transformation of α -methylphenylacetic acid. Note that without the pre-irradiation of the Ce catalyst, the acid absorption does not change. Based on the previous reports,⁴⁷⁻⁴⁹ these observations indicate that active Ce(IV) species, transformed from Ce(III) species under blue light irradiation and O₂,⁵⁰⁻⁵¹ may trigger the decarboxylation of acids. Further insight can be obtained from Figure 3.6(b). In the spectrum of a mixture of CeBr₃ and α -methylphenylacetic acid (1:1), the absorption bands of CeBr₃ and α -methylphenylacetic acid were observed at around 302 nm and 258 nm. Upon blue light irradiation, these peaks were replaced with absorptions at around 251 nm and 267 nm that might be attributed to carboxylate-coordinated Ce(IV) species [c.f. Figure 3.3 (a); for the absorption of **1**, see Figure 3.7].

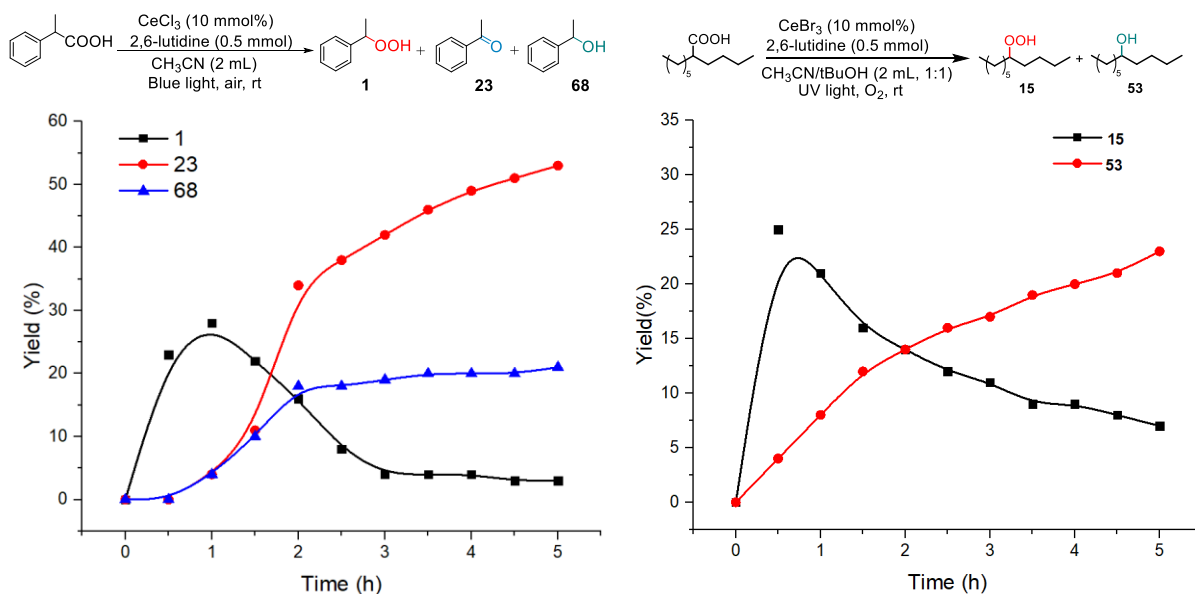


Figure 3.8 (a) Kinetic behaviour of α -methylphenylacetic acid in decarboxylative oxygenation. Conditions: CeCl₃ (0.05 mmol), α -methylphenylacetic acid (0.05 mmol), 1-bromo-3,5-bis(trifluoromethyl)benzene (0.2 mmol) as internal standard, CH₃CN (2 mL), air, blue light (465 nm); (b) Kinetic behaviour of 2-butyloctanoic acid in decarboxylative oxygenation. Conditions: CeBr₃ (0.05 mmol), α -methylphenylacetic acid (0.05 mmol), 1-bromo-3,5-bis(trifluoromethyl)benzene (0.2 mmol) as internal standard, CH₃CN (2 mL), CH₃CN/tBuOH (2 mL, 1:1), O₂, UV light (365 nm).

In our decarboxylative oxygenation reactions, alkyl hydroperoxides are likely to be a key intermediate.¹⁸ They may be generated from the reaction of a decarboxylated radical with O₂. This possibility is revealed by the kinetic profile of the reaction of α -methylphenylacetic acid. As is seen in Figure 3.8(a), the formation of the hydroperoxide **1** is rapid and precedes that of the ketone **23** and alcohol **68**. Its decrease after 1 h is coincided with the rise of the latter two. A similar trend is seen in the decarboxylative oxygenation of 2-butyloctanoic acid (Figure 3.8(b)). Furthermore, products **23** and **68** were formed in 77% and 22% yields, respectively, when the isolated **1** was subjected to the conditions of CeCl₃, 2,6-lutidine and blue light (Figure 3.9).

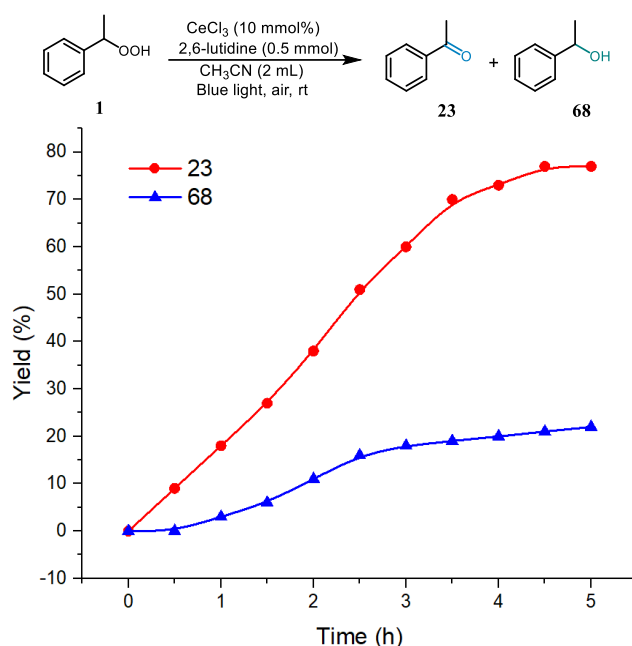
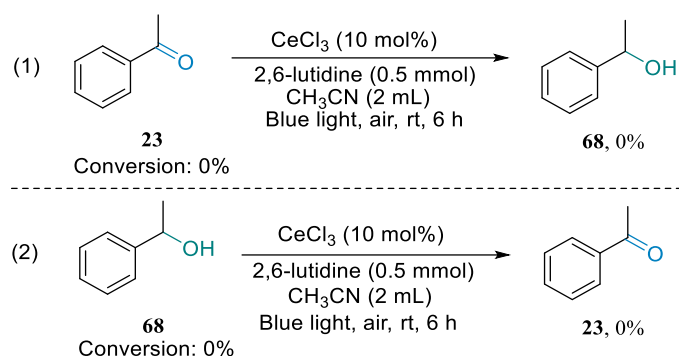


Figure 3.9 Decarboxylative oxygenation of **1**. Conditions: CeCl₃ (0.05 mmol), **1** (0.05 mmol), 1-bromo-3,5-bis(trifluoromethyl)benzene (0.2 mmol) as internal standard, CH₃CN (2 mL), air, blue light (465 nm).

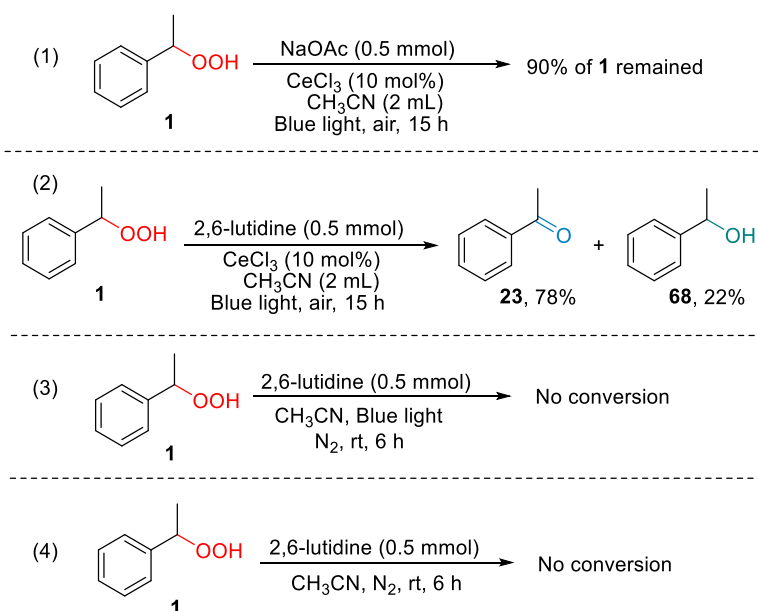
Thus, it is reasonable to conclude that the carbonyl and alcohol products result from the peroxide intermediate. However, the differing rate of formation of the ketone and alcohol indicates that they are formed by two different pathways, and it is possible that the alcohol is not an intermediate for ketone in the reaction. Consistent with this conjecture, both **23** and **68** showed no reactivity under the standard reaction conditions, as shown in Scheme 3.8. These

results are in line with the previous observations that show alcohols require a strong stoichiometric oxidant to be oxidised or are not oxidised by Ce(IV).^{16, 18}



Scheme 3.8 Exploration of Transformation between **23** and **68**.

The question then is why the peroxides are not reacting further in the presence of NaOAc, as is usually observed? Table 3.1 indicates that the base plays a critical role. This is more clearly manifested when the isolated peroxide **1** was subjected to blue light irradiation with different base. Peroxide **1** remained largely intact when NaOAc was used as the base, whereas **1** was fully converted to **23** and **68** when 2,6-lutidine was used (Scheme 3.9, eqs 1-2). A possible explanation is that the coordination of the peroxide to cerium was prevented by acetate anion, which could coordinate to cerium in the reaction. 2,6-Lutidine could not play such a role.



Scheme 3.9 Transformation of **1** in the presence of NaOAc or 2,6-lutidine.

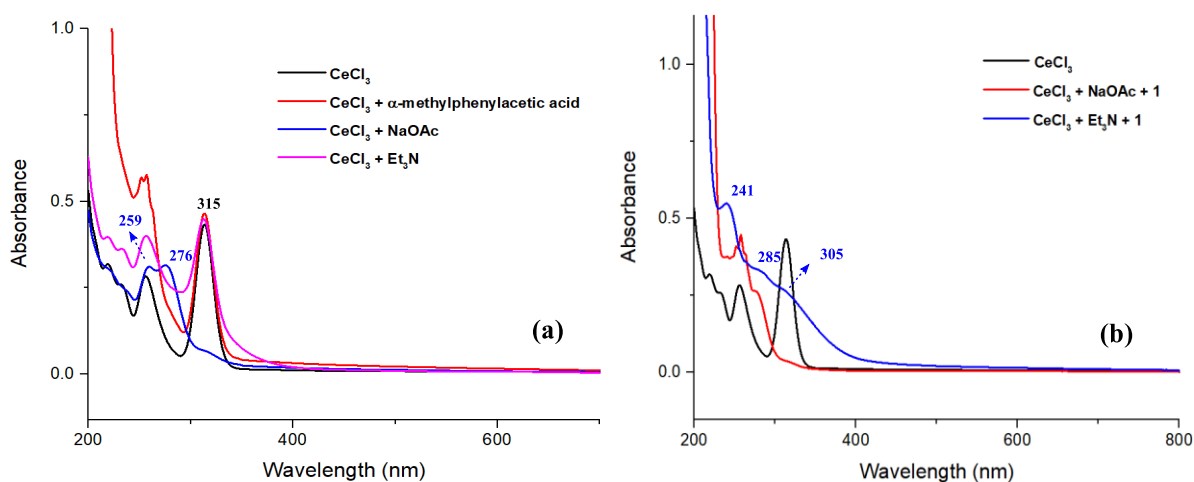


Figure 3.10 (a) UV-Vis spectra of CeCl_3 , the mixture of CeCl_3 and α -methylphenylacetic acid, the mixture of CeCl_3 and NaOAc, and the mixture of CeCl_3 and Et_3N . Conditions: CeCl_3 (0.05 mmol), α -methylphenylacetic acid (0.1 mmol), $\text{CH}_3\text{CN}/t\text{BuOH}$ (2 mL, 1:1), base (0.1 mmol); (b) UV-Vis spectra of CeCl_3 , the mixture of CeCl_3 , NaOAc and **1** and the mixture of CeCl_3 , Et_3N and **1**. Conditions: CeCl_3 (0.05 mmol), **1** (0.1 mmol), $\text{CH}_3\text{CN}/t\text{BuOH}$ (2 mL, 1:1), base (0.1 mmol). Details can be seen in Section 3.3.3.

To explore this possibility, UV-Vis experiments were attempted. However, the UV-Vis spectrum of the mixture of CeCl_3 and 2,6-lutidine is overwhelmed by the absorption of the latter (Figure 3.13). Hence, Et_3N was used instead of 2,6-lutidine. The UV-Vis spectra of CeCl_3 in the presence of NaOAc or Et_3N with or without phenylacetic acid show a peak at around 315 nm, assignable to CeCl_3 (Figure, 3.10(a)).⁵² However, two stronger absorption bands at around 259 and 276 nm were shown in the spectrum of CeCl_3 and NaOAc. This result may indicate the coordination of NaOAc to CeCl_3 .⁵³ This coordination could inhibit further transformation of hydroperoxides by Ce species. More evidence can be found in Figure 3.10(b). The mixture of CeCl_3 , NaOAc and the peroxide **1** showed the visible absorption band of **1** at around 251 nm (for the spectrum of **1**, see Figure 3.7). Interestingly, the mixture of CeCl_3 , Et_3N and **1** showed a new absorption peak and two broad peaks at around 241, 285 and 305 nm, respectively. Meanwhile, the absorption of **1** disappeared. These results appear to indicate the coordination of the peroxide to Ce species in the presence of Et_3N , whereas the coordination is inhibited by acetate. The complex formation constant between Ce(III) and acetate is about 70/M.⁴³

The formation of alcohols from the peroxides is an apparent reduction process, which would require a reducing agent. Could the base 2,6-lutidine be the electron donor? As shown in Scheme 3.9, no reaction of the peroxide **1** was observed in the presence of 2,6-lutidine under dark or blue light irradiation. These results ruled out the possibility that the base played a role as reductant. To explore whether the solvent CH₃CN works as the hydrogen donor in the decarboxylative oxygenation process,⁵⁴ a radical trap 1,1-diphenylethylene was introduced to intercept possible radical species generated from CH₃CN. As shown in Figure 3.11, 4,4-diphenylbutanenitrile was detected by GC-MS, which indicates the homolytic cleavage of C-H bond in CH₃CN. Therefore, this result suggests the possibility of the solvent acting as a hydrogen donor in forming the alcohols. In addition, acetone was detected with ¹³C NMR (Figure 3.12), indicating the oxidation of *t*BuOH and its role as a hydrogen donor as well.

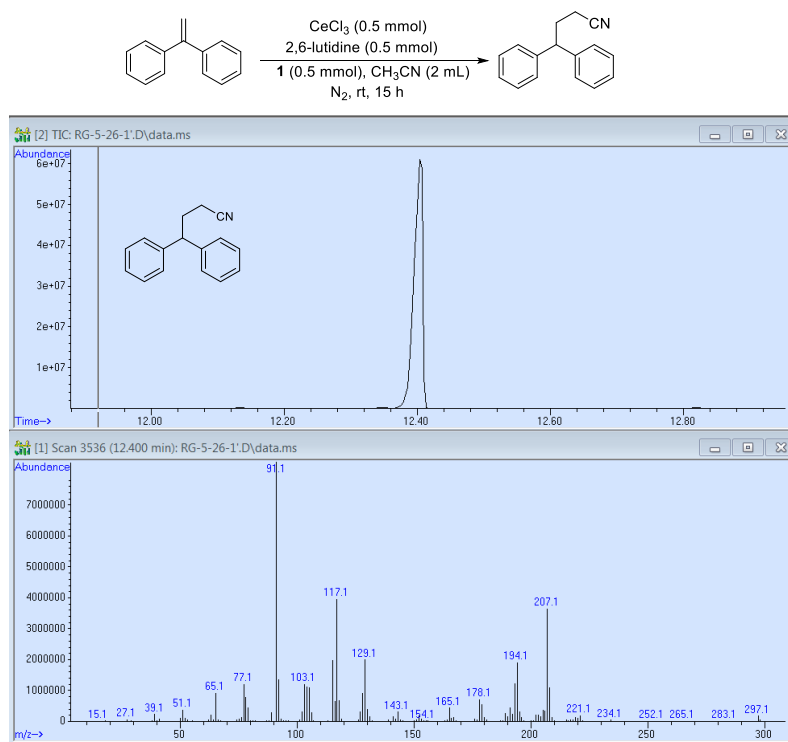


Figure 3.11 GC-MS spectrum of 4,4-diphenylbutanenitrile. Top: GC peak of 4,4-diphenylbutanenitrile (12.4 min); Bottom: MS peaks of 4,4-diphenylbutanenitrile (m/z: 221.1).

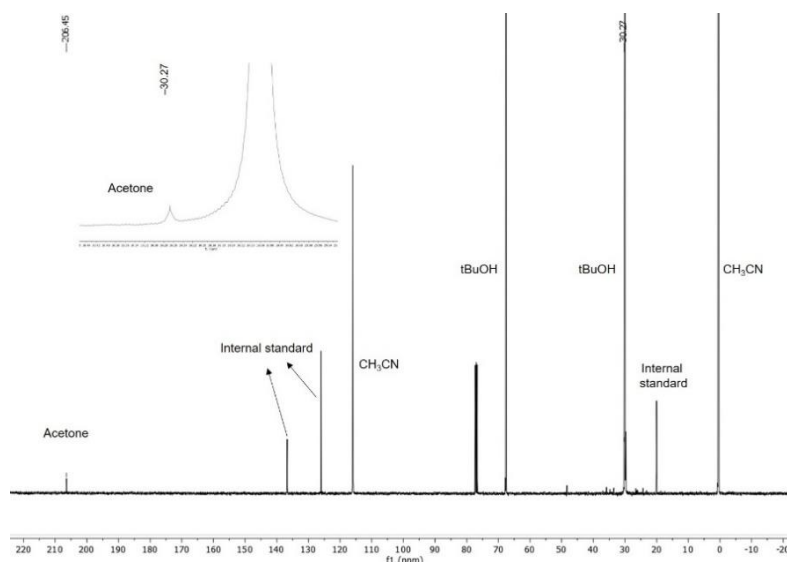
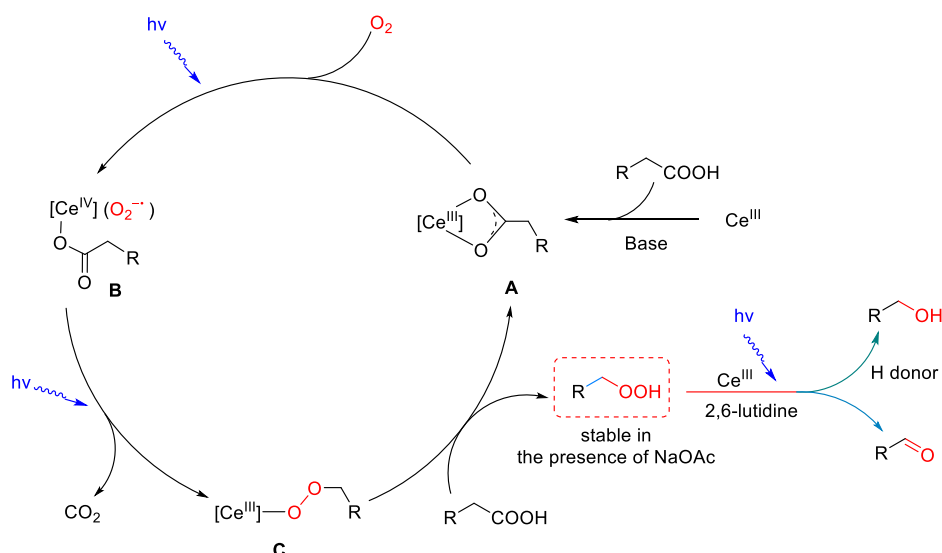


Figure 3.12 ¹³C NMR detection of acetone possibly resulting from the reaction of *t*BuOH.

Based on the above observations and previous literature,^{18, 25-26} a possible mechanism of this selective decarboxylative oxygenation reaction is suggested (Scheme 3.10). The transformation starts from the reaction of a Ce(III) compound with a carboxylic acid in the presence of a base, which affords the complex **A**. Then, the complex **A** is oxidized by O₂ to afford a Ce(IV)-superoxide species **B** under light irradiation.¹⁸ It is well-known that Ce(IV) carboxylate undergoes facile decarboxylation via light-promoted homolysis of the Ce-oxygen bond. The resulting alkyl radical would be easily trapped by the superoxide radical, affording a Ce(III) peroxide species **C**. Metathesis of the Ce(III) peroxide species **C** with a free carboxylic acid releases the observed alkyl hydroperoxide. However, the oxidation of α -methylphenylacetic acid in the dark with pre-irradiated CeBr₃ indicates that light may not be necessary for the conversion of **B** to **C**. The decarboxylation could be facilitated by the superoxide radical attacking the α carbon, a process reminiscent of an iron catalysed oxidation of ethers.⁵⁵ The peroxide product from **C** is stable in the presence of NaOAc, but is transformed to a carbonyl or an alcohol when using 2,6-lutidine as base. Light is necessary to promote the single-electron reduction of O₂ by Ce(III) species and the transformation of the peroxide to the aldehyde or alcohol.^{18, 26}



Scheme 3.10 Proposed mechanism of selective decarboxylative oxygenation of carboxylic acids.

3.3 Conclusions

In conclusion, a Ce(III)-catalysed selective decarboxylative oxygenation of carboxylic acids to widely different products has been developed in this chapter. The selectivity of this decarboxylative oxygenation process can be turned with a simple change of base. With this protocol, a wide range of carboxylic acids have been selectively transformed to hydroperoxides, aldehydes, ketones and alcohols in good yields with O_2 under mild conditions. In particular, the selective transformation of aliphatic acids and fatty acids to alcohols has been demonstrated for the first time, opening up a new, de-homologation pathway to access alcohols from carboxylic acids.

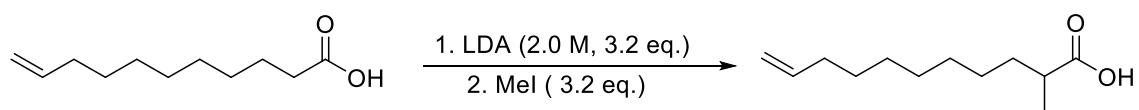
3.4 Experimental details

3.4.1 Details of photoreactors

Detail information of photoreactors can be seen in Section 2.3.

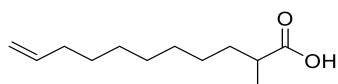
3.4.2 Preparation of substrates

Synthesis of 2-methylundec-10-enoic acid



2-Methylundec-10-enoic acid was synthesized according to the literature.⁵⁶ Under an argon atmosphere, undec-10-enoic acid (10 mmol, 1.0 eq.) in dry THF (10 mL) was added

slowly (over 20 min) into a LDA solution in a Schlenk tube cooled with an ice-water bath. After that, the reaction mixture was warmed to 45 °C, stirred for 3 h, and cooled to -78 °C. Then, MeI (32 mmol, 3.2 eq.) was added into the solution dropwise, and the resulting mixture was warmed to room temperature and stirred overnight. The reaction mixture was quenched by adding water (80 mL) slowly, followed by adding 2.0 M NaOH (aq.) to adjust the pH to 14. The resulting mixture was extracted with diethyl ether (50 mL × 2) and DCM (50 mL × 2). Then, 3.0 M HCl (aq.) was added into the aqueous phase to adjust the pH to 1-2 and the mixture was extracted with EtOAc (100 mL). Finally, the organic layer was dried over Na₂SO₄ and concentrated to obtain 2-methylundec-10-enoic acid.

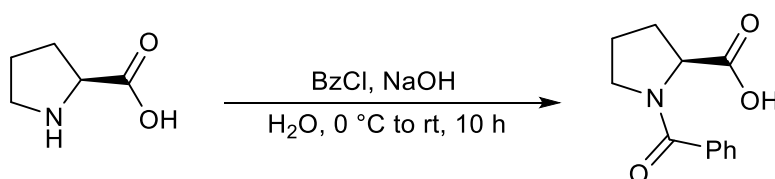


2-Methylundec-10-enoic acid⁵⁷

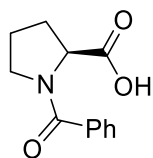
¹H NMR (400 MHz, Chloroform-*d*) δ 5.86-5.76 (m, 1H), 5.01-4.92 (m, 2H), 2.50-2.41 (m, 1H), 2.06-2.01 (m, 2H), 1.46 – 1.12 (m, 15H).

¹³C NMR (101 MHz, Chloroform-*d*) δ 183.03, 139.17, 114.13, 39.31, 33.77, 33.51, 29.42, 29.28, 29.04, 28.88, 27.10, 16.82.

Synthesis of *N*-benzoyl-*L*-proline



N-Benzoyl-*L*-proline was synthesized according to the literature.⁵⁸ To a solution of *L*-proline (4.00 g, 34.7 mmol) and NaOH (2.78 g, 69.5 mmol) in H₂O (64 mL), benzoyl chloride (BzCl, 4.0 mL, 34.7 mmol) was added dropwise at 0 °C. The mixture was stirred for 10 h at room temperature. The mixture was diluted with H₂O and washed with Et₂O (× 1). The aqueous layer was acidified with 10% HCl to pH = 1 and extracted with ethyl acetate. The organic layer was dried over MgSO₄ and evaporated to afford *N*-benzoyl-*L*-proline as colourless crystals.

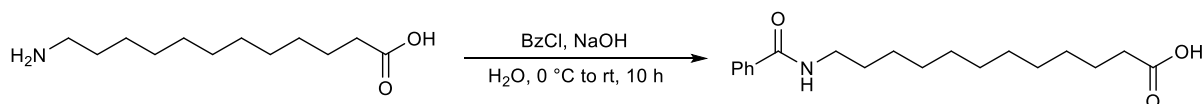


N-Benzoyl-L-proline⁵⁸

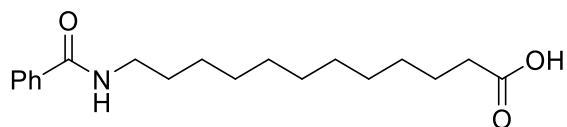
¹H NMR (400 MHz, Chloroform-*d*) δ 10.07 (s, 1H), 7.59-7.55 (m, 2H), 7.46-7.40 (m, 3H), 4.76 (t, *J* = 6.0 Hz, 1H), 3.58 (m, 2H), 2.35-2.23 (m, 2H), 2.09-1.98 (m, 1H), 1.95-1.85 (m, 1H).

¹³C NMR (101 MHz, Chloroform-*d*) δ 174.85, 170.86, 135.38, 130.42, 128.27, 127.18, 59.53, 50.23, 28.76, 25.11.

Synthesis of 12-benzamidododecanoic acid



12-Benzamidododecanoic acid was synthesized by the same steps. To a solution of 12-aminododecanoic acid (7.47 g, 34.7 mmol) and NaOH (2.78 g, 69.5 mmol) in H₂O (64 mL) was added benzoyl chloride (BzCl, 4.0 mL, 34.7 mmol) dropwise at 0 °C. The mixture was stirred for 10 h at room temperature. The mixture was diluted with H₂O and washed with Et₂O (\times 1). The aqueous layer was acidified with 10% HCl to pH = 1 and extracted with ethyl acetate. The organic layer was dried over MgSO₄ and evaporated to afford 12-benzamidododecanoic acid as colourless crystals.



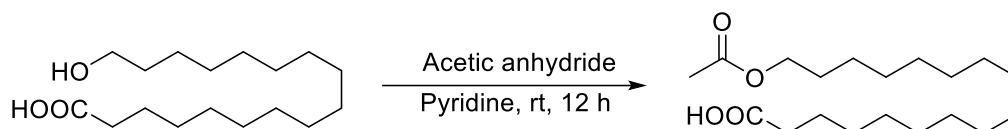
12-Benzamidododecanoic acid

¹H NMR (400 MHz, DMSO-*d*₆) δ 11.96 (s, 1H), 8.41 (t, *J* = 8.0 Hz, 1H), 7.82 (d, *J* = 7.5 Hz, 2H), 7.53 – 7.41 (m, 3H), 3.24 (q, *J* = 8.0 Hz, 2H), 2.18 (t, *J* = 7.4 Hz, 2H), 1.54-1.44 (m, 4H), 1.31-1.24 (m, 14H).

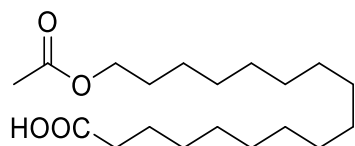
¹³C NMR (101 MHz, DMSO-*d*₆) δ 174.52, 166.06, 134.74, 130.96, 128.21, 127.11, 33.68, 30.70, 29.10, 28.99, 28.96, 28.92, 28.79, 28.76, 28.56, 26.49, 24.51.

HRMS (ESI) calcd for C₁₉H₂₉NO₃ [M+Na]⁺: 342.2045; found: 342.2043.

Synthesis of 17-acetoxyheptadecanoic acid



17-Acetoxyheptadecanoic acid was synthesized according to the literature.⁵⁹ Acetic anhydride (1.88 g, 18.47 mmol) was added to a stirred solution of 17-hydroxyheptadecanoic acid (2.1 g, 7.39 mmol) in pyridine (10 mL), and the reaction mixture was stirred for 12 h at room temperature. The reaction mixture was diluted with ethyl acetate (200 mL), the solution was washed with 2 N HCl (50 mL × 3) and brine, dried over anhydrous Na₂SO₄, and filtered, and the solvent was removed by rotary evaporation to furnish the crude product. The crude compound was chromatographed on silica gel using hexane/ethyl acetate as the mobile phase to afford 17-acetoxyheptadecanoic acid.



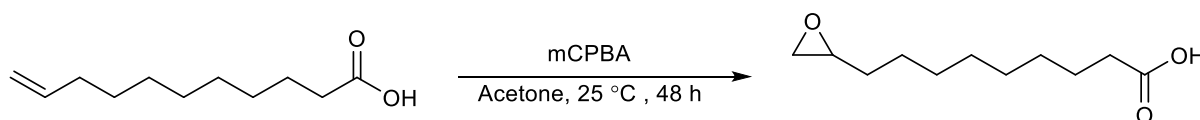
17-Acetoxyheptadecanoic acid

¹H NMR (400 MHz, Chloroform-*d*) δ 4.05 (t, *J* = 6.8 Hz, 2H), 2.34 (t, *J* = 7.5 Hz, 2H), 2.04 (s, 3H), 1.64-1.59 (m, 4H), 1.34-1.25 (m, 24H).

¹³C NMR (101 MHz, Chloroform-*d*) δ 179.69, 171.34, 64.69, 33.98, 29.60, 29.55, 29.54, 29.49, 29.40, 29.23, 29.21, 29.04, 28.57, 25.88, 24.66, 21.00.

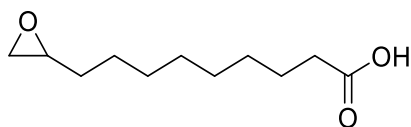
HRMS (ESI) calcd for C₁₉H₃₆O₄ [M+Na]⁺: 351.2506; found: 351.2511.

Synthesis of 9-(oxiran-2-yl)nonanoic acid



9-(Oxiran-2-yl)nonanoic acid was synthesized according to the literature.⁶⁰ The mixture of undec-10-enoic acid (10 mmol) and mCPBA (1.4 eq.) in acetone (10 mL) was stirred at 25 °C for 48 h. After the reaction, the solvent was removed by rotary evaporation to furnish the

crude product. The crude product was purified via flash chromatography on silica gel to afford 9-(oxiran-2-yl)nonanoic acid.

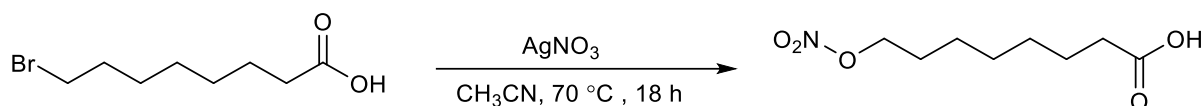


9-(Oxiran-2-yl)nonanoic acid⁶¹

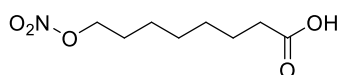
¹H NMR (400 MHz, Chloroform-*d*) δ 2.91 (m, 1H), 2.76-2.74 (m, 1H), 2.47-2.45 (m, 1H), 2.34 (t, $J = 7.5$ Hz, 2H), 1.66-1.59 (m, 2H), 1.55-1.50 (m, 2H), 1.44 (m, 2H), 1.35-1.31 (m, 8H).

¹³C NMR (101 MHz, Chloroform-*d*) δ 179.77, 52.44, 47.14, 33.98, 32.40, 29.30, 29.27, 29.08, 28.96, 25.89, 24.61.

Synthesis of 8-(nitrooxy)octanoic acid



8-(Nitrooxy)octanoic acid was synthesized according to the literature.⁶² The mixture of 8-bromooctanoic acid (1.45 g, 6.53 mmol) and silver nitrate (1.66 g, 9.80 mmol) in acetonitrile (30 mL) was stirred at 70 °C for 18 h. After the reaction, the solvent was removed by rotary evaporation to furnish the crude product. The crude product was purified via flash chromatography on silica gel to afford 8-(nitrooxy)octanoic acid.

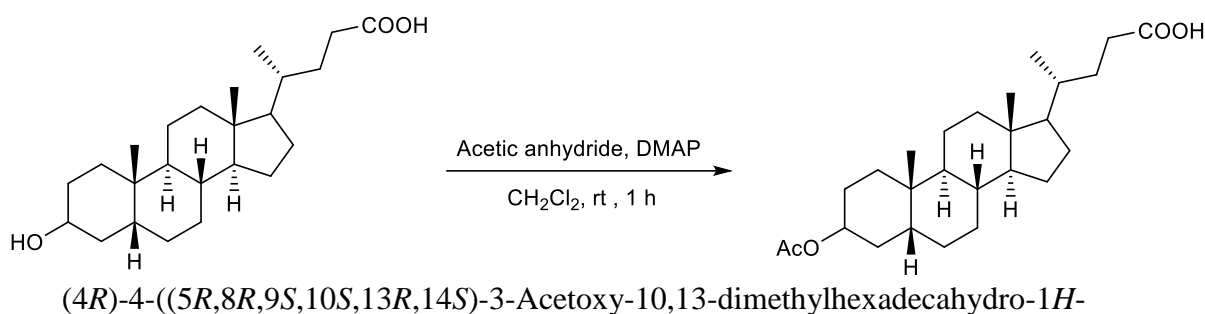


8-(Nitrooxy)octanoic acid⁶³

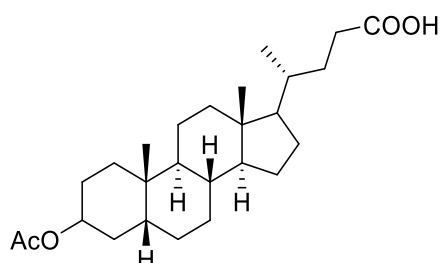
¹H NMR (400 MHz, Chloroform-*d*) δ 4.44 (t, $J = 6.7$ Hz, 2H), 2.35 (t, $J = 7.4$ Hz, 2H), 1.77-1.57 (m, 4H), 1.47-1.28 (m, 6H).

¹³C NMR (101 MHz, Chloroform-*d*) δ 180.04, 73.28, 33.90, 28.72, 28.70, 26.65, 25.42, 24.42.

Synthesis of (4*R*)-4-((5*R*,8*R*,9*S*,10*S*,13*R*,14*S*)-3-acetoxy-10,13-dimethylhexadecahydro-1*H*-cyclopenta[*a*]phenanthrene-17-yl)pentanoic acid



cyclopenta[*a*]phenanthrene-17-yl)pentanoic acid was synthesized according to the literature.⁶⁴ Acetic anhydride (26.43 mmol, 2.5 mL) was added dropwise to a solution of lithocholic acid (7.34 mmol) and DMAP (1.47 mmol, 180 mg) in CH₂Cl₂ (30 mL). The reaction mixture was stirred at room temperature under nitrogen atmosphere for 1 h. The mixture was then washed with HCl 1 N aqueous solution (3 × 30 mL), 5% NaHCO₃ solution (3 × 30 mL), saturated NaCl solution (3 × 20 mL) and water (1 × 20 mL). The organic layer was dried over MgSO₄ and concentrated. The crude product was purified by column chromatography (silica gel, cyclohexane/ethyl acetate, 8:2) to afford (4R)-4-((5R,8R,9S,10S,13R,14S)-3-acetoxy-10,13-dimethylhexadecahydro-1H-cyclopenta[*a*]phenanthrene-17-yl)pentanoic acid.

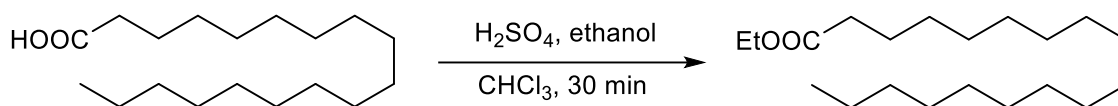


cyclopenta[*a*]phenanthren-17-yl)pentanoic acid⁶⁴

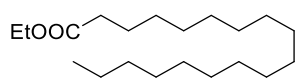
¹H NMR (400 MHz, Chloroform-*d*) δ 4.76-4.68 (m, 1H), 2.43-2.36 (m, 1H), 2.31-2.21 (m, 1H), 2.03 (s, 3H), 1.96 (d, *J* = 11.5 Hz, 1H), 1.88-1.74 (m, 5H), 1.70-1.66 (m, 1H), 1.61-1.49 (m, 2H), 1.47-1.31 (m, 8H), 1.30-0.99 (m, 9H), 0.95-0.90 (m, 6H), 0.64 (s, 3H).

¹³C NMR (101 MHz, Chloroform-*d*) δ 179.90, 170.71, 74.41, 56.48, 55.96, 42.74, 41.87, 40.39, 40.13, 35.78, 35.29, 35.02, 34.57, 32.23, 30.92, 30.75, 28.16, 27.00, 26.61, 26.30, 24.16, 23.31, 21.47, 20.82, 18.23, 12.03.

Synthesis of ethyl stearate



Ethyl stearate (**8**) was synthesized according to the literature.⁶⁵ Stearic acid (1 g) were solubilized in chloroform (2 mL) and ethylated with 2 % sulfuric acid in ethanol (4 mL) in a boiling flask equipped with a reflux condenser for 30 min. After being cooled to room temperature, the product was washed with water. The chloroform layer containing ethyl stearate was passed through an anhydrous sodium sulfate column, solvent removed in a rotary vacuum evaporator, and then completely dried under a nitrogen flush.



Ethyl stearate⁶⁶

¹H NMR (400 MHz, Chloroform-*d*) δ 4.12 (q, $J = 7.1$ Hz, 2H), 2.28 (t, $J = 7.6$ Hz, 2H), 1.65-1.57 (m, 2H), 1.36-1.18 (m, 31H), 0.88 (t, $J = 6.6$ Hz, 3H).

¹³C NMR (101 MHz, Chloroform-*d*) δ 173.93, 60.13, 34.40, 31.92, 29.68, 29.64, 29.59, 29.45, 29.35, 29.26, 29.14, 24.99, 22.68, 14.24, 14.10.

3.4.3 Mechanistic studies

Estimation of solubility of bases in selective decarboxylative oxygenation

To a sample tube (14 mL), NaOAc (500 mg) was added. The total weight of tube and NaOAc was measured. Then, CH₃CN (3.0 mL, used as received; the same as one used in catalysis) was added, and the tube was allowed to stir for 30 min at room temperature. To remove the solvent, the sample tube was placed in an oven under 100 °C until the NaOAc was completely dried. The weight of the tube and NaOAc was measured again and the lost weight was used to estimate the solubility (wt. %) of NaOAc in CH₃CN. The solubility of KOAc, LiOAc and CsOAc was estimated similarly.

Selective decarboxylative oxygenation of esters

Decarboxylative oxygenation of ethyl phenylacetate to **8**: To an oven dried Schlenk tube, CeCl₃ (10 mol%), NaOAc (0.5 mmol), ethyl phenylacetate (0.5 mmol) and 2 mL of CH₃CN were added under air. The Schlenk tube was allowed to stir under blue light (465 nm) for 15 h. After the reaction, water (2 mL), chloroform-*d* (1 mL), and mesitylene (17.3 mg) were added. The product yield of **8** was obtained by ¹H NMR analysis of the organic layer.

Decarboxylative oxygenation of ethyl phenylacetate to **33**: To an oven dried Schlenk tube, CeCl₃ (10 mol%), 2,6-lutidine (0.5 mmol), ethyl phenylacetate (0.5 mmol) and 2 mL of CH₃CN were added under air. The Schlenk tube was allowed to stir under blue light (465 nm) for 15 h. After the reaction, water (2 mL), chloroform-*d* (1 mL), and mesitylene (17.3 mg) were added. The product yield of **33** was obtained by ¹H NMR analysis of the organic layer.

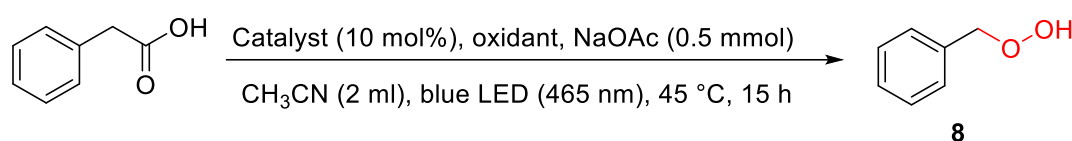
Decarboxylative oxygenation of ethyl stearate to **46**: To an oven dried Schlenk tube, CeBr₃ (10 mol%), 2,6-lutidine (0.5 mmol), ethyl stearate (0.5 mmol) and 2 mL of CH₃CN/*t*BuOH (1:1) were added under air. The Schlenk tube was allowed to stir under blue light (465 nm) for 15 h. After the reaction, water (2 mL), chloroform-*d* (1 mL), and mesitylene (17.3 mg) were added. The product yield of **46** was obtained by ¹H NMR analysis of the organic layer.

Selective decarboxylative oxygenation of carboxylic acids by well-known photosensitizers capable of producing singlet oxygen or peroxides

Decarboxylative oxygenation of phenylacetic acid to **8** by peroxides: To an oven dried Schlenk tube, CeCl₃ (10 mol%), NaOAc (0.5 mmol) and phenylacetic acid (0.5 mmol) were added under nitrogen. Then the reaction tube was allowed to be vacuumed and purged with nitrogen three times. After that, a peroxide (1.5 mmol) and CH₃CN (2 mL) were added under nitrogen. The reaction tube was allowed to stir at room temperature under light irradiation for 15 h. After the reaction, mesitylene (17.3 mg) as internal standard, water (2 mL) and CDCl₃ (2 mL) were added. Finally, the product yield of **8** was obtained by ¹H NMR analysis of the organic layer.

Decarboxylative oxygenation of phenylacetic acid to **8** by well-known photosensitizers: To an oven dried Schlenk tube, a photosensitizer (10 mol%), phenylacetic acid (0.5 mmol), NaOAc (0.5 mmol) and CH₃CN (2 mL) were added under air. The reaction tube was allowed to stir at room temperature under light irradiation for 15 h. After the reaction, mesitylene (17.3 mg) as internal standard, water (2 mL) and CDCl₃ (2 mL) were added. Finally, the product yield of **8** was obtained by ¹H NMR analysis of the organic layer.

Table 3.5 Transformation of phenylacetic acid to **8** by well-known photosensitizers capable of producing singlet oxygen or peroxides^{a,b}

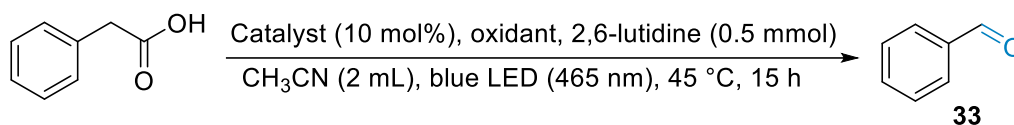


Entry	Catalyst	Oxidant	Yield (%)
1	CeCl ₃	TBHP (70% in water)	0
2	CeCl ₃	DTBP	0
3	CeCl ₃	Benzoyl peroxide	0
4	Eosin Y disodium salt	air	0
5	Rose bengal	air	0

^aReaction conditions: Phenylacetic acid (0.5 mmol), catalyst (10 mol%), peroxides (1.5 mmol) or air, NaOAc (0.5 mmol), CH₃CN (2 mL), air (1 atm), blue LED (465 nm, 9W), room temperature, 15 h.

^bNMR yields are given.

Table 3.6 Transformation of phenylacetic acid to **33** by well-known photosensitizers capable of producing singlet oxygen or peroxides^{a,b}



Entry	Catalyst	Oxidant	Yield (%)
1	CeCl ₃	TBHP (70% in water)	0
2	CeCl ₃	DTBP	0
3	CeCl ₃	Benzoyl peroxide	0
4	Eosin Y disodium salt	air	0
5	Rose bengal	air	0

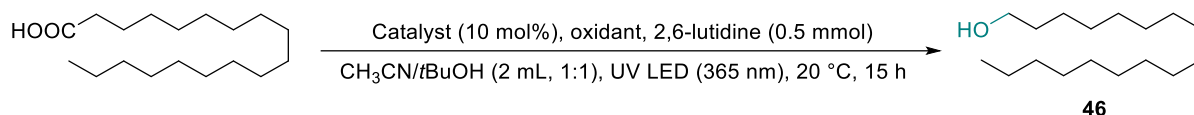
^aReaction conditions: Phenylacetic acid (0.5 mmol), catalyst (10 mol%), peroxides (1.5 mmol) or air, 2,6-lutidine (0.5 mmol), CH₃CN/*t*BuOH (2 mL), air (1 atm), UV LED (365 nm, 9W), room temperature,

15 h. ^bNMR yields are given.

Decarboxylative oxygenation of phenylacetic acid to **33** by peroxides: To an oven dried Schlenk tube, CeCl₃ (10 mol%), and phenylacetic acid (0.5 mmol) were added under nitrogen. Then the reaction tube was allowed to be vacuumed and purged with nitrogen three times. After that, a peroxide (1.5 mmol), 2,6-lutidine (0.5 mmol) and CH₃CN (2 mL) were added under nitrogen. The reaction tube was allowed to stir at room temperature under light irradiation for 15 h. After the reaction, mesitylene (17.3 mg) as internal standard, water (2 mL) and CDCl₃ (2 mL) were added. Finally, the product yield of **33** was obtained by ¹H NMR analysis of the organic layer.

Decarboxylative oxygenation of phenylacetic acid to **33** by well-known photosensitizers: To an oven dried Schlenk tube, a photosensitizer (10 mol%), phenylacetic acid (0.5 mmol), 2,6-lutidine (0.5 mmol) and CH₃CN (2 mL) were added under air. The reaction tube was allowed to stir at room temperature under light irradiation for 15 h. After the reaction, mesitylene (17.3 mg) as internal standard, water (2 mL) and CDCl₃ (2 mL) were added. Finally, the product yield of **33** was obtained by ¹H NMR analysis of the organic layer.

Table 3.7 Transformation of stearic acid to **46** by well-known photosensitizers capable of producing singlet oxygen or peroxides^{a,b}



Entry	Catalyst	Oxidant	Yield (%)
1	CeBr ₃	TBHP (70% in water)	0
2	CeBr ₃	DTBP	0
3	CeBr ₃	Benzoyl peroxide	0
4	Eosin Y disodium salt	O ₂	0
5	Rose bengal	O ₂	0

^aReaction conditions: Stearic acid (0.5 mmol), catalyst (10 mol%), 2,6-lutidine (0.5 mmol), oxidant (1.5 mmol) or O₂ (1 atm), CH₃CN/*t*BuOH (2 mL, 1:1), UV LED (365 nm, 9 W), room temperature, 15 h.

^bNMR yields are given.

Decarboxylative oxygenation of stearic acid to **46** by peroxides: To an oven dried Schlenk tube, CeBr₃ (10 mol%), and stearic acid (0.5 mmol) were added under nitrogen. Then the

reaction tube was allowed to be vacuumed and purged with nitrogen three times. After that, a peroxide (1.5 mmol), 2,6-lutidine (0.5 mmol) and CH₃CN/*t*BuOH (2 mL, 1:1) were added under nitrogen. The reaction tube was allowed to stir at room temperature under light irradiation for 15 h. After the reaction, mesitylene (17.3 mg) as internal standard, water (2 mL) and CDCl₃ (2 mL) were added. Finally, the product yield of **46** was obtained by ¹H NMR analysis of the organic layer.

Decarboxylative oxygenation of stearic acid to **46** by well-known photosensitizers: To an oven dried Schlenk tube, a photosensitizer (10 mol%), stearic acid (0.5 mmol), 2,6-lutidine (0.5 mmol) and CH₃CN/*t*BuOH (2 mL, 1:1) were added under O₂. The reaction tube was allowed to stir at room temperature under light irradiation for 15 h. After the reaction, mesitylene (17.3 mg) as internal standard, water (2 mL) and CDCl₃ (2 mL) were added. Finally, the product yield of **46** was obtained by ¹H NMR analysis of the organic layer.

The results above (Tables 3.5-3.7) indicate that singlet O₂ and peroxides are not involved as active oxygen species that enable the decarboxylative oxygenation under question.

XPS of CeCl₃

Preparation of CeCl₃ sample: To an oven dried Schlenk tube, 0.5 mmol of CeCl₃ and 4 mL of CH₃CN were added. The mixture was stirred at room temperature with air under dark for 2 h. Then, the solvent was removed in a rotary vacuum evaporator, and the CeCl₃ powder was placed at vacuum for 1 h.

Preparation of irradiated CeCl₃ sample: To an oven dried Schlenk tube, 0.5 mmol of CeCl₃ and 4 mL of CH₃CN were added. The mixture was stirred at room temperature with air under blue light (465 nm) for 2 h. Then, the solvent was removed in a rotary vacuum evaporator, and the CeCl₃ powder was placed at vacuum for 1 h.

After preparation, CeCl₃ and irradiated CeCl₃ samples were examined using a Kratos Supra spectrometer. All data were recorded using a monochromatic Al K α source. The powder

samples were mounted onto carbon tape on silicon substrates. A number of analysis positions were chosen per sample. An automatic, electron charge neutraliser system was used. The peak of irradiated CeCl_3 observed at 913.5 eV corresponds to the peak of Ce(IV) in $(\text{NH}_3)_2\text{Ce}(\text{NO}_3)_6$.

UV-Vis experiment

UV-Vis spectra of CeBr_3

CeBr_3 with air under blue light: To an oven dried Schlenk tube, CeBr_3 (0.05 mmol) and $\text{CH}_3\text{CN}/t\text{BuOH}$ (2 mL, 1:1) were added under air. The reaction tube was allowed to stir at room temperature under blue light irradiation (465 nm). Every 10 min, 0.1 mL of the solution was then taken out and diluted to 5 mL for UV-Vis analysis.

CeBr_3 (Blue light irradiation for 30 min) and α -methylphenylacetic acid with air under dark: To an oven dried Schlenk tube, CeBr_3 (0.05 mmol) and $\text{CH}_3\text{CN}/t\text{BuOH}$ (2 mL, 1:1) were added under air. The reaction tube was allowed to stir at room temperature under blue light irradiation (465 nm). After 30 min, the reaction tube was taken out and placed under dark, and α -methylphenylacetic acid (0.5 mmol) was added. Every 10 min, 0.1 mL of the solution was then taken out and diluted to 5 mL for UV-Vis analysis.

CeBr_3 with N_2 under blue light: To an oven dried Schlenk tube, CeBr_3 (0.05 mmol) was added under nitrogen. Then the reaction tube was allowed to be vacuumed and purged with nitrogen three times. After that, $\text{CH}_3\text{CN}/t\text{BuOH}$ (2 mL, 1:1) was added under nitrogen. The reaction tube was allowed to stir at room temperature under blue light irradiation (465 nm). Every 10 min, 0.1 mL of the solution was then taken out and diluted to 5 μL for UV-Vis analysis.

CeBr_3 with air under dark: To an oven dried Schlenk tube, CeBr_3 (0.05 mmol) and $\text{CH}_3\text{CN}/t\text{BuOH}$ (2 mL, 1:1) were added under air. The reaction tube was allowed to stir at room temperature under dark. Every 10 min, 5 μL of the solution was then taken out and diluted to 5 mL for UV-Vis analysis.

UV-Vis spectra of CeCl₃ in the presence of NaOAc and Et₃N

CeCl₃: To an oven dried Schlenk tube, CeCl₃ (0.05 mmol) and CH₃CN/MeOH (2 mL, 1:1) were added. The reaction tube was allowed to stir 5 min at room temperature. 0.01 mL of the solution was then taken out and diluted to 5 mL for UV-Vis analysis.

CeCl₃ + α -methylphenylacetic acid: To an oven dried Schlenk tube, CeCl₃ (0.05 mmol), α -methylphenylacetic acid (0.1 mmol) and CH₃CN/MeOH (2 mL, 1:1) were added. The reaction tube was allowed to stir 5 min at room temperature. 0.01 mL of the solution was then taken out and diluted to 5 mL for UV-Vis analysis.

CeCl₃ + NaOAc: To an oven dried Schlenk tube, CeCl₃ (0.05 mmol), NaOAc (0.1 mmol) and CH₃CN/MeOH (2 mL, 1:1) were added. The reaction tube was allowed to stir 5 min at room temperature. 0.01 mL of the solution was then taken out and diluted to 5 mL for UV-Vis analysis.

CeCl₃ + Et₃N: To an oven dried Schlenk tube, CeCl₃ (0.05 mmol), Et₃N (0.1 mmol) and CH₃CN/MeOH (2 mL, 1:1) were added. The reaction tube was allowed to stir 5 min at room temperature. 0.01 mL of the solution was then taken out and diluted to 5 mL for UV-Vis analysis.

CeCl₃ + 2,6-lutidine: To an oven dried Schlenk tube, CeCl₃ (0.05 mmol), 2,6-lutidine (0.1 mmol) and CH₃CN/MeOH (2 mL, 1:1) were added. The reaction tube was allowed to stir 5 min at room temperature. 0.01 mL of the solution was then taken out and diluted to 5 mL for UV-Vis analysis.

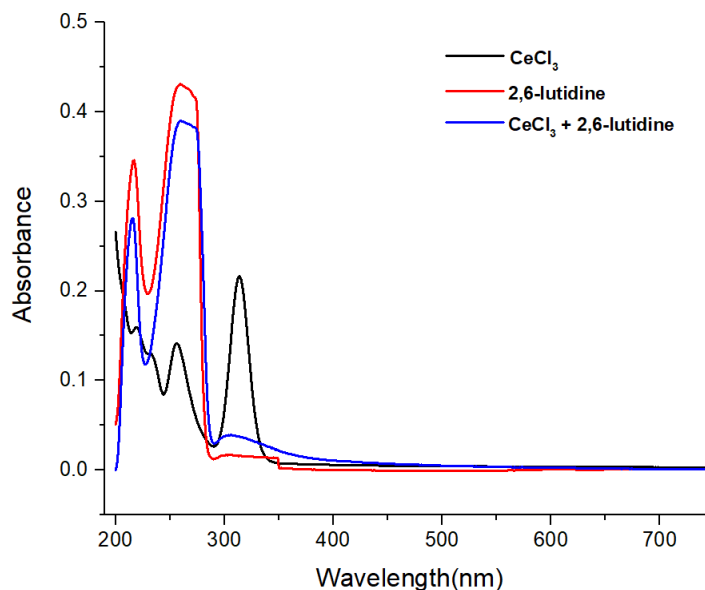


Figure 3.13 UV-Vis spectra of CeCl₃, 2,6-lutidine and the mixture of CeCl₃ and 2,6-lutidine.

UV-Vis spectra of the mixture of CeCl₃ and **1** in the presence of NaOAc and Et₃N

CeCl₃ + **1** + NaOAc: To an oven dried Schlenk tube, CeCl₃ (0.05 mmol), **1** (0.1 mmol), NaOAc (0.1 mmol) and CH₃CN/MeOH (2 mL, 1:1) were added. The reaction tube was allowed to stir 5 min at room temperature. 0.01 mL of the solution was then taken out and diluted to 5 mL for UV-Vis analysis.

CeCl₃ + **1** + Et₃N: To an oven dried Schlenk tube, CeCl₃ (0.05 mmol), **1** (0.1 mmol), Et₃N (0.1 mmol) and CH₃CN/MeOH (2 mL, 1:1) were added. The reaction tube was allowed to stir 5 min at room temperature. 0.01 mL of the solution was then taken out and diluted to 5 mL for UV-Vis analysis.

UV-Vis spectra of α -methylphenylacetic acid, **1**, NaOAc and Et₃N

α -Methylphenylacetic acid: To an oven dried Schlenk tube, α -methylphenylacetic acid (0.1 mmol) and CH₃CN/MeOH (2 mL, 1:1) were added. The reaction tube was allowed to stir 5 min at room temperature. 0.01 mL of the solution was then taken out and diluted to 5 mL for UV-Vis analysis.

1: To an oven dried Schlenk tube, **1** (0.1 mmol) and CH₃CN/MeOH (2 mL, 1:1) were added. The reaction tube and was allowed to stir 5 min at room temperature. 0.01 mL of the solution was then taken out and diluted to 5 mL for UV-Vis analysis.

NaOAc: To an oven dried Schlenk tube, NaOAc (0.1 mmol) and CH₃CN/MeOH (2 mL, 1:1) were added. The reaction tube was allowed to stir 5 min at room temperature. 0.01 mL of the solution was then taken out and diluted to 5 mL for UV-Vis analysis.

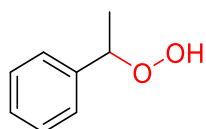
Et₃N: To an oven dried Schlenk tube, Et₃N (0.1 mmol) and CH₃CN/MeOH (2 mL, 1:1) were added. The reaction tube was allowed to stir 5 min at room temperature. 0.01 mL of the solution was then taken out and diluted to 5 mL for UV-Vis analysis.

UV-Vis spectra of CeBr₃ and α -methylphenylacetic acid

To an oven dried Schlenk tube, CeBr₃ (0.05 mmol) and α -methylphenylacetic acid (0.05 mmol) was added under air, and CH₃CN/*t*BuOH (2 mL, 1:1) was added then. The reaction tube was allowed to stir at room temperature under dark condition for 10 min. Then, 0.01 mL of the solution was then taken out and diluted to 5 mL for UV-Vis analysis. After that, the reaction tube was allowed to stir at room temperature under blue light irradiation (465 nm). Every 10 min, 0.1 mL of the solution was then taken out and diluted to 5 mL for UV-Vis analysis.

3.5 Analytical data of products

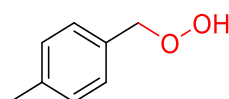
3.5.1 Hydroperoxide products



(1-Hydroperoxyethyl)benzene (**1**)⁶⁷

¹H NMR (400 MHz, Chloroform-*d*) δ 7.85 (s, 1H), 7.42 – 7.28 (m, 5H), 5.08 (q, *J* = 6.6 Hz, 1H), 1.48 (d, *J* = 6.6 Hz, 3H).

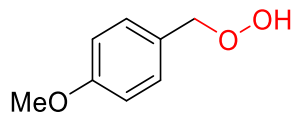
¹³C NMR (101 MHz, Chloroform-*d*) δ 141.36, 128.63, 128.23, 126.50, 83.74, 20.04.



1-(Hydroperoxymethyl)-4-methylbenzene (2)¹²

¹H NMR (400 MHz, Chloroform-*d*) δ 7.90 (s, 1H), 7.29 (d, $J = 7.8$ Hz, 2H), 7.20 (d, $J = 7.8$ Hz, 2H), 4.97 (s, 2H), 2.37 (s, 3H).

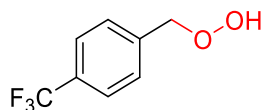
¹³C NMR (101 MHz, Chloroform-*d*) δ 138.52, 132.61, 129.29, 129.10, 79.09, 21.22.



1-(Hydroperoxymethyl)-4-methoxybenzene (3)¹²

¹H NMR (400 MHz, Chloroform-*d*) δ 8.06 (s, 1H), 7.32 (d, $J = 8.6$ Hz, 2H), 6.91 (d, $J = 8.6$ Hz, 2H), 4.94 (s, 2H), 3.81 (s, 3H).

¹³C NMR (101 MHz, Chloroform-*d*) δ 159.88, 130.72, 127.68, 113.94, 78.83, 55.27.

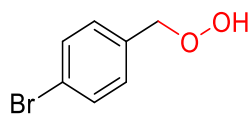


1-(hydroperoxymethyl)-4-(trifluoromethyl)benzene (4)

¹H NMR (400 MHz, Chloroform-*d*) δ 8.09 (d, $J = 1.5$ Hz, 1H), 7.65 (d, $J = 7.9$ Hz, 2H), 7.52 (d, $J = 7.9$ Hz, 2H), 5.06 (s, 2H).

¹³C NMR (101 MHz, Chloroform-*d*) δ 139.99, 130.67 (q, $J_{C-F} = 32.32$ Hz), 128.81, 125.54 (q, $J_{C-F} = 3.8$ Hz), 124.01 (q, $J_{C-F} = 273.7$ Hz), 78.21.

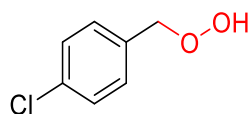
HRMS (ESI) calcd for C₈H₇F₃O₂ [M+Na]⁺: 215.0290; found: 215.0283.



1-Bromo-4-(hydroperoxymethyl)benzene (5)¹²

¹H NMR (400 MHz, Chloroform-*d*) δ 8.09 (s, 1H), 7.42 (d, $J = 8.3$ Hz, 2H), 7.17 (d, $J = 8.3$ Hz, 2H), 4.85 (s, 2H).

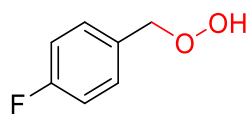
¹³C NMR (101 MHz, Chloroform-*d*) δ 134.77, 131.70, 130.53, 122.63, 78.31.



1-Chloro-4-(hydroperoxymethyl)benzene (6)¹²

^1H NMR (400 MHz, Chloroform-*d*) δ 8.09 (s, 1H), 7.38 – 7.30 (m, 4H), 4.96 (s, 2H).

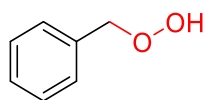
^{13}C NMR (101 MHz, Chloroform-*d*) δ 134.48, 134.27, 130.26, 128.76, 78.30.



1-Fluoro-4-(hydroperoxymethyl)benzene (7)¹²

^1H NMR (400 MHz, Chloroform-*d*) δ 8.06 (s, 1H), 7.41 – 7.33 (m, 2H), 7.09 – 7.05 (m, 2H), 4.96 (s, 2H).

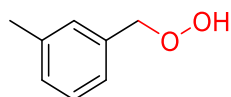
^{13}C NMR (101 MHz, Chloroform-*d*) δ 162.90 (d, $J_{\text{C-F}} = 247.1$ Hz), 131.52 (d, $J_{\text{C-F}} = 3.1$ Hz), 130.89 (d, $J_{\text{C-F}} = 8.4$ Hz), 115.50 (d, $J = 21.4$ Hz), 78.38.



(Hydroperoxymethyl)benzene (8)¹²

^1H NMR (400 MHz, Chloroform-*d*) δ 8.02 (s, 1H), 7.43 – 7.33 (m, 5H), 5.01 (s, 2H).

^{13}C NMR (101 MHz, Chloroform-*d*) δ 135.73, 128.97, 128.60, 79.21.

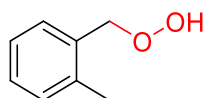


1-(Hydroperoxymethyl)-3-methylbenzene (9)

^1H NMR (400 MHz, Chloroform-*d*) δ 8.04 (s, 1H), 7.32 – 7.26 (m, 1H), 7.22 – 7.17 (m, 3H), 4.98 (s, 2H), 2.38 (s, 3H).

^{13}C NMR (101 MHz, Chloroform-*d*) δ 138.31, 135.59, 129.67, 129.34, 128.49, 126.00, 79.24, 21.31.

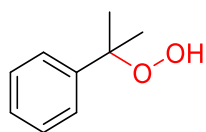
HRMS (ESI) calcd for $\text{C}_8\text{H}_{10}\text{O}_2$ [$\text{M}+\text{Na}$]⁺: 161.0573; found: 161.0571.



1-(Hydroperoxymethyl)-2-methylbenzene (10)¹²

^1H NMR (400 MHz, Chloroform-*d*) δ 8.02 (s, 1H), 7.36 – 7.31 (m, 1H), 7.30 – 7.25 (m, 1H), 7.24 – 7.18 (m, 2H), 5.06 (s, 2H), 2.40 (s, 3H).

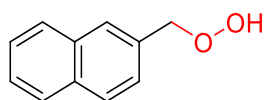
^{13}C NMR (101 MHz, Chloroform-*d*) δ 137.82, 133.31, 130.50, 130.42, 128.90, 125.92, 77.34, 18.87.



(2-Hydroperoxypropan-2-yl)benzene (11)⁶⁷

^1H NMR (400 MHz, Chloroform-*d*) δ 7.51 – 7.46 (m, 2H), 7.41 – 7.38 (m, 3H), 7.33 – 7.28 (m, 1H), 1.62 (s, 6H).

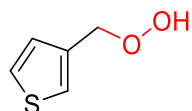
^{13}C NMR (101 MHz, Chloroform-*d*) δ 144.56, 128.51, 127.43, 125.36, 83.93, 26.04.



2-(Hydroperoxymethyl)naphthalene (12)¹²

^1H NMR (400 MHz, Chloroform-*d*) δ 8.07 (s, 1H), 7.91 – 7.82 (m, 4H), 7.56 – 7.48 (m, 3H), 5.17 (s, 2H).

^{13}C NMR (101 MHz, Chloroform-*d*) δ 133.33, 133.16, 128.43, 128.30, 127.99, 127.71, 126.35, 126.31, 79.32.

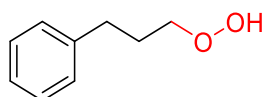


3-(Hydroperoxymethyl)thiophene (13)

^1H NMR (400 MHz, Chloroform-*d*) δ 8.06 (s, 1H), 7.37 – 7.32 (m, 2H), 7.16 – 7.11 (m, 1H), 5.02 (s, 2H).

^{13}C NMR (101 MHz, Chloroform-*d*) δ 136.73, 127.94, 126.29, 125.33, 73.77.

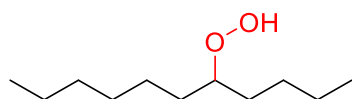
HRMS (ESI) calcd for $\text{C}_5\text{H}_6\text{O}_2\text{S}$ [$\text{M}+\text{Na}$]⁺: 152.9981; found: 152.9987.



(3-Hydroperoxypropyl)benzene (14)⁶⁸

^1H NMR (400 MHz, Chloroform-*d*) δ 7.82 (s, 1H), 7.32 – 7.26 (m, 2H), 7.21-7.18 (m, 3H), 4.05 (t, J = 6.4 Hz, 2H), 2.71(t, J = 8.0 Hz, 2H), 2.04 – 1.94 (m, 2H).

^{13}C NMR (101 MHz, Chloroform-*d*) δ 141.47, 128.42, 125.96, 76.22, 32.01, 29.14.

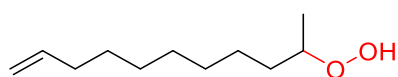


5-Hydroperoxyundecane (15)

^1H NMR (400 MHz, Chloroform-*d*) δ 7.57 (s, 1H), 3.92 – 3.86 (m, 1H), 1.69 – 1.55 (m, 2H), 1.55 – 1.43 (m, 2H), 1.40-1.25 (m, 12H), 0.95-0.86 (m, 6H).

^{13}C NMR (101 MHz, Chloroform-*d*) δ 85.74, 31.99, 31.78, 31.68, 29.42, 27.54, 25.33, 22.81, 22.60, 14.05, 14.00.

HRMS (ESI) calcd for $\text{C}_{11}\text{H}_{24}\text{O}_2$ $[\text{M}+\text{Na}]^+$: 211.1669; found: 211.1671.

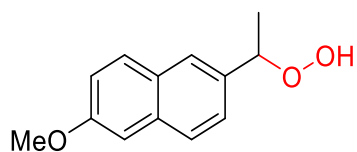


10-Hydroperoxyundec-1-ene (16)

^1H NMR (400 MHz, Chloroform-*d*) δ 7.64 (s, 1H), 5.86-5.76 (m, 1H), 5.02 – 4.88 (m, 2H), 4.10 – 4.02 (m, 1H), 2.08 – 1.98 (m, 2H), 1.69 – 1.55 (m, 2H), 1.40 – 1.27 (m, 10H), 1.22 (d, $J = 6.1$ Hz, 3H).

^{13}C NMR (101 MHz, Chloroform-*d*) δ 139.18, 114.13, 81.71, 33.97, 33.76, 29.60, 29.36, 29.02, 28.88, 25.37, 18.14.

HRMS (ESI) calcd for $\text{C}_{11}\text{H}_{22}\text{O}_2$ $[\text{M}+\text{Na}]^+$: 209.1512; found: 209.1511.

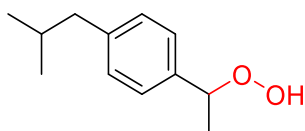


2-(1-Hydroperoxyethyl)-6-methoxynaphthalene (17)

^1H NMR (400 MHz, Chloroform-*d*) δ 7.91 (s, 1H), 7.75 (t, $J = 10.0$ Hz, 3H), 7.47 (dd, $J = 8.5$, 1.8 Hz, 1H), 7.20 – 7.10 (m, 2H), 5.21 (q, $J = 6.6$ Hz, 1H), 3.92 (s, 3H), 1.56 (d, $J = 6.6$ Hz, 3H).

^{13}C NMR (101 MHz, Chloroform-*d*) δ 157.83, 136.32, 134.48, 129.43, 128.65, 127.36, 125.79, 124.66, 119.07, 105.67, 83.85, 55.28, 19.95.

HRMS (ESI) calcd for $\text{C}_{13}\text{H}_{14}\text{O}_3$ $[\text{M}+\text{Na}]^+$: 241.0835; found: 241.0842.

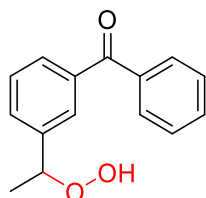


1-(1-Hydroperoxyethyl)-4-isobutylbenzene (18)

^1H NMR (400 MHz, Chloroform-*d*) δ 7.89 (s, 1H), 7.29 (d, $J = 8.0$ Hz, 2H), 7.17 (d, $J = 8.0$ Hz, 2H), 5.06 (q, $J = 6.6$ Hz, 1H), 2.49 (d, $J = 7.2$ Hz, 2H), 1.95 – 1.81 (m, 1H), 1.48 (d, $J = 6.6$ Hz, 3H), 0.93 (d, $J = 6.6$ Hz, 6H).

^{13}C NMR (101 MHz, Chloroform-*d*) δ 141.83, 138.40, 129.32, 126.39, 83.59, 45.09, 30.15, 22.35, 22.34, 19.88.

HRMS (ESI) calcd for $\text{C}_{12}\text{H}_{18}\text{O}_2$ $[\text{M}+\text{Na}]^+$: 217.1199; found: 217.1203.

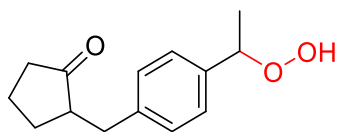


3-(1-Hydroperoxyethyl)phenyl(phenyl)methanone (19)

^1H NMR (400 MHz, Chloroform-*d*) δ 8.65 (s, 1H), 7.83 – 7.75 (m, 3H), 7.69 (d, $J = 7.6$ Hz, 1H), 7.61 – 7.57 (m, 2H), 7.49-7.44 (m, 3H), 5.13 (q, $J = 6.6$ Hz, 1H), 1.48 (d, $J = 6.6$ Hz, 3H).

^{13}C NMR (101 MHz, Chloroform-*d*) δ 196.87, 142.28, 137.73, 137.27, 132.59, 130.54, 130.08, 129.85, 128.43, 128.29, 127.93, 83.09, 20.18.

HRMS (ESI) calcd for $\text{C}_{15}\text{H}_{14}\text{O}_3$ $[\text{M}+\text{Na}]^+$: 265.0835; found: 265.0829.

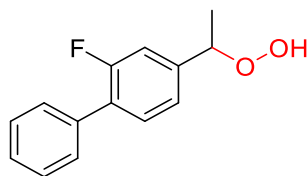


2-(4-(1-Hydroperoxyethyl)benzyl)cyclopentan-1-one (20)

^1H NMR (400 MHz, Chloroform-*d*) δ 8.29 (s, 1H), 7.30 (d, $J = 8.0$ Hz, 2H), 7.18 (d, $J = 8.0$ Hz, 2H), 5.06 (q, $J = 6.6$ Hz, 1H), 3.14 (dd, $J = 13.2, 5.0$ Hz, 1H), 2.60 – 2.50 (m, 1H), 2.39 – 2.31 (m, 2H), 2.17 – 2.04 (m, 2H), 2.01 – 1.93 (m, 1H), 1.81 – 1.67 (m, 1H), 1.62 – 1.51 (m, 1H), 1.48 (d, $J = 6.6$ Hz, 3H).

^{13}C NMR (101 MHz, Chloroform-*d*) δ 139.93, 139.21, 129.03, 126.65, 83.33, 50.90, 50.88, 38.09, 35.19, 29.12, 20.44, 19.93.

HRMS (ESI) calcd for $\text{C}_{14}\text{H}_{18}\text{O}_3$ $[\text{M}+\text{Na}]^+$: 257.1148; found: 257.1148.

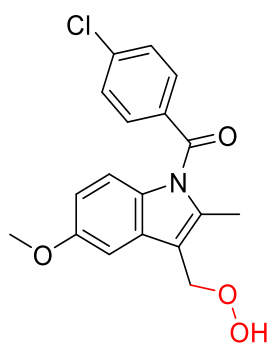


2-Fluoro-4-(1-hydroperoxyethyl)-1,1'-biphenyl (21)

^1H NMR (400 MHz, Chloroform-*d*) δ 8.00 (s, 1H), 7.58 – 7.55 (m, 2H), 7.50 – 7.44 (m, 3H), 7.42 – 7.36 (m, 1H), 7.25 – 7.17 (m, 2H), 5.12 (q, $J = 6.6$ Hz, 1H), 1.51 (d, $J = 6.6$ Hz, 3H).

^{13}C NMR (101 MHz, Chloroform-*d*) δ 159.81 (d, $J_{\text{C-F}} = 248.8$ Hz), 143.13 (d, $J_{\text{C-F}} = 7.1$ Hz), 135.41 (d, $J_{\text{C-F}} = 1.4$ Hz), 130.95 (d, $J_{\text{C-F}} = 3.8$ Hz), 128.94 (d, $J_{\text{C-F}} = 2.8$ Hz), 128.79 (d, $J_{\text{C-F}} = 13.8$ Hz), 128.44, 127.74, 122.36 (d, $J_{\text{C-F}} = 3.4$ Hz), 114.08 (d, $J_{\text{C-F}} = 23.6$ Hz), 82.89 (d, $J_{\text{C-F}} = 1.5$ Hz), 20.00.

HRMS (ESI) calcd for $\text{C}_{14}\text{H}_{13}\text{FO}_2$ $[\text{M}+\text{Na}]^+$: 255.0792; found: 255.0789.



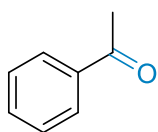
(4-Chlorophenyl)(3-(hydroperoxymethyl)-5-methoxy-2-methyl-1H-indol-1-yl)methanone (22)

^1H NMR (400 MHz, Chloroform-*d*) δ 8.05 (s, 1H), 7.67 (d, $J = 6.6$ Hz, 2H), 7.48 (d, $J = 6.6$ Hz, 2H), 7.07 (s, 1H), 6.84 (d, $J = 9.1$ Hz, 1H), 6.70 – 6.67 (m, 1H), 5.18 (s, 2H), 3.84 (s, 3H), 2.45 (s, 3H).

^{13}C NMR (101 MHz, Chloroform-*d*) δ 168.43, 156.19, 139.62, 138.78, 133.51, 131.26, 130.83, 130.32, 129.20, 114.92, 113.64, 112.12, 101.14, 69.25, 55.73, 13.16.

HRMS (ESI) calcd for C₁₈H₁₆ClNO₄ [M+Na]⁺: 368.0660; found: 368.0662.

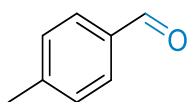
3.5.2 Aldehyde and ketone products



Acetophenone (23)⁶⁹

¹H NMR (400 MHz, Chloroform-*d*) δ 7.96 (d, *J* = 7.2 Hz, 2H), 7.57 (t, *J* = 7.4 Hz, 1H), 7.47 (t, *J* = 7.8 Hz, 2H), 2.61 (s, 3H).

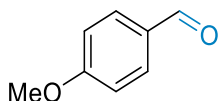
¹³C NMR (101 MHz, Chloroform-*d*) δ 198.15, 137.13, 133.09, 128.56, 128.30, 26.60.



4-Methylbenzaldehyde (24)⁶⁹

¹H NMR (400 MHz, Chloroform-*d*) δ 9.97 (s, 1H), 7.78 (d, *J* = 8.0 Hz, 2H), 7.33 (d, *J* = 8.0 Hz, 2H), 2.44 (s, 3H).

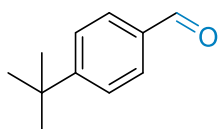
¹³C NMR (101 MHz, Chloroform-*d*) δ 192.01, 145.54, 134.19, 129.85, 129.70, 21.86.



4-Methoxybenzaldehyde (25)⁷⁰

¹H NMR (400 MHz, Chloroform-*d*) δ 9.88 (s, 1H), 7.83 (d, *J* = 8.7 Hz, 2H), 7.00 (d, *J* = 8.7 Hz, 2H), 3.88 (s, 3H).

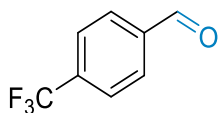
¹³C NMR (101 MHz, Chloroform-*d*) δ 190.80, 164.56, 131.95, 129.90, 114.26, 55.54.



4-(*tert*-butyl)benzaldehyde (26)⁶⁹

¹H NMR (400 MHz, Chloroform-*d*) δ 9.98 (s, 1H), 7.82 (d, *J* = 8.3 Hz, 2H), 7.55 (d, *J* = 8.3 Hz, 2H), 1.35 (s, 9H).

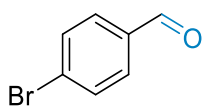
¹³C NMR (101 MHz, Chloroform-*d*) δ 192.04, 158.42, 134.04, 129.67, 125.96, 35.32, 31.03.



4-(Trifluoromethyl)benzaldehyde (27)⁷¹

¹H NMR (400 MHz, Chloroform-*d*) δ 9.56 (s, 1H), 7.47 (d, $J = 8.0$ Hz, 2H), 7.27 (d, $J = 8.0$ Hz, 2H).

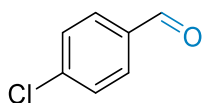
¹³C NMR (101 MHz, Chloroform-*d*) δ 191.06, 138.65, 135.60 (q, $J_{C-F} = 32.6$ Hz), 129.90, 126.10 (q, $J_{C-F} = 3.8$ Hz), 123.43 (q, $J_{C-F} = 273.7$ Hz).



4-Bromobenzaldehyde (28)⁶⁹

¹H NMR (400 MHz, Chloroform-*d*) δ 9.97 (s, 1H), 7.74 (d, $J = 8.4$ Hz, 2H), 7.68 (d, $J = 8.4$ Hz, 2H).

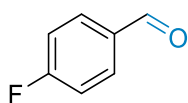
¹³C NMR (101 MHz, Chloroform-*d*) δ 191.01, 135.05, 132.41, 130.94, 129.74.



4-Chlorobenzaldehyde (29)⁶⁹

¹H NMR (400 MHz, Chloroform-*d*) δ 9.99 (s, 1H), 7.83 (d, $J = 8.4$ Hz, 2H), 7.52 (d, $J = 8.4$ Hz, 2H).

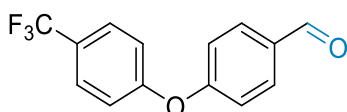
¹³C NMR (101 MHz, Chloroform-*d*) δ 190.73, 140.80, 134.61, 130.79, 129.33.



4-Fluorobenzaldehyde (30)⁷²

¹H NMR (400 MHz, Chloroform-*d*) δ 9.96 (s, 1H), 7.93 – 7.88 (m, 2H), 7.24 – 7.17 (m, 2H).

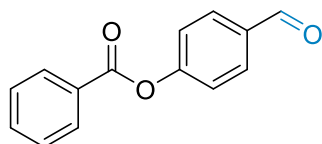
¹³C NMR (101 MHz, Chloroform-*d*) δ 190.47, 166.51 (d, $J_{C-F} = 256.8$ Hz), 132.95 (d, $J_{C-F} = 2.8$ Hz), 132.21 (d, $J_{C-F} = 9.7$ Hz), 116.33 (d, $J_{C-F} = 22.3$ Hz).



4-(4-(Trifluoromethyl)phenoxy)benzaldehyde (31)⁷³

^1H NMR (400 MHz, Chloroform-*d*) δ 9.96 (s, 1H), 7.97 – 7.83 (m, 2H), 7.66 (d, $J = 8.4$ Hz, 2H), 7.21 – 7.07 (m, 4H).

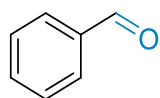
^{13}C NMR (101 MHz, Chloroform-*d*) δ 190.64, 161.64, 158.34, 132.21, 132.03, 127.49 (q, $J_{\text{C-F}} = 3.7$ Hz), 126.64 (q, $J_{\text{C-F}} = 33.0$ Hz), 123.92 (q, $J_{\text{C-F}} = 272.7$ Hz), 119.73, 118.65.



4-Formylphenyl benzoate (32)⁷⁴

^1H NMR (400 MHz, Chloroform-*d*) δ 10.03 (s, 1H), 8.21 (d, $J = 7.2$ Hz, 2H), 7.98 (d, $J = 8.6$ Hz, 2H), 7.69 – 7.61 (m, 1H), 7.54 (t, $J = 7.8$ Hz, 2H), 7.42 (d, $J = 8.5$ Hz, 2H).

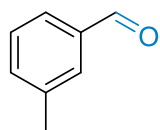
^{13}C NMR (101 MHz, Chloroform-*d*) δ 190.92, 164.47, 155.67, 134.04, 133.99, 131.24, 130.25, 128.88, 128.69, 122.51.



Benzaldehyde (33)⁷⁰

^1H NMR (400 MHz, Chloroform-*d*) δ 10.02 (s, $J = 1.8$ Hz, 1H), 7.92 – 7.83 (m, 2H), 7.65 – 7.61 (m, 1H), 7.52 (t, $J = 8.0$ Hz, 2H).

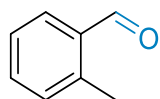
^{13}C NMR (101 MHz, Chloroform-*d*) δ 192.38, 136.36, 134.43, 129.70, 128.95.



3-Methylbenzaldehyde (34)⁷⁵

^1H NMR (400 MHz, Chloroform-*d*) δ 9.99 (s, 1H), 7.72 – 7.65 (m, 2H), 7.47 – 7.39 (m, 2H), 2.44 (s, 3H).

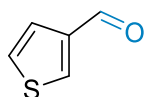
^{13}C NMR (101 MHz, Chloroform-*d*) δ 192.60, 138.90, 136.47, 135.27, 130.00, 128.86, 127.21, 21.17.



2-Methylbenzaldehyde (35)⁷⁶

^1H NMR (400 MHz, Chloroform-*d*) δ 10.28 (s, 1H), 7.80 (dd, $J = 7.7, 1.5$ Hz, 1H), 7.48 (td, $J = 7.5, 1.5$ Hz, 1H), 7.36 (t, $J = 7.5$ Hz, 1H), 7.27 (d, $J = 4.0$ Hz, 1H), 2.68 (s, 3H).

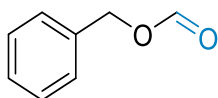
^{13}C NMR (101 MHz, Chloroform-*d*) δ 192.83, 140.62, 134.14, 133.64, 132.04, 131.76, 126.31, 19.57.



Thiophene-3-carbaldehyde (36)⁷⁷

^1H NMR (400 MHz, Chloroform-*d*) δ 9.94 (s, 1H), 8.13 – 8.12 (m, 1H), 7.55 – 7.54 (m, 1H), 7.38 (m, 1H).

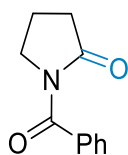
^{13}C NMR (101 MHz, Chloroform-*d*) δ 184.95, 143.03, 136.68, 127.38, 125.37.



Benzyl formate (37)⁷⁸

^1H NMR (400 MHz, Chloroform-*d*) δ 8.15 (s, 1H), 7.42 – 7.30 (m, 5H), 5.21 (s, 2H).

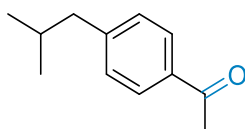
^{13}C NMR (101 MHz, Chloroform-*d*) δ 160.76, 135.16, 128.64, 128.49, 128.34, 65.68.



1-Benzoylpyrrolidin-2-one (38)⁷⁹

^1H NMR (400 MHz, Chloroform-*d*) δ 7.60 (d, $J = 7.8$ Hz, 2H), 7.51 (t, $J = 7.4$ Hz, 1H), 7.41 (t, $J = 7.4$ Hz, 2H), 3.96 (t, $J = 7.1$ Hz, 2H), 2.61 (t, $J = 8.0$ Hz, 2H), 2.19 – 2.11 (m, 2H).

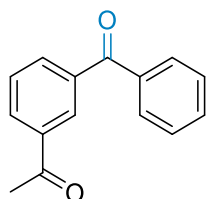
^{13}C NMR (101 MHz, Chloroform-*d*) δ 174.50, 170.69, 134.31, 131.89, 128.89, 127.76, 46.51, 33.29, 17.65.



1-(4-Isobutylphenyl)ethan-1-one (39)⁸⁰

^1H NMR (400 MHz, Chloroform-*d*) δ 7.88 (d, $J = 8.3$ Hz, 2H), 7.23 (d, $J = 8.3$ Hz, 2H), 2.59 (s, 3H), 2.53 (d, $J = 7.2$ Hz, 2H), 1.96 – 1.82 (m, 1H), 0.91 (d, $J = 6.6$ Hz, 6H).

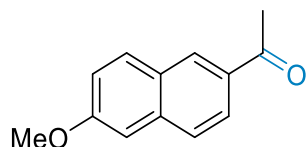
^{13}C NMR (101 MHz, Chloroform-*d*) δ 197.91, 147.59, 134.96, 129.27, 128.29, 45.37, 30.10, 26.53, 22.31.



1-(3-Benzoylphenyl)ethan-1-one (40)⁸⁰

^1H NMR (400 MHz, Chloroform-*d*) δ 8.36 (s, 1H), 8.18 (d, $J = 7.8$ Hz, 1H), 7.99 (d, $J = 7.8$ Hz, 1H), 7.80 (d, $J = 7.6$ Hz, 2H), 7.61 (q, $J = 7.6$ Hz, 2H), 7.51 (t, $J = 7.6$ Hz, 2H), 2.65 (s, 3H).

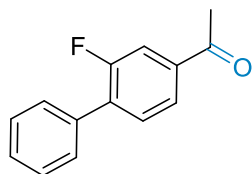
^{13}C NMR (101 MHz, Chloroform-*d*) δ 197.27, 195.83, 138.05, 137.16, 136.98, 134.22, 132.86, 131.73, 130.01, 129.67, 128.72, 128.48, 26.72.



1-(6-Methoxynaphthalen-2-yl)ethan-1-one (41)⁸⁰

^1H NMR (400 MHz, Chloroform-*d*) δ 8.38 (s, 1H), 8.00 (dd, $J = 8.6, 1.8$ Hz, 1H), 7.84 (d, $J = 8.9$ Hz, 1H), 7.75 (d, $J = 8.6$ Hz, 1H), 7.21-7.14 (m, 2H), 3.94 (s, 3H), 2.69 (s, 3H).

^{13}C NMR (101 MHz, Chloroform-*d*) δ 197.80, 159.70, 137.22, 132.56, 131.06, 130.00, 127.76, 127.03, 124.60, 119.66, 105.70, 55.36, 26.49.

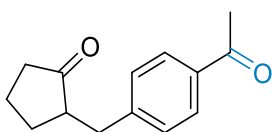


1-(2-Fluoro-[1,1'-biphenyl]-4-yl)ethan-1-one (42)¹⁶

^1H NMR (400 MHz, Chloroform-*d*) δ 7.81 (dd, $J = 8.0, 1.7$ Hz, 1H), 7.74 (dd, $J = 11.2, 1.7$ Hz, 1H), 7.61 – 7.52 (m, 3H), 7.51 – 7.39 (m, 3H), 2.63 (s, 3H).

^{13}C NMR (101 MHz, Chloroform-*d*) δ 196.49 (d, $J_{\text{C-F}} = 1.9$ Hz), 159.68 (d, $J_{\text{C-F}} = 249.9$ Hz), 137.81 (d, $J_{\text{C-F}} = 6.4$ Hz), 134.67 (d, $J_{\text{C-F}} = 1.0$ Hz), 133.80 (d, $J_{\text{C-F}} = 13.7$ Hz), 130.93 (d, $J_{\text{C-F}}$

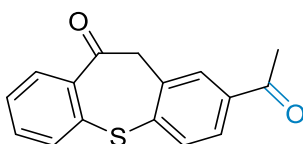
= 3.4 Hz), 129.00 (d, $J_{C-F} = 3.1$ Hz), 128.61, 128.50, 124.33 (d, $J_{C-F} = 3.5$ Hz), 115.91 (d, $J_{C-F} = 24.1$ Hz), 26.65.



2-(4-Acetylbenzyl)cyclopentan-1-one (43)⁸¹

¹H NMR (400 MHz, Chloroform-*d*) δ 7.91 (d, $J = 8.2$ Hz, 2H), 7.29 (d, $J = 8.2$ Hz, 2H), 3.22 (dd, $J = 13.9, 4.3$ Hz, 1H), 2.70 – 2.63 (m, 1H), 2.61 (s, 3H), 2.43 – 2.33 (m, 2H), 2.19 – 2.07 (m, 2H), 2.04-1.96 (m, 1H), 1.84-1.72 (m, 1H), 1.62 – 1.46 (m, 1H).

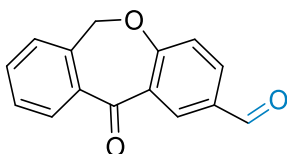
¹³C NMR (101 MHz, Chloroform-*d*) δ 219.49, 197.70, 145.76, 135.30, 129.05, 128.51, 50.58, 37.96, 35.47, 29.04, 26.48, 20.43.



2-Acetyldibenzo[b,f]thiepin-10(11H)-one (44)¹⁶

¹H NMR (400 MHz, Chloroform-*d*) δ 8.20 (d, $J = 7.9$ Hz, 1H), 7.99 (s, 1H), 7.78 (d, $J = 8.1$ Hz, 1H), 7.72 (d, $J = 8.1$ Hz, 1H), 7.60 (d, $J = 7.8$ Hz, 1H), 7.45 (t, $J = 7.5$ Hz, 1H), 7.33 (t, $J = 7.5$ Hz, 1H), 4.41 (s, 2H), 2.59 (s, 3H).

¹³C NMR (101 MHz, Chloroform-*d*) δ 196.89, 190.65, 140.04, 139.01, 138.13, 137.90, 135.98, 132.75, 131.56, 131.42, 130.89, 129.09, 127.14, 126.88, 50.95, 26.69.

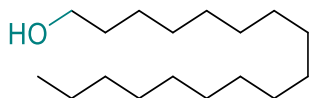


11-Oxo-6,11-dihydrodibenzo[b,e]oxepine-2-carbaldehyde (45)⁸²

¹H NMR (400 MHz, Chloroform-*d*) δ 10.00 (s, 1H), 8.73 (d, $J = 2.1$ Hz, 1H), 8.03 (dd, $J = 8.6, 2.1$ Hz, 1H), 7.89 (d, $J = 7.6$, 1H), 7.61 (t, $J = 7.6$, 1H), 7.51 (t, $J = 7.6$, 1H), 7.41 (d, $J = 7.4$, 1H), 7.17 (d, $J = 8.6$ Hz, 1H), 5.29 (s, 2H).

^{13}C NMR (101 MHz, Chloroform-*d*) δ 190.38, 190.17, 165.54, 140.32, 137.46, 134.51, 133.41, 133.20, 130.93, 129.73, 129.39, 128.14, 125.01, 122.16, 73.61.

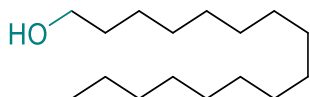
3.5.3 Alcohol products



Heptadecan-1-ol (46)⁸³

^1H NMR (400 MHz, Chloroform-*d*) δ 3.63 (t, $J = 6.6$ Hz, 2H), 1.59 – 1.52 (m, 2H), 1.39 – 1.18 (m, 28H), 0.87 (t, $J = 6.7$ Hz, 3H).

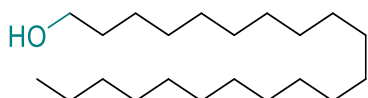
^{13}C NMR (101 MHz, Chloroform-*d*) δ 63.06, 32.79, 31.91, 29.67, 29.64, 29.60, 29.58, 29.42, 29.34, 25.72, 22.67, 14.09.



Hexadecan-1-ol (47)⁸⁴

^1H NMR (400 MHz, Chloroform-*d*) δ 3.63 (t, $J = 6.6$ Hz, 2H), 1.59 – 1.52 (m, 2H), 1.38 – 1.20 (m, 26H), 0.87 (t, $J = 6.8$ Hz, 3H).

^{13}C NMR (101 MHz, Chloroform-*d*) δ 63.06, 32.79, 31.91, 29.67, 29.64, 29.60, 29.58, 29.42, 29.34, 25.72, 22.67, 14.09.

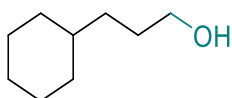


Henicosan-1-ol (48)

^1H NMR (400 MHz, Chloroform-*d*) δ 3.64 (t, $J = 6.6$ Hz, 2H), 1.62 – 1.51 (m, 3H), 1.36 – 1.25 (m, 35H), 0.88 (t, $J = 6.7$ Hz, 3H).

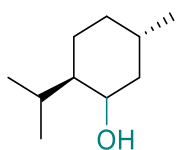
^{13}C NMR (101 MHz, Chloroform-*d*) δ 63.11, 32.81, 31.92, 29.69, 29.66, 29.61, 29.59, 29.43, 29.35, 25.73, 22.68, 14.11.

HRMS (CI) calcd for $\text{C}_{21}\text{H}_{44}\text{O}$ $[\text{M}+\text{H}]^+$: 313.3465; found: 313.3470.



3-Cyclohexylpropan-1-ol (49)⁸⁵

HRMS (ESI) calcd for C₉H₁₈O [M+Na]⁺: 165.1250; found: 165.1254.

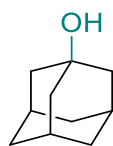


(2*R*,5*S*)-2-Isopropyl-5-methylcyclohexan-1-ol (50)

¹H NMR (400 MHz, Chloroform-*d*) δ 3.41 (td, *J* = 10.4, 4.3 Hz, 1H), 2.20 – 2.12 (m, 1H), 1.99 – 1.93 (m, 1H), 1.69 – 1.58 (m, 2H), 1.49 – 1.36 (m, 2H), 1.14 – 1.07 (m, 1H), 0.97 – 0.89 (m, 7H), 0.81 (d, *J* = 7.0 Hz, 3H).

¹³C NMR (101 MHz, Chloroform-*d*) δ 71.55, 50.14, 45.04, 34.53, 31.62, 25.84, 23.13, 22.20, 20.99, 16.09.

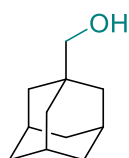
HRMS (ESI) calcd for C₁₀H₂₀O [M+H]⁺: 157.1587; found: 157.1591.



(3*s*,5*s*,7*s*)-Adamantan-1-ol (51)³²

¹H NMR (400 MHz, Chloroform-*d*) δ 2.17 – 2.11 (m, 3H), 1.71 (s, 6H), 1.65 – 1.57 (m, 6H).

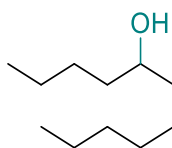
¹³C NMR (101 MHz, Chloroform-*d*) δ 68.22, 45.33, 36.06, 30.71.



((3*r*,5*r*,7*r*)-Adamantan-1-yl)methanol (52)³²

¹H NMR (400 MHz, Chloroform-*d*) δ 3.20 (s, 2H), 2.01 – 1.97 (m, 3H), 1.76 – 1.71 (m, 3H), 1.67 – 1.62 (m, 3H), 1.51 (d, *J* = 2.9 Hz, 6H).

¹³C NMR (101 MHz, Chloroform-*d*) δ 73.87, 39.02, 37.16, 28.16.

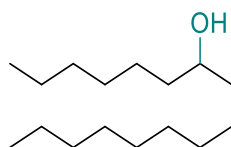


Undecan-5-ol (53)

^1H NMR (400 MHz, Chloroform-*d*) δ 3.61 – 3.55 (m, 1H), 1.48 – 1.25 (m, 17H), 0.92 – 0.87 (m, 6H).

^{13}C NMR (101 MHz, Chloroform-*d*) δ 72.01, 37.49, 37.17, 31.84, 29.37, 27.83, 25.61, 22.76, 22.61, 14.07.

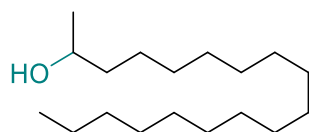
HRMS (ESI) calcd for $\text{C}_{11}\text{H}_{24}\text{O}$ $[\text{M}+\text{H}]^+$: 172.1900; found: 173.1901.



Hexadecan-7-ol (54)⁸⁶

^1H NMR (400 MHz, Chloroform-*d*) δ 3.60 – 3.56 (m, 1H), 1.52 – 1.16 (m, 26H), 0.88 (t, J = 6.4 Hz, 6H).

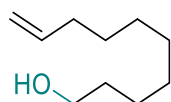
^{13}C NMR (101 MHz, Chloroform-*d*) δ 72.02, 37.48, 31.87, 31.84, 29.71, 29.59, 29.37, 29.27, 25.65, 25.61, 22.66, 22.61, 14.09, 14.07.



Octadecan-2-ol (55)⁸⁷

^1H NMR (400 MHz, Chloroform-*d*) δ 3.83 – 3.75 (m, 1H), 1.52 – 1.13 (m, 33H), 0.88 (t, J = 6.7 Hz, 3H).

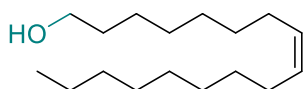
^{13}C NMR (101 MHz, Chloroform-*d*) δ 68.19, 39.38, 31.92, 29.69, 29.65, 29.62, 29.60, 29.35, 25.77, 23.47, 22.68, 14.11.



Dec-9-en-1-ol (56)⁸⁸

^1H NMR (400 MHz, Chloroform-*d*) δ 5.86 – 5.76 (m, 1H), 5.01 – 4.92 (m, 2H), 3.64 (t, J = 6.6 Hz, 2H), 2.07 – 2.01 (m, 2H), 1.60 – 1.53 (m, 2H), 1.42 – 1.30 (m, 10H).

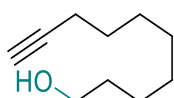
^{13}C NMR (101 MHz, Chloroform-*d*) δ 139.19, 114.13, 63.08, 33.77, 32.78, 29.42, 29.35, 29.04, 28.89, 25.70.



(Z)-Heptadec-8-en-1-ol (57)⁸⁹

¹H NMR (400 MHz, Chloroform-*d*) δ 5.39 – 5.33 (m, 2H), 3.63 (t, $J = 6.7$ Hz, 2H), 2.03 – 1.94 (m, 4H), 1.60 – 1.53 (m, 2H), 1.35 – 1.26 (m, 20H), 0.88 (t, $J = 6.6$ Hz, 3H).

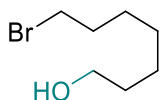
¹³C NMR (101 MHz, Chloroform-*d*) δ 130.46, 129.99, 63.06, 32.78, 31.89, 29.75, 29.67, 29.51, 29.31, 29.23, 29.16, 29.07, 27.20, 27.16, 25.69, 22.66, 14.09.



Dec-9-yn-1-ol (58)⁹⁰

¹H NMR (400 MHz, Chloroform-*d*) δ 3.65 (t, $J = 7.0$ Hz, 2H), 2.20 – 2.16 (m, 2H), 1.94 – 1.93 (m, 1H), 1.58 – 1.50 (m, 3H), 1.42-1.25 (m, 9H).

¹³C NMR (101 MHz, Chloroform-*d*) δ 85.92, 68.07, 63.04, 32.75, 29.25, 29.03, 28.64, 28.43, 25.66, 18.36.



7-Bromoheptan-1-ol (59)⁸⁴

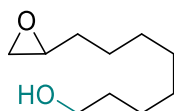
HRMS (ESI) calcd for C₇H₁₅BrO [M+H]⁺: 195.0379; found: 195.0384.



16-Hydroxyhexadecyl acetate (60)⁹¹

¹H NMR (400 MHz, Chloroform-*d*) δ 4.04 (t, $J = 6.8$ Hz, 2H), 3.62 (t, $J = 6.6$ Hz, 2H), 2.03 (s, 3H), 1.64 – 1.52 (m, 5H), 1.35 – 1.21 (m, 23H).

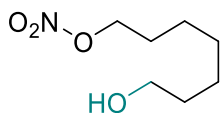
¹³C NMR (101 MHz, Chloroform-*d*) δ 171.27, 64.65, 63.02, 32.77, 29.60, 29.57, 29.55, 29.52, 29.47, 29.40, 29.21, 28.56, 25.87, 25.71, 20.99.



8-(Oxiran-2-yl)octan-1-ol (61)⁹²

¹H NMR (400 MHz, Chloroform-*d*) δ 3.63 (t, J = 6.6 Hz, 2H), 2.92-2.88 (m, 1H), 2.81 – 2.68 (m, 1H), 2.46 (dd, J = 5.1, 2.8 Hz, 1H), 1.62 – 1.23 (m, 14H).

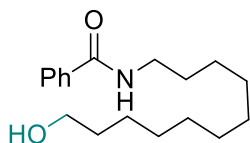
¹³C NMR (101 MHz, Chloroform-*d*) δ 63.01, 52.39, 47.11, 32.74, 32.44, 29.45, 29.32, 29.27, 25.92, 25.67.



7-Hydroxyheptyl nitrate (62)⁹³

¹H NMR (400 MHz, Chloroform-*d*) δ 4.44 (t, J = 6.3 Hz, 2H), 3.41 (t, J = 6.7 Hz, 2H), 1.90 – 1.83 (m, 2H), 1.79 – 1.70 (m, 2H), 1.50 – 1.24 (m, 6H).

¹³C NMR (101 MHz, Chloroform-*d*) δ 73.24, 33.71, 32.53, 28.24, 27.86, 26.64, 25.48.

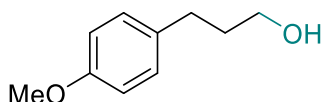


N-(11-Hydroxyundecyl)benzamide (63)

¹H NMR (400 MHz, Chloroform-*d*) δ 7.75 (d, J = 7.1 Hz, 2H), 7.50 – 7.40 (m, 3H), 7.42 (t, J = 7.4 Hz, 2H), 6.18 (s, 1H), 3.63 (t, J = 6.6 Hz, 2H), 3.44 (q, J = 7.2 Hz, 2H), 1.65 – 1.51 (m, 4H), 1.40 – 1.23 (m, 14H).

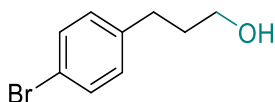
¹³C NMR (101 MHz, Chloroform-*d*) δ 167.52, 134.83, 131.29, 128.52, 126.80, 63.01, 40.09, 32.75, 29.63, 29.48, 29.43, 29.40, 29.33, 29.23, 26.93, 25.68.

HRMS (CI) calcd for C₁₈H₂₉NO₂ [M+H]⁺: 292.2271; found: 292.2270.



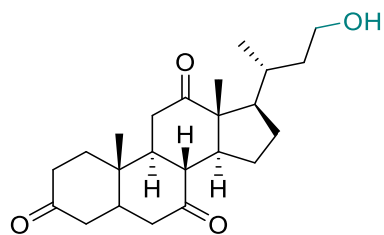
3-(4-Methoxyphenyl)propan-1-ol (64)⁹⁴

HRMS (ESI) calcd for C₁₀H₁₄O₂ [M+Na]⁺: 189.0886; found: 189.0885.



3-(4-Bromophenyl)propan-1-ol (65)⁹⁵

HRMS (ESI) calcd for C₇H₁₅BrO [M+H]⁺: 195.0379; found: 195.0380.

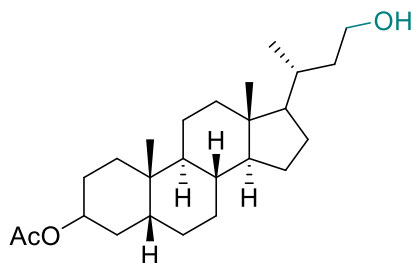


(8*R*,9*S*,10*S*,13*R*,14*S*,17*R*)-17-((*R*)-4-hydroxybutan-2-yl)-10,13-dimethyldodecahydro-3*H*-cyclopenta[*a*]phenanthrene-3,7,12(2*H*,4*H*)-trione (66)

¹H NMR (400 MHz, Chloroform-*d*) δ 4.19 – 3.94 (m, 2H), 2.98 – 2.77 (m, 3H), 2.41 – 2.08 (m, 9H), 2.04 – 1.78 (m, 6H), 1.65 – 1.56 (m, 1H), 1.39 (s, 3H), 1.30 – 1.22 (m, 3H), 1.07 (s, 3H), 0.89 (dd, *J* = 24.2, 6.0 Hz, 3H).

¹³C NMR (101 MHz, Chloroform-*d*) δ 212.10, 209.17, 208.77, 75.12, 56.89, 51.74, 48.94, 46.80, 45.93, 45.51, 44.93, 42.74, 38.58, 36.43, 35.98, 35.23, 33.22, 33.00, 27.73, 25.10, 21.86, 19.11, 11.79.

HRMS (CI) calcd for C₂₃H₃₄O₄ [M+H]⁺: 391.2479; found: 391.2483.



(5*R*,8*R*,9*S*,10*S*,13*R*,14*S*)-17-((*R*)-4-hydroxybutan-2-yl)-10,13-dimethylhexadecahydro-1*H*-cyclopenta[*a*]phenanthren-3-yl acetate (67)

¹H NMR (400 MHz, Chloroform-*d*) δ 4.75 – 4.67 (m, 1H), 3.71 – 3.62 (m, 2H), 2.02 (s, 3H), 2.00 – 1.95 (m, 1H), 1.89 – 1.78 (m, 5H), 1.71 – 1.64 (m, 2H), 1.58 – 1.51 (m, 3H), 1.47 – 1.36 (m, 7H), 1.29 – 1.17 (m, 6H), 1.12 – 1.01 (m, 5H), 0.92 (s, 3H), 0.65 (s, 3H).

¹³C NMR (101 MHz, Chloroform-*d*) δ 170.65, 74.40, 60.91, 56.55, 56.51, 42.77, 41.88, 40.40, 40.16, 38.98, 35.77, 35.02, 34.57, 32.88, 32.24, 28.40, 27.01, 26.62, 26.31, 24.18, 23.31, 21.47, 20.81, 18.81, 11.99.

HRMS (CI) calcd for C₂₅H₄₂O₃ [M+H]⁺: 391.3207; found: 391.3202.

3.6 References

1. Clayden, J.; Greeves, N.; Warren, S., *Organic Chemistry*. Oxford University Press: **2012**.
2. Patai, S.; Rappoport, Z., *The Chemistry of Functional Groups*. Wiley: **1964**.
3. Wei, Y.; Hu, P.; Zhang, M.; Su, W., Metal-Catalyzed Decarboxylative C-H Functionalization. *Chem. Rev.* **2017**, *117*, 8864-8907.
4. Patra, T.; Maiti, D., Decarboxylation as the Key Step in C-C Bond-Forming Reactions. *Chemistry* **2017**, *23*, 7382-7401.
5. Schwarz, J.; König, B., Decarboxylative Reactions with and without Light-A Comparison. *Green Chem.* **2018**, *20*, 323-361.
6. Majumdar, N., Carboxylic Acids as Building Blocks in Catalytic Asymmetric Reactions. *ACS Catal.* **2022**, *12*, 8291-8324.
7. Warren, S., *Chemistry of the Carbonyl Group-Programmed Approach to Organic Reaction Method*. Wiley-Blackwell: **1974**.
8. Simmonds, C., *Alcohol, Its Production, Properties, Chemistry, and Industrial Applications: With Chapters on Methyl Alcohol, Fusel Oil, and Spirituous Beverages*. Macmillan and Company, Limited: **1919**.
9. Yaremenko, I. A.; Vil, V. A.; Demchuk, D. V.; Terent'ev, A. O., Rearrangements of Organic Peroxides and Related Processes. *Beilstein J. Org. Chem.* **2016**, *12*, 1647-1748.
10. Ma, Z.; Mahmudov, K. T.; Aliyeva, V. A.; Gurbanov, A. V.; Guedes da Silva, M. F. C.; Pombeiro, A. J. L., Peroxides in Metal Complex Catalysis. *Coord. Chem. Rev.* **2021**, *437*, 213859.
11. Weissermel, K.; Arpe, H. J., *Industrial Organic Chemistry*. John Wiley & Sons: **2008**.
12. Hou, Y.; Hu, J.; Xu, R.; Pan, S.; Zeng, X.; Zhong, G., Iridium-Mediated Synthesis of Benzylic Hydroperoxides. *Org. Lett.* **2019**, *21*, 4428-4432.
13. Kyasa, S.; Puffer, B. W.; Dussault, P. H., Synthesis of Alkyl Hydroperoxides via Alkylation of Gem-Dihydroperoxides. *J. Org. Chem.* **2013**, *78*, 3452-3456.
14. Sánchez, M. A.; Torres, G. C.; Mazzieri, V. A.; Pieck, C. L., Selective Hydrogenation of Fatty Acids and Methyl Esters of Fatty Acids to Obtain Fatty Alcohols-A Review. *J. Chem. Technol. Biotechnol.* **2017**, *92*, 27-42.
15. Tamura, M.; Nakagawa, Y.; Tomishige, K., Recent Developments of Heterogeneous Catalysts for Hydrogenation of Carboxylic Acids to their Corresponding Alcohols. *Asian J. Org. Chem.* **2020**, *9*, 126-143.

16. Sakakibara, Y.; Cooper, P.; Murakami, K.; Itami, K., Photoredox-Catalyzed Decarboxylative Oxidation of Arylacetic Acids. *Chem. Asian J.* **2018**, *13*, 2410-2413.
17. Bazyar, Z.; Hosseini-Sarvari, M., On/Off O₂ Switchable Photocatalytic Oxidative and Protodecarboxylation of Carboxylic Acids. *J. Org. Chem.* **2019**, *84*, 13503-13515.
18. Shirase, S.; Tamaki, S.; Shinohara, K.; Hirosawa, K.; Tsurugi, H.; Satoh, T.; Mashima, K., Cerium(IV) Carboxylate Photocatalyst for Catalytic Radical Formation from Carboxylic Acids: Decarboxylative Oxygenation of Aliphatic Carboxylic Acids and Lactonization of Aromatic Carboxylic Acids. *J. Am. Chem. Soc.* **2020**, *142*, 5668-5675.
19. Araghi, M.; Bokaei, F., Manganese(III) Porphyrin Supported on Multi-Wall Carbon Nanotubes: A Highly Efficient and Reusable Biomimetic Catalyst for Oxidative Decarboxylation of α -Arylcarboxylic Acids and Oxidation of Alkanes with Sodium Periodate. *Polyhedron* **2013**, *53*, 15-19.
20. Tangestaninejad, S.; Mirkhani, V., Efficient and Mild Oxidative Decarboxylation of Aryl-substituted Carboxylic Acids by Iron and Manganese Porphyrin Periodate Systems. *J. Chem. Res.* **1998**, *12*, 820-821.
21. Farhadi, S.; Zaringhadam, P.; Sahamieh, R. Z., Photolytic Decarboxylation of α -Arylcarboxylic Acids Mediated by HgF₂ under a Dioxygen Atmosphere. *Tetrahedron Lett.* **2006**, *47*, 1965-1968.
22. Pocker, Y.; Davis, B. C., Oxidative Cleavage by Lead(IV). I. The Mechanism of Decarboxylation of 2-Hydroxycarboxylic Acids. *J. Am. Chem. Soc.* **1973**, *95*, 6216-6223.
23. Gholamreza, K.; Roxana, A., Biomimetic Decarboxylation of Carboxylic Acids with PhI(OAc)₂ Catalyzed by Manganese Porphyrin [Mn(TPP)OAc]. *Chem. Res. Chin. Uni.* **2008**, *24*, 464-468.
24. Mete, T. B.; Khopade, T. M.; Bhat, R. G., Oxidative Decarboxylation of Arylacetic Acids in Water: One-Pot Transition-Metal-Free Synthesis of Aldehydes and Ketones. *Tetrahedron Lett.* **2017**, *58*, 2822-2825.
25. Faraggi, T. M.; Li, W.; MacMillan, D. W. C., Decarboxylative Oxygenation via Photoredox Catalysis. *Israel J. Chem.* **2019**, *60*, 410-415.
26. Guan, R.; Bennett, E. L.; Huang, Z.; Xiao, J., Decarboxylative Oxygenation of Carboxylic Acids with O₂ via a Non-Heme Manganese Catalyst. *Green Chem.* **2022**, *24*, 2946-2952.
27. Sheldon, R. A.; Kochi, J. K., Photochemical and Thermal Reduction of Cerium(IV) Carboxylates. Formation and Oxidation of Alkyl Radicals. *J. Am. Chem. Soc.* **1968**, *90*, 6688-6698.

28. Trahanovsky, W. S.; Cramer, J.; Brixius, D. W., Oxidation of Organic Compounds with Cerium(IV). XVIII. Oxidative Decarboxylation of Substituted Phenylacetic Acids. *J. Am. Chem. Soc.* **1974**, *96*, 1077-1081.
29. Yatham, V. R.; Bellotti, P.; Konig, B., Decarboxylative Hydrazination of Unactivated Carboxylic Acids by Cerium Photocatalysis. *Chem. Commun.* **2019**, *55*, 3489-3492.
30. Wang, Y.; Li, L.; Fu, N., Electrophotocatalytic Decarboxylative Azidation of Aliphatic Carboxylic Acids. *ACS Catal.* **2022**, *12*, 10661-10667.
31. Song, H. T.; Ding, W.; Zhou, Q. Q.; Liu, J.; Lu, L. Q.; Xiao, W. J., Photocatalytic Decarboxylative Hydroxylation of Carboxylic Acids Driven by Visible Light and Using Molecular Oxygen. *J. Org. Chem.* **2016**, *81*, 7250-7255.
32. Khan, S. N.; Zaman, M. K.; Li, R.; Sun, Z., A General Method for Photocatalytic Decarboxylative Hydroxylation of Carboxylic Acids. *J. Org. Chem.* **2020**, *85*, 5019-5026.
33. Tsurugi, H.; Mashima, K., Renaissance of Homogeneous Cerium Catalysts with Unique Ce(IV/III) Couple: Redox-Mediated Organic Transformations Involving Homolysis of Ce(IV)-Ligand Covalent Bonds. *J. Am. Chem. Soc.* **2021**, *143*, 7879-7890.
34. Yang, Q.; Wang, Y. H.; Qiao, Y.; Gau, M.; Carroll, P. J.; Walsh, P. J.; Schelter, E. J., Photocatalytic C-H Activation and the Subtle Role of Chlorine Radical Complexation in Reactivity. *Science* **2021**, *372*, 847-852.
35. Abderrazak, Y.; Bhattacharyya, A.; Reiser, O., Visible-Light-Induced Homolysis of Earth-Abundant Metal-Substrate Complexes: A Complementary Activation Strategy in Photoredox Catalysis. *Angew. Chem. Int. Ed.* **2021**, *60*, 21100-21115.
36. Yang, Z.; Yang, D.; Zhang, J.; Tan, C.; Li, J.; Wang, S.; Zhang, H.; Huang, Z.; Lei, A., Electrophotocatalytic Ce-Catalyzed Ring-Opening Functionalization of Cycloalkanols under Redox-Neutral Conditions: Scope and Mechanism. *J. Am. Chem. Soc.* **2022**, *144*, 13895-13902.
37. Feng, Q.; Song, Q., Aldehydes and Ketones Formation: Copper-Catalyzed Aerobic Oxidative Decarboxylation of Phenylacetic Acids and α -Hydroxyphenylacetic Acids. *J. Org. Chem.* **2014**, *79*, 1867-1871.
38. Chauhan, S. M. S.; Sahoo, B. B., Biomimetic Oxidation of Ibuprofen with Hydrogen Peroxide Catalysed by Horseradish Peroxidase (HRP) and 5,10,15,20-Tetrakis-(2',6'-Dichloro-3'-Sulphonatophenyl)porphyrinatoiron(III) and Manganese(III) Hydrates in AOT Reverse Micelles. *Bioorg. Med. Chem.* **1999**, *7*, 2629-2634.
39. Foote, C. S.; Valentine, J. S.; Greenberg, A.; Liebman, J. F., *Active Oxygen in Chemistry*. Springer Science & Business Media: **2012**.

40. Bolm, C.; Beller, M., *Transition Metals for Organic Synthesis*. Wiley-VCH: Weinheim: **2004**.
41. Ojima, I. X., *Catalytic Asymmetric Synthesis*. John Wiley & Sons: **2010**.
42. Marques, E. F.; Burrows, H. D.; da Graca Miguel, M., The Structure and Thermal Behaviour of Some Long Chain Cerium(III) Carboxylates. *J. Chem. Soc. Faraday Trans.* **1998**, *94*, 1729-1736.
43. Oh, E. M.; Nagasawa, A., Interactions Between Hydrated Cerium(III) Cations and Carboxylates in an Aqueous Solution: Anomalous Strong Complex Formation with Diglycolate, Suggesting a Chelate Effect. *ACS Omega* **2020**, *5*, 31880-31890.
44. Naik, S.; Naik, P. P.; Krishnamurthy, G.; Venugopal, N.; Naik, N.; Naik, T. R. R., Synthesis, Characterization, DFT Studies and Biological Activity of Ru(III), La(III) and Ce(III) Triphenylphosphine Complexes Containing 2-Aminothiazole and 2-Aminotriazole. *J. Inorg. Organomet. Polym. Mater.* **2020**, *30*, 3332-3356.
45. Moiseev, Y.; Ben-Eliyahu, Y.; Audras, M.; Berthon, L.; Moisy, P.; Bettelheim, A.; Zilbermann, I., Spectroscopic, Electrochemical, and Structural Aspects of the Ce(IV)/Ce(III) DOTA Redox Couple Chemistry in Aqueous Solutions. *J. Coord. Chem.* **2016**, *69*, 2895-2907.
46. Mathey, L.; Paul, M.; Coperet, C.; Tsurugi, H.; Mashima, K., Cerium(IV) Hexanuclear Clusters from Cerium(III) Precursors: Molecular Models for Oxidative Growth of Ceria Nanoparticles. *Chemistry* **2015**, *21*, 13454-13461.
47. Guo, J. J.; Hu, A.; Chen, Y.; Sun, J.; Tang, H.; Zuo, Z., Photocatalytic C-C Bond Cleavage and Amination of Cycloalkanols by Cerium(III) Chloride Complex. *Angew. Chem. Int. Ed.* **2016**, *55*, 15319-15322.
48. Hu, A.; Guo, J. J.; Pan, H.; Tang, H.; Gao, Z.; Zuo, Z., δ -Selective Functionalization of Alkanols Enabled by Visible-Light-Induced Ligand-to-Metal Charge Transfer. *J. Am. Chem. Soc.* **2018**, *140*, 1612-1616.
49. Hu, A.; Chen, Y.; Guo, J. J.; Yu, N.; An, Q.; Zuo, Z., Cerium-Catalyzed Formal Cycloaddition of Cycloalkanols with Alkenes through Dual Photoexcitation. *J. Am. Chem. Soc.* **2018**, *140*, 13580-13585.
50. Lonnberg, T.; Aiba, Y.; Hamano, Y.; Miyajima, Y.; Sumaoka, J.; Komiyama, M., Oxidation of an Oligonucleotide-Bound Ce(III)/Multiphosponate Complex for Site-Selective DNA Scission. *Chemistry* **2010**, *16*, 855-859.
51. Shekunova, T. O.; Lapkina, L. A.; Shcherbakov, A. B.; Meshkov, I. N.; Ivanov, V. K.; Yu. Tsvadze, A.; Gorbunova, Y. G., Deactivation of Singlet Oxygen by Cerium Oxide Nanoparticles. *J. Photochem. Photobiol. A. Chem.* **2019**, *382*, 111925.

52. Stahl, J.; Yatham, V. R.; Crespi, S.; König, B., Cesium Carbonate Catalyzed Oxa-Michael Addition of Oximes to Acrylonitrile. *ChemistrySelect* **2021**, *6*, 4107-4111.
53. Azenha, M. E.; Burrows, H. D.; Fonseca, S. M.; Ramos, M. L.; Rovisco, J.; de Melo, J. S.; Sobral, A. J. F. N.; Kogej, K., Luminescence from Cerium(III) Acetate Complexes in Aqueous Solution: Considerations on the Nature of Carboxylate Binding to Trivalent Lanthanides. *New J. Chem.* **2008**, *32*, 1531-1535.
54. Yin, H.; Jin, Y.; Hertzog, J. E.; Mullane, K. C.; Carroll, P. J.; Manor, B. C.; Anna, J. M.; Schelter, E. J., The Hexachloroacetate(III) Anion: A Potent, Benchtop Stable, and Readily Available Ultraviolet A Photosensitizer for Aryl Chlorides. *J. Am. Chem. Soc.* **2016**, *138*, 16266-16273.
55. Gonzalez-de-Castro, A.; Robertson, C. M.; Xiao, J., Dehydrogenative α -Oxygenation of Ethers with an Iron Catalyst. *J. Am. Chem. Soc.* **2014**, *136*, 8350-8360.
56. Liao, Y.; Zhou, Y.; Zhang, Z.; Fan, J.; Liu, F.; Shi, Z., Intramolecular Oxidative Coupling between Unactivated Aliphatic C-H and Aryl C-H Bonds. *Org. Lett.* **2021**, *23*, 1251-1257.
57. Bachmann, J. P., α -Branched Silkenoic Scids and the Use of α -Branched Alkanoic and Alkenoic Acids as a Fragrance. *U.S. Patent No. 9,745,245*. **2017**.
58. Sasano, Y.; Nagasawa, S.; Yamazaki, M.; Shibuya, M.; Park, J.; Iwabuchi, Y., Highly Chemoselective Aerobic Oxidation of Amino Alcohols into Amino Carbonyl Compounds. *Angew. Chem. Int. Ed.* **2014**, *53*, 3236-3240.
59. Kancharla, P.; Lu, W.; Salem, S. M.; Kelly, J. X.; Reynolds, K. A., Stereospecific Synthesis of 23-Hydroxyundecylprodiginines and Analogues and Conversion to Antimalarial Premarinesosins via a Rieske Oxygenase Catalyzed Bicyclization. *J. Org. Chem.* **2014**, *79*, 11674-11689.
60. Chai, K. B.; Sampson, P., A Convenient and Efficient Three-Step Synthesis of α -Chloro Keto Acids. *Tetrahedron Lett.* **1992**, *33*, 585-588.
61. Cravotto, G.; Calcio Gaudino, E.; Barge, A.; Binello, A.; Albertino, A.; Aghemo, C., Synthesis of 1-Octacosanol and GC-C-IRMS Discrimination of Samples from Different Origin. *Nat. Prod. Res.* **2010**, *24*, 428-439.
62. O, E. A., Nicoletta; S, Laura, Preparation of Quinone Based Nitric Oxide Donating Compounds for Ophthalmic Use. *World Intellectual Property Organization, WO2014063923 A1*. **2014**.
63. Barraud, N., Kumar, Naresh, Kutty, Samuel Kunjunju, Rice, Scott., Preparation of Dual Action Nitric Oxide Donors and Their Use as Antimicrobial Agents. *World Intellectual Property Organization, WO2014071457 A1*. **2014**.

64. Brossard, D.; Lechevrel, M.; El Kihel, L.; Quesnelle, C.; Khalid, M.; Moslemi, S.; Reimund, J. M., Synthesis and Biological Evaluation of Bile Carboxamide Derivatives with Pro-Apoptotic Effect on Human Colon Adenocarcinoma Cell Lines. *Eur. J. Med. Chem.* **2014**, *86*, 279-290.
65. Kim, S.; Kim, I. H.; Akoh, C. C.; Kim, B. H., Enzymatic Production of Cocoa Butter Equivalents High in 1-Palmitoyl-2-Oleoyl-3-Stearin in Continuous Packed Bed Reactors. *J. Am. Oil Chem. Soc.* **2014**, *91*, 747-757.
66. Wang, Y.; Huang, Z.; Leng, X.; Zhu, H.; Liu, G.; Huang, Z., Transfer Hydrogenation of Alkenes Using Ethanol Catalyzed by a NCP Pincer Iridium Complex: Scope and Mechanism. *J. Am. Chem. Soc.* **2018**, *140*, 4417-4429.
67. Sugamoto, K.; Matsushita, Y. i.; Matsui, T., Direct Hydroperoxygenation of Conjugated Olefins Catalyzed by Cobalt(II) Porphyrin. *J. Chem. Soc. Perkin Trans.* **1998**, *23*, 3989-3998.
68. Kyasa, S.; Meier, R. N.; Pardini, R. A.; Truttman, T. K.; Kuwata, K. T.; Dussault, P. H., Synthesis of Ethers via Reaction of Carbanions and Monoperoxyacetals. *J. Or.g Chem.* **2015**, *80*, 12100-12214.
69. Wang, Y.; Li, P.; Wang, J.; Liu, Z.; Wang, Y.; Lu, Y.; Liu, Y.; Duan, L.; Li, W.; Sarina, S.; Zhu, H.; Liu, J., Visible-Light Photocatalytic Selective Oxidation of C(sp³)-H Bonds by Anion-Cation Dual-Metal-Site Nanoscale Localized Carbon Nitride. *Catal. Sci.Technol.* **2021**, *11*, 4429-4438.
70. Cui, T.; Ma, L.; Wang, S.; Ye, C.; Liang, X.; Zhang, Z.; Meng, G.; Zheng, L.; Hu, H. S.; Zhang, J.; Duan, H.; Wang, D.; Li, Y., Atomically Dispersed Pt-N₃C₁ Sites Enabling Efficient and Selective Electrocatalytic C-C Bond Cleavage in Lignin Models under Ambient Conditions. *J. Am. Chem. Soc.* **2021**, *143*, 9429-9439.
71. Meng, S. S.; Lin, L. R.; Luo, X.; Lv, H. J.; Zhao, J. L.; Chan, A. S. C., Aerobic Oxidation of Alcohols with Air Catalyzed by Decacarbonyldimanganese. *Green Chem.* **2019**, *21*, 6187-6193.
72. Uyanik, M.; Fukatsu, R.; Ishihara, K., Bromine-Catalyzed Aerobic Oxidation of Alcohols. *Chem. Asian J.* **2010**, *5*, 456-460.
73. Chen, J.; Wang, X.; Zheng, X.; Ding, J.; Liu, M.; Wu, H., Ligand-Free Copper-Catalyzed *O*-Arylation of Nitroarenes with Phenols. *Tetrahedron* **2012**, *68*, 8905-8907.
74. Gennari, C.; Ceccarelli, S.; Piarulli, U.; Aboutayab, K.; Donghi, M.; Paterson, I., Stereocontrolled Synthesis of Polyketide Libraries: Boron-Mediated Aldol Reactions with Aldehydes on Solid Support. *Tetrahedron* **1998**, *54*, 14999-15016.

75. Uygur, M.; Kuhlmann, J. H.; Pérez-Aguilar, M. C.; Piekarski, D. G.; García Mancheño, O., Metal- and Additive-Free C-H Oxygenation of Alkylarenes by Visible-Light Photoredox Catalysis. *Green Chem.* **2021**, *23*, 3392-3399.
76. Behera, P. K.; Choudhury, P.; Sahu, S. K.; Sahu, R. R.; Harvat, A. N.; McNulty, C.; Stitgen, A.; Scanlon, J.; Kar, M.; Rout, L., Oxygen Bridged Bimetallic CuMoO₄ Nanocatalyst for Benzylic Alcohol Oxidation; Mechanism and DFT Study. *Asian J. Org. Chem.* **2021**, *10*, 1117-1122.
77. Dharpure, P. D.; Bhowmick, A.; Warghude, P. K.; Bhat, R. G., Visible-Light Mediated Facile Dithiane Deprotection under Metal Free Conditions. *Tetrahedron Lett.* **2020**, *61*, 151407.
78. Li, Z.; Chu, J.; Meng, D.; Wen, Y.; Xing, X.; Miao, H.; Hu, M.; Yu, C.; Wei, Z.; Yang, Y.; Li, Y., Photocatalytic Chemical CO₂ Fixation by Cu-BDC Nanosheet@Macroporous–Mesoporous-TiO₂ under Mild Conditions. *ACS Catal.* **2019**, *9*, 8659-8668.
79. Humphries, P. S.; Bersot, R.; Kincaid, J.; Mabery, E.; McCluskie, K.; Park, T.; Renner, T.; Riegler, E.; Steinfeld, T.; Turtle, E. D.; Wei, Z. L.; Willis, E., Carbazole-Containing Amides and Ureas: Discovery of Cryptochrome Modulators as Antihyperglycemic Agents. *Bioorg. Med. Chem. Lett.* **2018**, *28*, 293-297.
80. Gangadurai, C.; Illa, G. T.; Reddy, D. S., FeCl₃-Catalyzed Oxidative Decarboxylation of Aryl/Heteroaryl Acetic Acids: Preparation of Selected API Impurities. *Org. Biomol. Chem.* **2020**, *18*, 8459-8466.
81. Kawai, N.; Kato, N.; Hamada, Y.; Shioiri, T., New Methods and Reagents in Organic Synthesis. 35. A New Synthesis of Some Non-Steroidal Anti-Inflammatory Agents with the 2-Arylpropionic Acid Skeleton by the Use of Diphenyl Phosphorazidate (DPPA) as a 1,3-Dipole. *Chem. Pharma. Bull.* **1983**, *31*, 3139-3148.
82. Ge, L.; Wang, D. X.; Xing, R.; Ma, D.; Walsh, P. J.; Feng, C., Photoredox-Catalyzed Oxo-Amination of Aryl Cyclopropanes. *Nat. Commun.* **2019**, *10*, 4367.
83. Al-Dulayymi, J. a. R.; Baird, M. S.; Mohammed, H.; Roberts, E.; Clegg, W., The Synthesis of One Enantiomer of the α -Methyl-*trans*-Cyclopropane Unit of Mycolic Acids. *Tetrahedron* **2006**, *62*, 4851-4862.
84. Ohta, T.; Kamiya, M.; Nobutomo, M.; Kusui, K.; Furukawa, I., Reduction of Carboxylic Acid Derivatives Using Diphenylsilane in the Presence of a Rh–PPh₃ Complex. *Bull. Chem. Soc. Jpn.* **2005**, *78*, 1856-1861.

85. Zhang, J.; Li, Y.; Zhang, F.; Hu, C.; Chen, Y., Generation of Alkoxy Radicals by Photoredox Catalysis Enables Selective C(sp³)-H Functionalization under Mild Reaction Conditions. *Angew. Chem. Int. Ed.* **2016**, *55*, 1872-1875.
86. Saes, B. W. H.; Wienk, M. M.; Janssen, R. A. J., The Effect of α -Branched Side Chains on the Structural and Opto-Electronic Properties of Poly(Diketopyrrolopyrrole-*alt*-Terthiophene). *Chemistry* **2020**, *26*, 14221-14228.
87. Puls, F.; Linke, P.; Kataeva, O.; Knolker, H. J., Iron-Catalyzed Wacker-type Oxidation of Olefins at Room Temperature with 1,3-Diketones or Neocuproine as Ligands*. *Angew. Chem. Int. Ed.* **2021**, *60*, 14083-14090.
88. Sytniczuk, A.; Forcher, G.; Grotjahn, D. B.; Grela, K., Sequential Alkene Isomerization and Ring-Closing Metathesis in Production of Macrocyclic Musks from Biomass. *Chemistry* **2018**, *24*, 10403-10408.
89. Subba Reddy, B. V.; Anusha, B.; Subba Reddy, U. V.; Yadav, J. S.; Suresh Reddy, C., A Concise and Convergent Total Synthesis of Two Novel Cytotoxic Hydroquinones, Lannequinol and (*R*)-2'-Hydroxylannequinol. *Helv. Chim. Acta* **2013**, *96*, 1983-1990.
90. Takai, K.; Takagi, T.; Baba, T.; Kanamori, T., Highly Fluorinated C₁₈ Fatty Acids: Synthesis and Interfacial Properties. *J. Fluor. Chem.* **2004**, *125*, 1959-1964.
91. Das, B.; Srinivas, K. V.; Mahender, I., Selective Monoacetylation of Symmetrical Diols and Selective Monode-Acetylation of Symmetrical Diacetates Using HY-Zeolite as Reusable Heterogeneous Catalyst. *Synlett* **2003**, *15*, 2419-2421.
92. Yoshino, H.; Matsumoto, K.; Hagiwara, R.; Ito, Y.; Oshima, K.; Matsubara, S., Fluorination with Ionic Liquid EMIMF(HF)_{2.3} as Mild HF Source. *J. Fluor. Chem.* **2006**, *127*, 29-35.
93. Garvey, D. S., Letts, L.G., Earl, R.A., Ezawa, M., Fang, X., Gaston, R.D., Khanapure, S.P., Lin, C.E., Ranatunge, R.R., Stevenson, C.A. and Wey, S.J., Nitric Oxide Enhancing Diuretic Compounds, Compositions and Methods of Use. *U.S. Patent 7,396,829*. **2008**.
94. Bodnar, B. S.; Vogt, P. F., An Improved Bouveault-Blanc Ester Reduction with Stabilized Alkali Metals. *J. Org. Chem.* **2009**, *74*, 2598-2600.
95. Geurink, P. P.; Klein, T.; Prèly, L.; Paal, K.; Leeuwenburgh, M. A.; van der Marel, G. A.; Kauffman, H. F.; Overkleeft, H. S.; Bischoff, R., Design of Peptide Hydroxamate-Based Photoreactive Activity-Based Probes of Zinc-Dependent Metalloproteases. *Eur. J. Org. Chem.* **2010**, *2010*, 2100-2112.

Chapter 4

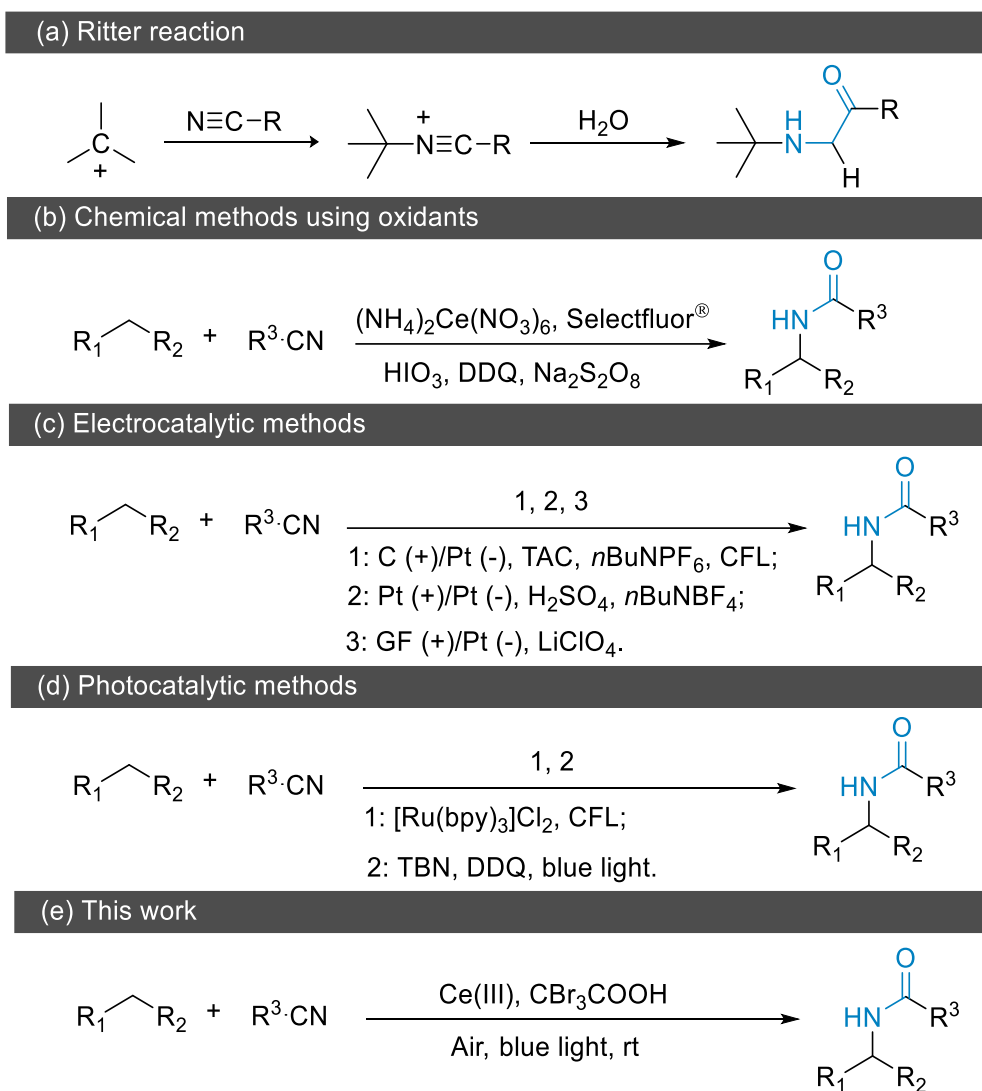
Photocatalytic Ritter-Type Benzylic C-H Amidation of Alkylarenes

4.1 Introduction

The amide functionality is one of the most important building blocks in nature. It not only plays an important role in constituting the backbone of proteins but also is present in a large amount of pharmacological active compounds and materials.¹⁻² One of the most convenient methods for synthesizing amides is condensation of a carboxylic acid and an amine. However, the harsh conditions, limited substrate scope and the formation of byproducts restrict the preparative value of this process.³ Therefore, tremendous efforts have been made by chemists to synthesize functionalised amides. A variety of strategies for synthesis of amides have been developed, using starting materials such as alcohols, alkenes, nitriles, aldehydes and aryl halides.³⁻⁴ Among them, the Ritter reaction has received wide attention, which enables the formation of amides by the electrophilic addition of a carbocations to a nitrile followed by hydrolyzation (Scheme 4.1a). It provides a rapid and efficient method for the preparation of sterically hindered amides using alcohols and alkenes as starting materials.⁵⁻⁷

Functionalization of saturated hydrocarbons via C-H activation is an interesting and challenging issue for chemists. Inspired by Ritter reaction, the catalytic Ritter-type reaction via C-H activation has been proposed. It allows the selective synthesis of amides from non-functionalized alkanes, with the carbocation intermediate generated from C(sp³)-H bond oxidation.⁸ However, Ritter-type C(sp³)-H amidation of hydrocarbons is a challenging reaction, though it has attracted wide attentions in recent years. Most reported methods often rely on the use of stoichiometric amounts of oxidants, such as (NH₄)₂Ce(NO₃)₆,⁹ Selectfluor[®],¹⁰ HIO₃,¹¹ DDQ,¹² and Na₂S₂O₈ (Scheme 4.1b).¹³ These oxidants lead to a limited substrate scope due to

incompatible functional groups. Meanwhile, high temperature and formation of unwanted by-products also restrict the application of these methods.¹⁰⁻¹¹



Scheme 4.1 Ritter type C-H amidation of hydrocarbons.

Recently, electrochemistry and photochemistry have been introduced in Ritter-type reaction in seeking more applicable strategies. The construction of C-N bonds via electrochemical oxidative C(sp³)-H functionalization has been reported by the Lambert group and Ye group. Lambert and co-workers employed trisaminocyclopropenium (TAC) ion as the mediator in electrophotocatalytic Ritter-type C-H amidation of alkylarenes with acetonitrile.¹⁴ A wide range of alkylarenes with benzylic sites can be transformed to corresponding amides in moderate to good yields. The TAC radical dication or anode led to the formation of carbon

cation for classic Ritter steps. Although good results have been obtained in their work, their strategy suffers the limit nitrile scope and the requirement of acetonitrile as solvent.

Subsequently, Ye and co-workers employed sulfate radical anion as hydrogen atom transfer agent in Ritter-type amidation of C(sp³)-H bonds.¹⁵ A wide substrate scope, including benzylic alkylarenes and alkanes, and good functional tolerance were observed in their work. The scope of nitriles also has been explored. Several alkyl nitriles were tolerated in their strategy. The carbon cation was formed by a sulfate radical anion-mediated hydrogen atom transfer process. A following work reported by Sun and co-workers realized benzylic C-H amidation without the addition of external mediator and oxidant (Scheme 4.1c).¹⁶

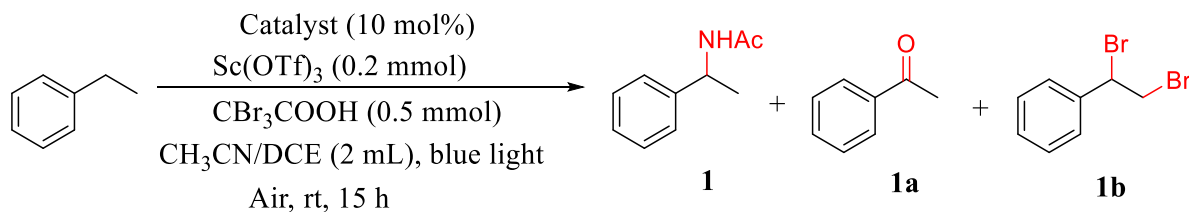
On the other hand, two reports have demonstrated the C-H amidation via photochemistry (Scheme 4.1d). Ritter-type amidation of benzylic sites and tertiary carbon was reported by Chen and co-workers, where an expensive Ru catalyst and toxic hypervalent iodine(III) reagents were required.¹⁷ Shen and co-workers firstly realized the aerobic photocatalytic C-H amidation of diarylmethanes using O₂ as terminal oxidant. The carbon cation was formed by a hydrogen atom transfer reaction and subsequent single electron transfer between DDQ and diarylmethanes. However, their strategy is only applicable to diarylmethanes.⁸

Considering the high efficiency of Ce(III) catalysts in C-H functionalization of carboxylic acids, we examined Ce(III) catalysts in the functionalization of alkylarenes. In this chapter, we report a photocatalytic method that enables the benzylic C(sp³)-H amidation via a simple, cheap Ce(III) iodide as catalyst and CBr₃COOH as the bromide source to access carbon cation. A variety of nitriles are tolerated in the C-H amidation, with a few equivalents of a nitrile being feasible. Note most previous work suffers from the limited nitrile scope or the requirement of nitriles as solvent.

4.2 Results and Discussion

4.2.1 Optimization experiments

Table 4.1 Optimization of photocatalytic C-H amidation of ethylbenzene^{a,b}



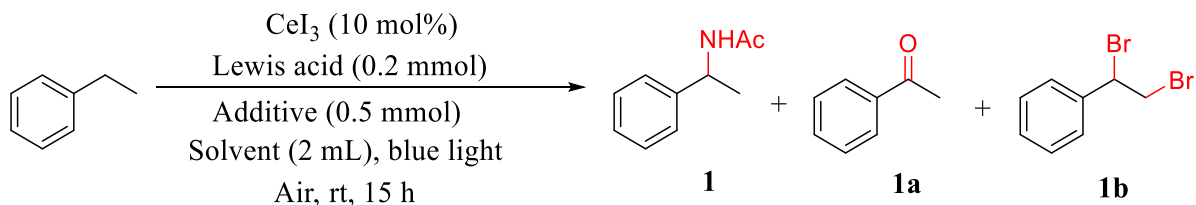
Entry	Catalyst	Lewis acid	Additive	Yield (%)		
				1	1a	1b
1	CeI ₃	Sc(OTf) ₃	CBr ₃ COOH	70	5	5
2	CeI ₃	Sc(OTf) ₃	/	0	0	0
3	CeI ₃	/	CBr ₃ COOH	47	34	7
4	/	Sc(OTf) ₃	CBr ₃ COOH	0	0	0
5 ^c	CeI ₃	Sc(OTf) ₃	CBr ₃ COOH	0	0	0
6 ^d	CeI ₃	Sc(OTf) ₃	CBr ₃ COOH	45	0	10
7	CeCl ₃	Sc(OTf) ₃	CBr ₃ COOH	4	0	1
8	CeBr ₃	Sc(OTf) ₃	CBr ₃ COOH	60	13	0
9	CeF ₃	Sc(OTf) ₃	CBr ₃ COOH	0	0	0
10	Ce(OAc) ₃	Sc(OTf) ₃	CBr ₃ COOH	0	51	10
11	Ce(OTf) ₃	Sc(OTf) ₃	CBr ₃ COOH	0	0	0
12	Ce(OTf) ₄	Sc(OTf) ₃	CBr ₃ COOH	0	0	0
13	CeF ₄	Sc(OTf) ₃	CBr ₃ COOH	0	0	0

^aReaction conditions: ethylbenzene (0.5 mmol), CeI₃ (10 mol%), Lewis acid (0.2 mmol), Additive (0.5 mmol), CH₃CN/DCE (2 mL, 1:1), under air, blue light (465 nm, 9 W), room temperature, 15 h. ^bNMR yields are given, determined using mesitylene (20 μL) as internal standard. ^cReaction in dark. ^dN₂ instead of air.

We started from the finding and optimising conditions for photocatalytic C-H amidation using ethylbenzene as the standard substrate and CH₃CN as the nitrogen source. We envisioned that the addition of Lewis acid may promote the formation of carbon cation. Therefore, different Lewis acids and acid additive were employed. As shown in Table 4.1, 70% of **1** was afforded when CeI₃, Sc(OTf)₃ and CBr₃COOH were employed as catalyst, Lewis acid and additive, respectively (entry 1). A similar yield of **1** was afforded in a mixture of CH₃CN/DCE or in pure CH₃CN (Table 4.1, entry 1 vs Table 4.2, entry 1). Therefore, DCE is a suitable solvent

to replace part of a nitrile, particularly when it is expensive one. We chose the mixture of CH₃CN and DCE as the solvent for further exploration of potential nitrile scope.

Table 4.2 Optimization of photocatalytic C-H amidation of ethylbenzene^{a,b}

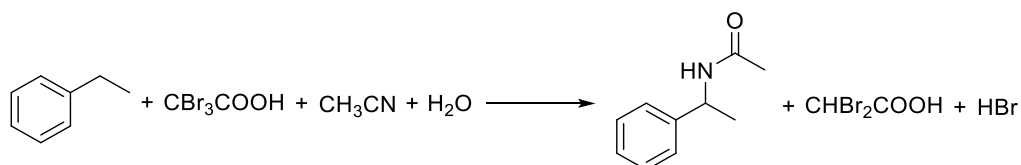


Entry	Solvent	Lewis acid	Additive	Yield (%)		
				1	1a	1b
1	CH ₃ CN	Sc(OTf) ₃	CBr ₃ COOH	70	14	10
2 ^c	Dried CH ₃ CN	Sc(OTf) ₃	CBr ₃ COOH	15	82	0
3 ^d	Dried CH ₃ CN	Sc(OTf) ₃	CBr ₃ COOH	72	12	4
4	CH ₃ CN/EtOAc	Sc(OTf) ₃	CBr ₃ COOH	58	14	13
5	CH ₃ CN/EtOH	Sc(OTf) ₃	CBr ₃ COOH	0	24	0
6	CH ₃ CN/toluene	Sc(OTf) ₃	CBr ₃ COOH	43	0	0
7	CH ₃ CN/diethyl ether	Sc(OTf) ₃	CBr ₃ COOH	50	0	10
8	CH ₃ CN/DCE	Yt(OTf) ₃	CBr ₃ COOH	29	33	33
9	CH ₃ CN/DCE	La(OTf) ₃	CBr ₃ COOH	49	20	25
10	CH ₃ CN/DCE	Sc(OTf) ₃	CCl ₃ COOH	0	0	0
11	CH ₃ CN/DCE	Sc(OTf) ₃	CCl ₂ COOH	0	0	0
12	CH ₃ CN/DCE	Sc(OTf) ₃	CF ₃ COOH	0	0	0

^aReaction conditions: ethylbenzene (0.5 mmol), CeI₃ (10 mol%), Lewis acid (0.2 mmol), additive (0.5 mmol), solvent (2 mL, 1:1), under blue LED light (465 nm, 9 W) at rt under air atmosphere (1 atm) for 15 h; ^bNMR yields are given, determined using mesitylene (20 μL) as internal standard. ^cUnder O₂ atmosphere (1 atm). ^dUnder O₂ atmosphere (1 atm), H₂O (3.6 mmol). Details of CH₃CN, dried CH₃CN and DCE can be seen in Section 4.4.3.

Meanwhile, the replacement of CeI₃ by other Ce catalysts (Table 4.1, entries 7-13), such as CeCl₃, CeF₃, Ce(OAc)₃, Ce(OTf)₃, Ce(OTf)₄, and CeF₄, only led to no or trace of **1**, though 60% yield of **1** was obtained when CeBr₃ was employed. CeI₃, CBr₃COOH and blue light irradiation all are important components for the transformation of ethylbenzene to **1** (Table 4.1, entries 2-5). Also worth noting is that this transformation can happen under N₂ (Table 4.1, entry 6). Then, the screen of different solvents, Lewis acids and additives were conducted (Table 4.2). However, only lower yields of **1** were obtained. It is worth noting that the employment of

dried CH₃CN only led to 15% yield of **1** (Table 4.2, entry 2). With the addition of H₂O (3.6 mmol) in dried CH₃CN, 72% of **1** was afforded (Table 4.2, entry 2). Therefore, H₂O contained in commercial CH₃CN played an important role in the reaction. On the basis of the need for CBr₃COOH and H₂O, the amidation reaction could be expressed by the equation 4.1 shown below.



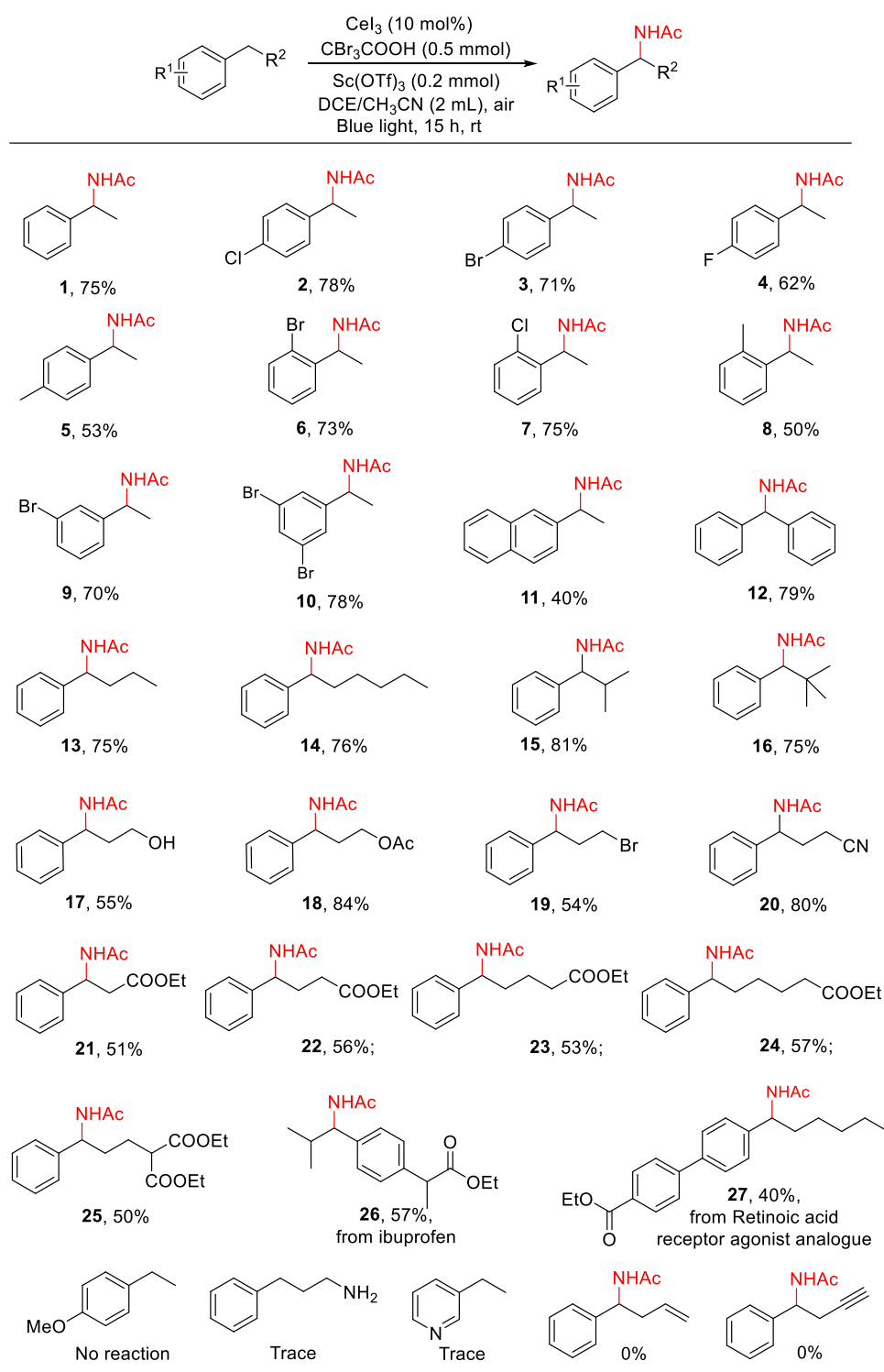
Equation 4.1 A stoichiometric representation of the amidation reaction.

4.2.2 Substrate scope

With these optimum experimental conditions in hand, we investigated the photocatalytic Ritter type C-H amidation of a variety of alkylarenes. Firstly, the scope of ethylbenzenes with a range of functional groups was examined. As shown in Scheme 4.2, ethylbenzenes bearing electron-withdrawing and electron-donating groups proceeded successfully, affording the corresponding amides in good yields (40-78%). All the halogen-substituted ethylbenzene was tolerated (*p*-Cl, *p*-Br, *p*-F, *o*-Br, *o*-Cl and *m*-Br). The position of substitutes may not affect the reaction a lot, as ethylbenzene with Br and Cl groups on different positions afforded the corresponding amides in similar yields (**6-10**). Meanwhile, naphthalene (**11**) and diphenylmethane (**12**) proceeded successfully, affording the corresponding amides in good yields.

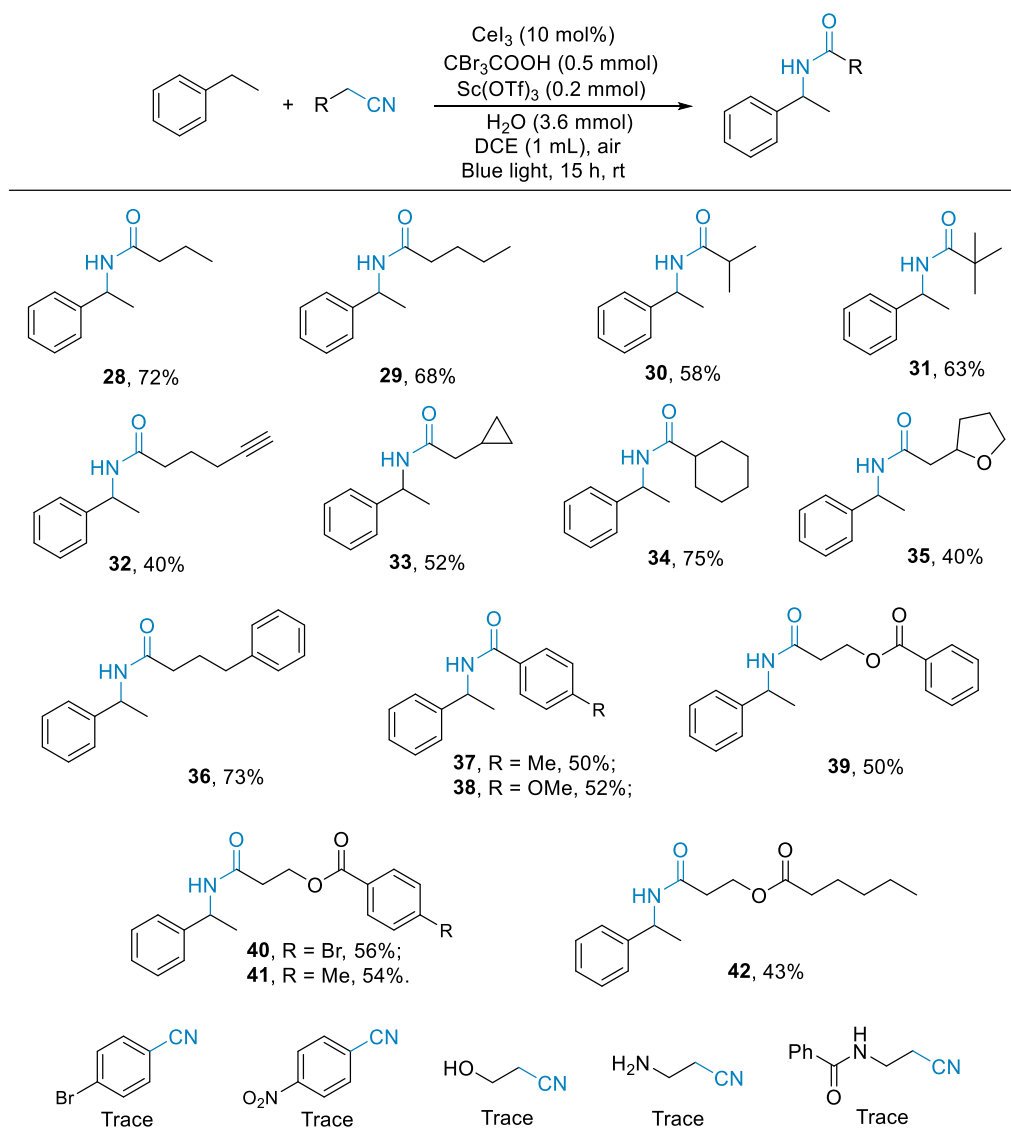
Substrates bearing different alkyl substituents (**13-25**) could also be tolerated. Notably, a range of functional substitutes including alcohol (**17**), ketone (**18**), halide (**19**), nitrile (**20**) and ester (**21-25**) survived the C-H amidation procedure, demonstrating the good functional compatibility of the protocol. For those esters (**22-25**), the length of carbon chain may not affect the C-H amidation due to similar yields of corresponding amide products being obtained. In

addition, the drug molecule ibuprofen (**26**) and retinoic acid receptor agonist analogue (**27**) were also tolerated in the reaction, giving the corresponding amide in good yields.



Scheme 4.2 Photocatalytic Ritter-type C-H amidation of benzylic C-H bonds.^{a,b} ^aReaction conditions: substrate (0.5 mmol), CeI₃ (10 mol%), CBr₃COOH (0.5 mmol), Sc(OTf)₃ (0.2 mmol), DCE/CH₃CN (2 mL, 1:1), blue light (465 nm, 9 W), air, room temperature, 15 h. ^bIsolated yields are given.

On the other hand, some limitations of the substrate scope were observed. The more electron-donating methoxy-substituted ethylbenzene and amino-substituted ethylbenzene, showed almost no reactivity in the reaction. Similarly, 3-ethylpyridine proceeded unsuccessfully. For substrates bearing C=C and C≡C bonds, no amide products were formed. Cleavage of the C=C and C≡C bonds was observed in the reaction.



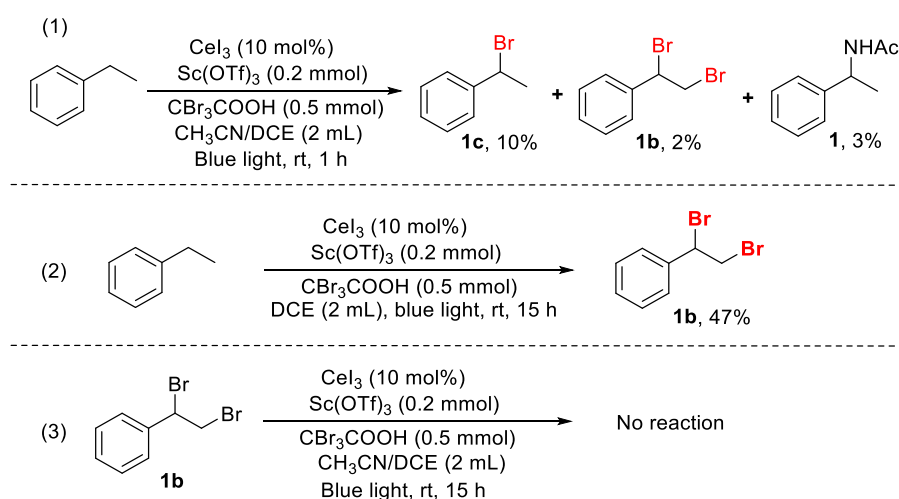
Scheme 4.3 Photocatalytic Ritter-type C-H amidation of ethylbenzene with different nitrile source.^{a,b}

^aReaction conditions: ethylbenzene (0.5 mmol), nitrile (2 mmol), CeI_3 (10 mol%), CBr_3COOH (0.5 mmol), $\text{Sc}(\text{OTf})_3$ (0.2 mmol), DCE (1 mL), H_2O (3.6 mmol), blue light (465 nm, 9 W), air, room temperature, 15 h. ^bIsolated yields are given.

We also examined the scope of nitriles to further demonstrate the generality of our strategy. A wide range of aromatic and aliphatic nitriles (**28-42**) underwent C-H amidation of

ethylbenzene to afford corresponding amides in moderate to good yields (40-72%). As shown in Scheme 4.3, good functional group compatibility was observed, as isopropyl (**30**), *tert*-butyl (**31**), alkynyl (**32**), cycle (**33-34**) and heterocycle (**35**) were tolerated in the reaction. Meanwhile, aromatic nitriles bearing electron-donating groups (**37-38**) worked well, whereas those bearing electron-withdrawing groups, such as bromo and nitro, showed almost no reactivity, presumably due to reduced nucleophilicity of the nitrile. Moreover, nitriles bearing ester (**39-42**) groups also proceeded well to afford corresponding amides. However, some functionalized aliphatic nitriles, such as 3-hydroxypropanenitrile, 3-aminopropanenitrile and *N*-(2-cyanoethyl)benzamide, only afforded trace of products.

4.2.3 Exploration of possible mechanism



Scheme 4.4 Formation and reaction of bromide intermediates. NMR yields are given, determined using mesitylene (20 μL) as internal standard.

We have performed a series of experiments to explore the possible mechanism of this benzylic Ritter-type C-H amidation. Ethylbenzene was used as the standard substrate. Firstly, some intermediates were detected in the reaction. As shown in Scheme 4.4 (Eq. 1), apart from the amide product **1**, two bromide species, (1-bromoethyl)benzene (**1c**) and (1,2-dibromoethyl)benzene (**1b**), were detected. To confirm the formation of **1b** and **1c** in the reaction, the ^1H NMR spectrum of purified **1b** and **1c** was collected (Figure 4.1). The peaks of

1b were observed at around δ 5.15 (dd, $J = 10.6, 5.5$ Hz, 1H) and δ 4.11-4.00 (m, 2H), while those of **1c** were detected at around δ 5.23 (q, $J = 6.9$ Hz, 1H) and δ 2.06 (d, $J = 6.9$ Hz, 3H).

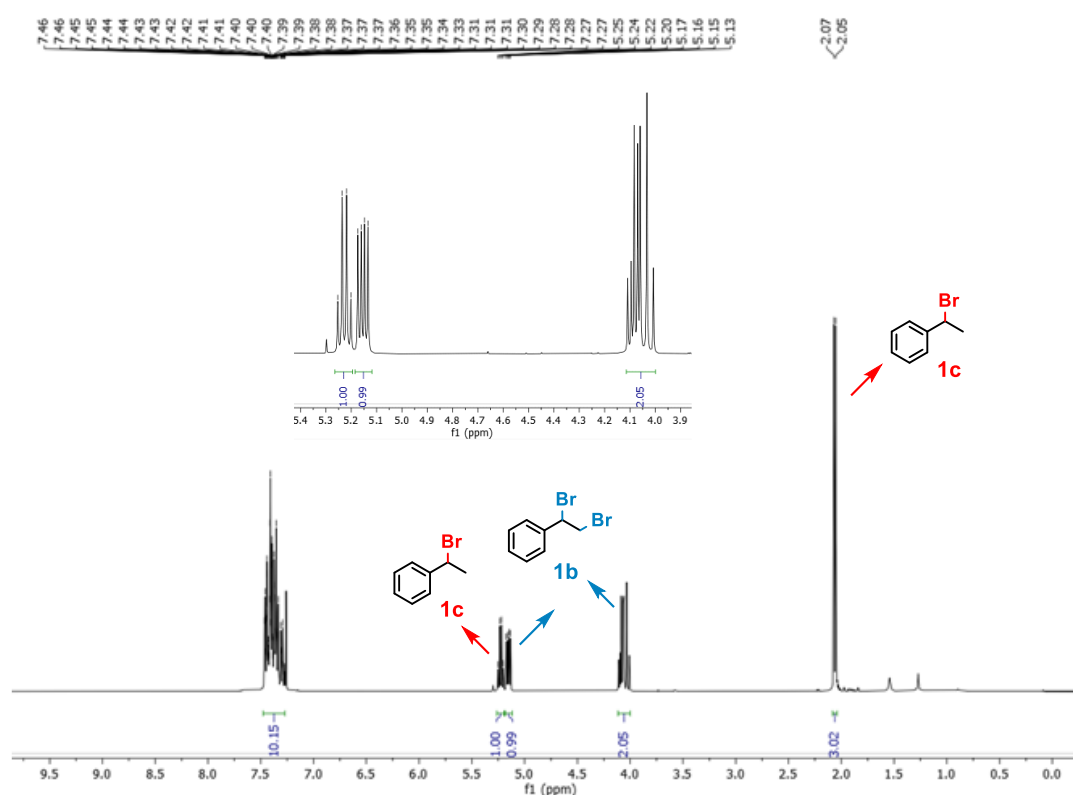


Figure 4.1 ¹H NMR spectrum of purified bromide species. Conditions: CeI₃ (10 mol%), Sc(OTf)₃, CBr₃COOH (0.5mmol), CH₃CN/DCE (2 mL), blue light, rt, 8 h. Four batches of reactions were conducted at the same time. After reaction, these batches were mixed together and then purified by silica gel column chromatography to afford bromide species.

Some control experiments were conducted. As shown in Scheme 4.4 (Eq. 2), without the addition of CH₃CN, only **1b** was formed as the final product. Moreover, **1b** cannot be further transformed under the standard conditions (Scheme 4.4, Eq. 3). More insight can be found in the kinetic study of C-H amidation of ethylbenzene. As presented in Figure 4.2, **1**, **1b** and **1c** all were detected in the reaction. **1c** increased in the first 4 h and then it started to decrease, which may indicate the transformation of **1c** to **1** and **1b**. The formation of **1c** was faster than **1** in the first 5 h. These observations indicated the transformation of **1c** to **1**, and the formation of **1** may not be turnover-limited by the benzylic C-H bond cleavage. As well, the slow increase of **1b** was observed, which may indicate the transformation of **1c** to **1b** as byproduct.

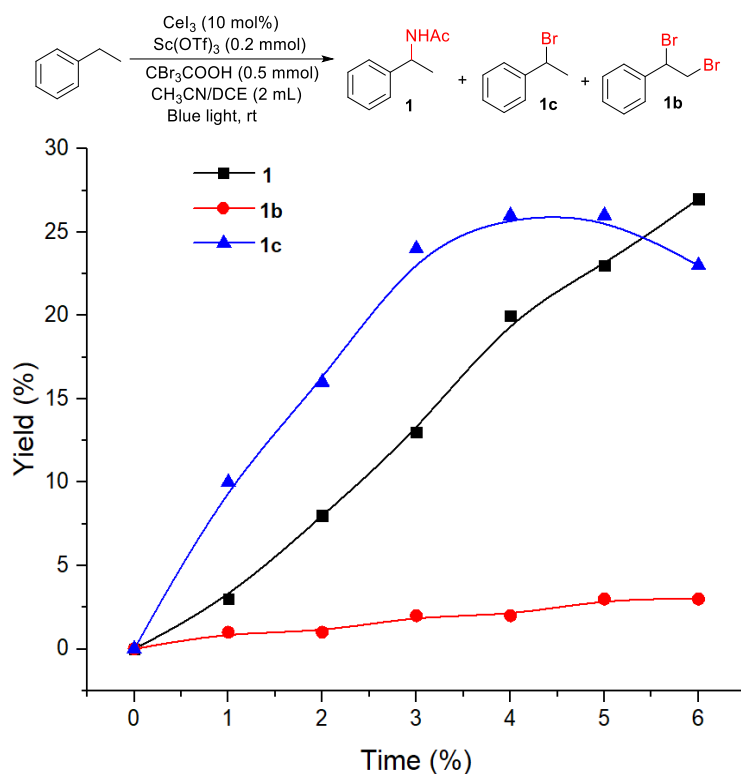


Figure 4.2 Kinetic study of C-H amidation of ethylbenzene. Conditions: CeI_3 (10 mol%), ethylbenzene (0.5 mmol), CBr_3COOH (0.5 mmol), $\text{Sc}(\text{OTf})_3$ (0.2 mmol), 1-bromo-3,5-bis(trifluoromethyl)benzene (0.2 mmol) as internal standard, $\text{CH}_3\text{CN}/\text{DCM}$ (2 mL, 1:1), blue light (465 nm, 9 W), air, room temperature.

CBr_3COOH is the only Br source in the reaction and is involved in the formation of the amides. To gain more evidence, we have performed the HRMS detection. As shown in Figure 4.3, three acid intermediates CHBr_2COOH , CH_2BrCOOH and CH_3COOH , possibly formed by CBr_3COOH , were detected. Based on these results, CBr_3COOH is the Br donor in the reactions, leading to the formation of **1c** as the main intermediate in the Ritter-type reaction with itself being reduced. The possibility of employing CBr_3COOH as the $\cdot\text{Br}$ radical source has been demonstrated by Cui's work.¹⁸ Their DFT calculation results demonstrated the use of CBr_3COOH as halogen reagent in $\text{Mn}(\text{OAc})_3$ -mediated halotrifluoromethylation reactions. To examine this possibility in our reactions, 1,1-diphenylethylene and styrene were employed as the radical trap to capture the potential Br radical species from CBr_3COOH . As shown in Scheme 4.5, both (2-bromoethene-1,1-diyl)dibenzene and **1b** were detected (Detailed NMR data can be seen in section 4.4.3).

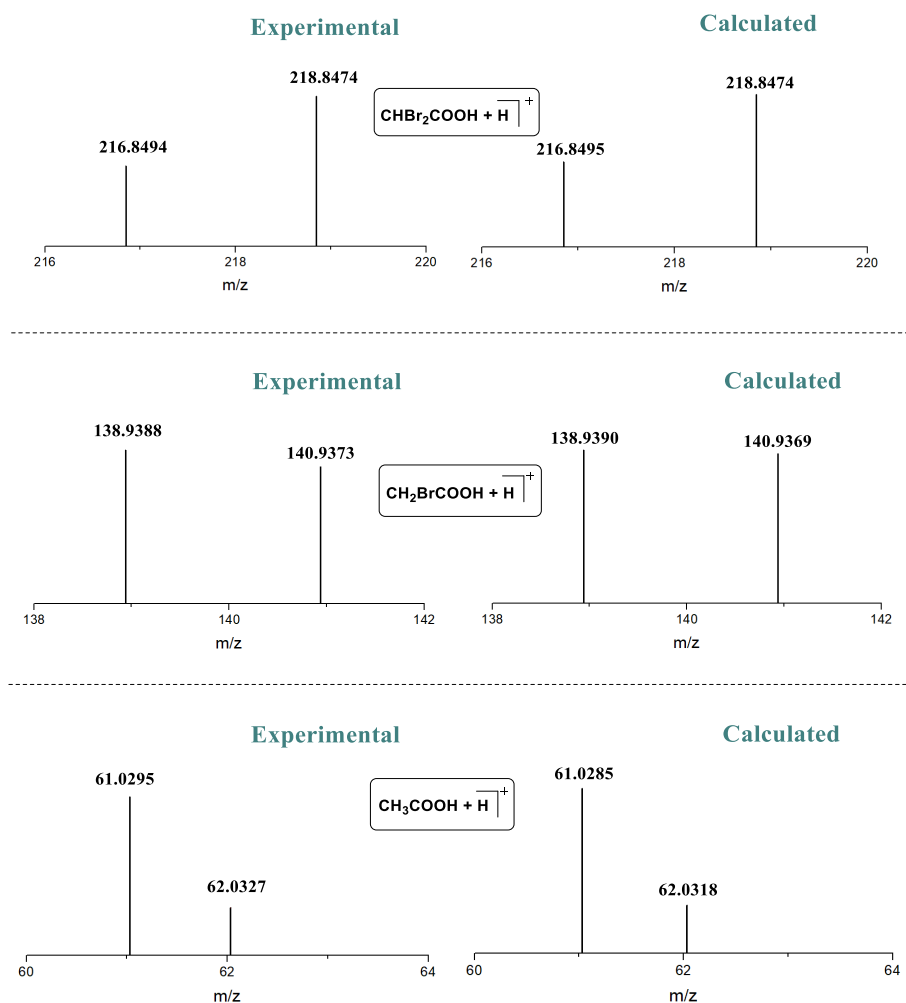
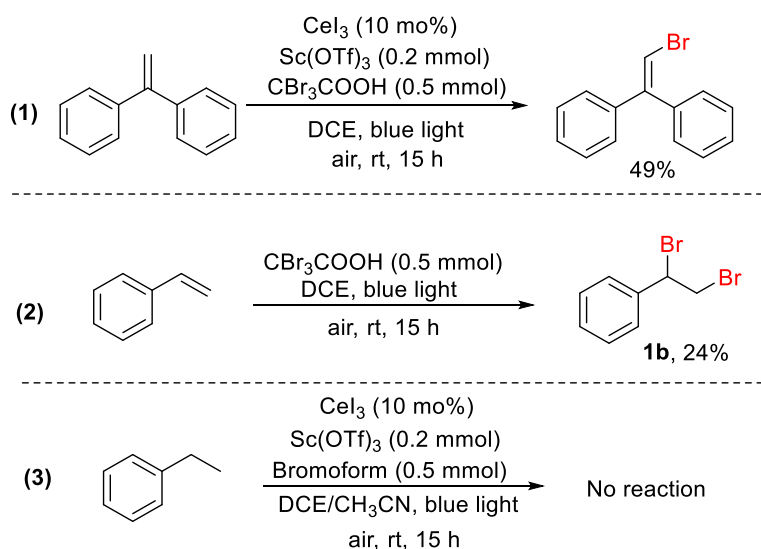
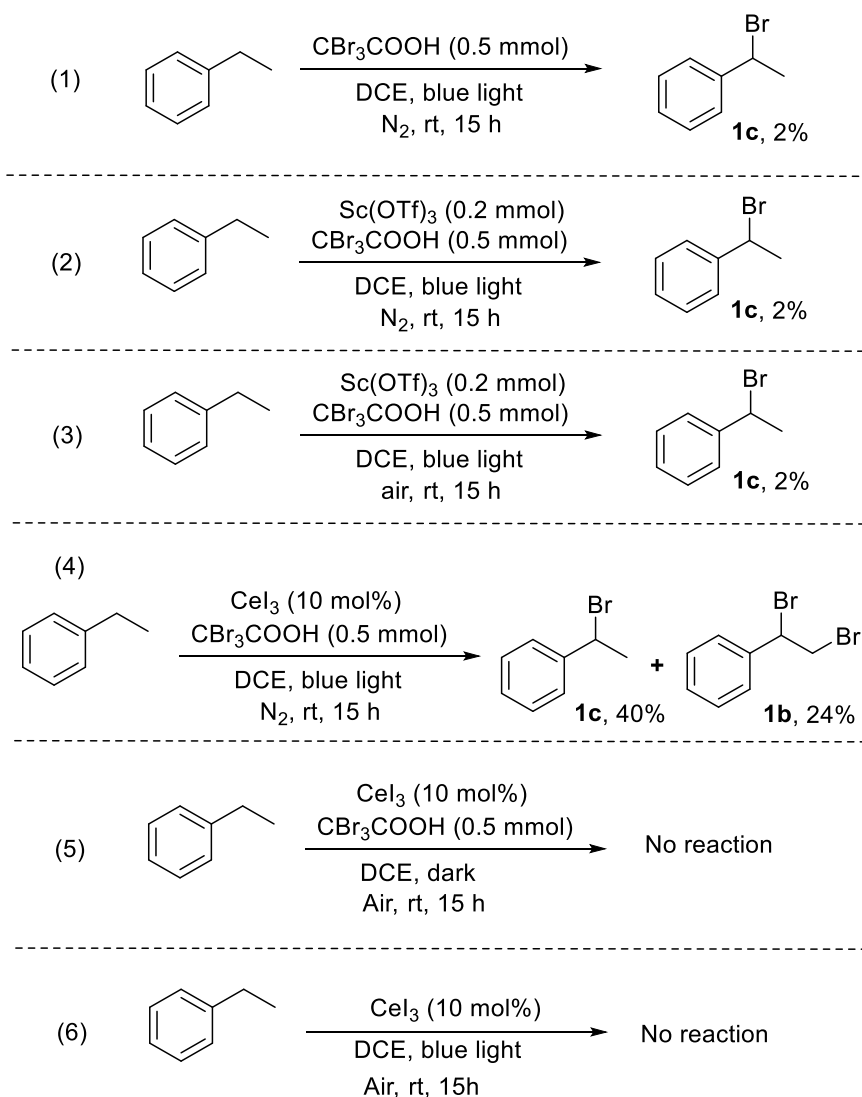


Figure 4.3 HRMS spectra of detected CHBr₂COOH, CH₂BrCOOH and CH₃COOH (m/z value = M + H). Conditions: CeI₃ (10 mol%), ethylbenzene (0.5 mmol), CBr₃COOH (0.5 mmol), Sc(OTf)₃ (0.2 mmol), CH₃CN/DCM (2 mL, 1:1), blue light (465 nm, 9 W), air, room temperature, 2 h.



Scheme 4.5 Exploration of Br radical from CBr₃COOH.

On the other hand, it is possible that decarboxylation of CBr_3COOH to form CBr_3H may happen in the reaction. To test this possibility of CBr_3COOH participating in the reaction, bromoform was employed to replace CBr_3COOH . As shown in Scheme 4.5 (Eq. 3), no reaction happened. This result can partly rule out the possibility of CBr_3H as the bromide source in the reaction.



Scheme 4.6 Control experiments to detect **1c** intermediate. NMR yields are given, determined using mesitylene (20 μL) as internal standard.

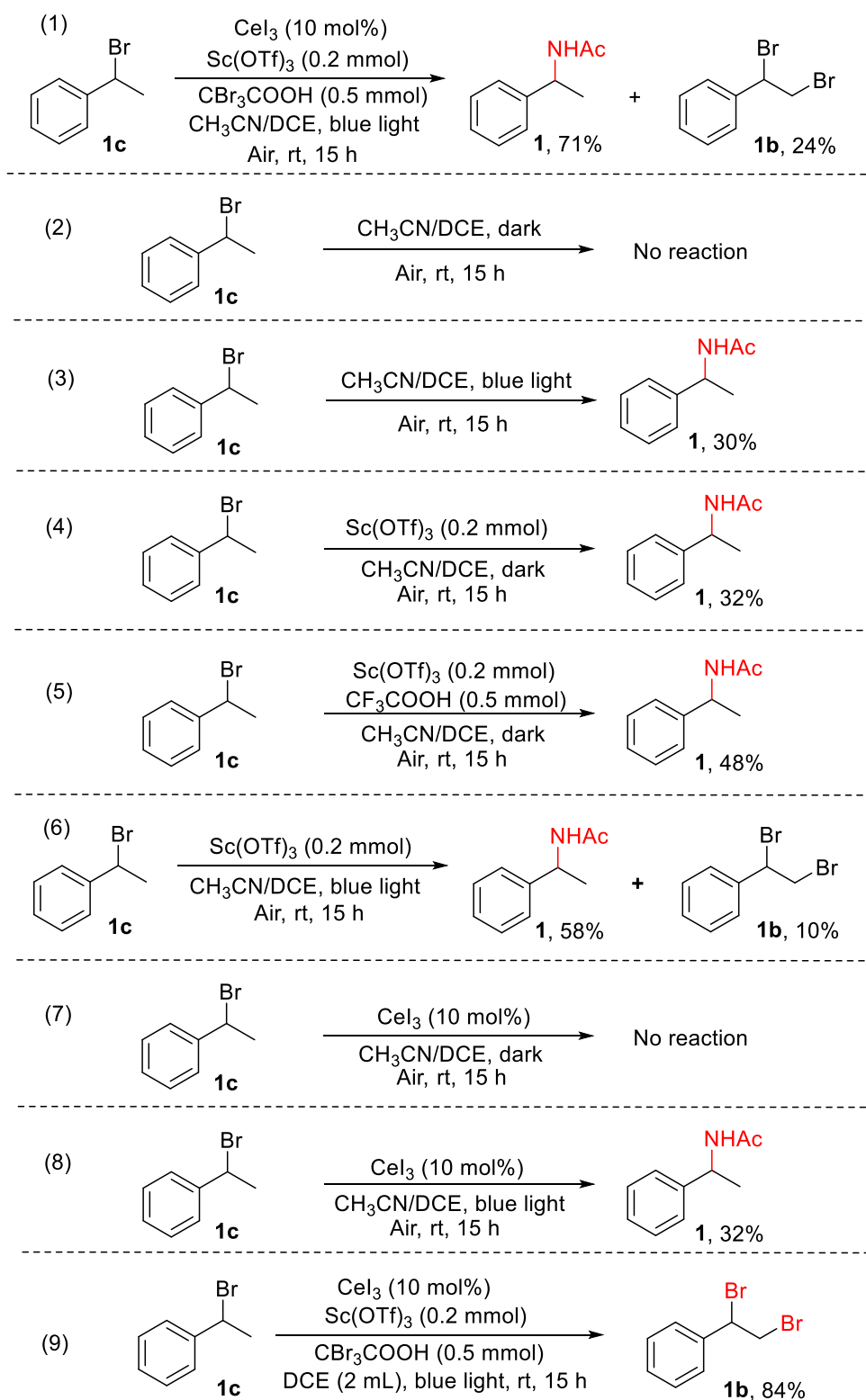
It is important to figure out the key conditions for the formation of **1c** intermediate in the reactions. As shown in Scheme 4.6 (Eqs. 1-3), only a trace of **1c** was detected, indicating the necessity of CeI_3 . Bromide products **1b** and **1c** can be formed without air (Scheme 4.6, Eq. 4), which is in line with the previous result in Table 4.1 (entry 6). As well, no products can be seen

without light or CBr_3COOH (Scheme 4.6, Eqs. 5-6). Therefore, the participation of CeI_3 , CBr_3COOH and light all are required for the formation of **1c** intermediate.

A similar yield of **1** was observed when **1c** was employed as the substrate under standard conditions (Scheme 4.7, Eq. 1). No transformation of **1c** was detected without $\text{Sc}(\text{OTf})_3$ and light irradiation (Scheme 4.7, Eq. 2), whereas around 30% yield of **1** was observed with the employment of $\text{Sc}(\text{OTf})_3$ in the dark or blue light without Lewis acid (Scheme 4.7, Eqs. 3-4). Furthermore, the addition of CF_3COOH and $\text{Sc}(\text{OTf})_3$ led to a higher yield of **1** (Scheme 4.7, Eq. 5). Based on these results, the added $\text{Sc}(\text{OTf})_3$ and CF_3COOH may promote the formation of carbon cation from **1c**. Heterolysis of C-Br of **1c** may happen under blue light irradiation, affording a carbon cation and a Br^- anion.¹⁹⁻²⁰ Notably, the transformation of **1c** to **1** didn't require the assistance of Ce catalysts (Scheme 4.7, Eqs. 3-5, 7-8). No change of the yields of **1** was observed with the employment of CeI_3 (Scheme 4.7, Eqs. 3 vs 8, 2 vs 7). Meanwhile, **1c** was transformed to **1b** without the addition of CH_3CN (Scheme 4.7, Eq. 9).

Then, UV-Vis analysis of a mixture of CeI_3 and CBr_3COOH was conducted. In Figure 4.4(a), a new peak at around 258 nm can be seen in the spectrum of the mixture of CeI_3 and CBr_3COOH . This result may indicate the coordination of CeI_3 with CBr_3COOH in the reaction. Furthermore, UV-Vis monitoring of the change of CBr_3COOH upon irradiation was conducted. As shown in Figure 4.4(b), the absorption of CBr_3COOH was observed at around 225 nm, which decreased with the extension of irradiation time. Meanwhile, a new peak appeared at around 416 nm and it increased with the extension of irradiation time. Based on previous reports,²¹⁻²² this peak could be assigned to Br_2 formed from $\bullet\text{Br}$ radicals. UV-Vis monitoring of CBr_3COOH under blue light irradiation and N_2 showed a similar spectrum (See Section 4.4.4), which indicated that air is not involved in the cleavage of C-Br bond of CBr_3COOH . Therefore, $\bullet\text{Br}$ radicals may be formed by cleavage of C-Br bond of CBr_3COOH under light irradiation.²³

Based on these results, we envision that the Ce catalyst may play an important role in stabilizing unstable Br species, which may be a crucial step for the formation of **1c**.



Scheme 4.7 Control experiments using **1c** as the standard substrate.

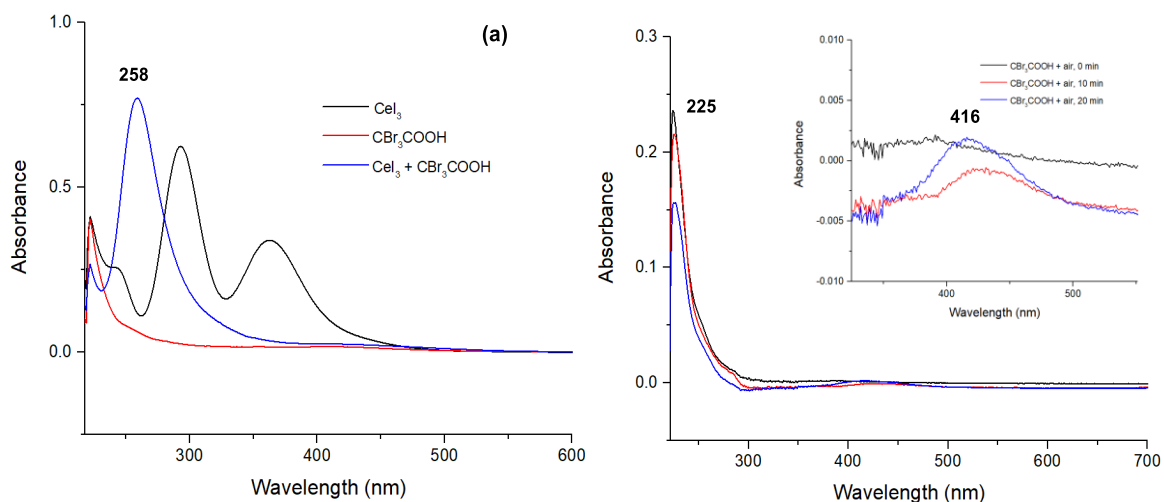


Figure 4.4 (a) UV-Vis analysis of the mixture of CeI_3 and CBr_3COOH . Conditions: CeI_3 (0.05 mmol), CBr_3COOH (0.1 mmol), $\text{CH}_3\text{CN}/\text{DCM}$ (2 mL, 1:1), air; (b) UV-Vis analysis of CBr_3COOH under blue light irradiation. Conditions: CBr_3COOH (0.1 mmol), $\text{CH}_3\text{CN}/\text{DCM}$ (2 mL, 1:1), air, blue light (465 nm).

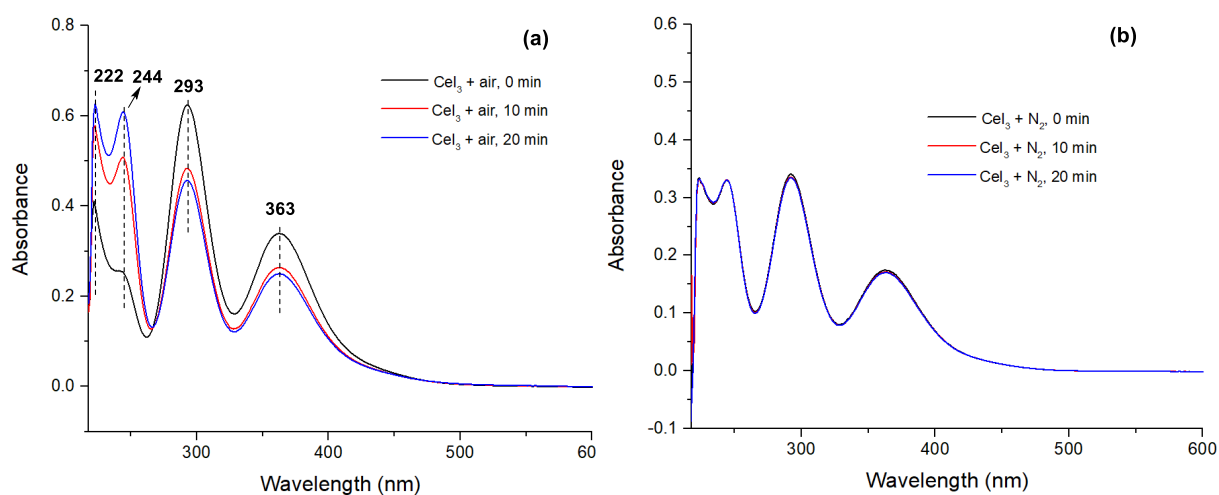


Figure 4.5 UV-Vis analysis of blue light irradiation of CeI_3 under air (a) or N_2 (b). Conditions: CeI_3 (0.05 mmol), $\text{CH}_3\text{CN}/\text{DCM}$ (2 mL, 1:1), air or N_2 , blue light (465 nm).

Then, UV-Vis analysis of CeI_3 under air or N_2 was conducted. In Figure 4.5(a), four peaks at around 222, 244, 293, 363 nm can be observed without blue light irradiation. Under blue light irradiation and air, the peaks at around 293 and 363 nm decreased with the extension of irradiation time, whereas the peaks at around 244 nm increased obviously. Meanwhile, no changes can be observed in the spectra of CeI_3 under N_2 (Figure 4.5(b)). This observation may indicate the transformation of Ce(III) to Ce(IV) species.²⁴ A similar result on the formation of

Ce(IV) species in the selective transformation of carboxylic acids can be seen in our previous work (See Chapter 3.2.3).²⁵

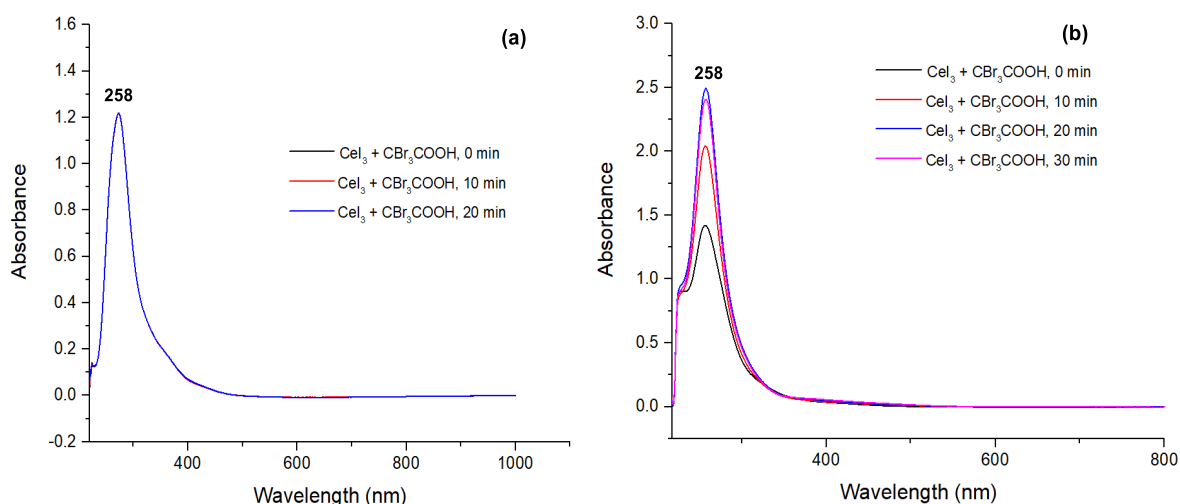
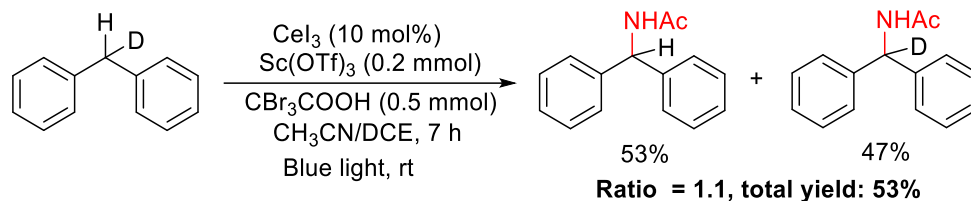


Figure 4.6 (a) UV-Vis analysis of the mixture of CeI_3 and CBr_3COOH (CeI_3 : CBr_3COOH = 1:2) Conditions: CeI_3 (0.05 mmol), CBr_3COOH (0.1 mmol), $\text{CH}_3\text{CN}/\text{DCM}$ (2 mL, 1:1), N_2 , blue light (465 nm); (b) UV-Vis analysis of the mixture of CeI_3 and CBr_3COOH (CeI_3 : CBr_3COOH = 1:10). Conditions: CeI_3 (0.05 mmol), CBr_3COOH (0.5 mmol), $\text{CH}_3\text{CN}/\text{DCM}$ (2 mL, 1:1), N_2 , blue light (465 nm).

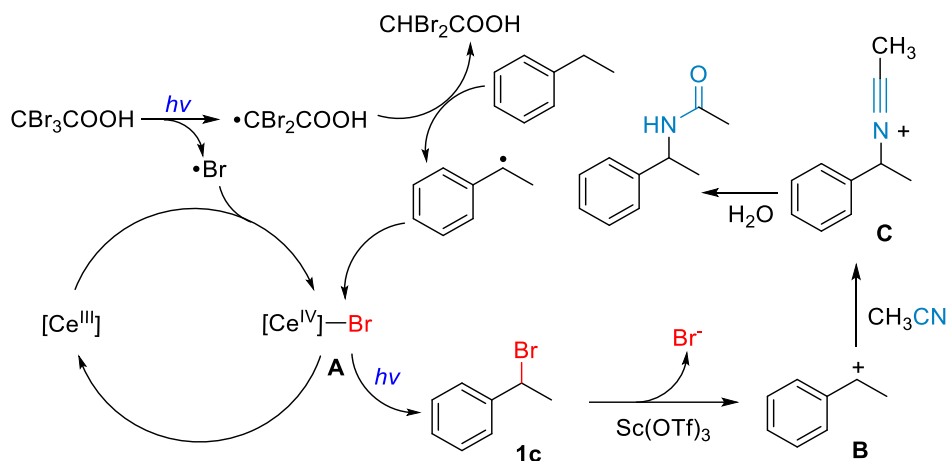


Scheme 4.8 Detection of the C-H amidation of deuterium substrate.

On the other hand, the spectra of the mixture of CeI_3 and CBr_3COOH (molar ratio of CeI_3 and CBr_3COOH = 1:2) under light irradiation and N_2 only show a peak at around 258 nm, which had no change with extension of irradiation time (Figure 4.6(a)). It is interesting to find that this peak increased in the first 20 min and then decreased under N_2 when excessive CBr_3COOH (molar ratio of CeI_3 and CBr_3COOH = 1:10) was added (Figure 4.6(b)). This observation may indicate the transformation of Ce(III) to Ce(IV) species,²⁴ which may result from homolysis of C-Br bond in CBr_3COOH , generating $\cdot\text{Br}$ radicals that react with Ce(III) to afford Ce(IV) species.

The C-H amidation of (methylene-*d*)dibenzene has been conducted to examine if there is any KIE in the reaction. As shown in Scheme 4.8, similar yields of *N*-benzhydrylacetamide and

N-(diphenylmethyl-*d*)acetamide were observed, indicating that C-H activation on the benzylic position is less likely to be involved in the turnover limiting step, considering the insignificant KIE.



Scheme 4.9 Possible mechanism of Ritter-type C-H amidation reaction.

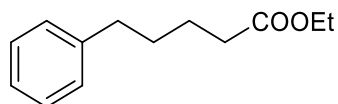
Based on the above observations and previous literature,¹⁴⁻¹⁵ a possible mechanism of this photocatalytic Ritter-type reaction is proposed using ethylbenzene as an example substrate reacting with acetonitrile (Scheme 4.9). The reaction is initiated through the cleavage of C-Br bond of CBr_3COOH under blue light irradiation, affording a $\cdot\text{Br}$ radical and a $\cdot\text{CBr}_2\text{COOH}$ radical. The Ce(IV)-Br species **A** is formed after the reaction of $\cdot\text{Br}$ radical with Ce(III) species. The unstable $\cdot\text{CBr}_2\text{COOH}$ radical attacks the benzylic site of ethylbenzene, affording CHBr_2COOH and a benzylic radical. The following reaction between the benzylic radical and Ce(IV)-Br species **A** afforded bromide intermediate **1c** and regenerates Ce(III) species. A carbon cation **B** formed from bromide intermediate **1c** in the presence of Sc(OTf)_3 which is trapped by a CH_3CN molecule to generate a nitrilium cation **C**, which undergoes hydrolysis to afford the final amide product.

4.3 Conclusions

In conclusion, a photocatalytic Ritter-type C-H amidation strategy has been developed, which employs a CeI_3 as catalyst and CBr_3COOH as bromine. With this strategy, a series of alkylarenes can be transformed to corresponding amides with good yields and high selectivity.

^1H NMR (400 MHz, Chloroform-*d*) δ 7.32 – 7.26 (m, 2H), 7.22 – 7.16 (m, 3H), 4.13 (q, J = 7.2 Hz, 2H), 2.66 (t, J = 7.5 Hz, 2H), 2.32 (t, J = 7.5 Hz, 2H), 2.00 – 1.93 (m, 2H), 1.26 (t, J = 7.1 Hz, 3H).

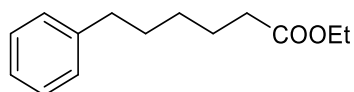
^{13}C NMR (101 MHz, Chloroform-*d*) δ 173.49, 141.43, 128.47, 128.35, 125.94, 60.23, 35.13, 33.66, 26.53, 14.23.



Ethyl 5-phenylpropanoate²⁹

^1H NMR (400 MHz, Chloroform-*d*) δ 7.34 – 7.27 (m, 2H), 7.21 – 7.19 (m, 3H), 4.15 (q, J = 7.1 Hz, 2H), 2.66 (t, J = 7.1 Hz, 2H), 2.35 (t, J = 7.1 Hz, 2H), 1.71 – 1.68 (m, 4H), 1.28 (t, J = 7.1 Hz, 3H).

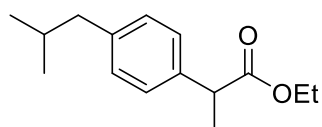
^{13}C NMR (101 MHz, Chloroform-*d*) δ 173.62, 142.14, 128.35, 128.28, 125.73, 60.19, 35.55, 34.18, 30.88, 24.58, 14.22.



Ethyl 6-phenylpropanoate³⁰

^1H NMR (400 MHz, Chloroform-*d*) δ 7.33 – 7.26 (m, 2H), 7.22 – 7.18 (m, 3H), 4.14 (q, J = 7.1 Hz, 2H), 2.67 – 2.64 (t, J = 7.5 Hz, 2H), 2.32 (t, J = 7.5 Hz, 2H), 1.72 – 1.63 (m, 4H), 1.45 – 1.34 (m, 2H), 1.27 (t, J = 7.1 Hz, 3H).

^{13}C NMR (101 MHz, Chloroform-*d*) δ 173.79, 142.50, 128.36, 128.24, 125.64, 60.17, 35.70, 34.27, 31.07, 28.73, 24.81, 14.22.

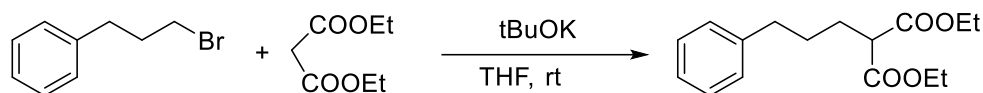


Ethyl 2-(4-isobutylphenyl)propanoate³¹

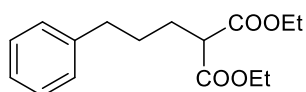
^1H NMR (400 MHz, Chloroform-*d*) δ 7.20 (d, J = 8.1 Hz, 2H), 7.09 (d, J = 8.2 Hz, 2H), 4.17 – 4.07 (m, 2H), 3.68 (q, J = 7.2 Hz, 1H), 2.45 (d, J = 7.2 Hz, 2H), 1.90 – 1.80 (m, 1H), 1.48 (d, J = 7.2 Hz, 3H), 1.21 (t, J = 7.2 Hz, 3H), 0.90 (d, J = 6.6 Hz, 6H).

^{13}C NMR (101 MHz, Chloroform-*d*) δ 174.77, 140.42, 137.88, 129.27, 127.11, 60.62, 45.15, 45.03, 30.16, 22.37, 18.59, 14.10.

Synthesis of diethyl 2-(3-phenylpropyl)malonate



Diethyl 2-(3-phenylpropyl)malonate was synthesized according to the literature.³² Malonic acid diethyl ester (0.80 g, 5.02 mmol) was added to a mixture of anhydrous potassium *tert*-butoxide (0.56 g, 5.02 mmol) and anhydrous THF (50 mL). The mixture was stirred at room temperature for 15 min. Then, (3-bromo-propyl)-benzene (1.00 g, 5.02 mmol) was added and the mixture was stirred under reflux for a further 14 h. After filtration, the THF was removed under vacuum to leave a clear oil which was dissolved in DCM (40 mL). The mixture was washed with water (3 \times 50 mL), dried over anhydrous MgSO_4 and filtered. Finally, diethyl 2-(3-phenylpropyl)malonate was afforded as a clear oil.



Diethyl 2-(3-phenylpropyl)malonate³³

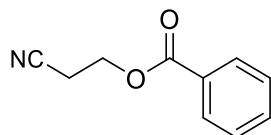
^1H NMR (400 MHz, Chloroform-*d*) δ 7.30 – 7.24 (m, 2H), 7.21 – 7.13 (m, 3H), 4.22 – 4.15 (m, 4H), 3.34 (t, $J = 7.5$ Hz, 1H), 2.65 (t, $J = 7.5$ Hz, 2H), 1.99 – 1.89 (m, 2H), 1.71 – 1.61 (m, 2H), 1.26 (t, $J = 7.1$ Hz, 6H).

^{13}C NMR (101 MHz, Chloroform-*d*) δ 169.40, 141.69, 128.33, 128.27, 125.85, 61.29, 51.89, 35.46, 29.07, 28.34, 14.05.

Synthesis of substituted cyanoethyl benzoate

A series of substituted cyanoethyl benzoate were synthesized according to the literature.³⁴ To a solution of 3-hydroxypropanenitrile (0.78g, 11 mmol) in CH_2Cl_2 (10 mL) cooled to 0 $^\circ\text{C}$ was added Et_3N (3.1 mL, 22 mmol) and the mixture was stirred at this temperature for 10 min. The substituted benzoyl chloride (10 mmol) was slowly added at 0 $^\circ\text{C}$; then the mixture was stirred at room temperature overnight. Water (30 mL) was added and the aqueous phase was

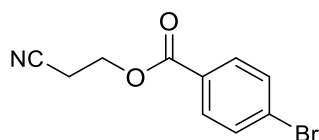
extracted with CH₂Cl₂ (3 × 30 mL). After drying over MgSO₄ and filtration, the organic fraction was concentrated under reduced pressure. The residue was purified by column chromatography (hexane/EtOAc, 10:1) to afford substituted cyanoethyl benzoate as products.



2-Cyanoethyl benzoate³⁴

¹H NMR (400 MHz, Chloroform-*d*) δ 8.06 (d, *J* = 5.5 Hz, 2H), 7.60 (t, *J* = 7.4 Hz, 1H), 7.46 (t, *J* = 7.8 Hz, 2H), 4.53 (t, *J* = 6.3 Hz, 2H), 2.85 (t, *J* = 6.3 Hz, 2H).

¹³C NMR (101 MHz, Chloroform-*d*) δ 165.93, 133.55, 129.77, 129.05, 128.52, 116.76, 59.09, 18.15.

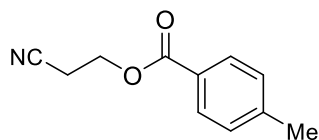


2-Cyanoethyl 4-bromobenzoate

¹H NMR (400 MHz, Chloroform-*d*) δ 7.90 (d, *J* = 8.6 Hz, 2H), 7.59 (d, *J* = 8.6 Hz, 2H), 4.51 (t, *J* = 6.3 Hz, 2H), 2.83 (t, *J* = 6.3 Hz, 2H).

¹³C NMR (101 MHz, Chloroform-*d*) δ 165.14, 131.85, 131.19, 128.73, 127.89, 116.65, 59.27, 18.07.

HRMS (ESI) calcd for C₁₀H₈BrNO₂ [M+Na]⁺: 275.9631, 277.9611; found: 275.9631, 277.9611.



2-Cyanoethyl 4-methylbenzoate

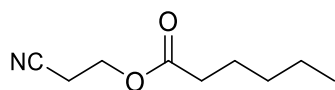
¹H NMR (400 MHz, Chloroform-*d*) δ 7.97 (d, *J* = 8.3 Hz, 2H), 7.27 (d, *J* = 8.3 Hz, 2H), 4.53 (t, *J* = 6.3 Hz, 2H), 2.85 (t, *J* = 6.3 Hz, 2H), 2.43 (s, 3H).

^{13}C NMR (101 MHz, Chloroform-*d*) δ 165.94, 144.32, 129.75, 129.18, 126.27, 116.82, 58.90, 21.64, 18.10.

HRMS (ESI) calcd for $\text{C}_{11}\text{H}_{11}\text{NO}_2$ $[\text{M}+\text{Na}]^+$: 212.0682; found: 212.0683.

Synthesis of 2-cyanoethyl hexanoate

2-Cyanoethyl hexanoate was synthesized according to the literature.³⁴ To a solution of 3-hydroxypropanenitrile (0.78g, 11 mmol) in CH_2Cl_2 (10 mL) cooled to 0 °C was added Et_3N (3.1 mL, 22 mmol) and the mixture was stirred at this temperature for 10 min. The hexanoyl chloride (1.1g, 10 mmol) was slowly added at 0 °C and then the mixture was stirred at room temperature overnight. Water (30 mL) was added and the aqueous phase was extracted with CH_2Cl_2 (3 \times 30 mL). After drying over MgSO_4 and filtration, the organic fraction was concentrated under reduced pressure. The residue was purified by column chromatography (hexane/EtOAc, 30:1) to afford 2-cyanoethyl hexanoate as product.



2-Cyanoethyl hexanoate³⁵

^1H NMR (400 MHz, Chloroform-*d*) δ 4.27 (t, $J = 6.3$ Hz, 2H), 2.70 (t, $J = 6.3$ Hz, 2H), 2.35 (t, $J = 7.6$ Hz, 2H), 1.69 – 1.58 (m, 2H), 1.37 – 1.26 (m, 4H), 0.89 (t, $J = 7.0$ Hz, 3H).

^{13}C NMR (101 MHz, Chloroform-*d*) δ 173.24, 116.76, 58.41, 33.87, 31.16, 24.41, 22.21, 17.99, 13.82.

4.4.3 Details of solvents

CH_3CN (HPLC gradient grade) was purchased from Fisher Scientific. It was opened on Sept. 1, 2022 and used immediately. Dry CH_3CN (anhydrous, 99.8%) was purchased from Sigma Aldrich. It was opened on Nov. 11, 2022 and used immediately. DCE (anhydrous, 99.8%) was purchased from Sigma Aldrich. It was opened at Mar. 2, 2023 and used immediately. Dried solvents were dry solvents pretreated by molecular sieves (3A, 2-5 mm beads) to remove potential water before using in the experiments. To an oven dried round-

bottom flask, 20 mL of dry solvents and activated molecular sieves (2g, activated at 300 °C) were added at N₂. Then, the mixture was placed for 24 h before use.

4.4.4 Mechanistic studies

Kinetic study of C-H amidation of ethylbenzene

To an oven dried Schlenk tube, CeI₃ (10 mol%), ethylbenzene (0.5 mmol), Sc(OTf)₃ (0.2 mmol), CBr₃COOH (0.5 mmol) and CH₃CN/DCE (2 mL, 1:1) were added under air. Then, 1-bromo-3,5-bis(trifluoromethyl)benzene (0.2 mmol) was added as the internal standard. The reaction tube was allowed to stir at room temperature under blue light. Every 1 h, 0.1 mL of the reaction mixture was taken out for ¹H NMR analysis.

Mass detection of acid intermediates

To an oven dried Schlenk tube, CeI₃ (10 mol%), ethylbenzene (0.5 mmol), Sc(OTf)₃ (0.2 mmol), CBr₃COOH (0.5 mmol) and CH₃CN/DCE (2 mL, 1:1) were added under air. The reaction tube was allowed to stir at room temperature under blue light. Then, the reaction mixture was taken out for mass analysis.

UV-Vis detection

CeI₃ + air: To an oven dried Schlenk tube, CeI₃ (0.05 mmol) and CH₃CN/DCM (2 mL, 1:1) were added under air. The reaction tube was allowed to stir at room temperature under blue light. Every 10 min, 0.05 mL of the reaction mixture was taken out and diluted to 50 mL for ¹H NMR analysis.

CeI₃ + N₂: To an oven dried Schlenk tube, CeI₃ (0.05 mmol) and CH₃CN/DCM (2 mL, 1:1) were added under N₂. The reaction tube was allowed to stir at room temperature under blue light. Every 10 min, 0.05 mL of the reaction mixture was taken out and diluted to 50 mL for ¹H NMR analysis.

CeI₃ + CBr₃COOH + air: To an oven dried Schlenk tube, CeI₃ (0.05 mmol), CBr₃COOH (0.1 mmol) and CH₃CN/DCM (2 mL, 1:1) were added under air. The reaction tube was allowed

to stir at room temperature under blue light. Every 10 min, 0.05 mL of the reaction mixture was taken out and diluted to 50 mL for ^1H NMR analysis.

$\text{CeI}_3 + \text{CBr}_3\text{COOH} + \text{N}_2$: To an oven dried Schlenk tube, CeI_3 (0.05 mmol), CBr_3COOH (0.1 mmol) and $\text{CH}_3\text{CN}/\text{DCM}$ (2 mL, 1:1) were added under air. The reaction tube was allowed to stir at room temperature under blue light. Every 10 min, 0.05 mL of the reaction mixture was taken out and diluted to 50 mL for ^1H NMR analysis.

$\text{CeI}_3 + \text{CBr}_3\text{COOH} + \text{N}_2$: To an oven dried Schlenk tube, CeI_3 (0.05 mmol), CBr_3COOH (0.5 mmol) and $\text{CH}_3\text{CN}/\text{DCM}$ (2 mL, 1:1) were added under air. The reaction tube was allowed to stir at room temperature under blue light. Every 10 min, 0.05 mL of the reaction mixture was taken out and diluted to 50 mL for ^1H NMR analysis.

$\text{CBr}_3\text{COOH} + \text{air}$: To an oven dried Schlenk tube, CBr_3COOH (0.1 mmol) and $\text{CH}_3\text{CN}/\text{DCM}$ (2 mL, 1:1) were added under air. The reaction tube was allowed to stir at room temperature under blue light. Every 10 min, 0.05 mL of the reaction mixture was taken out and diluted to 50 mL for ^1H NMR analysis.

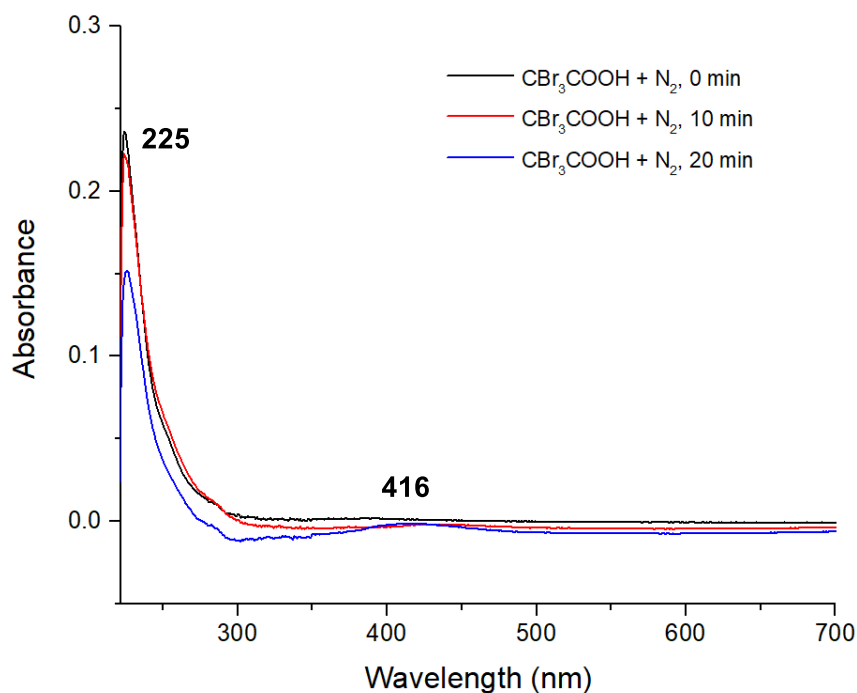
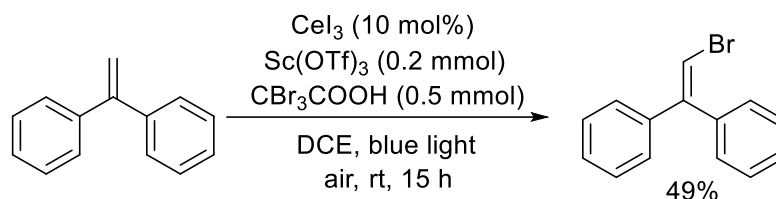


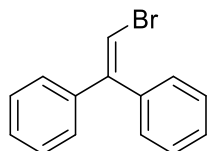
Figure 4.7 UV-Vis analysis of CBr_3COOH with N_2 under blue light irradiation.

$\text{CBr}_3\text{COOH} + \text{N}_2$: To an oven dried Schlenk tube, CBr_3COOH (0.1 mmol) and $\text{CH}_3\text{CN}/\text{DCM}$ (2 mL, 1:1) were added under N_2 . The reaction tube was allowed to stir at room temperature under blue light. Every 10 min, 0.05 mL of the reaction mixture was taken out and diluted to 50 mL for ^1H NMR analysis.

Trapping of Br radical species



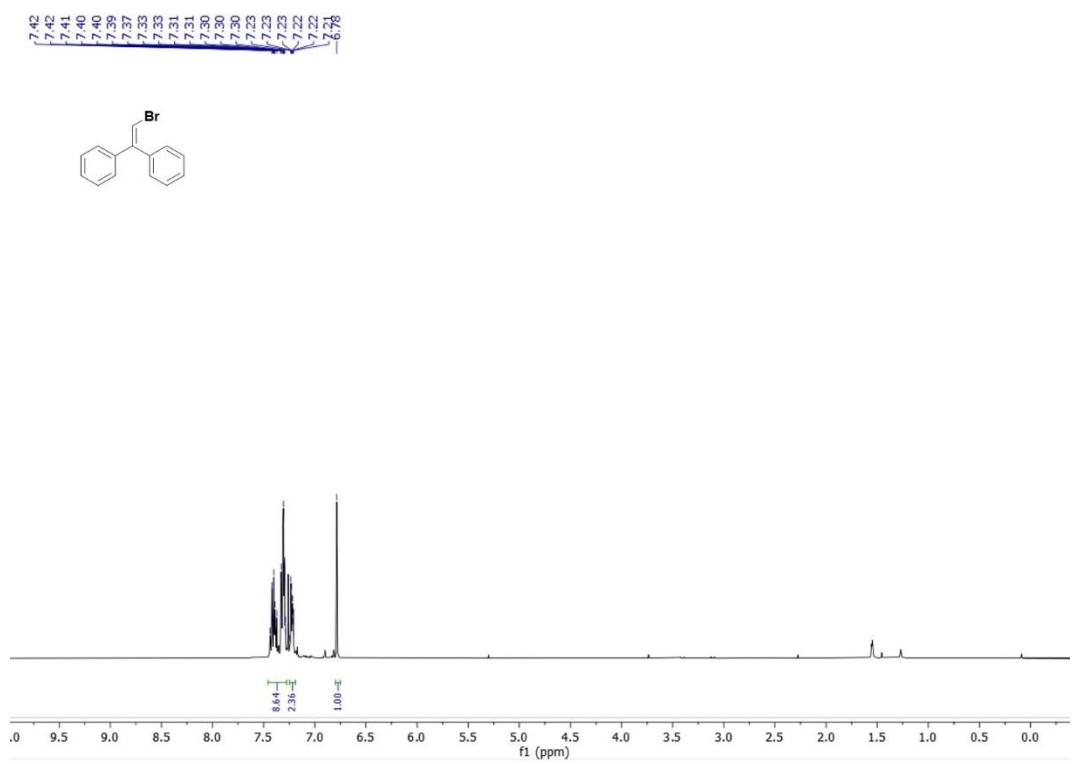
To an oven dried Schlenk tube, CeI_3 (10 mol%), 1,1-diphenylethylene (0.5 mmol), $\text{Sc}(\text{OTf})_3$ (0.2 mmol), CBr_3COOH (0.5 mmol) and DCE (2 mL) were added under air. The reaction tube was allowed to stir at room temperature under blue light for 15 h. After reaction, the bromide product was purified by silica gel column chromatography (Hexane: ethyl acetate = 40:1).



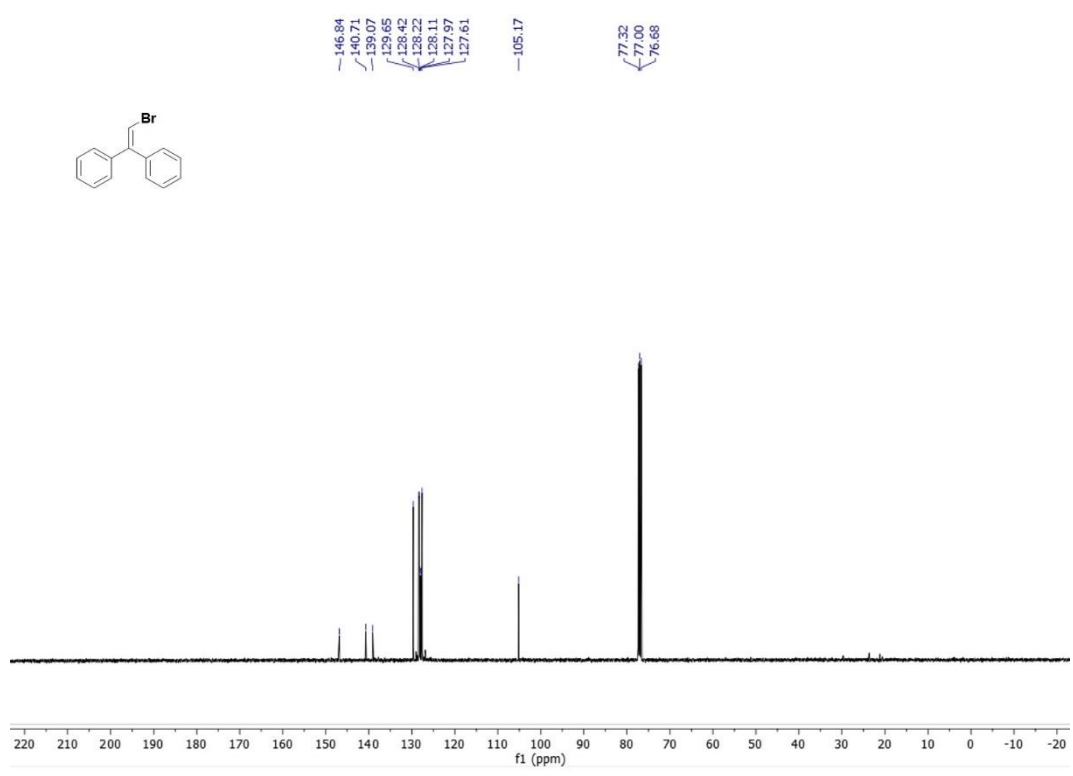
(2-Bromoethene-1,1-diyl)dibenzene³⁶

^1H NMR (400 MHz, Chloroform-*d*) δ 7.46 – 7.28 (m, 8H), 7.25 – 7.19 (m, 2H), 6.78 (s, 1H).

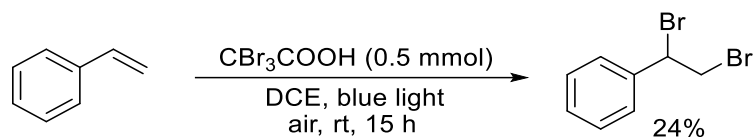
^{13}C NMR (101 MHz, Chloroform-*d*) δ 146.84, 140.71, 139.07, 129.65, 128.42, 128.22, 128.11, 127.97, 127.61, 105.17.



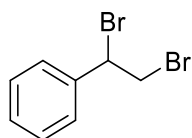
¹H NMR



¹³C NMR



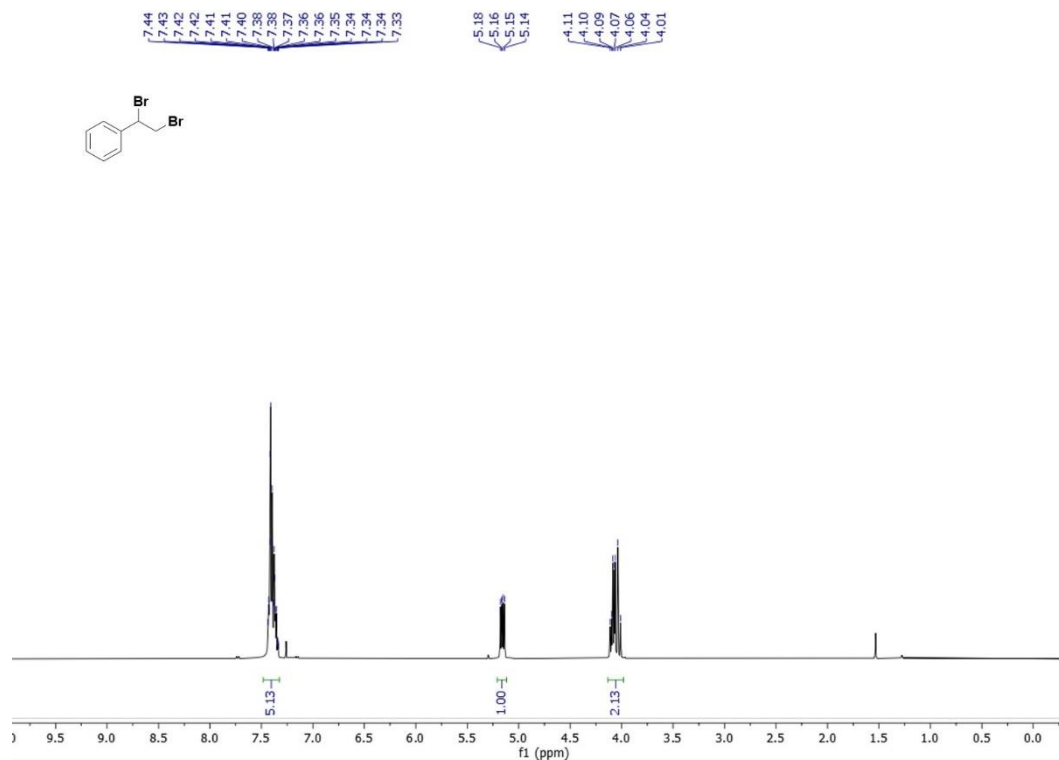
To an oven dried Schlenk tube, styrene (0.5 mmol), CBr_3COOH (0.5 mmol) and DCE (2 mL) were added under air. The reaction tube was allowed to stir at room temperature under blue light for 15 h. After the reaction, the bromide product was purified by silica gel column chromatography (Hexane: ethyl acetate = 40:1).



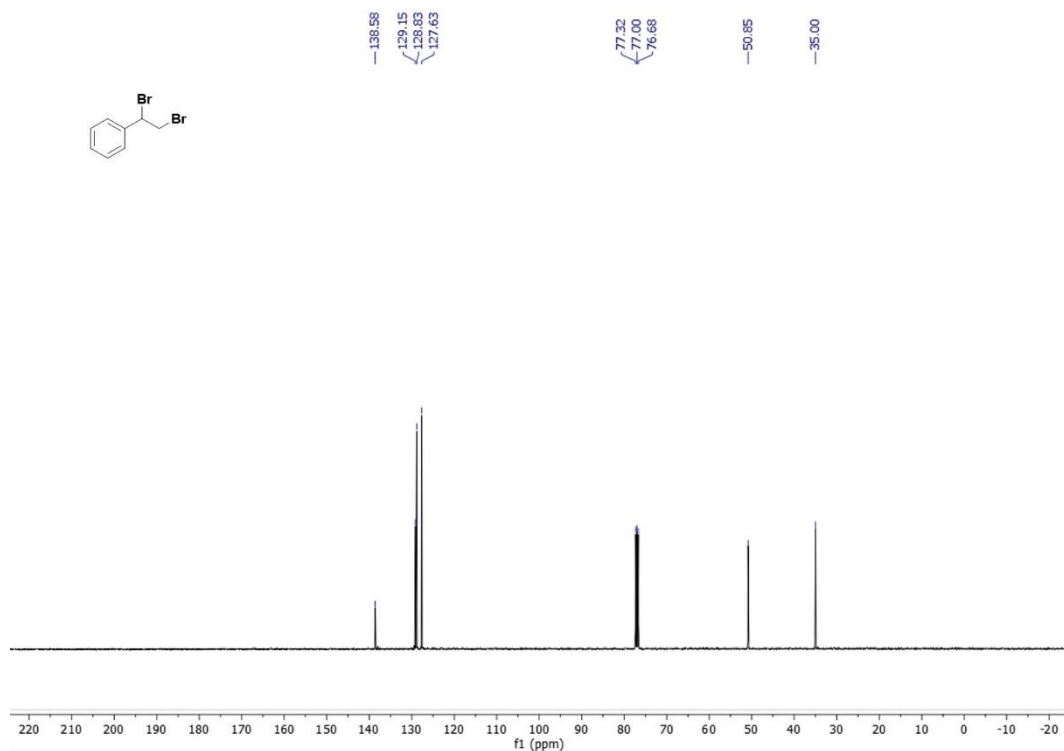
(1,2-Dibromoethyl)benzene³⁷

$^1\text{H NMR}$ (400 MHz, Chloroform-*d*) δ 7.48 – 7.33 (m, 5H), 5.16 (dd, $J = 10.5, 5.5$ Hz, 1H), 4.13 – 3.98 (m, 2H).

$^{13}\text{C NMR}$ (101 MHz, Chloroform-*d*) δ 138.58, 129.15, 128.83, 127.63, 50.85, 35.00.

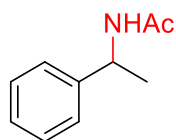


$^1\text{H NMR}$



^{13}C NMR

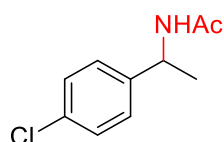
4.5 Analytical data of products



N-(1-phenylethyl)acetamide (**1**)³⁸

^1H NMR (400 MHz, Chloroform-*d*) δ 7.41 – 7.21 (m, 5H), 6.04 (d, $J = 8.0$ Hz, 1H), 5.17 – 5.09 (m, 1H), 1.98 (s, 3H), 1.49 (d, $J = 6.9$ Hz, 3H).

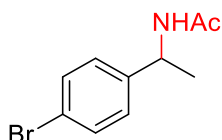
^{13}C NMR (101 MHz, CDCl_3) δ 169.12, 143.16, 128.58, 127.27, 126.13, 48.72, 23.31, 21.67.



N-(1-(4-chlorophenyl)ethyl)acetamide (**2**)³⁹

^1H NMR (400 MHz, Chloroform-*d*) δ 7.31 – 7.24 (m, 4H), 5.97 (d, $J = 7.8$ Hz, 1H), 5.12 – 5.05 (m, 1H), 1.98 (s, 3H), 1.46 (d, $J = 6.9$ Hz, 3H).

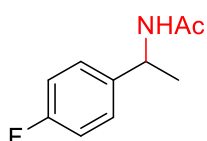
^{13}C NMR (101 MHz, Chloroform-*d*) δ 169.18, 141.78, 132.95, 128.68, 127.52, 48.16, 23.29, 21.66.



***N*-(1-(4-bromophenyl)ethyl)acetamide (3)**³⁸

¹H NMR (400 MHz, Chloroform-*d*) δ 7.43 (d, J = 8.4 Hz, 2H), 7.17 (d, J = 8.4 Hz, 2H), 5.95 (d, J = 7.6 Hz, 1H), 5.08 – 5.01 (m, 1H), 1.96 (s, 3H), 1.44 (d, J = 6.9 Hz, 3H).

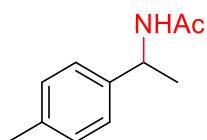
¹³C NMR (101 MHz, Chloroform-*d*) δ 169.19, 142.31, 131.64, 127.88, 121.04, 48.23, 23.29, 21.63.



***N*-(1-(4-fluorophenyl)ethyl)acetamide (4)**⁴⁰

¹H NMR (400 MHz, Chloroform-*d*) δ 7.32 – 7.24 (m, 2H), 7.03 – 6.99 (m, 2H), 6.06 (d, J = 6.7 Hz, 1H), 5.13 – 5.05 (m, 1H), 1.97 (s, 3H), 1.46 (d, J = 6.9 Hz, 3H).

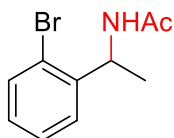
¹³C NMR (101 MHz, Chloroform-*d*) δ 169.21, 161.87 (d, $J_{\text{C-F}}$ = 245.4 Hz), 139.03 (d, $J_{\text{C-F}}$ = 3.1 Hz), 127.74 (d, $J_{\text{C-F}}$ = 8.1 Hz), 115.32 (d, $J_{\text{C-F}}$ = 21.4 Hz), 48.09, 23.26, 21.73.



***N*-(1-(*p*-tolyl)ethyl)acetamide (5)**⁴¹

¹H NMR (400 MHz, Chloroform-*d*) δ 7.23 – 7.08 (m, 4H), 5.91 (br, s, 1H), 5.12 – 5.05 (m, 1H), 2.33 (s, 3H), 1.99 (s, 3H), 1.48 (d, J = 6.9 Hz, 3H).

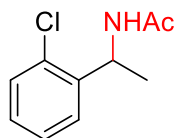
¹³C NMR (101 MHz, Chloroform-*d*) δ 169.65, 139.87, 137.16, 129.34, 126.12, 48.75, 23.26, 21.56, 21.01.



***N*-(1-(2-bromophenyl)ethyl)acetamide (6)**⁴²

^1H NMR (400 MHz, Chloroform-*d*) δ 7.56 (d, $J = 7.9$ Hz, 1H), 7.38 – 7.25 (m, 2H), 7.17 – 7.08 (m, 1H), 6.15 (d, $J = 8.4$ Hz, 1H), 5.39 – 5.32 (m, 1H), 2.00 (s, 3H), 1.48 (d, $J = 6.9$ Hz, 3H).

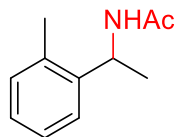
^{13}C NMR (101 MHz, Chloroform-*d*) δ 169.07, 142.14, 133.35, 128.68, 127.68, 127.05, 122.94, 49.13, 23.21, 20.96.



***N*-(1-(2-chlorophenyl)ethyl)acetamide (7)**⁴³

^1H NMR (400 MHz, Chloroform-*d*) δ 7.36 – 7.11 (m, 4H), 6.27 (d, $J = 7.3$ Hz, 1H), 5.41 – 5.34 (m, 1H), 1.96 (s, 3H), 1.45 (d, $J = 6.9$ Hz, 3H).

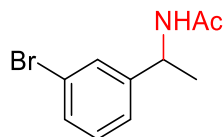
^{13}C NMR (101 MHz, Chloroform-*d*) δ 169.14, 140.57, 132.73, 130.01, 128.35, 127.06, 127.05, 47.08, 23.16, 20.83.



***N*-(1-(*o*-tolyl)ethyl)acetamide (8)**⁴³

^1H NMR (400 MHz, Chloroform-*d*) δ 7.32 – 7.27 (m, 1H), 7.24 – 7.14 (m, 3H), 5.60 (br, s, 1H), 5.34 – 5.27 (m, 1H), 2.38 (s, 3H), 1.97 (s, 3H), 1.48 (d, $J = 6.8$ Hz, 3H).

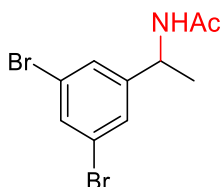
^{13}C NMR (101 MHz, Chloroform-*d*) δ 168.92, 140.92, 136.04, 130.77, 127.40, 126.30, 124.64, 45.36, 23.34, 20.98, 19.15.



***N*-(1-(3-bromophenyl)ethyl)acetamide (9)**⁴⁴

^1H NMR (400 MHz, Chloroform-*d*) δ 7.44 – 7.34 (m, 2H), 7.24 – 7.13 (m, 2H), 6.15 (d, $J = 8.1$ Hz, 1H), 5.08 – 5.01 (m, 1H), 1.96 (s, 3H), 1.43 (d, $J = 7.0$ Hz, 3H).

^{13}C NMR (101 MHz, Chloroform-*d*) δ 169.34, 145.69, 130.30, 130.17, 129.09, 124.92, 122.64, 48.36, 23.22, 21.76.

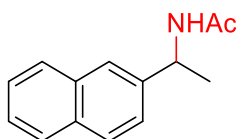


***N*-(1-(3,5-dibromophenyl)ethyl)acetamide (10)**

^1H NMR (400 MHz, Chloroform-*d*) δ 7.55 (t, $J = 1.8$ Hz, 1H), 7.37 (d, $J = 1.7$ Hz, 2H), 5.75 (br, s, 1H), 5.07 – 5.00 (m, 1H), 2.02 (s, 3H), 1.45 (d, $J = 7.0$ Hz, 3H).

^{13}C NMR (101 MHz, Chloroform-*d*) δ 169.43, 147.26, 132.98, 128.11, 123.18, 48.19, 23.32, 21.80.

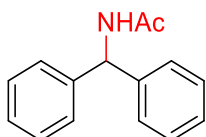
HRMS (ESI) calcd for $\text{C}_{10}\text{H}_{11}\text{Br}_2\text{NO}$ $[\text{M}+\text{Na}]^+$: 341.9100, 343.9080, 345.9059; found: 341.9100, 343.9081, 345.9059.



***N*-(1-(naphthalen-2-yl)ethyl)acetamide (11)³⁸**

^1H NMR (400 MHz, Chloroform-*d*) δ 7.85 – 7.78 (m, 3H), 7.77 – 7.73 (m, 1H), 7.51 – 7.41 (m, 3H), 5.83 (br, s, 1H), 5.35 – 5.23 (m, 1H), 2.01 (s, 3H), 1.58 (d, $J = 6.9$ Hz, 3H).

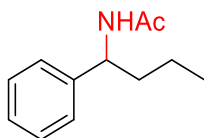
^{13}C NMR (101 MHz, Chloroform-*d*) δ 169.13, 140.46, 133.30, 132.70, 128.49, 127.85, 127.59, 126.24, 125.89, 124.72, 124.52, 48.81, 23.48, 21.59.



***N*-benzhydrylacetamide (12)³⁸**

^1H NMR (400 MHz, Chloroform-*d*) δ 7.43 – 7.17 (m, 10H), 6.43 (d, $J = 7.8$ Hz, 1H), 6.26 (d, $J = 8.1$ Hz, 1H), 2.02 (s, 3H).

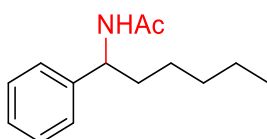
^{13}C NMR (101 MHz, Chloroform-*d*) δ 169.16, 141.49, 128.56, 127.37, 127.35, 56.90, 23.16.



***N*-(1-phenylbutyl)acetamide (13)**⁴⁵

¹H NMR (400 MHz, Chloroform-*d*) δ 7.39 – 7.25 (m, 5H), 6.13 (d, *J* = 7.7 Hz, 1H), 4.96 (q, *J* = 7.7 Hz, 1H), 2.02 (s, 3H), 1.88 – 1.71 (m, 2H), 1.44 – 1.20 (m, 2H), 0.94 (t, *J* = 7.3 Hz, 3H).

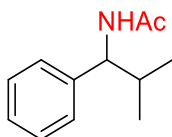
¹³C NMR (101 MHz, Chloroform-*d*) δ 170.06, 142.06, 128.67, 127.41, 126.58, 53.68, 38.20, 23.20, 19.44, 13.77.



***N*-(1-phenylhexyl)acetamide (14)**⁴⁴

¹H NMR (400 MHz, Chloroform-*d*) δ 7.51 – 7.15 (m, 5H), 5.91 (d, *J* = 8.4 Hz, 1H), 4.96 (q, *J* = 7.7 Hz, 1H), 2.02 (s, 3H), 1.85 – 1.74 (m, 2H), 1.38 – 1.21 (m, 6H), 0.88 (t, *J* = 6.5 Hz, 3H).

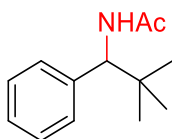
¹³C NMR (101 MHz, Chloroform-*d*) δ 169.60, 142.22, 128.67, 127.37, 126.58, 53.72, 36.08, 31.53, 25.86, 23.37, 22.46, 13.97.



***N*-(2-methyl-1-phenylpropyl)acetamide (15)**⁴²

¹H NMR (400 MHz, Chloroform-*d*) δ 7.35 – 7.17 (m, 5H), 6.17 (d, *J* = 9.2 Hz, 1H), 4.73 (t, *J* = 8.6 Hz, 1H), 2.04 – 1.97 (m, 4H), 0.96 (d, *J* = 6.7 Hz, 3H), 0.81 (d, *J* = 6.7 Hz, 3H).

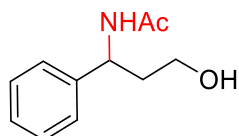
¹³C NMR (101 MHz, Chloroform-*d*) δ 169.49, 141.58, 128.35, 127.03, 126.94, 59.22, 33.30, 23.35, 19.69, 18.85.



***N*-(2,2-dimethyl-1-phenylpropyl)acetamide (16)**⁴²

^1H NMR (400 MHz, Chloroform-*d*) δ 7.36 – 7.19 (m, 5H), 6.12 (d, $J = 8.8$ Hz, 1H), 4.85 (d, $J = 9.5$ Hz, 1H), 2.04 (s, 3H), 0.95 (s, 9H).

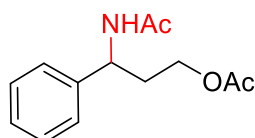
^{13}C NMR (101 MHz, Chloroform-*d*) δ 169.31, 140.00, 128.08, 127.80, 127.03, 61.61, 34.81, 26.71, 23.57.



***N*-(3-hydroxy-1-phenylpropyl)acetamide (17)**⁴⁶

^1H NMR (400 MHz, Chloroform-*d*) δ 7.43 – 7.27 (m, 5H), 6.12 (d, $J = 8.3$ Hz, 1H), 5.11 (q, $J = 7.6$ Hz, 1H), 3.38 – 3.20 (m, 2H), 2.47 – 2.25 (m, 2H), 1.98 (s, 3H).

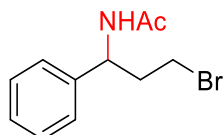
^{13}C NMR (101 MHz, Chloroform-*d*) δ 170.03, 140.57, 128.94, 127.88, 126.60, 67.74, 52.61, 38.97, 23.39.



3-Acetamido-3-phenylpropyl acetate (18)¹⁴

^1H NMR (400 MHz, Chloroform-*d*) δ 7.37 – 7.25 (m, 5H), 6.20 (d, $J = 8.4$ Hz, 1H), 5.12 (q, $J = 7.7$ Hz, 1H), 4.14 – 3.98 (m, 2H), 2.19 – 2.08 (m, 2H), 2.02 (s, 3H), 1.98 (s, 3H).

^{13}C NMR (101 MHz, Chloroform-*d*) δ 170.99, 169.37, 141.23, 128.75, 127.58, 126.43, 61.37, 50.66, 34.70, 23.28, 20.84.

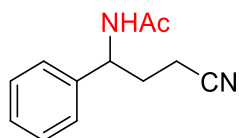


***N*-(3-bromo-1-phenylpropyl)acetamide (19)**

^1H NMR (400 MHz, Chloroform-*d*) δ 7.36 – 7.26 (m, 5H), 6.24 (d, $J = 8.3$ Hz, 1H), 5.11 (q, $J = 7.6$ Hz, 1H), 3.39 – 3.19 (m, 2H), 2.47 – 2.23 (m, 2H), 1.94 (s, 3H).

^{13}C NMR (101 MHz, Chloroform-*d*) δ 169.78, 140.67, 128.90, 127.82, 126.59, 52.54, 38.97, 29.42, 23.36.

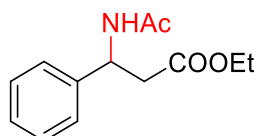
HRMS (ESI) calcd for C₁₀H₁₄BrNO [M+Na]⁺: 278.0151, 280.0131; found: 278.0153, 280.0132.



N-(3-cyano-1-phenylpropyl)acetamide (20)⁴⁷

¹H NMR (400 MHz, Chloroform-*d*) δ 7.43 – 7.23 (m, 5H), 6.37 (d, *J* = 8.3 Hz, 1H), 5.05 (td, *J* = 8.2, 6.6 Hz, 1H), 2.35 (t, *J* = 7.1 Hz, 2H), 2.29 – 2.09 (m, 2H), 2.01 (s, 3H).

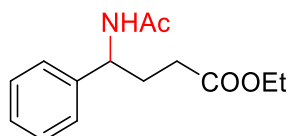
¹³C NMR (101 MHz, Chloroform-*d*) δ 170.04, 139.94, 129.08, 128.18, 126.49, 119.29, 52.76, 31.58, 23.22, 14.47.



Ethyl 3-acetamido-3-phenylpropanoate (21)⁴⁸

¹H NMR (400 MHz, Chloroform-*d*) δ 7.40 – 7.22 (m, 5H), 6.19 (d, *J* = 8.1 Hz, 1H), 5.01 (td, *J* = 8.3, 6.3 Hz, 1H), 4.14 (q, *J* = 7.1 Hz, 2H), 2.89 (dd, *J* = 15.6, 5.9 Hz, 1H), 2.79 (dd, *J* = 15.6, 6.0 Hz, 1H), 2.00 (s, 3H), 1.27 (t, *J* = 7.1 Hz, 3H).

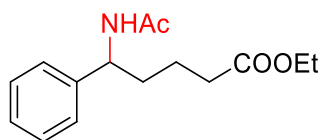
¹³C NMR (101 MHz, Chloroform-*d*) δ 173.64, 169.72, 141.34, 128.79, 127.63, 126.47, 60.68, 53.38, 40.21, 23.27, 14.16.



Ethyl 4-acetamido-4-phenylbutanoate (22)⁴⁹

¹H NMR (400 MHz, Chloroform-*d*) δ 7.38 – 7.23 (m, 5H), 6.18 (d, *J* = 8.3 Hz, 1H), 5.00 (td, *J* = 8.3, 6.3 Hz, 1H), 4.13 (q, *J* = 7.1 Hz, 2H), 2.44 – 2.27 (m, 2H), 2.23 – 2.05 (m, 2H), 1.98 (s, 3H), 1.26 (t, *J* = 7.1 Hz, 3H).

¹³C NMR (101 MHz, Chloroform-*d*) δ 173.57, 169.40, 141.51, 128.73, 127.54, 126.45, 60.61, 53.17, 31.23, 30.80, 23.33, 14.14.

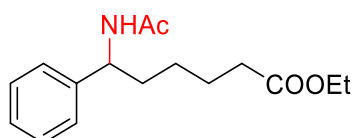


Ethyl 5-acetamido-5-phenylpentanoate (23)

^1H NMR (400 MHz, Chloroform-*d*) δ 7.36 – 7.23 (m, 5H), 6.10 (d, J = 8.3 Hz, 1H), 4.97 (q, J = 7.6 Hz, 1H), 4.12 (q, J = 7.1 Hz, 2H), 2.35 – 2.31 (td, J = 7.2, 3.2 Hz, 2H), 1.99 (s, 3H), 1.89 – 1.76 (m, 2H), 1.70 – 1.48 (m, 2H), 1.25 (t, J = 7.1 Hz, 3H).

^{13}C NMR (101 MHz, Chloroform-*d*) δ 173.43, 169.52, 141.91, 128.66, 127.39, 126.48, 60.33, 53.21, 35.33, 33.68, 23.30, 21.47, 14.15.

HRMS (ESI) calcd for $\text{C}_{15}\text{H}_{21}\text{NO}_3$ $[\text{M}+\text{Na}]^+$: 286.1414; found: 286.1417.

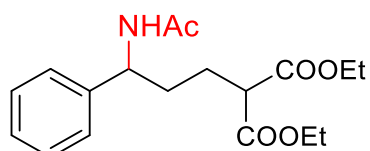


Ethyl 6-acetamido-6-phenylhexanoate (24)

^1H NMR (400 MHz, Chloroform-*d*) δ 7.40 – 7.21 (m, 5H), 5.93 (d, J = 8.4 Hz, 1H), 4.96 (q, J = 7.7 Hz, 1H), 4.11 (q, J = 7.2 Hz, 2H), 2.28 (t, J = 7.5 Hz, 2H), 1.98 (s, 3H), 1.87 – 1.76 (m, 2H), 1.69 – 1.61 (m, 2H), 1.43 – 1.32 (m, 2H), 1.24 (t, J = 7.1 Hz, 3H).

^{13}C NMR (101 MHz, Chloroform-*d*) δ 173.56, 169.28, 142.08, 128.64, 127.36, 126.52, 60.22, 53.31, 35.68, 34.03, 25.68, 24.62, 23.36, 14.16.

HRMS (ESI) calcd for $\text{C}_{16}\text{H}_{23}\text{NO}_3$ $[\text{M}+\text{Na}]^+$: 300.1571; found: 300.1572.

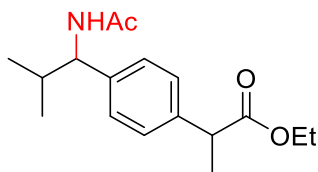


Diethyl 2-(3-acetamido-3-phenylpropyl)malonate (25)

^1H NMR (400 MHz, Chloroform-*d*) δ 7.51 – 7.17 (m, 5H), 5.91 (d, J = 8.1 Hz, 1H), 5.04 – 4.97 (m, 1H), 4.44 – 4.00 (m, 4H), 3.37 (t, J = 6.6 Hz, 1H), 2.17 – 1.78 (m, 7H), 1.28 (t, J = 7.1 Hz, 6H).

^{13}C NMR (101 MHz, Chloroform-*d*) δ 169.43, 169.24, 141.58, 128.78, 127.56, 126.47, 61.46, 53.17, 51.45, 33.47, 25.35, 23.39, 14.03.

HRMS (ESI) calcd for $\text{C}_{18}\text{H}_{25}\text{NO}_5$ $[\text{M}+\text{Na}]^+$: 358.1625; found: 358.1627.

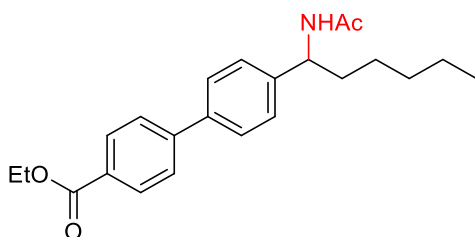


Ethyl 2-(4-(1-acetamido-2-methylpropyl)phenyl)propanoate (26)

^1H NMR (400 MHz, Chloroform-*d*) δ 7.29 – 7.16 (m, 4H), 5.97 (d, $J = 9.2$ Hz, 1H), 4.75 (t, $J = 8.5$ Hz, 1H), 4.20 – 4.03 (m, 2H), 3.69 (q, $J = 7.2$ Hz, 1H), 1.99 (s, 3H), 1.48 (d, $J = 7.2$ Hz, 3H), 1.22 (t, $J = 7.1$ Hz, 3H), 0.96 (d, $J = 6.7$ Hz, 3H), 0.83 (d, $J = 6.7$ Hz, 3H).

^{13}C NMR (101 MHz, Chloroform-*d*) δ 174.52, 169.34, 140.35, 139.33, 127.48, 127.12, 60.69, 58.76, 45.10, 33.28, 23.40, 19.72, 18.77, 18.48, 14.05.

HRMS (ESI) calcd for $\text{C}_{17}\text{H}_{25}\text{NO}_3$ $[\text{M}+\text{Na}]^+$: 314.1727; found: 314.1728.

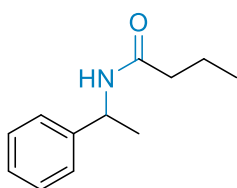


Ethyl 4'-(1-acetamidohexyl)-[1,1'-biphenyl]-4-carboxylate (27)

^1H NMR (400 MHz, Chloroform-*d*) δ 8.11 – 8.06 (m, 2H), 7.63 – 7.56 (m, 4H), 7.40 – 7.33 (m, 2H), 5.93 (d, $J = 8.2$ Hz, 1H), 4.98 (q, $J = 7.6$ Hz, 1H), 4.39 (q, $J = 7.1$ Hz, 2H), 2.00 (s, 3H), 1.83 – 1.77 (m, 2H), 1.41 (t, $J = 7.1$ Hz, 3H), 1.32 – 1.23 (m, 6H), 0.87 (t, $J = 6.8$ Hz, 3H).

^{13}C NMR (101 MHz, Chloroform-*d*) δ 169.42, 166.48, 145.00, 142.55, 138.94, 130.02, 129.19, 127.46, 127.13, 126.83, 60.95, 53.27, 36.10, 31.52, 25.88, 23.43, 22.45, 14.31, 13.96.

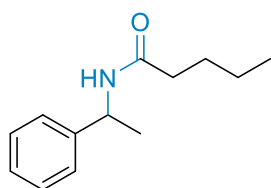
HRMS (ESI) calcd for $\text{C}_{23}\text{H}_{29}\text{NO}_3$ $[\text{M}+\text{Na}]^+$: 390.2040; found: 390.2040.



***N*-(1-phenylethyl)butyramide (28)**⁵⁰

¹H NMR (400 MHz, Chloroform-*d*) δ 7.41 – 7.20 (m, 5H), 5.98 (d, J = 6.4 Hz, 1H), 5.18 – 5.11 (m, 1H), 2.16 (t, J = 7.2 Hz, 2H), 1.71 – 1.62 (m, 2H), 1.49 (d, J = 6.9 Hz, 3H), 0.94 (t, J = 7.4 Hz, 3H).

¹³C NMR (101 MHz, Chloroform-*d*) δ 172.12, 143.27, 128.54, 127.19, 126.09, 48.50, 38.63, 21.69, 19.11, 13.65.

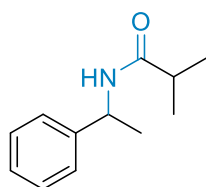


***N*-(1-phenylethyl)pentanamide (29)**

¹H NMR (400 MHz, Chloroform-*d*) δ 7.40 – 7.20 (m, 5H), 5.93 (d, J = 6.0 Hz, 1H), 5.19 – 5.11 (m, 1H), 2.23 – 2.11 (m, 2H), 1.66 – 1.59 (m, 2H), 1.49 (d, J = 6.9 Hz, 3H), 1.39 – 1.30 (m, 2H), 0.92 (t, J = 7.3 Hz, 3H).

¹³C NMR (101 MHz, Chloroform-*d*) δ 172.20, 143.29, 128.55, 127.20, 126.10, 48.48, 36.51, 27.76, 22.31, 21.68, 13.72.

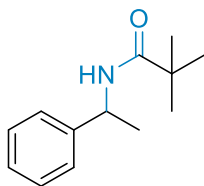
HRMS (ESI) calcd for C₁₃H₁₉NO₃ [M+Na]⁺: 228.1359; found: 228.1359.



***N*-(1-phenylethyl)isobutyramide (30)**⁵¹

¹H NMR (400 MHz, Chloroform-*d*) δ 7.39 – 7.24 (m, 5H), 5.86 (br, s, 1H), 5.17 – 5.10 (m, 1H), 2.42 – 2.32 (m, 1H), 1.50 (d, J = 6.9 Hz, 3H), 1.18 (d, J = 6.9 Hz, 3H), 1.15 (d, J = 6.9 Hz, 3H).

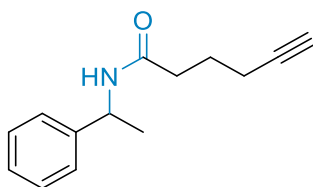
¹³C NMR (101 MHz, Chloroform-*d*) δ 176.01, 143.34, 128.58, 127.20, 126.04, 48.35, 35.56, 21.68, 19.53, 19.49.



N-(1-phenylethyl)pivalamide (31)⁵²

¹H NMR (400 MHz, Chloroform-*d*) δ 7.39 – 7.24 (m, 5H), 5.86 (br, s, 1H), 5.17 – 5.09 (m, 1H), 1.50 (d, J = 6.9 Hz, 3H), 1.22 (s, 9H).

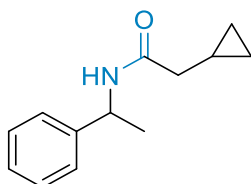
¹³C NMR (101 MHz, Chloroform-*d*) δ 177.41, 143.45, 128.60, 127.18, 125.97, 48.40, 38.53, 27.50, 21.67.



N-(1-phenylethyl)hex-5-ynamide (32)⁵³

¹H NMR (400 MHz, Chloroform-*d*) δ 7.38 – 7.23 (m, 5H), 5.74 (br, s, 1H), 5.17 – 5.10 (m, 1H), 2.35 – 2.18 (m, 4H), 1.96 (t, J = 2.7 Hz, 1H), 1.97 – 1.82 (m, 2H), 1.49 (d, J = 6.9 Hz, 3H)

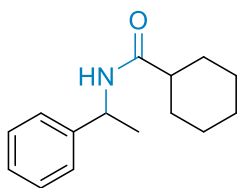
¹³C NMR (101 MHz, Chloroform-*d*) δ 171.22, 143.15, 128.67, 127.37, 126.15, 83.51, 69.20, 48.73, 35.12, 24.07, 21.74, 17.76.



2-Cyclopropyl-N-(1-phenylethyl)acetamide (33)⁵⁴

¹H NMR (400 MHz, Chloroform-*d*) δ 7.39 – 7.20 (m, 5H), 6.20 (br, s, 1H), 5.20 – 5.13 (m, 1H), 2.16 (d, J = 7.2 Hz, 2H), 1.50 (d, J = 6.9 Hz, 3H), 1.00 – 0.93 (m, 1H), 0.66 – 0.55 (m, 2H), 0.26 – 0.15 (m, 2H).

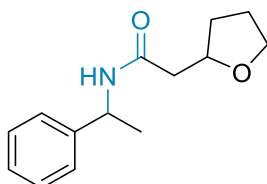
¹³C NMR (101 MHz, Chloroform-*d*) δ 171.57, 143.24, 128.64, 127.27, 126.04, 48.50, 41.47, 21.90, 7.11, 4.58, 4.56.



***N*-(1-phenylethyl)cyclohexanecarboxamide (34)**⁵¹

¹H NMR (400 MHz, Chloroform-*d*) δ 7.40 – 7.22 (m, 5H), 5.88 (d, J = 8.0 Hz, 1H), 5.17 – 5.10 (m, 1H), 2.13 – 2.05 (m, 1H), 1.92 – 1.74 (m, 4H), 1.70 – 1.63 (m, 1H), 1.52 – 1.38 (m, 5H), 1.31 – 1.18 (m, 3H).

¹³C NMR (101 MHz, Chloroform-*d*) δ 175.13, 143.39, 128.53, 127.13, 126.02, 48.18, 45.44, 29.61, 29.54, 25.65, 21.69.

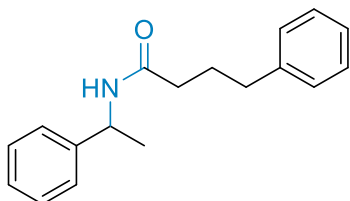


***N*-(1-phenylethyl)-2-(tetrahydrofuran-2-yl)acetamide (35)**

¹H NMR (400 MHz, Chloroform-*d*) δ 7.40 – 7.19 (m, 5H), 6.88 (d, J = 8.0 Hz, 1H), 5.18 – 5.11 (m, 1H), 4.18 – 4.10 (m, 1H), 3.99 – 3.71 (m, 2H), 2.55 – 2.37 (m, 2H), 2.16 – 1.78 (m, 4H), 1.49 (d, J = 7.0 Hz, 3H).

¹³C NMR (101 MHz, Chloroform-*d*) δ 170.18, 143.48, 128.53, 127.05, 125.93, 75.73, 68.04, 48.43, 42.09, 31.08, 25.41, 22.03.

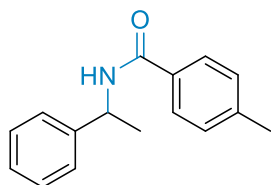
HRMS (ESI) calcd for C₁₄H₁₉NO₂ [M+Na]⁺: 256.1308; found: 256.1311.



3-Phenyl-*N*-(1-phenylethyl)propenamide (36)⁵⁵

¹H NMR (400 MHz, Chloroform-*d*) δ 7.38 – 7.15 (m, 10H), 5.82 (d, J = 7.9 Hz, 1H), 5.20 – 5.13 (m, 1H), 2.66 (t, J = 7.4 Hz, 2H), 2.23 – 2.17 (m, 2H), 2.03 – 1.96 (m, 2H), 1.50 (d, J = 6.9 Hz, 3H).

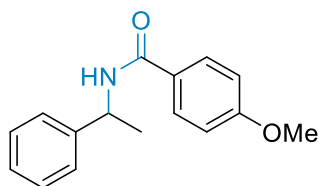
^{13}C NMR (101 MHz, Chloroform-*d*) δ 171.78, 143.14, 141.40, 128.61, 128.43, 128.32, 127.31, 126.12, 125.90, 48.61, 35.84, 35.06, 27.03, 21.64.



4-Methyl-*N*-(1-phenylethyl)benzamide (37)⁵⁵

^1H NMR (400 MHz, Chloroform-*d*) δ 7.67 (d, $J = 8.2$ Hz, 2H), 7.41 – 7.33 (m, 4H), 7.41 – 7.30 – 7.27 (m, 1H), 7.21 (d, $J = 7.9$ Hz, 2H), 6.34 (d, $J = 7.8$ Hz, 1H), 5.37 – 5.30 (m, 1H), 2.39 (s, 3H), 1.60 (d, $J = 6.9$ Hz, 3H).

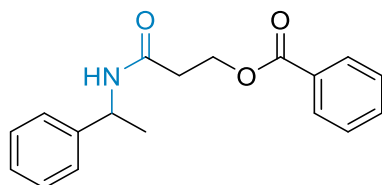
^{13}C NMR (101 MHz, Chloroform-*d*) δ 166.47, 143.21, 141.84, 131.69, 129.16, 128.69, 127.37, 126.89, 126.23, 49.08, 21.72, 21.39.



4-Methoxy-*N*-(1-phenylethyl)benzamide (38)⁵⁵

^1H NMR (400 MHz, Chloroform-*d*) δ 7.80 – 7.73 (m, 2H), 7.42 – 7.34 (m, 4H), 7.31 – 7.27 (m, 1H), 6.92 (d, $J = 8.8$ Hz, 2H), 6.39 (d, $J = 7.8$ Hz, 1H), 5.38 – 5.31 (m, 1H), 3.85 (s, 3H), 1.61 (d, $J = 6.9$ Hz, 3H).

^{13}C NMR (101 MHz, Chloroform-*d*) δ 166.05, 162.10, 143.32, 128.70, 128.65, 127.30, 126.80, 126.21, 113.65, 55.34, 49.06, 21.73.

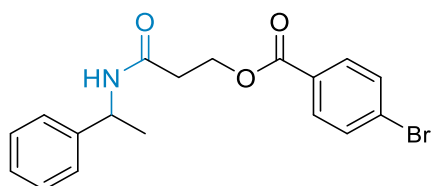


3-Oxo-3-((1-phenylethyl)amino)propyl benzoate (39)

^1H NMR (400 MHz, Chloroform-*d*) δ 7.97 (d, $J = 7.0$ Hz, 2H), 7.58 (t, $J = 7.4$ Hz, 1H), 7.42 (t, $J = 7.8$ Hz, 2H), 7.33 – 7.23 (m, 5H), 6.19 (d, $J = 7.9$ Hz, 1H), 5.22 – 5.15 (m, 1H), 4.63 (td, $J = 6.3, 2.1$ Hz, 2H), 2.66 (t, $J = 6.0$ Hz, 2H), 1.50 (d, $J = 6.9$ Hz, 3H).

^{13}C NMR (101 MHz, Chloroform-*d*) δ 168.98, 166.34, 142.83, 133.07, 129.78, 129.53, 128.62, 128.34, 127.35, 126.07, 61.17, 48.83, 36.25, 21.60.

HRMS (ESI) calcd for $\text{C}_{18}\text{H}_{19}\text{NO}_3$ $[\text{M}+\text{Na}]^+$: 320.1258; found: 320.1258.

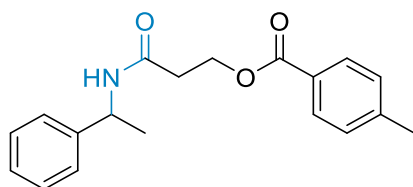


3-Oxo-3-((1-phenylethyl)amino)propyl 4-bromobenzoate (40)

^1H NMR (400 MHz, Chloroform-*d*) δ 7.79 (d, $J = 8.6$ Hz, 2H), 7.53 (d, $J = 8.6$ Hz, 2H), 7.31 – 7.25 (m, 5H), 5.91 (d, $J = 8.0$ Hz, 1H), 5.23 – 5.11 (m, 1H), 4.62 (td, $J = 6.2, 1.8$ Hz, 2H), 2.63 (t, $J = 6.0$, 2H), 1.49 (d, $J = 6.9$ Hz, 3H).

^{13}C NMR (101 MHz, Chloroform-*d*) δ 168.65, 165.62, 142.80, 131.77, 131.72, 131.07, 128.70, 128.23, 127.49, 126.11, 61.40, 48.86, 36.22, 21.59.

HRMS (ESI) calcd for $\text{C}_{18}\text{H}_{18}\text{NO}_3$ $[\text{M}+\text{Na}]^+$: 398.0363, 400.0342; found: 398.0362, 400.0343.

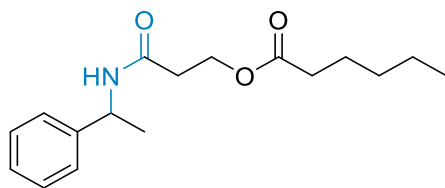


3-Oxo-3-((1-phenylethyl)amino)propyl 4-methylbenzoate (41)

^1H NMR (400 MHz, Chloroform-*d*) δ 7.86 (d, $J = 8.3$ Hz, 2H), 7.33 – 7.19 (m, 7H), 6.15 (d, $J = 8.0$ Hz, 1H), 5.22 – 5.15 (m, 1H), 4.61 (td, $J = 6.3, 2.2$ Hz, 2H), 2.65 (t, $J = 6.0$ Hz, 2H), 2.43 (s, 3H), 1.50 (d, $J = 6.9$ Hz, 3H).

^{13}C NMR (101 MHz, Chloroform-*d*) δ 168.98, 166.41, 143.79, 142.89, 129.57, 129.06, 128.61, 127.32, 127.05, 126.08, 61.00, 48.79, 36.34, 21.63, 21.38.

HRMS (ESI) calcd for $\text{C}_{19}\text{H}_{21}\text{NO}_3$ $[\text{M}+\text{Na}]^+$: 334.1414; found: 334.1415.



3-Oxo-3-((1-phenylethyl)amino)propyl hexanoate (42)

^1H NMR (400 MHz, Chloroform-*d*) δ 7.36 – 7.26 (m, 5H), 5.93 (d, J = 8.0 Hz, 1H), 5.18 – 5.11 (m, 1H), 4.35 (t, J = 6.2 Hz, 2H), 2.50 (t, J = 6.2 Hz, 2H), 2.24 (t, J = 7.6 Hz, 2H), 1.57 – 1.54 (m, 2H), 1.49 (d, J = 6.9 Hz, 3H), 1.33 – 1.23 (m, 4H), 0.88 (t, J = 6.9 Hz, 3H).

^{13}C NMR (101 MHz, Chloroform-*d*) δ 173.63, 168.85, 142.93, 128.66, 127.42, 126.09, 60.43, 48.78, 36.12, 34.11, 31.23, 24.50, 22.24, 21.66, 13.86.

HRMS (ESI) calcd for $\text{C}_{17}\text{H}_{25}\text{NO}_3$ $[\text{M}+\text{Na}]^+$: 314.1727; found: 314.1728.

4.6 References

1. Lundberg, H.; Tinnis, F.; Selander, N.; Adolfsson, H., Catalytic Amide Formation from Non-Activated Carboxylic Acids and Amines. *Chem. Soc. Rev.* **2014**, *43*, 2714-2742.
2. de Figueiredo, R. M.; Suppo, J. S.; Campagne, J. M., Nonclassical Routes for Amide Bond Formation. *Chem. Rev.* **2016**, *116*, 12029-12122.
3. Allen, C. L.; Williams, J. M., Metal-Catalysed Approaches to Amide Bond Formation. *Chem. Soc. Rev.* **2011**, *40*, 3405-3415.
4. Roy, S.; Roy, S.; Gribble, G. W., Metal-Catalyzed Amidation. *Tetrahedron* **2012**, *48*, 9867-9923.
5. Ritter, J. J.; Minieri, P. P., A New Reaction of Nitriles; Amides from Alkenes and Mononitriles. *J. Am. Chem. Soc.* **1948**, *70*, 4045-4048.
6. Ritter, J. J.; Kalish, J., A New Reaction of Nitriles; Synthesis of *t*-Carbinamines. *J. Am. Chem. Soc.* **1948**, *70*, 4048-4050.
7. Chen, M. E.; Chen, X. W.; Hu, Y. H.; Ye, R.; Lv, J. W.; Li, B.; Zhang, F. M., Recent Advances of Ritter Reaction and its Synthetic Applications. *Org. Chem. Front.* **2021**, *8*, 4623-4664.
8. Li, T.; Yang, J.; Yin, X.; Shi, J.; Cao, Q.; Hu, M.; Xu, X.; Li, M.; Shen, Z., Visible-Light-Mediated Aerobic Ritter-Type C-H Amination of Diarylmethanes Using DDQ/*tert*-Butyl Nitrite. *Org. Biomol. Chem.* **2022**, *20*, 8756-8760.

9. Sakaguchi, S.; Hirabayashi, T.; Ishii, Y., First Ritter-Type Reaction of Alkylbenzenes Using *N*-Hydroxyphthalimide as a Key Catalyst. *Chem. Commun.* **2002**, *5*, 516-517.
10. Michaudel, Q.; Thevenet, D.; Baran, P. S., Intermolecular Ritter-Type C-H Amination of Unactivated sp³ Carbons. *J. Am. Chem. Soc.* **2012**, *134*, 2547-2550.
11. Kiyokawa, K.; Takemoto, K.; Minakata, S., Ritter-Type Amination of C-H Bonds at Tertiary Carbon Centers Using Iodic Acid as an Oxidant. *Chem. Commun.* **2016**, *52*, 13082-13085.
12. Zhang, Y.; Dong, J.; Liu, L.; Liu, L.; Zhou, Y.; Yin, S. F., Manganese(III) Acetate Catalyzed Oxidative Amination of Benzylic C(sp³)-H Bonds with Nitriles. *Org. Biomol. Chem.* **2017**, *15*, 2897-2901.
13. Lai, H.; Xu, J.; Lin, J.; Su, B.; Zha, D., Chemo-Selective Control of Ritter-Type Reaction by Coordinatively Unsaturated Inorganic Salt Hydrates. *Org. Chem. Front.* **2022**, *9*, 1541-1549.
14. Shen, T.; Lambert, T. H., C-H Amination via Electrophotocatalytic Ritter-type Reaction. *J. Am. Chem. Soc.* **2021**, *143*, 8597-8602.
15. Zhang, L.; Fu, Y.; Shen, Y.; Liu, C.; Sun, M.; Cheng, R.; Zhu, W.; Qian, X.; Ma, Y.; Ye, J., Ritter-Type Amination of C(sp³)-H Bonds Enabled by Electrochemistry with SO₄²⁻. *Nat. Commun.* **2022**, *13*, 4138.
16. Sun, P.; Liu, P.; Chu, Q.; Zhou, Y.; Ji, C., Electrochemical Benzylic C(sp³)-H Amidation via Ritter-Type Reaction in the Absence of External Mediator and Oxidant. *Synthesis* **2022**, *55*, DOI: 10.1055/a-1992-7066.
17. Li, G. X.; Morales-Rivera, C. A.; Gao, F.; Wang, Y.; He, G.; Liu, P.; Chen, G., A Unified Photoredox-Catalysis Strategy for C(sp³)-H Hydroxylation and Amidation Using Hypervalent Iodine. *Chem. Sci.* **2017**, *8*, 7180-7185.
18. Sun, H.; Cui, G.; Shang, H.; Cui, B., Mn(OAc)₃-Mediated Addition Reactions of NaSO₂CF₃ and Perhalogenated Carboxylic Acids with Unactivated Alkenes Conjectured by a Single Electron Transfer and Halogen Abstraction Mechanism. *J. Org. Chem.* **2020**, *85*, 15241-15255.
19. Verga, D.; Doria, F.; Mella, M.; Freccero, M., Selective Arylation, Alkenylation, and Cyclization of Dibromonaphthols, Using Visible Light, via Carbene Intermediates. *J. Org. Chem.* **2009**, *74*, 5311-5319.
20. Situ, Z.; Chen, W.; Yang, S.; Fan, X.; Liu, F.; Wong, N. K.; Dang, L.; Phillips, D. L.; Li, M. D., Blue or Near-Infrared Light-Triggered Release of Halogens via Blebbistatin Photocage. *J. Phys. Chem. B.* **2022**, *126*, 3338-3346.

21. Goldschleger, I. U.; Senekerimyan, V.; Krage, M. S.; Seferyan, H.; Janda, K. C.; Apkarian, V. A., Quenched by Ice: Transient Grating Measurements of Vibronic Dynamics in Bromine-Doped Ice. *J. Chem. Phys.* **2006**, *124*, 204507.
22. Mohammad, M.; Tariq, M.; Soomro, M. T., "Long-Life" Atom-Free Radical: Generation and Reactions of Bromine Atom-Free Radical. *Collect. Czechoslovak. Chem. Commun.* **2010**, *75*, 1061-1074.
23. Li, X. C.; Ma, J.; Yue, S. Y., Total and Efficient Removal of Tribromoacetic Acid by Ultraviolet Irradiation. *Adv. Mater. Res.* **2012**, *518*, 2939-2943.
24. Moiseev, Y.; Ben-Eliyahu, Y.; Audras, M.; Berthon, L.; Moisy, P.; Bettelheim, A.; Zilbermann, I., Spectroscopic, Electrochemical, and Structural Aspects of the Ce(IV)/Ce(III) DOTA Redox Couple Chemistry in Aqueous Solutions. *J. Coord. Chem.* **2016**, *69*, 2895-2907.
25. Guan, R.; Chen, G.; Bennett, E. L.; Huang, Z.; Xiao, J., Chemoselective Decarboxylative Oxygenation of Carboxylic Acids To Access Ketones, Aldehydes, and Peroxides. *Org. Lett.* **2023**, *25*, 2482-2486.
26. Kim, S.; Kim, I. H.; Akoh, C. C.; Kim, B. H., Enzymatic Production of Cocoa Butter Equivalents High in 1-Palmitoyl-2-Oleoyl-3-Stearin in Continuous Packed Bed Reactors. *J. Am. Oil Chem. Soc.* **2014**, *91*, 747-757.
27. Flinker, M.; Yin, H.; Juhl, R. W.; Eikeland, E. Z.; Overgaard, J.; Nielsen, D. U.; Skrydstrup, T., Efficient Water Reduction with sp^3 - sp^3 Diboron(4) Compounds: Application to Hydrogenations, H-D Exchange Reactions, and Carbonyl Reductions. *Angew. Chem. Int. Ed.* **2017**, *56*, 15910-15915.
28. Everson, D. A.; Shrestha, R.; Weix, D. J., Nickel-Catalyzed Reductive Cross-Coupling of Aryl Halides with Alkyl Halides. *J. Am. Chem. Soc.* **2010**, *132*, 920-921.
29. Morimoto, N.; Yamamoto, S. i.; Takeuchi, Y.; Nishina, Y., Palladium on Graphene: the *in situ* Generation of a Catalyst for the Chemoselective Reduction of α,β -Unsaturated Carbonyl Compounds. *RSC Adv.* **2013**, *3*, 15608-15612.
30. Berger, A. L.; Donabauer, K.; Konig, B., Photocatalytic Carbanion Generation from C-H Bonds-Reductant Free Barbier/Grignard-Type Reactions. *Chem. Sci.* **2019**, *10*, 10991-10996.
31. Mueller, R.; Yang, J.; Duan, C.; Pop, E.; Geoffroy, O. J.; Zhang, L. H.; Huang, T. B.; Denisenko, S.; McCosar, B. H.; Oniciu, D. C.; Bisgaier, C. L.; Pape, M. E.; Freiman, C. D.; Goetz, B.; Cramer, C. T.; Hopson, K. L.; Dasseux, J. L., Long hydrocarbon Chain Keto Diols and Diacids that Favorably Alter Lipid Disorders in Vivo. *J. Med. Chem.* **2004**, *47*, 6082-6099.
32. Owen, C. P.; Shahid, I.; Olusanjo, M. S.; Patel, C. H.; Dhanani, S.; Ahmed, S., Synthesis, Biochemical Evaluation and Rationalisation of the Inhibitory Activity of a Range of Phenyl

- Alkyl Bimidazole-Based Compounds as Potent Inhibitors of the Enzyme Complex 17 α -hydroxylase/17,20-lyase (P450_{17 α}). *J. Steroid. Biochem. Mol. Biol.* **2008**, *111*, 117-127.
33. Kawasaki, M.; Toyooka, N.; Saka, T.; Goto, M.; Matsuya, Y.; Kometani, T., Lipase-Mediated Preparation of Optically Active Isomers of Rosaphen®. *J. Mol. Catal. B. Enzym.* **2010**, *67*, 135-142.
34. Setzer, P.; Forcher, G.; Boeda, F.; Pearson-Long, M. S. M.; Bertus, P., Titanium-Mediated Addition of Grignard Reagents to Acyl Cyanohydrins: Aminocyclopropane versus 1,4-Diketone Formation. *Eur. J. Org. Chem.* **2014**, *2014*, 171-180.
35. Shang, L.; Chang, Y.; Luo, F.; He, J. N.; Huang, X.; Zhang, L.; Kong, L.; Li, K.; Peng, B., Redox-Neutral α -Arylation of Alkyl Nitriles with Aryl Sulfoxides: A Rapid Electrophilic Rearrangement. *J. Am. Chem. Soc.* **2017**, *139*, 4211-4217.
36. Song, X.; Meng, S.; Zhang, H.; Jiang, Y.; Chan, A. S. C.; Zou, Y., Dibrominated Addition and Substitution of Alkenes Catalyzed by Mn₂CO₁₀. *Chem. Commun.* **2021**, *57*, 13385-13388.
37. Li, X.; He, J.; Zhang, Y., BBr₃-Assisted Preparation of Aromatic Alkyl Bromides from Lignin and Lignin Model Compounds. *J. Org. Chem.* **2018**, *83*, 11019-11027.
38. Nandy, S.; Das, A. K.; Bhar, S., Chemoselective Formation of C-N Bond in Wet Acetonitrile using Amberlyst®-15(H) as a Recyclable Catalyst. *Synth. Commun.* **2020**, *50*, 3326-3336.
39. Mondal, A.; Subaramanian, M.; Nandakumar, A.; Balaraman, E., Manganese-Catalyzed Direct Conversion of Ester to Amide with Liberation of H₂. *Org. Lett.* **2018**, *20*, 3381-3384.
40. Narobe, R.; Murugesan, K.; Haag, C.; Schirmer, T. E.; König, B., C(sp³)-H Ritter Amination by Excitation of *in situ* Generated Iodine(III)-BF₃ Complexes. *Chem. Commun.* **2022**, *58*, 8778-8781.
41. Ajvazi, N.; Stavber, S., Direct Substitution of the Hydroxy Group of Alcohols with *N*-Nucleophiles Mediated by the Substoichiometric Amount of Selectfluor™ F-TEDA-BF as a Precatalyst under Mild Reaction Conditions. *Tetrahedron Lett.* **2023**, *115*, 154318.
42. Sanz, R.; Martínez, A.; Guilarte, V.; Álvarez-Gutiérrez, J. M.; Rodríguez, F., The Ritter Reaction under Truly Catalytic Brønsted Acid Conditions. *Eur. J. Org. Chem.* **2007**, *2007*, 4642-4645.
43. Tang, Y. P.; Luo, Y. E.; Xiang, J. F.; He, Y. M.; Fan, Q. H., Rhodium-Catalyzed ON-OFF Switchable Hydrogenation Using a Molecular Shuttle Based on a [2]Rotaxane with a Phosphine Ligand. *Angew. Chem. Int. Ed.* **2022**, *61*, e202200638.
44. Gao, S.; Zhang, L. C.; Zhang, L.; Chen, B.; He, P.; Li, G., Polyoxometalate-Ionic Liquid-Catalyzed Ritter Reaction for Efficient Synthesis of Amides. *Synlett* **2022**, *33*, 1515-1518.

45. Qian, B.; Chen, S.; Wang, T.; Zhang, X.; Bao, H., Iron-Catalyzed Carboamination of Olefins: Synthesis of Amines and Disubstituted β -Amino Acids. *J. Am. Chem. Soc.* **2017**, *139*, 13076-13082.
46. Torre, O.; Gotor-Fernández, V.; Gotor, V., Lipase-Catalyzed Resolution of Chiral 1,3-Amino Alcohols: Application in the Asymmetric Synthesis of (*S*)-Dapoxetine. *Tetrahedron: Asymmetry*. **2006**, *17*, 860-866.
47. Zhu, N.; Wang, T.; Ge, L.; Li, Y.; Zhang, X.; Bao, H., γ -Amino Butyric Acid (GABA) Synthesis Enabled by Copper-Catalyzed Carboamination of Alkenes. *Org. Lett.* **2017**, *19*, 4718-4721.
48. Molander, G. A.; Stengel, P. J., Reduction of 2-Acylaziridines by Samarium(II) Iodide. An Efficient and Regioselective Route to β -Amino Ketones and Esters. *J. Org. Chem.* **2002**, *60*, 6660-6661.
49. Giedyk, M.; Goliszewska, K.; o Proinsias, K.; Gryko, D., Cobalt(I)-Catalysed CH-Alkylation of Terminal Olefins, and Beyond. *Chem. Commun.* **2016**, *52*, 1389-1392.
50. Xu, P.; Qi, F. L.; Han, F. S.; Wang, Y. H., Copper-Catalyzed Reductive *N*-Alkylation of Amides with *N*-Tosylhydrazones Derived from Ketones. *Chem. Asian J.* **2016**, *11*, 2030-2034.
51. Doan, S. H.; Hussein, M. A.; Nguyen, T. V., Tropylium-Promoted Ritter Reactions. *Chem. Commun.* **2021**, *57*, 8901-8904.
52. Biallas, P.; Haring, A. P.; Kirsch, S. F., Cleavage of 1,3-Dicarbonyls through Oxidative Amidation. *Org. Biomol. Chem.* **2017**, *15*, 3184-3187.
53. Czerwinski, P.; Michalak, M., NHC-Cu(I)-Catalyzed Friedlander-Type Annulation of Fluorinated *o*-Aminophenones with Alkynes on Water: Competitive Base-Catalyzed Dibenzo[*b,f*][1,5]diazocine Formation. *J. Org. Chem.* **2017**, *82*, 7980-7997.
54. Cazorla, C.; Métay, E.; Lemaire, M., Oxidative Nucleophilic Substitution: Transformation of Alkylboronic Derivatives. *Tetrahedron* **2011**, *67*, 8615-8621.
55. Dai, C.; Genovino, J.; Bechle, B. M.; Corbett, M. S.; Huh, C. W.; Rose, C. R.; Sun, J.; Warmus, J. S.; Blakemore, D. C., One-Pot Synthesis of α -Branched *N*-Acylamines via Titanium-Mediated Condensation of Amides, Aldehydes, and Organometallics. *Org. Lett.* **2017**, *19*, 1064-1067.

Chapter 5

Exploration of Photocatalytic Oxidation of Cycloalkanes

5.1 Introduction

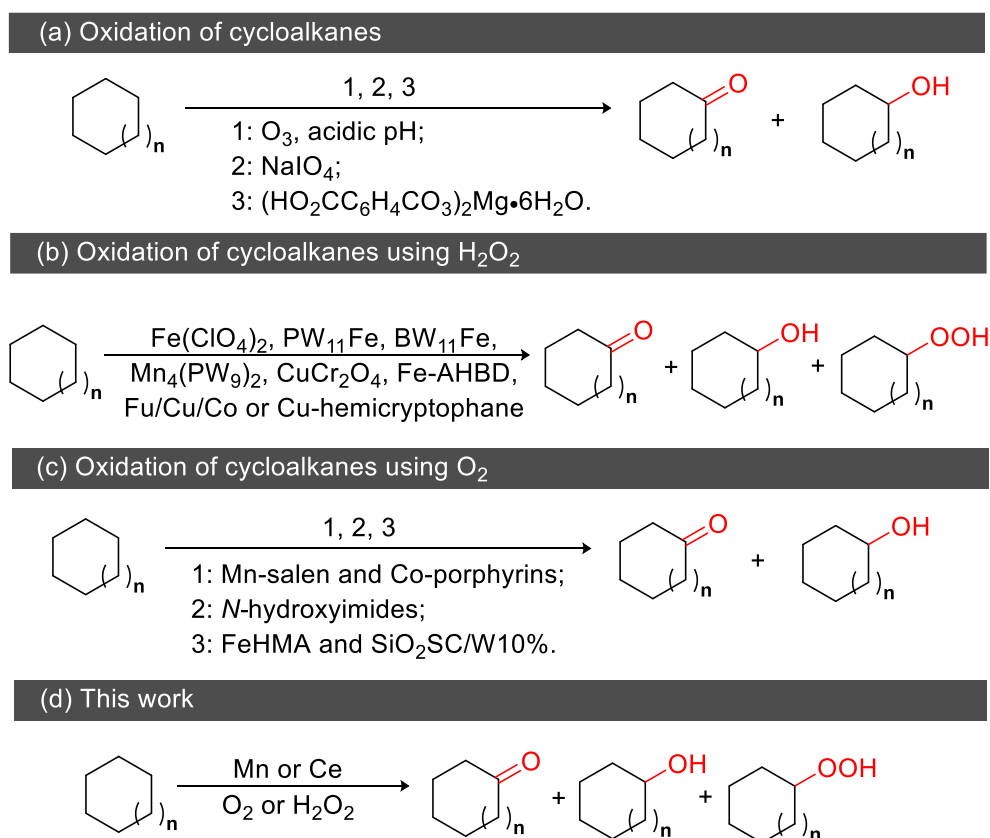
Selective oxidation of saturated alkanes is one of the most challenging issues in organic chemistry. Alkanes are weakly polar, saturated hydrocarbons with strong C-H (99 kcal/mol) and C-C bonds (88 kcal/mol) that tend to interact only weakly with many catalytic substrates.¹⁻⁵ Selective oxidation of alkanes is a key objective in synthetic chemistry.⁶⁻⁸ Although the process of alkane oxidation is favoured thermodynamically, the most significant difficulty associated with this oxidation process is the control of selectivity because complete oxidation of alkanes to CO₂ and H₂O is more favourable in this process. In particular, this overoxidation becomes more acute when high energy oxidants are employed.⁹ Therefore, increasing the selectivity and efficiency of alkane functionalization is the primary objective.

Oxidation of cycloalkanes is one of the most attractive reactions in organic synthesis and industry. The selective oxidation of cycloalkanes can afford a series of valuable products, such as ketones, alcohols and peroxides. For example, cyclohexanone and cyclohexanol afforded by selective oxidation of cyclohexane are important starting materials in industry for the production of nylon.¹⁰⁻¹¹ In addition, hydroperoxides are widely used as initiators for polymerization.¹²

To date, oxidation of cycloalkanes has attracted wide attention and a series of catalytic systems using different oxidants have been investigated. Ozonation of cycloalkanes was proposed early. Barletta and co-workers realized the ozonation of cycloalkanes to corresponding ketones and alcohols in acidic pH conditions (Scheme 5.1a).¹³ However, the low selectivity and unpleasant yields were encountered in their work. Meanwhile, the ozonation process is associated with intrinsic safety issues, the requirement of specialty equipment and

formation of over stoichiometric amounts of waste.¹⁴⁻¹⁵ In addition, stoichiometric amount of oxidants, such as NaIO_4 ¹⁶ and magnesium monoperoxyphthalate (MMPP),¹⁷ have been used in the oxidation of cycloalkanes.

Oxidation processes using green oxidants are needed for green chemistry. Therefore, benign and green oxidants, such as H_2O_2 and O_2 , are more attractive in oxidation reactions. Different catalytic systems using H_2O_2 as oxidants have been reported. A series of heterogenous catalysts, including $\text{Fe}(\text{ClO}_4)_2$,¹⁸ PW_{11}Fe ,¹⁹ BW_{11}Fe ,²⁰ $\text{Mn}_4(\text{PW}_9)_2$,²¹ CuCr_2O_4 ,²² Fe-arylhydrazone- β -diketone (AHBD) complex,²³ Fu/Cu/Co complex,²⁴ and Cu-hemicryptophane,²⁵ have been synthesized for oxidation of cycloalkanes, affording good selectivity of ketones and alcohols (Scheme 5.1b). However, low yields and limited substrate scope may restrict further application of these reactions.



Scheme 5.1 Oxidation of cycloalkanes.

Oxidation of cycloalkanes with molecular O_2 is one of the most attractive approaches to accessing the related ketones and alcohols.²⁶⁻²⁷ Many efforts have been made in this area

(Scheme 5.1c). A variety of metal complexes, such as Mn-salen²⁸ and Co-porphyrins complexes,²⁹⁻³¹ have been shown to be efficient in the oxygenation of cycloalkanes, affording corresponding ketones and alcohols. High temperature (80-120 °C) and pressure (10 atm) are generally required in those reports. Metal-free oxygenation of cycloalkanes has also been realized by using *N*-hydroxyimides as catalysts.³² However, the yields of alcohols and ketones are very low (less than 13%). In addition, some heterogenous catalysts have been proved to be efficient in oxygenation of cycloalkanes. Good yields of cycloalkanols and cycloalkanones have been obtained when iron-substituted hexagonal mesoporous aluminophosphate (FeHMA) molecular sieves and $(n\text{-Bu}_4\text{N})_4\text{W}_{10}\text{O}_{32}$ on amorphous MCM-41 silicas are employed as catalysts,³³⁻³⁴ though those catalysts have only been demonstrated for the oxidation of cyclohexane. The low selectivity is also a drawback shown in previous reports. In most cases, a mixture of cycloalkanones and cycloalkanols is afforded as products.

In this chapter, we attempt to realize the selective oxidation of cycloalkanes to corresponding ketones, alcohols and peroxides using cheap catalysts and green oxidants. Mn catalysts and Ce catalysts were employed, and O₂ and H₂O₂ were used as oxidants. Under optimised conditions, cyclododecane can be transformed to cyclododecanone, cyclododecanol and hydroperoxycyclododecane with good selectivity.

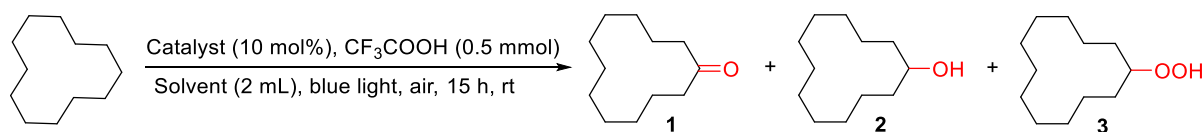
5.2 Exploration of oxygenation of cyclododecane

Selective oxygenation of cycloalkanes to corresponding ketones, alcohols and peroxides is interesting and challenging. Firstly, we aimed at the oxygenation of cycloalkanes to ketones. We started from the exploration of catalytic systems and optimum conditions for the oxidation of cycloalkanes using cyclododecane as the standard substrate. Considering the high efficiency of our Mn-catalytic system and Ce-catalytic systems in C-H functionalization of carboxylic acids to carbonyl products (Chapter 2 and Chapter 3), we started to try the [Mn(dtbpv)₂(OTf)₂]

complex (Chapter 2) and Ce catalysts in the oxidation of cyclododecane. The experiment was conducted under blue light irradiation (465 nm).

As shown in Table 5.1 (entry 1), 17% of cyclododecanone was obtained when $[\text{Mn}(\text{dtbpy})_2(\text{OTf})_2]$ was employed as catalyst. The change of solvent from MeOH to CH_3CN led to no product formation (Table 5.1, entry 2). A better yield (22%) of cyclododecanone was achieved when CeBr_3 was employed as the catalyst (Table 5.1, entry 3). Other Ce catalysts, including $(\text{NH}_4)\text{Ce}(\text{NO}_3)_6$, CeCl_3 , CeF_4 , $\text{Ce}(\text{OAc})_3$ and $\text{Ce}(\text{OTf})_3$, only afforded lower yields (Table 5.1, entries 4-8). We also tried dual-catalytic systems using $[\text{Mn}(\text{dtbpy})_2(\text{OTf})_2]$ combined with other catalysts, such as tetra-*n*-butylammonium decatungstate (TBADT) and 9-methyl-10-methylacridinium. Unfortunately, no good yields were obtained (Table 5.1, entries 9-10).

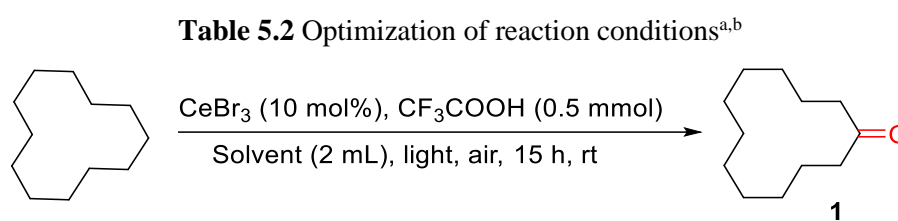
Table 5.1 Optimization of reaction conditions^{a,b}



Entry	Catalyst	Solvent	Yield (%)		
			1	2	3
1 ^c	$[\text{Mn}(\text{dtbpy})_2(\text{OTf})_2]$	MeOH	17	0	0
2 ^c	$[\text{Mn}(\text{dtbpy})_2(\text{OTf})_2]$	CH_3CN	0	0	0
3	CeBr_3	CH_3CN	22	6	5
4	$(\text{NH}_4)\text{Ce}(\text{NO}_3)_6$	CH_3CN	13	0	0
5	CeCl_3	CH_3CN	11	6	0
6	CeF_4	CH_3CN	0	0	0
7	$\text{Ce}(\text{OAc})_3$	CH_3CN	0	0	0
8	$\text{Ce}(\text{OTf})_3$	CH_3CN	8	2	0
9 ^d	$[\text{Mn}(\text{dtbpy})_2(\text{OTf})_2]$	MeOH	9	0	0
10 ^e	$[\text{Mn}(\text{dtbpy})_2(\text{OTf})_2]$	MeOH	0	0	0

^aReaction conditions: catalyst (10 mol%), cyclododecane (0.5 mmol), CF_3COOH (0.5 mmol), solvent (2 mL), blue light (465 nm), air, rt; ^bNMR yields, determined using mesitylene (20 μL) as internal standard; ^c $[\text{Mn}(\text{dtbpy})_2(\text{OTf})_2]$ (5 mol%); ^d $[\text{Mn}(\text{dtbpy})_2(\text{OTf})_2]$ (5 mol%), TBADT (2 mol%); ^e $[\text{Mn}(\text{dtbpy})_2(\text{OTf})_2]$ (5 mol%), 9-methyl-10-methylacridinium (2 mol%).

The employment of CeBr_3 as catalyst afforded the highest yield of cyclododecanone. Therefore, a series of optimization experiments using CeBr_3 as catalyst were conducted to seek better yields. As presented in Table 5.2 (entries 1-3), different light sources (465, 405 and 365 nm) were screened. However, similar yields of cyclododecanone were obtained even when light sources with higher energy were employed. Meanwhile, a variety of different solvents, such as MeOH, DCE, benzene, EtOH and ethyl acetate were screened, but they only afforded trace or none of cyclododecanone.



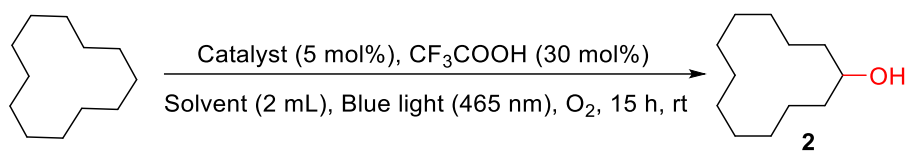
Entry	Solvent	Wavelength of light (nm)	Yield (%)
1	CH_3CN	465 nm	23
2	CH_3CN	405 nm	24
3	CH_3CN	365 nm	26
4	MeOH	465 nm	0
5	DCE	465 nm	2
6	Benzene	465 nm	0
7	EtOH	465 nm	0
8	Ethyl acetate	465 nm	0

^aReaction conditions: catalyst (10 mol%), cyclododecane (0.5 mmol), CF_3COOH (0.5 mmol), solvent (2 mL), blue light (465 nm), air, rt; ^bNMR yields, determined using mesitylene (20 μL) as internal standard.

In Table 5.1 (entry 1), 17% of cyclododecanone was obtained in the conditions of $[\text{Mn}(\text{dtbpy})_2(\text{OTf})_2]$ as catalyst and MeOH as solvent. It is interesting to find that the use of TFE led to a different product, cyclododecanol, in a good yield (36%, Table 5.3, entry 1). As well, cyclododecanol was obtained when DCE and ethyl acetate were used as the solvent, though low yields of cyclododecanol were obtained. After the screening of different solvents, TFE was shown to give highest yield of cyclododecanol. Blue light irradiation was required

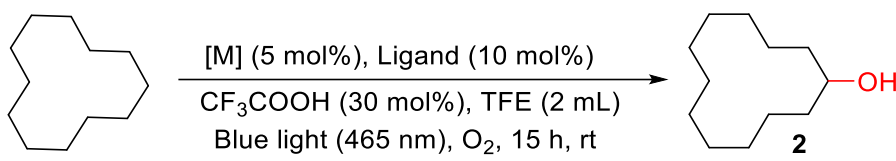
for this oxidation (Table 5.3, entry 12). The replacement of O₂ with H₂O₂ afforded no products (Table 5.3, entry 13). Decrease of the yield of cyclododecanol was observed when more [Mn(dtbp₂)(OTf)₂] and CF₃COOH were added in the reaction (Table 5.3, entries 14-18).

Table 5.3 Optimization of reaction`



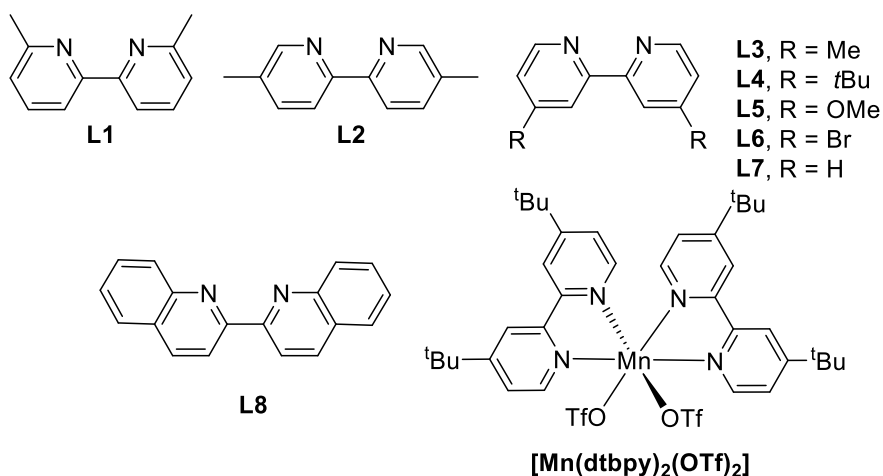
Entry	Catalyst	Solvent	Yield (%)
1	[Mn(dtbp ₂)(OTf) ₂]	TFE	36
2	[Mn(dtbp ₂)(OTf) ₂]	Toluene	0
3	[Mn(dtbp ₂)(OTf) ₂]	DCE	16
4	[Mn(dtbp ₂)(OTf) ₂]	Ethyl acetate	2
5	[Mn(dtbp ₂)(OTf) ₂]	TFE/MeOH	31
6	[Mn(dtbp ₂)(OTf) ₂]	TFE/toluene	0
7	[Mn(dtbp ₂)(OTf) ₂]	TFE/ Ethyl acetate	0
8	[Mn(dtbp ₂)(OTf) ₂]	TFE/Trifluorotoluene	21
9	[Mn(dtbp ₂)(OTf) ₂]	TFE/benzene	0
10	[Mn(dtbp ₂)(OTf) ₂]	TFE/chloroform	18
11	[Mn(dtbp ₂)(OTf) ₂]	TFE/DCE	27
12 ^c	[Mn(dtbp ₂)(OTf) ₂]	TFE	0
13 ^d	[Mn(dtbp ₂)(OTf) ₂]	TFE	0
14 ^e	[Mn(dtbp ₂)(OTf) ₂]	TFE	24
15 ^f	[Mn(dtbp ₂)(OTf) ₂]	TFE	15
16 ^g	[Mn(dtbp ₂)(OTf) ₂]	TFE	29
17 ^h	[Mn(dtbp ₂)(OTf) ₂]	TFE	30
18 ⁱ	[Mn(dtbp ₂)(OTf) ₂]	TFE	Trace

^aReaction conditions: catalyst (10 mol%), CF₃COOH (30 mol%), solvent (2 mL), blue light (465 nm), O₂, rt; ^bNMR yields, determined using mesitylene (20 μL) as internal standard; ^c40 °C; ^d40 °C, H₂O₂ (1 mmol); ^e[Mn(dtbp₂)(OTf)₂] (10 mol%); ^f[Mn(dtbp₂)(OTf)₂] (20 mol%); ^gCF₃COOH (60 mol%); ^hCF₃COOH (90 mol%); ⁱCF₃COOH (2 mmol).

Table 5.4 Optimization of reaction conditions^{a,b}

Entry	[M]	Ligand	Yield (%)
1	Mn(OTf) ₂	L4	36
2	MnBr ₂	L4	16
3	MnCl ₂	L4	18
4	MnF ₂	L4	11
5	MnF ₃	L4	23
6	Mn(OAc) ₃	L4	17
7	Cu(OAc) ₂	L4	0
8	Fe(OTf) ₂	L4	Trace
9	Mn(OTf) ₂	L1	0
10	Mn(OTf) ₂	L2	21
11	Mn(OTf) ₂	L3	28
12	Mn(OTf) ₂	L4	36
13	Mn(OTf) ₂	L5	17
14	Mn(OTf) ₂	L6	0
15	Mn(OTf) ₂	L7	Trace
16	Mn(OTf) ₂	L8	Trace

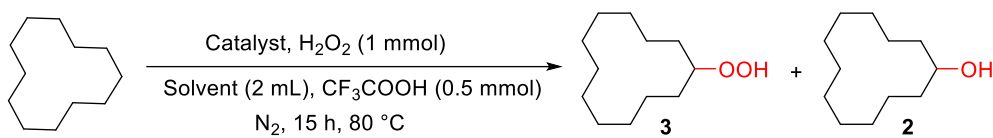
^aReaction conditions: catalyst (10 mol%), CF₃COOH (30 mol%), solvent (2 mL), blue light (465 nm), O₂, rt; ^bNMR yields, determined using mesitylene (20 μL) as internal standard.



After a series of attempts, the highest yield of cyclododecanol in our Mn-catalytic system was 36%. Although a good result has been obtained in the oxygenation of cyclododecane, this

yield is lower than our expectation. We then tried to seek for more effective Mn catalysts (Table 5.4). Firstly, a variety of Mn salts and other metal salts were tested. In comparison with Mn(OTf)₂, Mn salts, including MnBr₂, MnCl₂, MnF₂, MnF₃ and Mn(OAc)₃, all were less effective, affording lower yields of cyclododecanol. As well, other metal salts, such as Cu(OAc)₂ and Fe(OTf)₂, were investigated, but trace or no cyclododecanol was formed.

Table 5.5 Optimization of reaction conditions^{a,b}



Entry	Catalyst	Solvent	Yield (%)	
			3	2
1	5CeBa	iPrOH	10	7
2	5CeBa	Ethyl acetate	21	3
3	5CeBa	MeOH	0	0
4	5CeBa	Toluene	0	0
5	5CeBa	Hexane	0	0
6	5CeBa	DCE	0	0
7	5NiTi	Ethyl acetate	15	2
8	10CeTi	Ethyl acetate	0	2
9 ^c	5CeBa	Ethyl acetate	5	2
10 ^d	5CeBa	Ethyl acetate	8	2
11 ^e	5CeBa	Ethyl acetate	21	4
12 ^f	5CeBa	Ethyl acetate	0	0
13 ^g	5CeBa	Ethyl acetate	0	0
14 ^h	5CeBa	Ethyl acetate	0	0

^aReaction conditions: catalyst (10 mg), CF₃COOH (0.5 mmol), solvent (2 mL), H₂O₂ (1 mmol), N₂, 80 °C; ^bNMR yields, determined using mesitylene (20 μL) as internal standard; ^cH₂O₂ (0.25 mmol); ^dH₂O₂ (0.5 mmol); ^eH₂O₂ (2 mmol); ^f40 °C; ^gH₂O₂ (1 mmol), blue light, rt; ^hair, blue light, rt. The formulas of heterogeneous catalysts can be seen in Section 5.4.2.

On the other hand, the optimization of ligands was conducted. A series of bipyridine ligands with different functional groups were employed to coordinate with Mn(OTf)₂. Bipyridine ligands bearing Me groups on ortho, meta and para positions were tested firstly. No

product was formed when bipyridine bearing *o*-Me group was employed as ligand, whereas bipyridines bearing *m*-Me and *p*-Me group afforded 21 and 28% of cyclododecanol (Table 5.4, entries 9-11), respectively. Electron-donating groups and electron-withdrawing groups were explored, revealing **L4** to be better than other bipyridine ligands (Table 5.4, entries 11-15). 2,2'-Biquinoline was also employed; unfortunately, only a trace of cyclododecanol was detected.

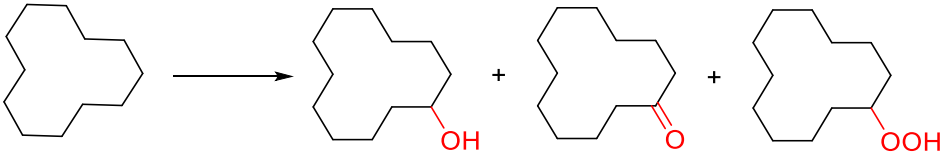
Apart from photocatalysis, we also explored thermal catalytic oxidation of cyclododecane with H₂O₂. We tested a series of heterogeneous catalysts, including (Ba_{0.95}Ce_{0.05})TiO₃ (5CeBa), (Ba_{0.95}Ni_{0.05})TiO₃ (5NiTi) and Ba(Ti_{0.9}Ce_{0.1})O₃ (10CeTi), prepared by Dr. Ilkan Calisir of our group (For details, see Section 5.4.2). Interestingly, selective oxidation of cyclododecane to hydroperoxycyclododecane can be realized with some of these heterogeneous catalysts. As shown in Table 5.5 (entry 1), 10% of hydroperoxycyclododecane was afforded in the presence of 5CeBa as catalyst and H₂O₂ as oxidant. The screening of different solvents, including ethyl acetate, MeOH, toluene, hexane and DCE, was conducted in the next step (Table 5.5, entries 2-6). The results revealed that ethyl acetate showed the highest yield of hydroperoxycyclododecane (21%). The screening of other heterogeneous catalysts, such as 5NiTi and 10CeTi, didn't afford better yields (Table 5.5, entries 7-8). A lower amount of H₂O₂ led to the decrease of the yield of hydroperoxycyclododecane (Table 5.5, entries 9-10). The effect of temperature was considered. However, no reaction was observed under a lower temperature (Table 5.5, entry 12). Blue light irradiation and air were also introduced in the oxidation of cyclododecane. However, no product was formed under blue light irradiation with H₂O₂ or air as oxidant (Table 5.5, entries 13-14).

In conclusion, we have explored three different catalytic systems for selective oxidation of cyclododecane. As is shown, cyclododecane can be selectively transformed to cyclododecanone, cyclododecanol and hydroperoxycyclododecane, respectively. Although the

current yields of cyclododecanone, cyclododecanol and hydroperoxycyclododecane are moderate, our methods show high potential for the selective oxidation of cycloalkanes to corresponding oxygenated products in good selectivity.

To illustrate the advantage of our systems, we looked into some previous reports about the oxidation of cyclododecane. As shown in Table 5.6, a series of different catalytic systems for oxidation of cyclododecane have been reported. However, all these methods afforded a mixture of cyclododecanone and cyclododecanol with or without hydroperoxycyclododecane as the final products. Although oxidation of cyclododecane proceeded successfully, low yields of oxidation products were obtained by the She group and Sheldon group.^{29, 35} Better yields of cyclododecanone and cyclododecanol were reported by Cavaleiro and Selvam.^{20, 33} The PW₁₁Fe-catalytic system needed high temperature, and the FeHMA-catalytic system required the assistance of methyl ethyl ketone as initiator and high temperature.

Table 5.6 Literature catalysts for oxidation of cyclododecane



The reaction scheme shows cyclododecane (a 12-membered ring) reacting to form three products: cyclododecanol (with an -OH group), cyclododecanone (with a =O group), and hydroperoxycyclododecane (with an -OOH group). The products are shown with red highlighting on the oxygen-containing functional groups.

Group	Catalyst	Yield (%)		
		Alcohol	Ketone	Peroxide
Cavaleiro ²⁰	PW ₁₁ Fe	13	32	18
She ²⁹	T(4-COOCH ₃)PPCo	4	12	8
Selvam ³³	FeHMA	41	39	0
Sheldon ³⁵	NHS/Co	17	7	0

5.3 Conclusions and future work

We have identified methods that can realize the transformation of cyclododecane to ketones and alcohols under mild conditions with O₂ as oxidant. Cheap and easily-available Mn and Ce were employed as catalysts. Good selectivity was obtained with our methods. In addition, oxidation of the cycloalkane to a hydroperoxide has been realized by using a

heterogenous 5CeBa catalyst with H₂O₂ as oxidant without byproducts. Unfortunately, only preliminary exploration and optimization of our strategies could be conducted because of limited time. I believe further optimization of these catalytic systems can realize the selective oxidation of cycloalkanes to alcohols, ketones or hydroperoxides with good selectivity, high yields and wide substrate scope.

5.4 Experimental details

5.4.1 Details of photoreactors

Detail information of photoreactors can be seen in Section 2.3.

5.4.2 Synthesis of catalysts

Synthesis of [Mn(dtbpv)₂(OTf)₂]³⁶

To an oven dried Schlenk tube, Mn(OTf)₂ (8.8 mg, 5 mol%) and 4,4'-di-tert-butyl-2,2'-bipyridine (13.4 mg, 10 mol%) were added. Then the reaction tube was placed under vacuum and purged with nitrogen at least three times. Then 1 mL of CH₃CN was added via syringe under N₂. The Schlenk tube was allowed to stir at 80 °C for 1 h to obtain [Mn(dtbpv)₂(OTf)₂] to be used in subsequent oxidation.

Synthesis of heterogenous catalysts

Ce-substituted ceramics were synthesised by Dr. Ilkan Calisir of the Xiao group. These ceramics were synthesised by the solid state reaction method, based on the chemical formulas of: a) Ba(Ti_{1-x}Ce_x)O₃ where $x = 0.10$ abbreviated as 10 CeTi; b) (Ba_{1-y}Ce_y)TiO₃ where $y = 0.05$ abbreviated as 5CeBa; c) (Ba_{1-z}Ni_z)TiO₃ where $z = 0.05$ abbreviated as 5NiTi. Starting powders used in the synthesis were BaCO₃, TiO₂, NiO and CeO₂ and these powders were mixed with ethanol and subjected to high-energy planetary milling for a duration of 4 hours. Following the milling process, the powders were dried overnight and calcined at 1050 °C for 4 hours using a high temperature furnace in an air environment. Subsequently, the calcined powders underwent an additional milling process for 6 hours, followed by another overnight drying period. The

resulting calcined powders were sintered at a temperature of 1300 °C for 4 hours in an air atmosphere. The resulting solid ceramics were then ground using a pestle and mortar for subsequent use in catalysis.

5.4.3 General procedure for selective oxidation of cyclododecane

General procedure for photocatalytic oxidation of cyclododecane of cyclododecanone

To an oven dried Schlenk tube, catalyst (5 mol%), cyclododecane (0.5 mmol), trifluoroacetic acid (30 mol%), solvent (2 mL) were added under air. The reaction tube was then allowed to stir at room temperature under blue light for 15 h. After reaction, mesitylene (17.3 mg) as internal standard, water (2 mL) and CDCl₃ (2 mL) were added. Finally, the product yield was obtained by ¹H NMR analysis of the organic layer.

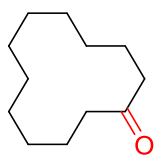
General procedure for photocatalytic oxidation of cyclododecane of cyclododecanol

To an oven dried Schlenk tube, [Mn(dtbp)₂(OTf)₂] (5 mol%) was in situ synthesized. Then, cyclododecane (0.5 mmol), trifluoroacetic acid (30 mol%), solvent (2 mL) were added under N₂. The reaction tube was then fitted with an oxygen balloon, and was allowed to stir at room temperature under blue light for 15 h. After reaction, mesitylene (17.3 mg) as internal standard, water (2 mL) and CDCl₃ (2 mL) were added. Finally, the product yield was obtained by ¹H NMR analysis of the organic layer.

General procedure for thermal oxidation of cyclododecane of hydroperoxycyclododecane

To an oven dried Schlenk tube, catalyst (10 mg), cyclododecane (0.5 mmol), were added under N₂. Then the reaction tube was placed under vacuum and purged with nitrogen at least three times. After that, H₂O₂ (1 mmol), trifluoroacetic acid (0.5 mmol) and solvent (2 mL) were added under N₂. The reaction tube was then allowed to stir at room temperature under blue light for 15 h. After reaction, mesitylene (17.3 mg) as internal standard, water (2 mL) and CDCl₃ (2 mL) were added. Finally, the product yield was obtained by ¹H NMR analysis of the organic layer.

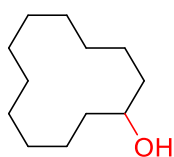
5.5 Analytical data of products



Cyclododecanone³⁷

¹H NMR (400 MHz, Chloroform-*d*) δ 2.52 – 2.40 (m, 4H), 1.77 – 1.65 (m, 4H), 1.37 – 1.16 (m, 14H).

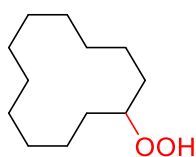
¹³C NMR (101 MHz, Chloroform-*d*) δ 212.92, 40.36, 24.73, 24.58, 24.21, 22.54, 22.32.



Cyclododecanol³⁸

¹H NMR (400 MHz, Chloroform-*d*) δ 3.93 – 3.80 (m, 1H), 1.79 – 1.00 (m, 22H).

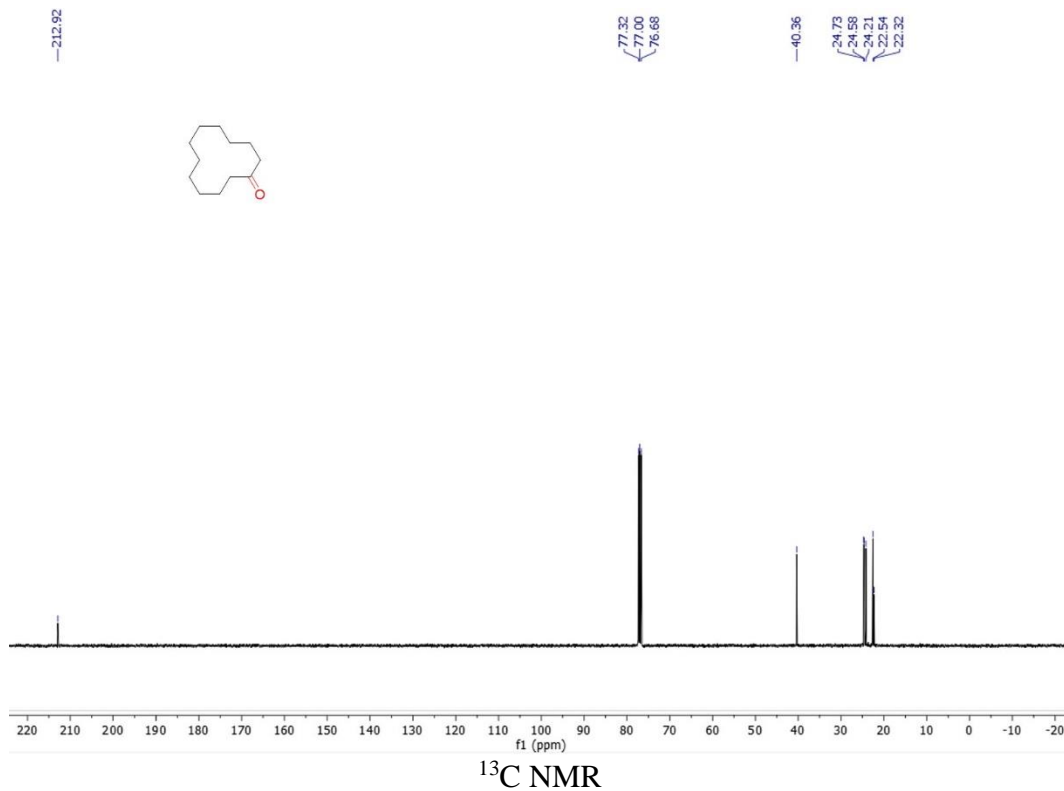
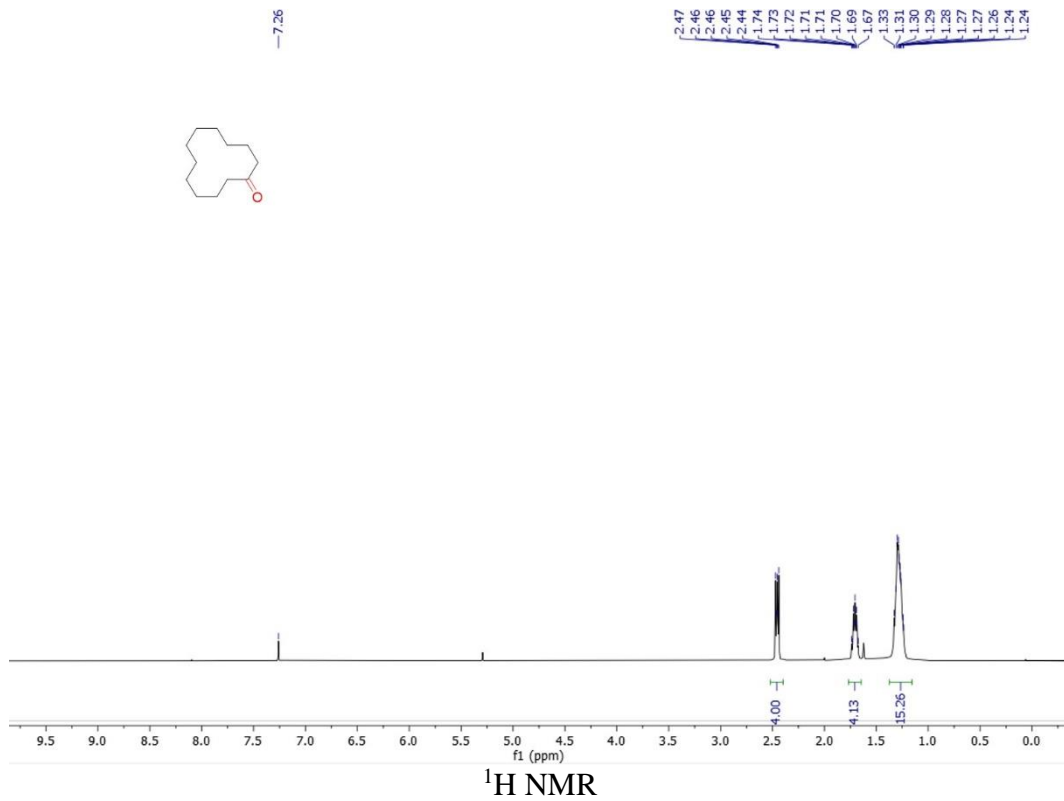
¹³C NMR (101 MHz, Chloroform-*d*) δ 69.21, 32.48, 24.21, 23.82, 23.36, 23.27, 20.96.

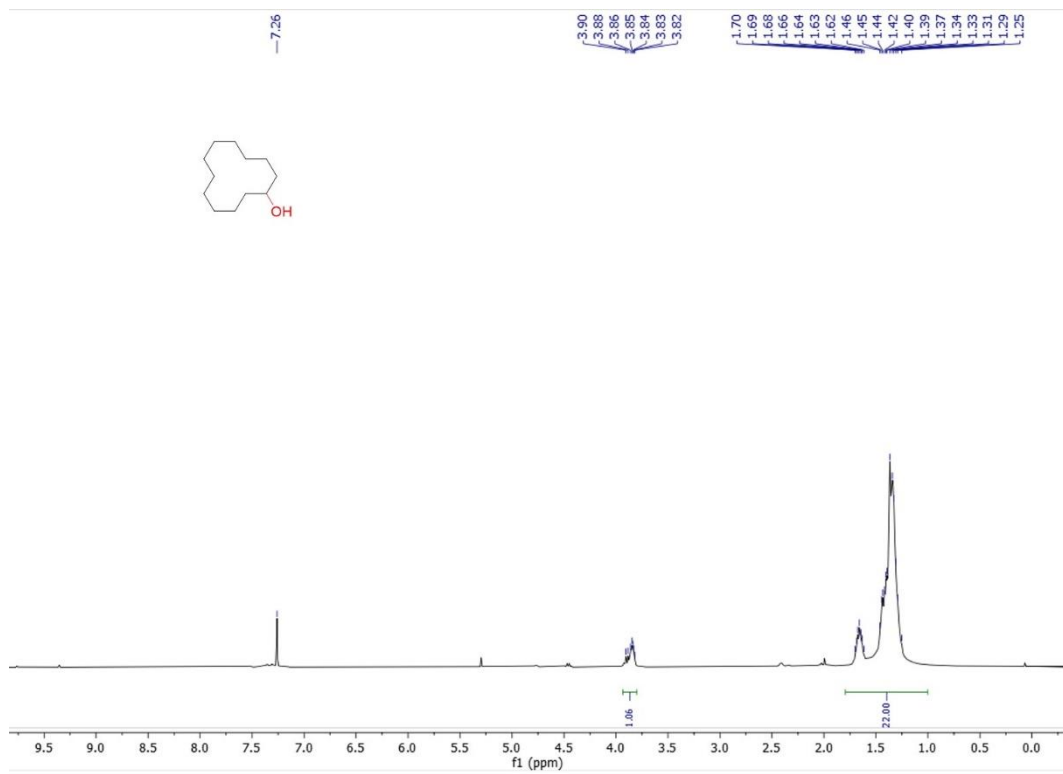


Hydroperoxycyclododecane³⁹

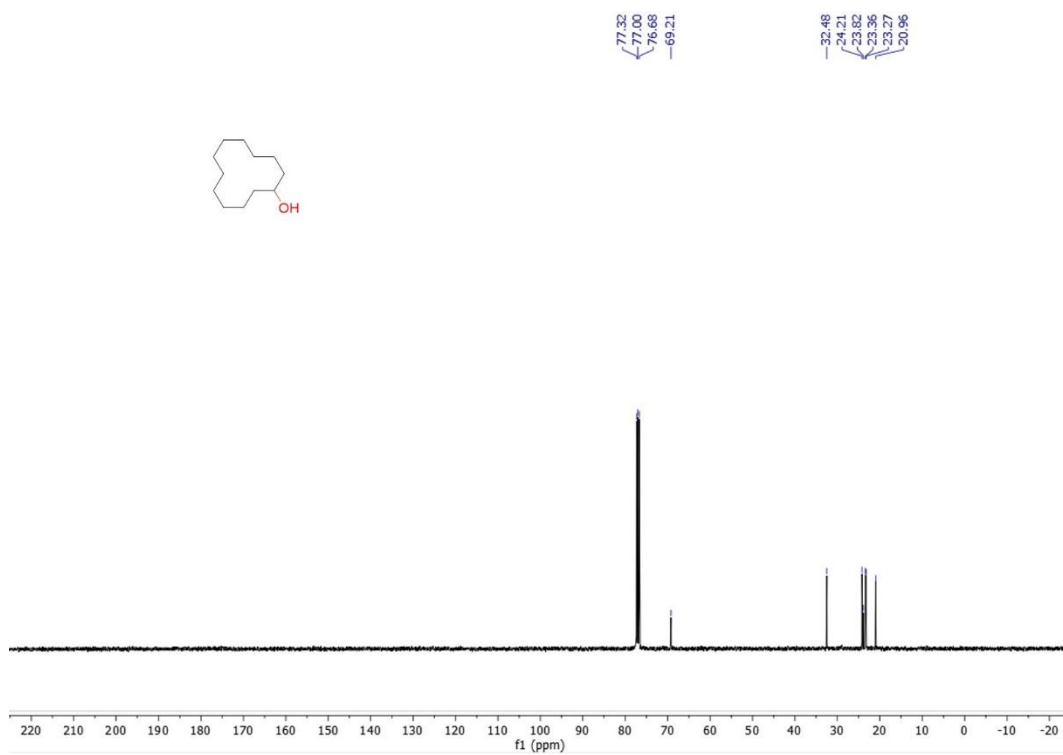
¹H NMR (400 MHz, Chloroform-*d*) δ 4.16 – 4.10 (m, 1H), 1.64 – 1.30 (m, 22H).

¹³C NMR (101 MHz, Chloroform-*d*) δ 83.38, 27.34, 24.38, 23.82, 23.34, 23.26, 21.07.

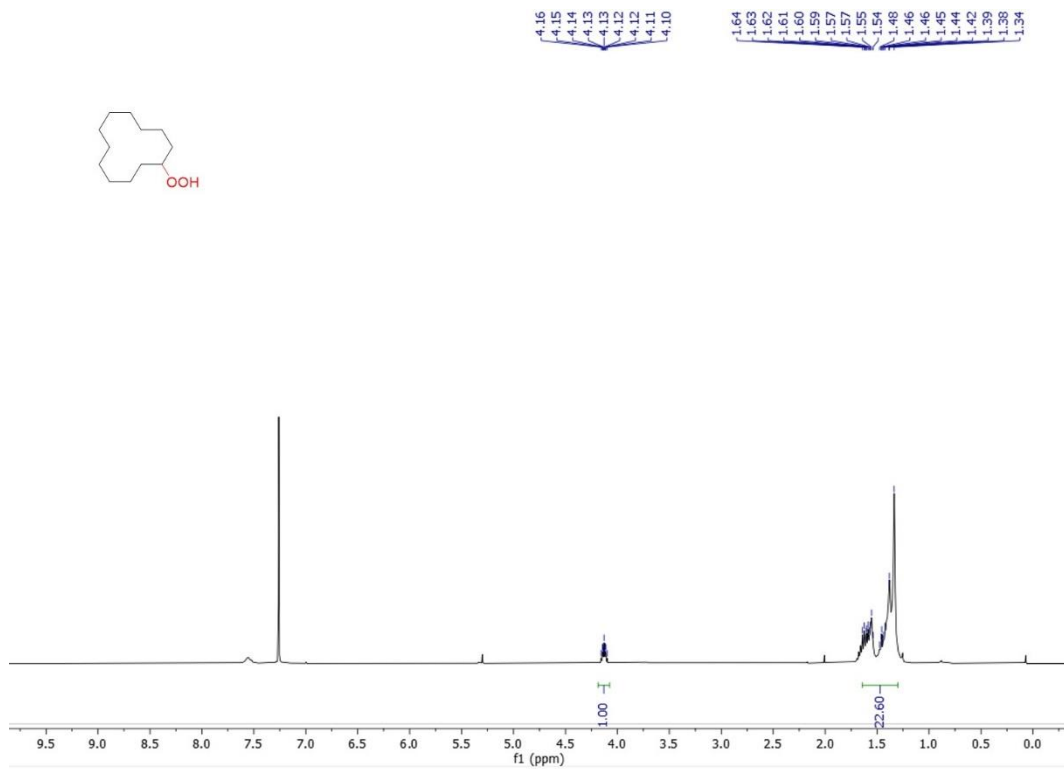




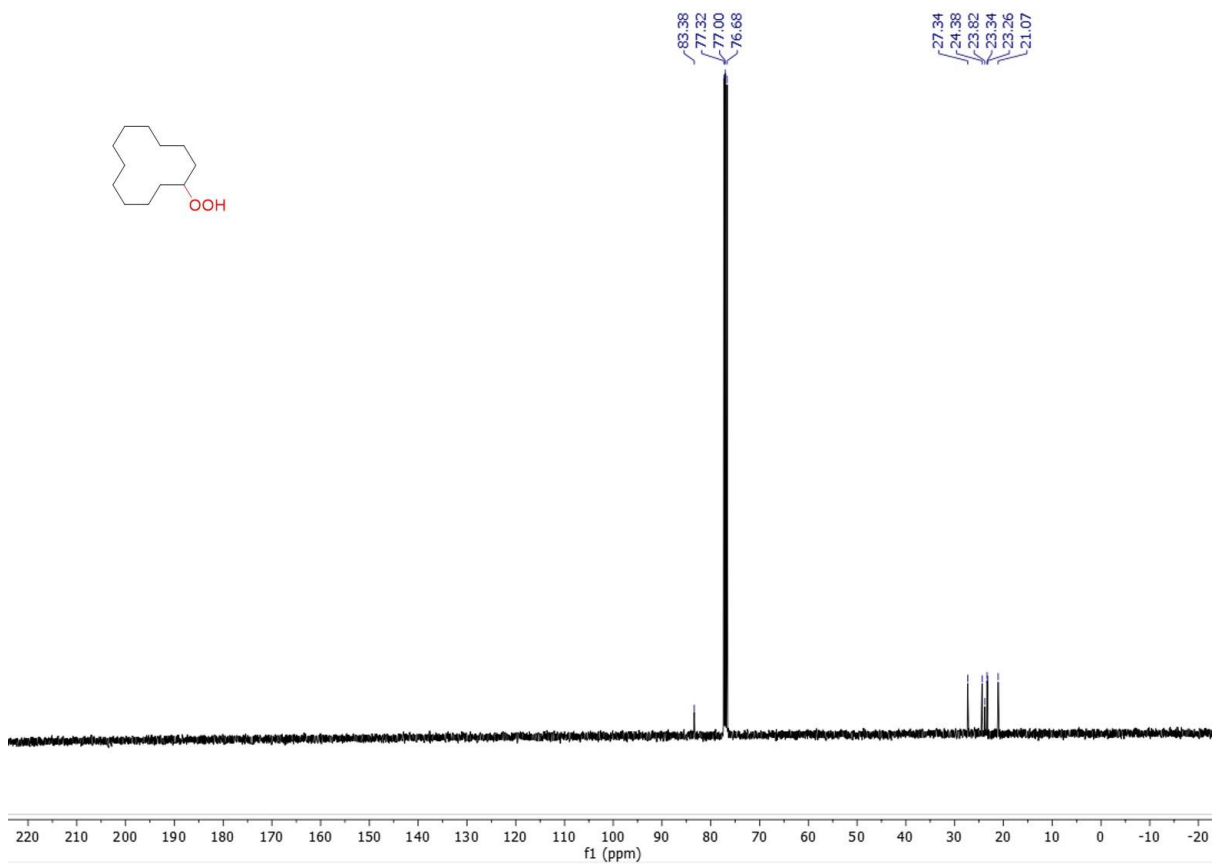
^1H NMR



^{13}C NMR



¹H NMR



¹³C NMR

5.6 References

1. Sheldon, R.; Kochi, J., *Metal-Catalyzed Oxidations of Organic Compound*. Academic Press, New York: **1981**.
2. Hill, C., *Activation and Functionalization of Alkanes*. Wiley, New York: **1989**.
3. Shilov, A.; Shul'pin, G., *Activation and Catalytic Reactions of Saturated Hydrocarbons in the Presence of Metal Complexes*. Springer Science & Business Media: **2001**.
4. Curci, R.; D'Accolti, L.; Fusco, C., A Novel Approach to the Efficient Oxygenation of Hydrocarbons under Mild Conditions. Superior Oxo Transfer Selectivity Using Dioxiranes. *Acc. Chem. Res.* **2006**, *39*, 1-9.
5. Luo, Y. R., *Handbook of Bond Dissociation Energies in Organic Compounds*. CRC Press: **2002**.
6. Rosenzweig, A. C., Biochemistry: Breaking Methane. *Nature* **2015**, *518*, 309-310.
7. Wang, V. C.; Maji, S.; Chen, P. P.; Lee, H. K.; Yu, S. S.; Chan, S. I., Alkane Oxidation: Methane Monooxygenases, Related Enzymes, and Their Biomimetics. *Chem. Rev.* **2017**, *117*, 8574-8621.
8. Sankaralingam, M.; Balamurugan, M.; Palaniandavar, M., Alkane and Alkene Oxidation Reactions Catalyzed by Nickel(II) Complexes: Effect of Ligand Factors. *Coord. Chem. Revi.* **2020**, *403*, 213085.
9. Martin, R.; Kim, M.; Asthagiri, A.; Weaver, J. F., Alkane Activation and Oxidation on Late-Transition-Metal Oxides: Challenges and Opportunities. *ACS Catal.* **2021**, *11*, 4682-4703.
10. Garcia Villaluenga, J. P.; Tabe-Mohammadi, A., A Review on the Separation of Benzene/Cyclohexane VMixtures by Pervaporation Processes. *J. Membr. Sci.* **2000**, *169*, 159-174.
11. Dintzner, M. R.; Kinzie, C. R.; Pulkrabek, K.; Arena, A. F., The Cyclohexanol Cycle and Synthesis of Nylon 6,6: Green Chemistry in the Undergraduate Organic Laboratory. *J. Chem. Edu.* **2011**, *89*, 262-264.
12. Wicklatz, J. E.; Kennedy, T. J.; Reynolds, W. B., Hydroperoxides as Initiators of Emulsion Polymerizations at Low Temperatures. *J. Poly. Sci.* **1951**, *6*, 45-58.
13. Barletta, B.; Bolzacchini, E.; Fossati, L.; Meinardi, S.; Orlandi, M.; Rindone, B., Metal-Free Functionalization of the Unactivated Carbon-Hydrogen Bond: the Oxidation of Cycloalkanes to Cycloalkanones with Ozone. *Ozone. Sci. Eng.* **1998**, *20*, 91-98.
14. Ogle, R. A.; Schumacher, J. L., Investigation of an Explosion and Flash Fire in a Fixed Bed Reactor. *Process. Saf. Prog.* **1998**, *17*, 127-133.

15. Koike, K.; Inoue, G.; Fukuda, T., Explosion Hazard of Gaseous Ozone. *J. Eng. Jap.* **1999**, *32*, 295-299.
16. Mohajer, D.; Tayebee, R.; Goudarziafshar, H., Oxidation of Cycloalkanes and Arylalkanes with Sodium Periodate Catalysed by Manganese Porphyrins. *J. Chem. Res.* **1998**, *12*, 822-823.
17. Połtowicz, J.; Pamin, K.; Haber, J., Influence of Manganese Tetraarylporphyrins Substituents on the Selectivity of Cycloalkanes Oxidation with Magnesium Monoperoxyphthalate. *J. Mol. Catal. A.* **2006**, *257*, 154-157.
18. Pavan, C.; Legros, J.; Bolm, C., Iron-Catalyzed Oxidation of Cycloalkanes and Alkylarenes with Hydrogen Peroxide. *Adv. Syn. Catal.* **2005**, *347*, 703-705.
19. Simões, M. M. Q.; Santos, I. C. M. S.; Balula, M. S. S.; Gamelas, J. A. F.; Cavaleiro, A. M. V.; Neves, M. G. P. M. S.; Cavaleiro, J. A. S., Oxidation of Cycloalkanes with Hydrogen Peroxide in the Presence of Keggin-Type Polyoxotungstates. *Catal. Today* **2004**, *91*, 211-214.
20. Cavaleiro, A.; Santos, I.; Simões, M.; Balula, M.; Neves, M.; Cavaleiro, J., A New Insight into the Oxidation of Cyclododecane with Hydrogen Peroxide in the Presence of Iron-Substituted Polyoxotungstates. *Synlett* **2008**, *2008*, 1623-1626.
21. Santos, I. C. M. S.; Gamelas, J. A. F.; Balula, M. S. S.; Simões, M. M. Q.; Neves, M. G. P. M. S.; Cavaleiro, J. A. S.; Cavaleiro, A. M. V., Sandwich-Type Tungstophosphates in the Catalytic Oxidation of Cycloalkanes with Hydrogen Peroxide. *J. Mol. Catal. A.* **2007**, *262*, 41-47.
22. Acharyya, S. S.; Ghosh, S.; Adak, S.; Tripathi, D.; Bal, R., Fabrication of CuCr_2O_4 Spinel Nanoparticles: A Potential Catalyst for the Selective Oxidation of Cycloalkanes via Activation of $\text{Csp}^3\text{-H}$ Bond. *Catal. Commun.* **2015**, *59*, 145-150.
23. Kopylovich, M. N.; MacLeod, T. C.; Haukka, M.; Amanullayeva, G. I.; Mahmudov, K. T.; Pombeiro, A. J., Aquasoluble Iron(III)-Arylhydrazone- β -Diketone Complexes: Structure and Catalytic Activity for the Peroxidative Oxidation of $\text{C}_5\text{-C}_8$ Cycloalkanes. *J. Inorg. Biochem.* **2012**, *115*, 72-77.
24. Nesterov, D. S.; Kokozay, V. N.; Dyakonenko, V. V.; Shishkin, O. V.; Jezierska, J.; Ozarowski, A.; Kirillov, A. M.; Kopylovich, M. N.; Pombeiro, A. J., An Unprecedented Heterotrimetallic Fe/Cu/Co Core for Mild and Highly Efficient Catalytic Oxidation of Cycloalkanes by Hydrogen Peroxide. *Chem. Commun.* **2006**, *44*, 4605-4607.
25. Perraud, O.; Sorokin, A. B.; Dutasta, J. P.; Martinez, A., Oxidation of Cycloalkanes by H_2O_2 Using a Copper-Hemicryptophane Complex as a Catalyst. *Chem. Commun.* **2013**, *49*, 1288-1290.

26. Barton, D. H.; Martell, A. E.; Sawyer, D. T., *The Activation of Dioxygen and Homogeneous Catalytic Oxidation*. Springer Science & Business Media: **2012**.
27. Ellis, P., Selective Air Oxidation of Light Alkanes Catalyzed by Activated Metalloporphyrins-The Search for a Suprabiotic System. *Coord. Chem. Rev.* **1990**, *105*, 181-193.
28. Pamin, K.; Pozzi, G.; Tabor, E.; Bukowski, W.; Połtowicz, J., Oxidation of Cycloalkanes with Molecular Oxygen in the Presence of Salen Metallocomplexes in Thermomorphic Conditions. *Catal. Commun.* **2013**, *39*, 102-105.
29. Shen, H. M.; Wang, X.; Ning, L.; Guo, A. B.; Deng, J. H.; She, Y. B., Efficient Oxidation of Cycloalkanes with Simultaneously Increased Conversion and Selectivity Using O₂ Catalyzed by Metalloporphyrins and Boosted by Zn(AcO)₂: A Practical Strategy to Inhibit the Formation of Aliphatic Diacids. *Appl. Catal. A.* **2021**, *609*, 117904.
30. Pamin, K.; Tabor, E.; Gorecka, S.; Kubiak, W. W.; Rutkowska-Zbik, D.; Poltowicz, J., Three Generations of Cobalt Porphyrins as Catalysts in the Oxidation of Cycloalkanes. *ChemSusChem* **2019**, *12*, 684-691.
31. Shen, H. M.; Wang, X.; Huang, H.; Liu, Q. P.; Lv, D.; She, Y. B., Staged Oxidation of Hydrocarbons with Simultaneously Enhanced Conversion and Selectivity Employing O₂ as Oxygen Source Catalyzed by 2D Metalloporphyrin-Based MOFs Possessing Bimetallic Active Centers. *Chem. Eng. J.* **2022**, *443*, 136126.
32. Lisicki, D.; Orlińska, B., Oxidation of Cycloalkanes Catalysed by *N*-Hydroxyimides in Supercritical Carbon Dioxide. *Chem. Pap.* **2019**, *74*, 711-716.
33. Mohapatra, S. K.; Selvam, P., Selective Oxidation of Cycloalkanes over Iron-Substituted Hexagonal Mesoporous Aluminophosphate Molecular Sieves. *Chem. Lett.* **2004**, *33*, 198-199.
34. Maldotti, A.; Molinari, A.; Varani, G.; Lenarda, M.; Storaro, L.; Bigi, F.; Maggi, R.; Mazzacani, A.; Sartori, G., Immobilization of (n-Bu₄N)₄W₁₀O₃₂ on Mesoporous MCM-41 and Amorphous Silicas for Photocatalytic Oxidation of Cycloalkanes with Molecular Oxygen. *J. Catal.* **2002**, *209*, 210-216.
35. Baucherel, X.; Gonsalvi, L.; Arends, I. W. C. E.; Ellwood, S.; Sheldon, R. A., Aerobic Oxidation of Cycloalkanes, Alcohols and Ethylbenzene Catalyzed by the Novel Carbon Radical Chain Promoter NHS (*N*-Hydroxysaccharin). *Adv. Syn. Catal.* **2004**, *346*, 286-296.
36. Guan, R.; Bennett, E. L.; Huang, Z.; Xiao, J., Decarboxylative Oxygenation of Carboxylic Acids with O₂ via a Non-Heme Manganese Catalyst. *Green Chem.* **2022**, *24*, 2946-2952.

37. Moriyama, K.; Takemura, M.; Togo, H., Selective Oxidation of Alcohols with Alkali Metal Bromides as Bromide Catalysts: Experimental Study of the Reaction Mechanism. *J. Org. Chem.* **2014**, *79*, 6094-6104.
38. Ahn, D. K.; Kang, Y. W.; Woo, S. K., Oxidative Deprotection of *p*-Methoxybenzyl Ethers via Metal-Free Photoredox Catalysis. *J Org Chem* **2019**, *84*, 3612-3623.
39. Klement, I.; Lütjens, H.; Knochel, P., Chemoselective Oxidation of Organozinc Reagents with Oxygen. *Tetrahedron* **1997**, *53*, 9135-9144.

Chapter 6

Conclusions and Perspectives

C-H functionalization of inert C-H bonds has been considered as a meaningful but challenging issue. This thesis describes several methodologies for the photocatalytic C-H functionalization of different aromatic and aliphatic hydrocarbons, including carboxylic acids, alkylarenes and cycloalkanes. C-H functionalization of these cheap, stable and easily-available substrates affords a wide range of valuable compounds, including aldehydes, ketones, alcohols, peroxides and amides.

We have developed a Mn-catalytic system for the decarboxylative oxygenation of carboxylic acids to corresponding aldehydes and ketones using a non-heme $[\text{Mn}(\text{dtbpy})_2(\text{OTf})_2]$ catalyst with O_2 as oxidant. A wide range of aromatic and aliphatic acids as well as drug molecules can be converted to target aldehydes and ketones in good yields under mild conditions. To explore the transformation of carboxylic acids to other oxidation products, such as alcohols and peroxides, we attempted to develop new catalytic systems for selective C-H functionalization of carboxylic acids.

We went on with the search and found a new Ce-catalytic system for selective transformation of carboxylic acids using a cheap and commercially available Ce(III) catalyst with air as oxidant. Not only could aldehydes and ketones be obtained, but also peroxides and alcohols were afforded as final products. A big challenge in this protocol is the control of the selectivity. It is interesting to find that the selection of base, i.e. NaOAc vs 2,6-lutidine, can adjust the selectivity of the reaction. A wide range of peroxides, aldehydes, ketones and alcohols resulting from aromatic acids, aliphatic acids and pharmaceutical drugs were afforded in good yields with high selectivity.

Apart from the transformation of carboxylic acids, a Ce(III)-catalysed Ritter-type C-H amidation of alkylarenes was developed. CBr_3COOH was employed as the Br source to access carbon cation. A wide range of alkylarenes as well as different nitriles were tolerated in this strategy, affording the corresponding amides in good yields and selectivity.

Finally, the oxidation of cycloalkanes was explored. Three catalytic systems have been investigated for the oxidation of cycloalkanes to ketones, alcohols and peroxides. Although the current yields of these products are moderate, the method shows promise and is worth further studying.

We hope that this research work can provide some thought towards the challenges associated with the C-H functionalization. However, some new questions require to be answered. Firstly, there still exists a need for a deep investigation of the mechanism of both Mn and Ce catalytic systems. As well, the specific structure of Ce(III) catalysts in Chapter 3 and 4 is not very clear. An endeavour must be made on the study of these catalysts. Furthermore, application of these catalytic systems in practical synthesis is worth being investigated. More work on oxidation of cycloalkanes is needed to improve the yields of ideal products.